2.6 Satellite Imagery

2.6.1 Methods

Data were obtained from the NOAA-9 satellite Advanced Very-High Resolution Radiometer (AVHRR) during the period 4/1/90–9/30/90. The thermal infrared channel was used to provide estimates of surface temperature. The resolution of the data is roughly 1 km, but in some cases it is degraded due to the satellite position. Satellite passes occurred twice per day, at approximately noon and midnight local time. Partial or total cloud cover obscured many of the images, but there were 26 images that were clear enough to provide useful oceanographic information.

The satellite data provide truly synoptic resolution of the surface temperature, complementing the other data types in the study. Because of the fairly consistent relationship between surface temperature and salinity during the spring and summer (fig. 2.6-1), the satellite data provide a means of identifying freshwater pulses that originate from the Gulf of Maine. The surface manifestation of upwelling is well resolved by the satellite data, particularly because upwelling conditions tend to occur with clear skies.

2.6.2 Satellite Observations

The times when good satellite images were obtained are indicated in the vertical lines in fig. 2.6-2. Temperature and salinity timeseries data are superimposed for comparison. Figures 2.6-3 through 2.6-15 include the actual satellite imagery, grouped in some cases when there is a chronological sequence of images. The coldest water is shown as white, and the warmest water as black, with the temperature range shown at the top of each figure. The land tends to show up dark in the pm images and light in the am images. Clouds are light (or white).

The images from the early spring period (figs. 2.6-3 and 2.6-4) show little temperature structure. Figure 2.6-4 provides a comparison with the April hydrographic measurements.

Figure 2.6-5 captures a major run-off event that occurred between May 11 and May 25, cresting on both the Merrimack and Charles Rivers around May 18. Broad Sound salinity hit a minimum of 30.2 psu on May 22, and Scituate salinity dropped to 30.7 psu 2 days later, then dropped again to 30.2 psu to on around May 30. The minimum salinity at U-6 of 29.4 psu occurred on May 29. Interpretation of the satellite imagery is based on the assumption that the low-salinity water emanating from the rivers is warmer than the ambient water. This is evident from the T-S relation of the moored data (fig. 2.6-1), which show that a 1 psu decrease in salinity

corresponds roughly to a 2°C increase in temperature.

The satellite image from 5/25/90 (fig. 2.6-5a) shows a distinct coastal current travelling down the western Gulf of Maine, apparently coming from the Kennebec–Androscoggen. A blob of warm water appears to be emanating from the mouth of the Merrimack. A warm feature along the coast south of Boston suggests a coastal flow from Boston Harbor. While it is a faint feature, this interpretation is supported by salinity data from Scituate. This feature extends approximately as far as Plymouth. Warm water south of Cape Ann may have come from the Merrimack.

The a.m. image on 5/27/90 (fig. 2.6-5c) shows that the blob has curved around Cape Ann toward Massachusetts Bay. A cold filament extending southeastward off the tip of Cape Ann strongly suggests that there is a coastal convergence and offshore flow there. The feature looks like a mushroom vortex, suggesting jet-like flow with recirculation on either side.

The p.m. image on 5/28/90 (fig. 2.6-5e) shows a southward continuation of the mushroom feature. Again there is distinct evidence of flow separation at Cape Ann, with cold water being pulled up on the seaward side. A cloud obscures the conditions in Cape Cod Bay.

Figures 2.6-6—2.6-11 indicate variations of near-surface temperature during a variety of wind forcing conditions in the Bays (see captions for details).

Figure 2.6-12 provides a sequence during which a persistent upwelling pattern is evident. The strongest upwelling event of the year occurred during this period (see also Section 3.3). Strong SW winds starting on 7/16/90 (fig. 2.1-1) initiated an upwelling period that was sustained for approximately 1 week, due to persistence of the SW wind regime. Large drops in surface water temperature at Scituate and Broad Sound were observed during this period.

Figure 2.6-12 shows the sequence of satellite images during this time interval, some of which are cloud-free. The am images (figs. 2.6-12 b, e and f) provide better resolution of the coastal temperature anomaly than the pm images. The clearest image is figure 2.6-12e, which shows a band of upwelled cold water starting just west of Barnstable Harbor and extending north to Cape Ann. The region from Boston to Cape Ann has a broad region of low temperature, extending 20 km from the coast, while the upwelling band is approximately 10 km wide in the southern part of Massachusetts Bay and Cape Cod Bay. Patches of cold water are observed offshore of Scituate and Manomet. These appear to be the result of offshore advection of upwelled water. The sequence of images shows that the structure and intensity of the upwelling varies through the course of the period.

Figure 2.6-13 indicates the temperature field resulting from strong northerly winds. There is no sign of upwelling, and warm water is found in southern Cape Cod

Bay. A curved frontal feature is found wrapping around Race Point.

Another upwelling sequence is included in figs. 2.6-14a–e. Unlike the previous upwelling sequence, wind forcing was more intermittent during this period, but still there was a marked upwelling signature. A persistent pool of warm water is found within Cape Cod Bay.

Downwelling conditions (NE winds) are depicted in figure 2.6-15. Warm water is found throughout the Bays, but particularly along the west coast and in Cape Cod Bay.

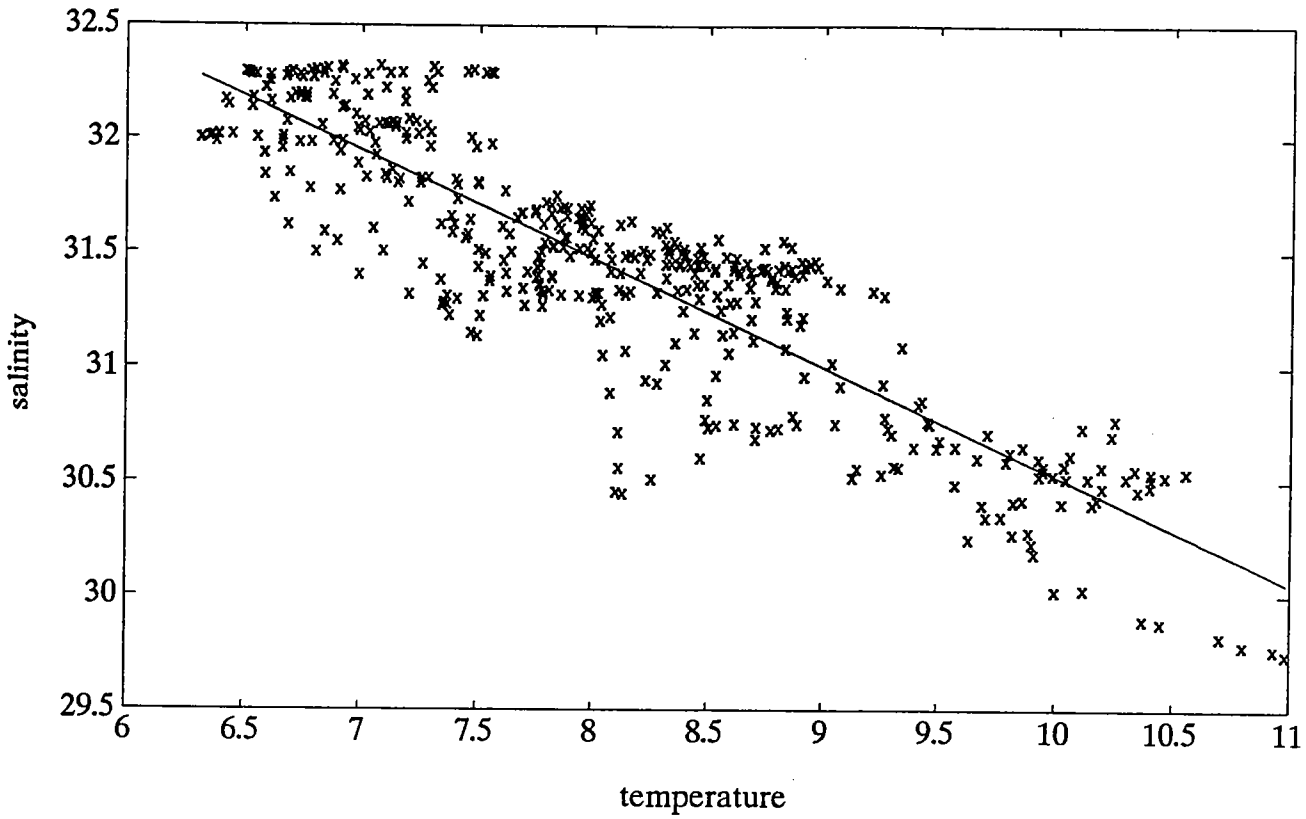

Figure 2.6-1 Temperature-Salinity (T-S) diagram for near-surface moored data from April–June, 1990, at Boston Buoy, Scituate and U6 moorings. The roughly linear relation allows temperature to be used as a proxy for salinity in tracking freshwater plumes from the Gulf of Maine with the satellite imagery.

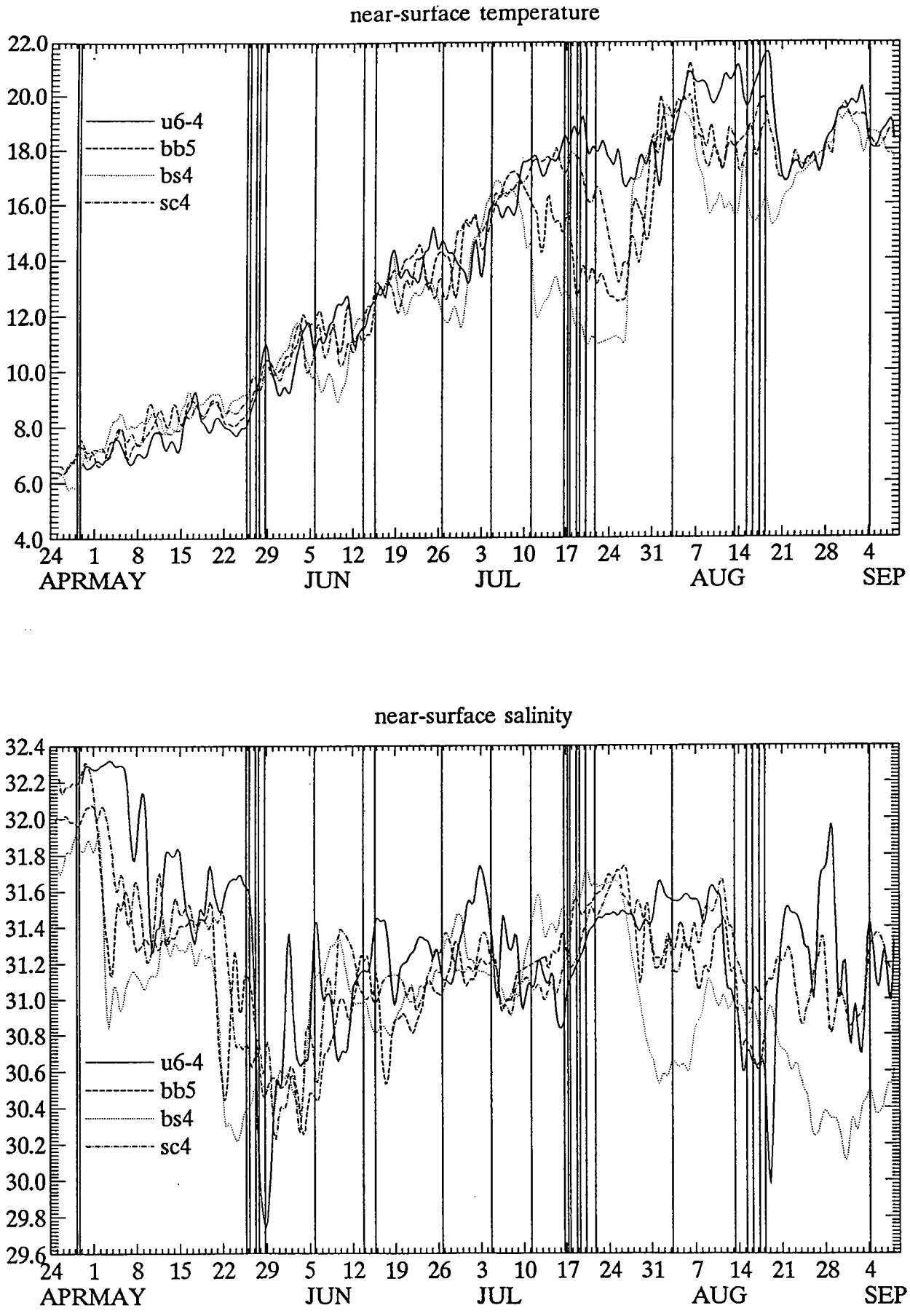

Figure 2.6-2 Times of good satellite images (vertical lines) superimposed on temperature (upper panel) and salinity timeseries (lower panel) for the period during which satellite data were collected. Temperature and salinity were recorded at the near-surface sensors at the U6, Boston Buoy, Broad Sound and Scituate moorings.

Figure 2.6-3 4/23/90. Just at the beginning of the Mass. Bays Program mooring deployment, weak gradients are observed throughout the region. There is some warm water north of Cape Ann, suggesting a coastal plume. The warmest water (darker) is in eastern Cape Cod Bay.

Figure 2.6-4a 4/28/90. Concurrent with spring hydrographic cruise. Weak southerly winds during the period. Buoyant water extending offshore north of Cape Ann. Mass. Bay mostly obscured.

Figure 2.6-4b 4/28/90. Buoyant plume has advected south, now trending southeastward off Cape Ann. Major freshening occurs several days later in Mass. Bay, as the freshwater is advected by strong northeasterly winds.

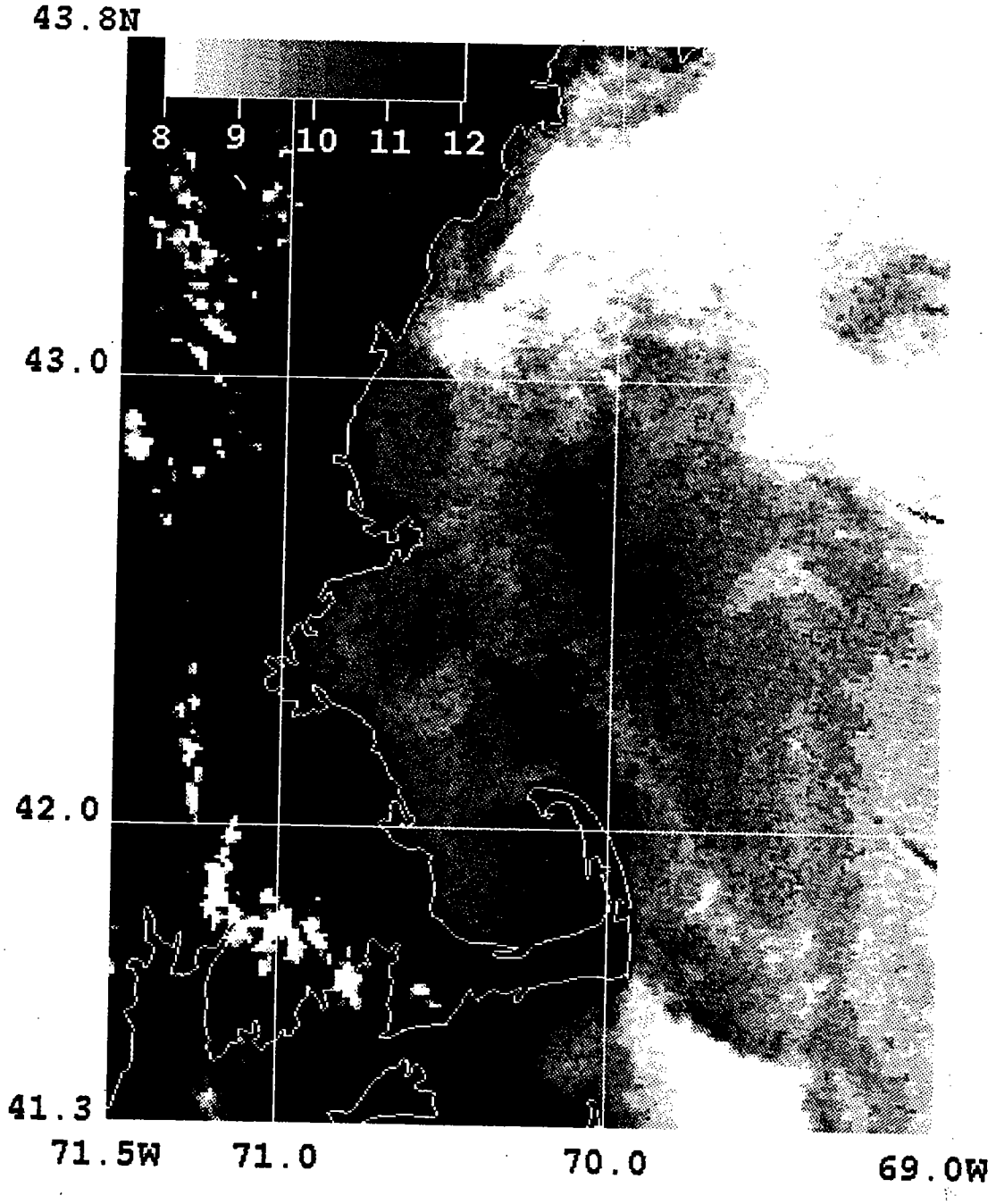

Figure 2.6-5a 5/25/90. Major freshwater inflow event. Winds during this period were weak southerlies. Salinity in Mass. Bay dropped by 1 psu during this period. Sequence of images shows plume starting out north of Cape Ann and then extending south into Massachusetts Bay (see text for detailed description).

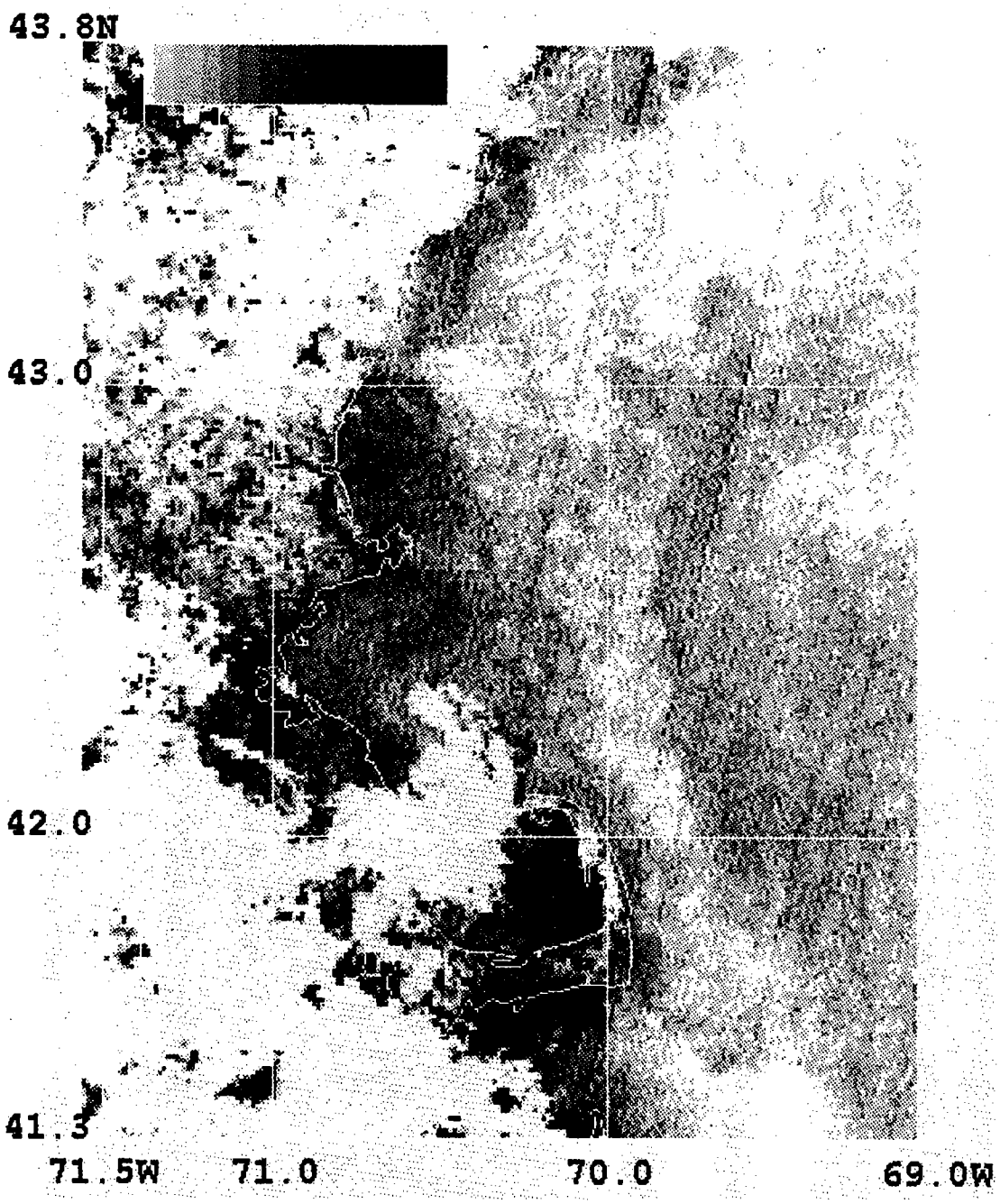

Figure 2.6-5b 5/26/90. Major freshwater inflow event.

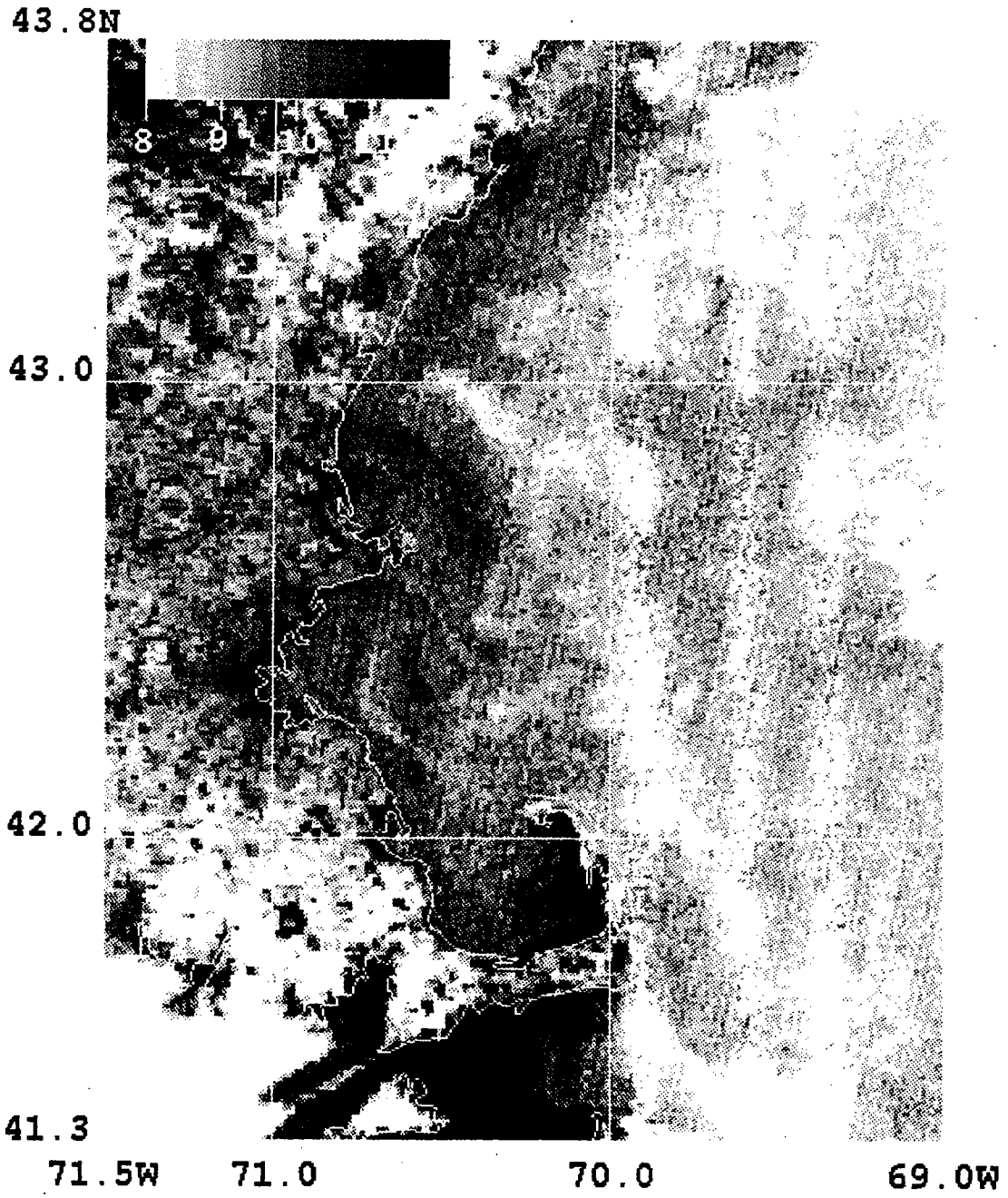

Figure 2.6-5c 5/27/90 (am). Major freshwater inflow event.

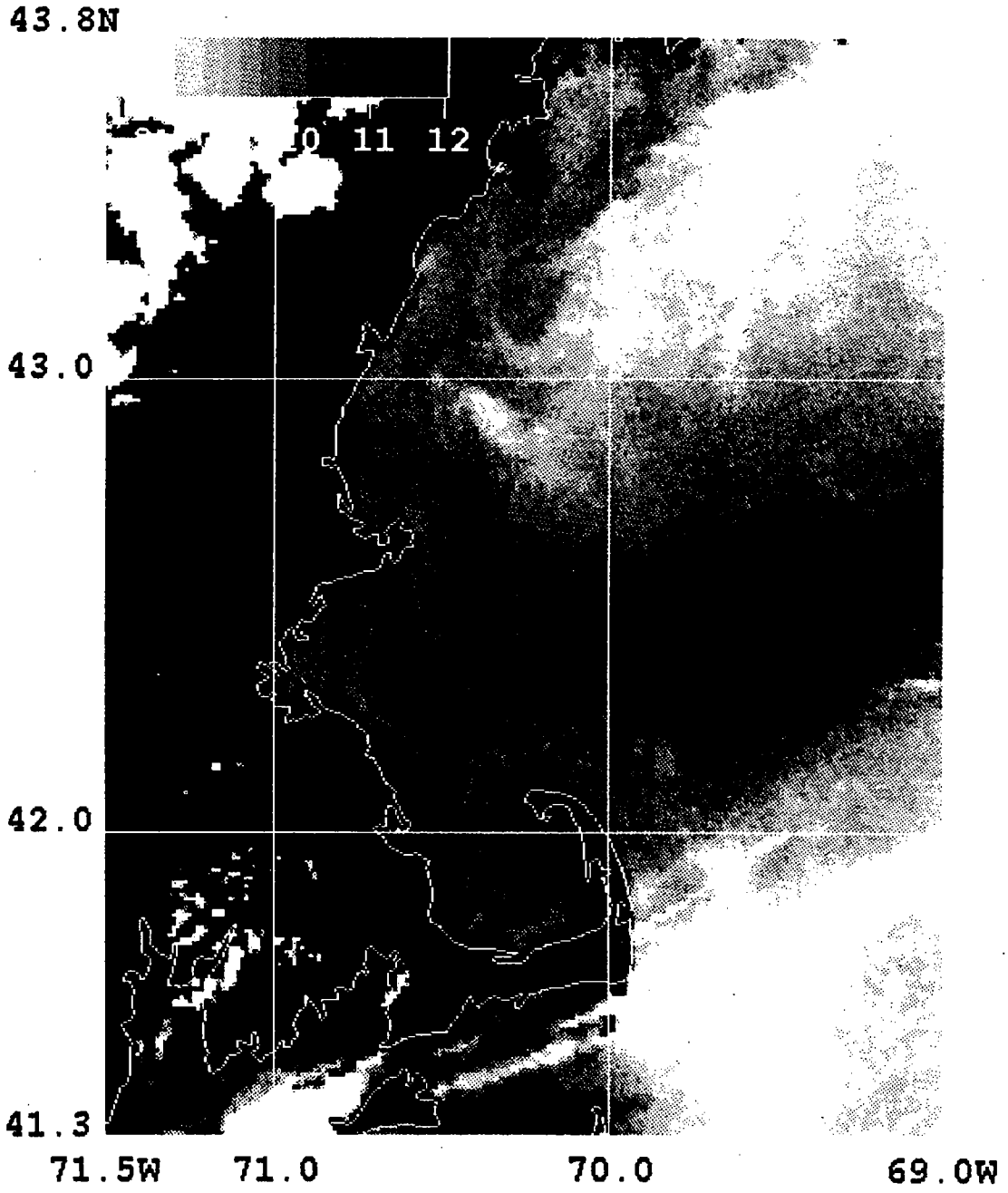

Figure 2.6-5d 5/27/90 (pm). Major freshwater inflow event.

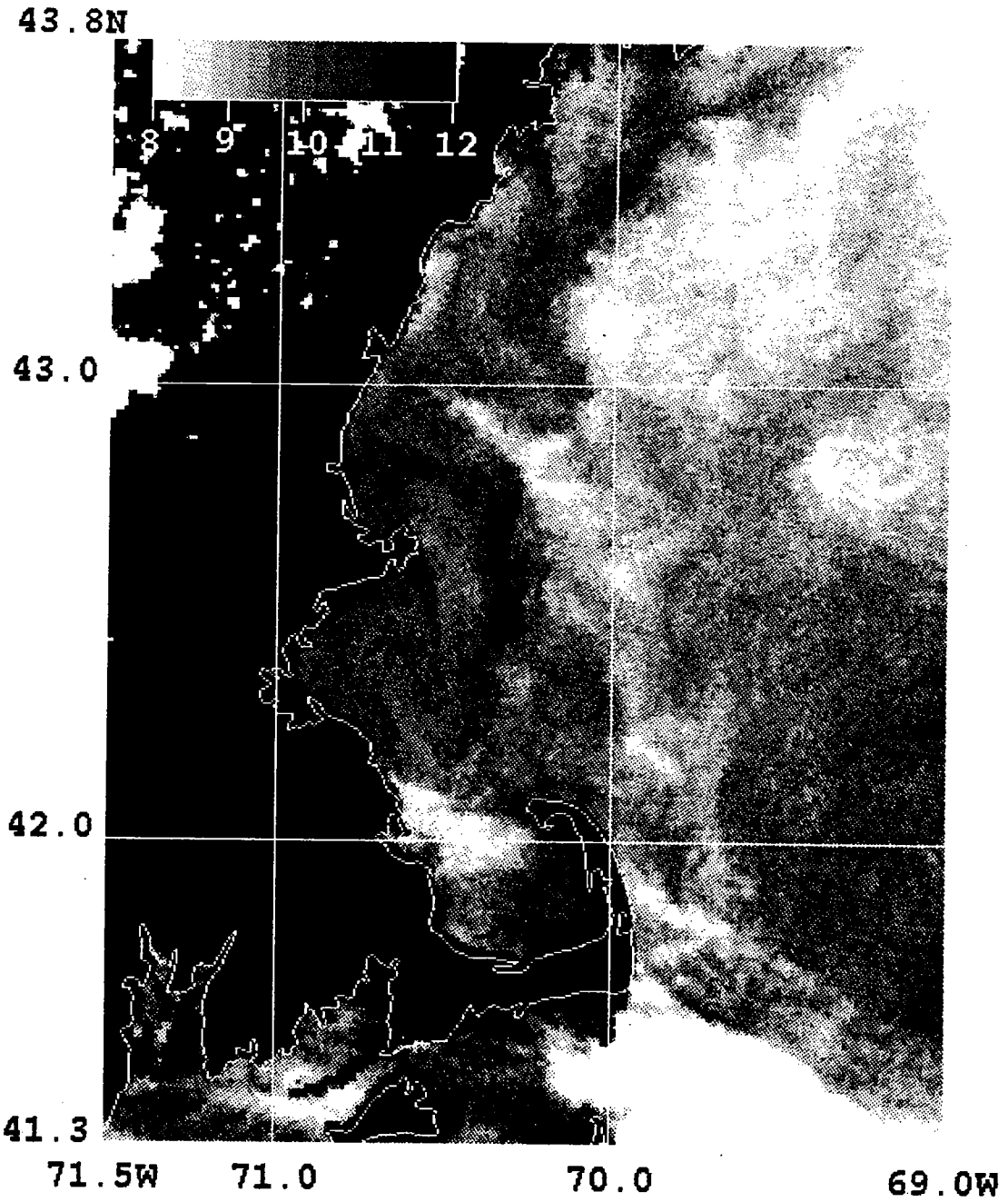

Figure 2.6-5e 5/28/90. Major freshwater inflow event.

Figure 2.6-6 6/5/90. Moderate northwesterly winds, end of freshening event. Southeast-trending gradients, with cold band extending across Stellwagen Bank from Cape Ann. Warm areas off Cohasset and in eastern Cape Cod Bay.

Figure 2.6-7 6/13/90. Weak SE winds, following strong northerlies. Cold water to north, warm water in Cape Cod Bay.

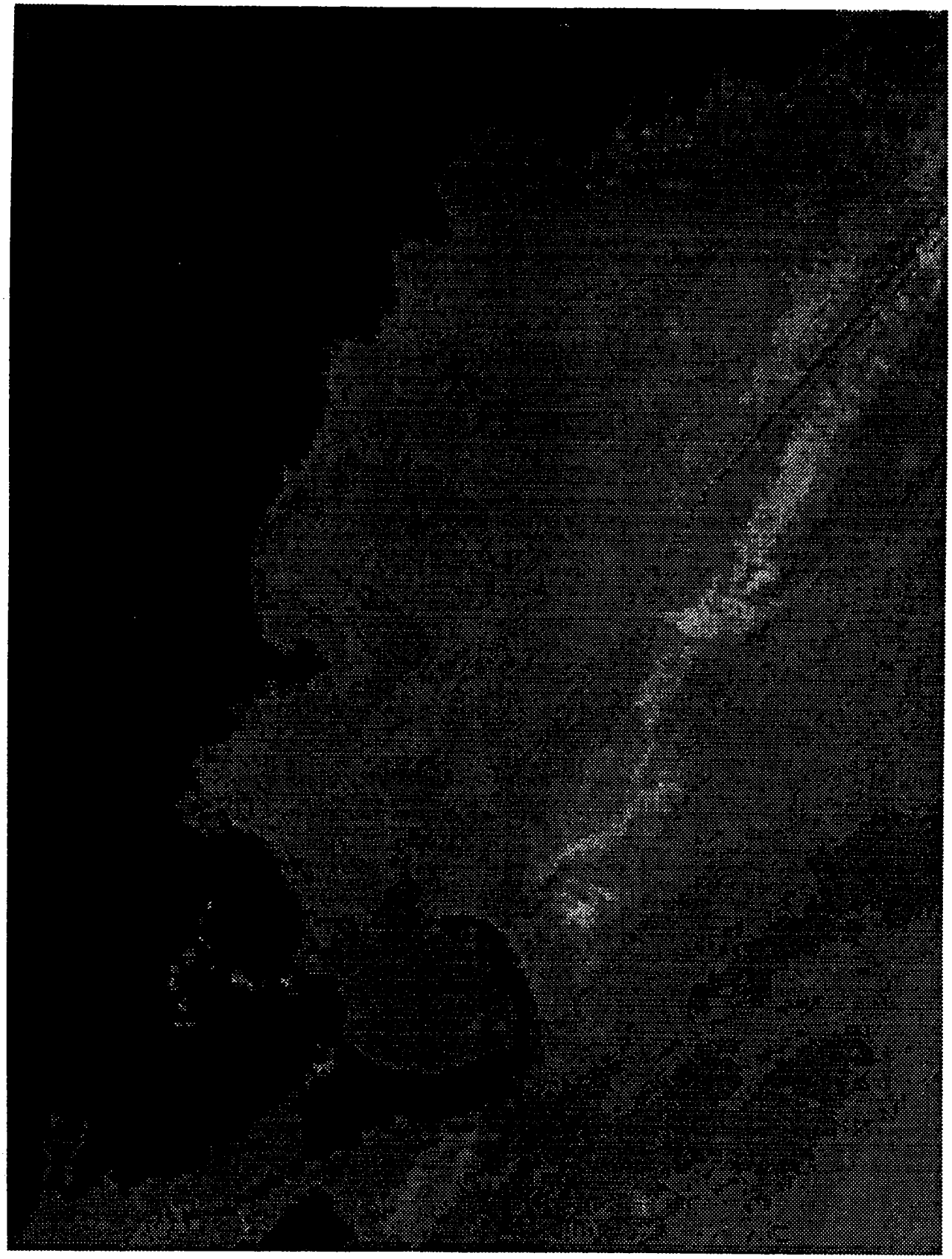

Figure 2.6-8 6/15/90. Weak SE winds. Warm water filling Cape Cod Bay, with suggestion of warm "burp" just west of Provincetown. Indication of coastal plume around Cape Ann.

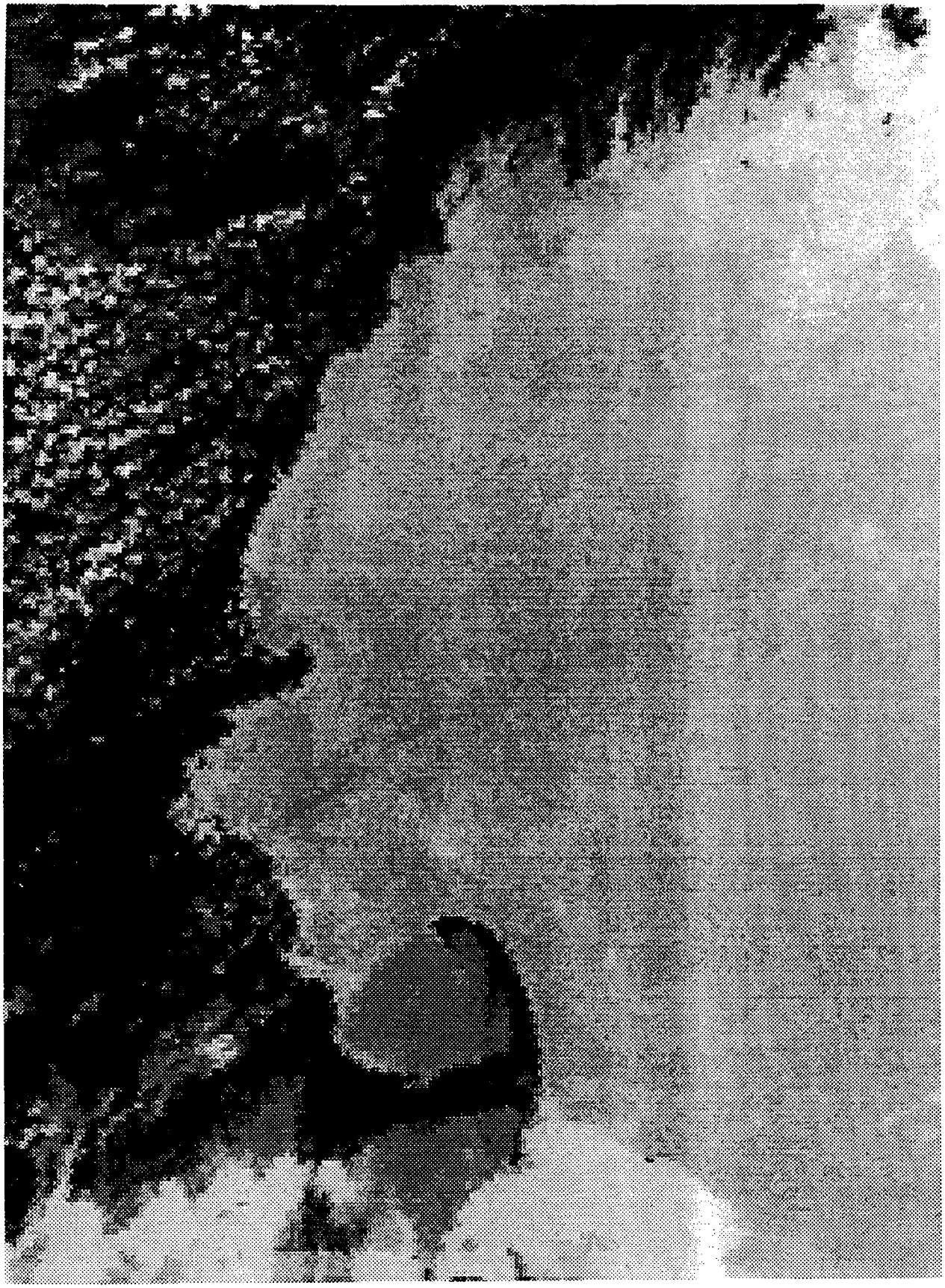

Figure 2.6-9 6/26/90. Persistent SW winds for several days, with evidence of coastal upwelling. Filament of cold water extending from Manomet to Race Point.

Figure 2.6-10 7/4/90. Strong WSW winds in Cape Cod. Some evidence of upwelling in Cape Cod Bay.

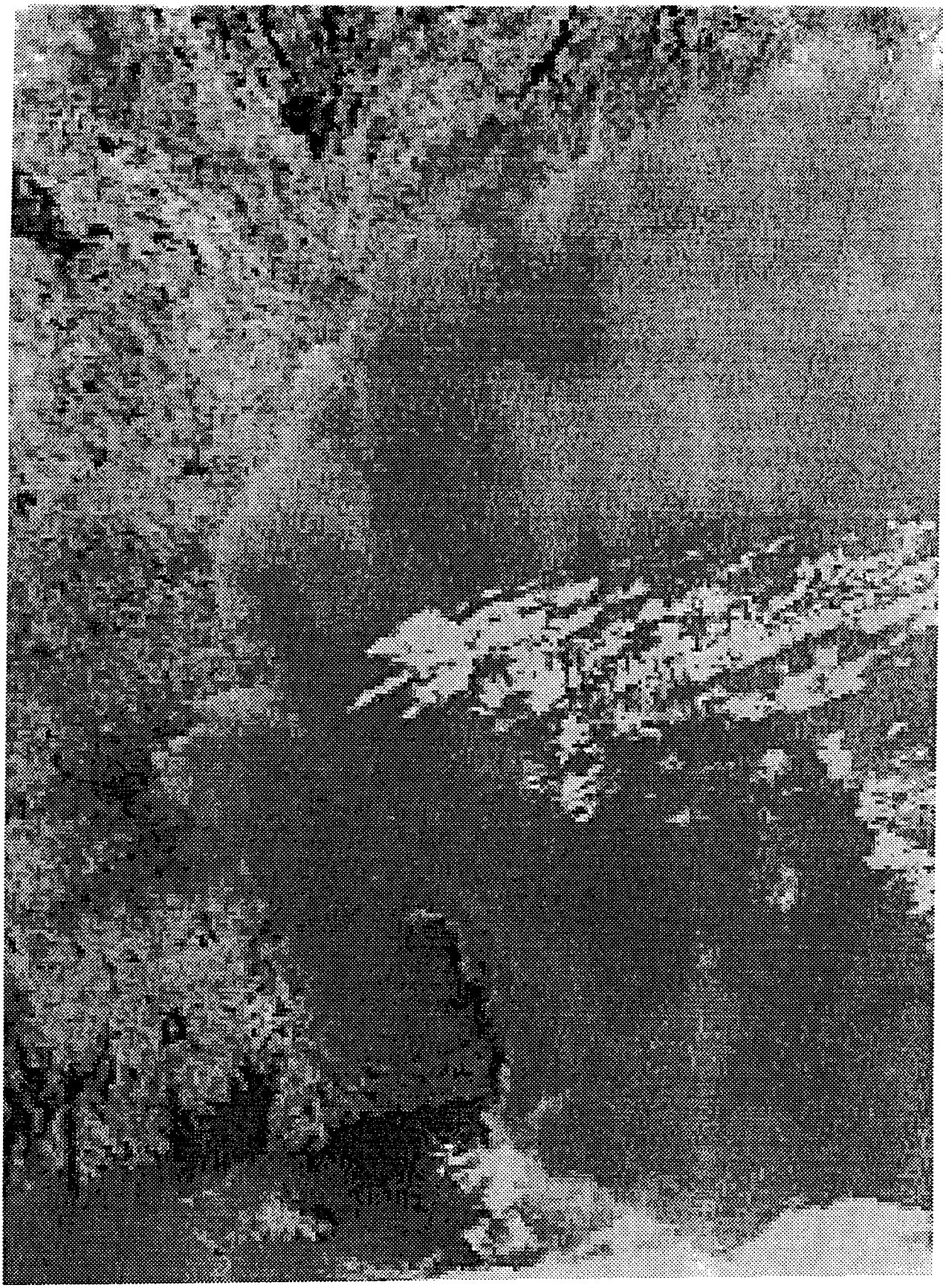

Figure 2.6-11 7/11/90. Moderate westerly winds. Upwelling north of Boston.

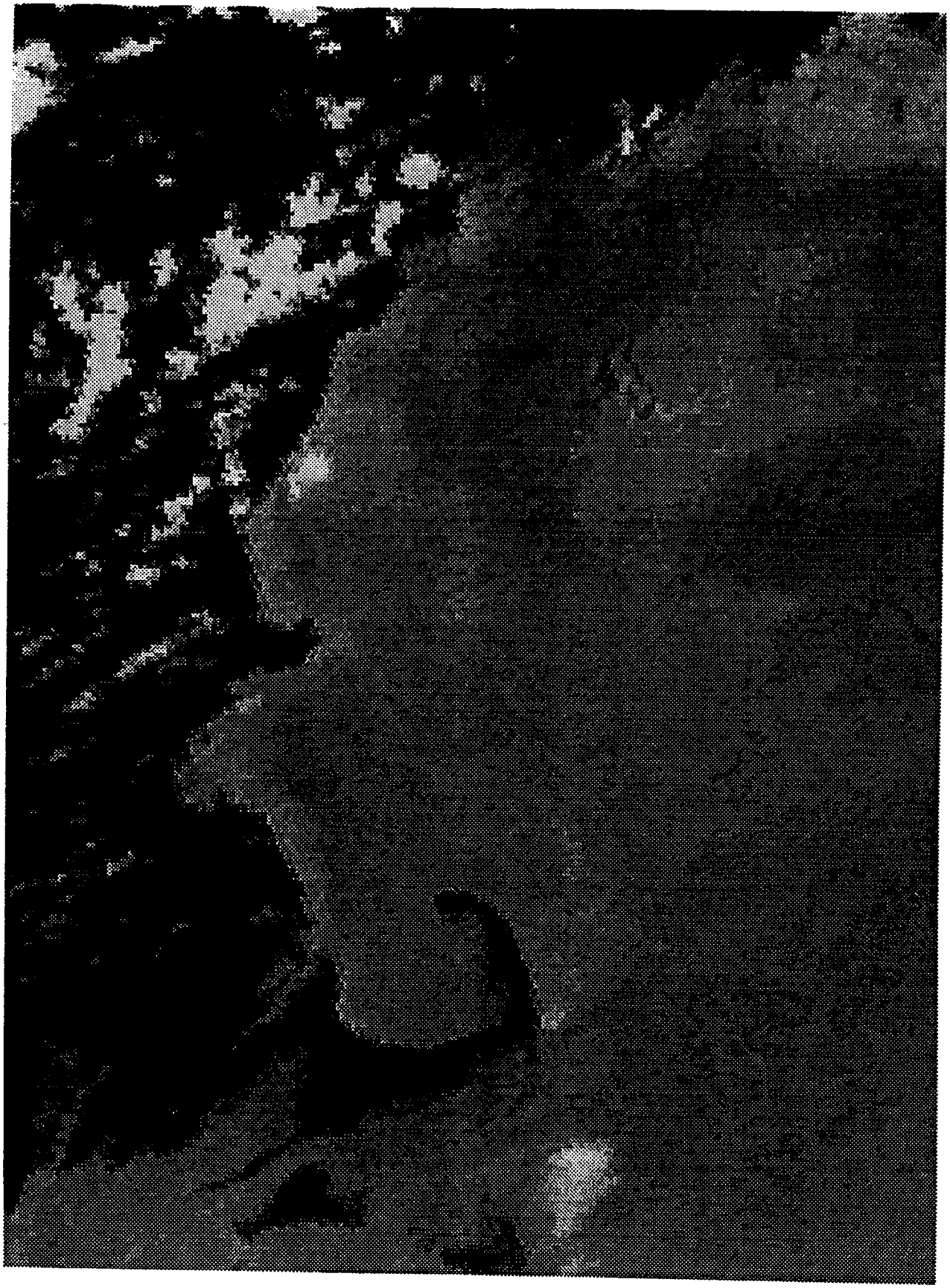

Figure 2.6-12a 7/16/90. Persistent upwelling driven by sustained SW winds. (See text for detailed description).

Figure 2.6-12b 7/17/90 (am). Persistent upwelling driven by sustained SW winds.

Figure 2.6-12c 7/17/90 (pm). Persistent upwelling driven by sustained SW winds.

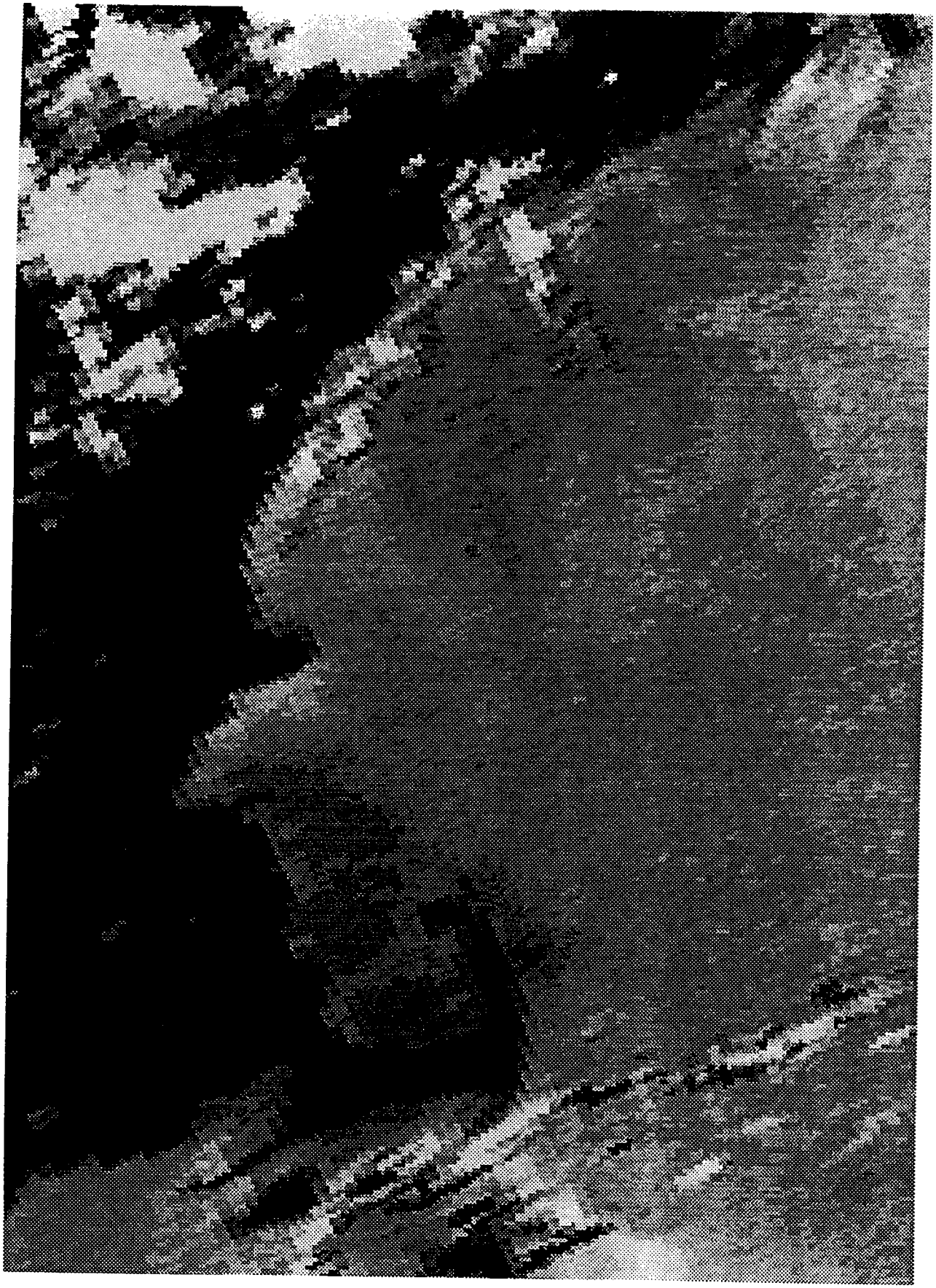

Figure 2.6-12d 7/18/90. Persistent upwelling driven by sustained SW winds.

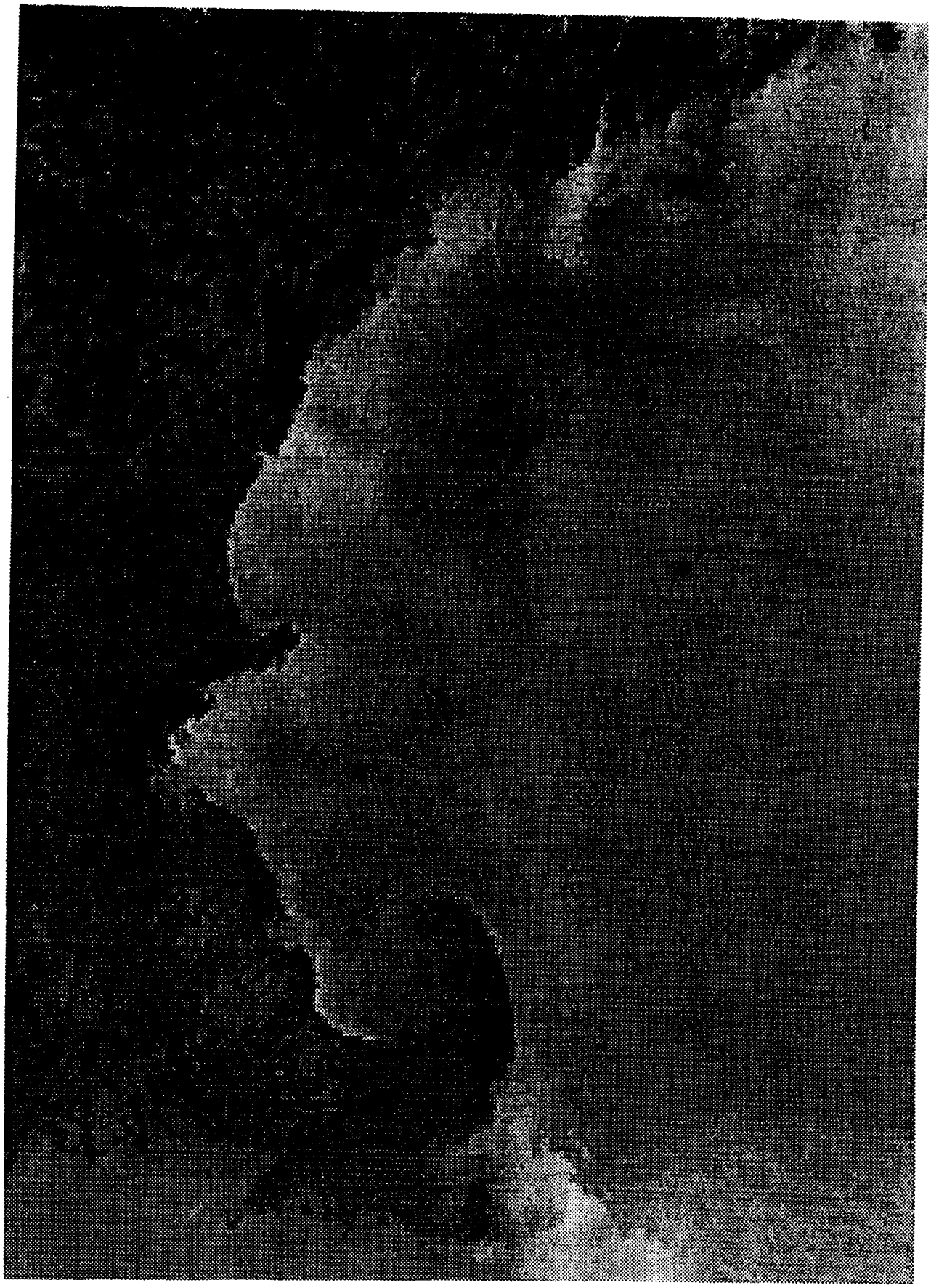

Figure 2.6-12e 7/19/90. Persistent upwelling driven by sustained SW winds.

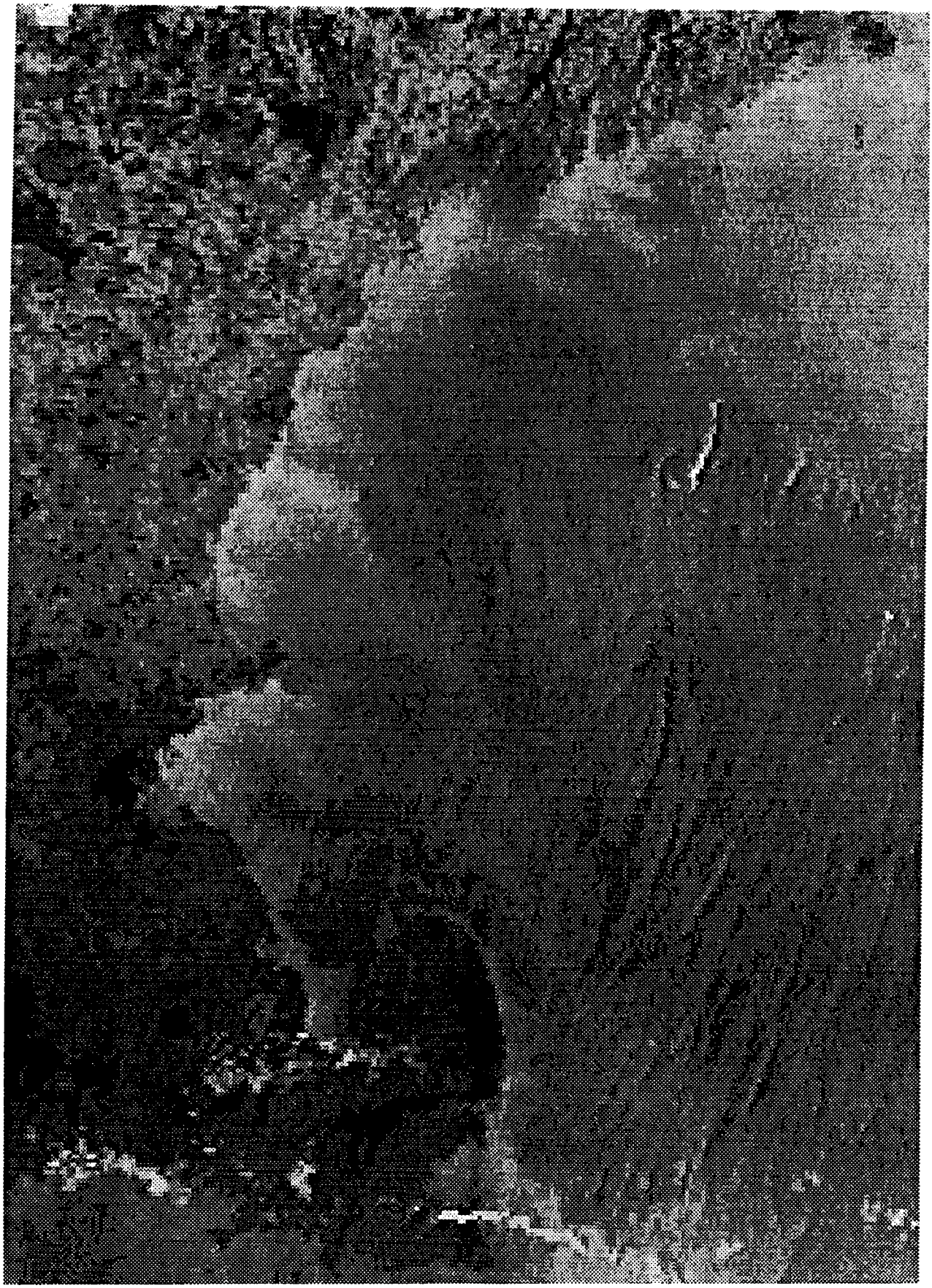

Figure 2.6-12f 7/20/90. Persistent upwelling driven by sustained SW winds.

Figure 2.6-12g 7/21/90. Persistent upwelling driven by sustained SW winds.

Figure 2.6-13 8/3/90. Two days after strong northerly winds. Curved temperature front around Race Point, with warm water in southern Cape Cod Bay.

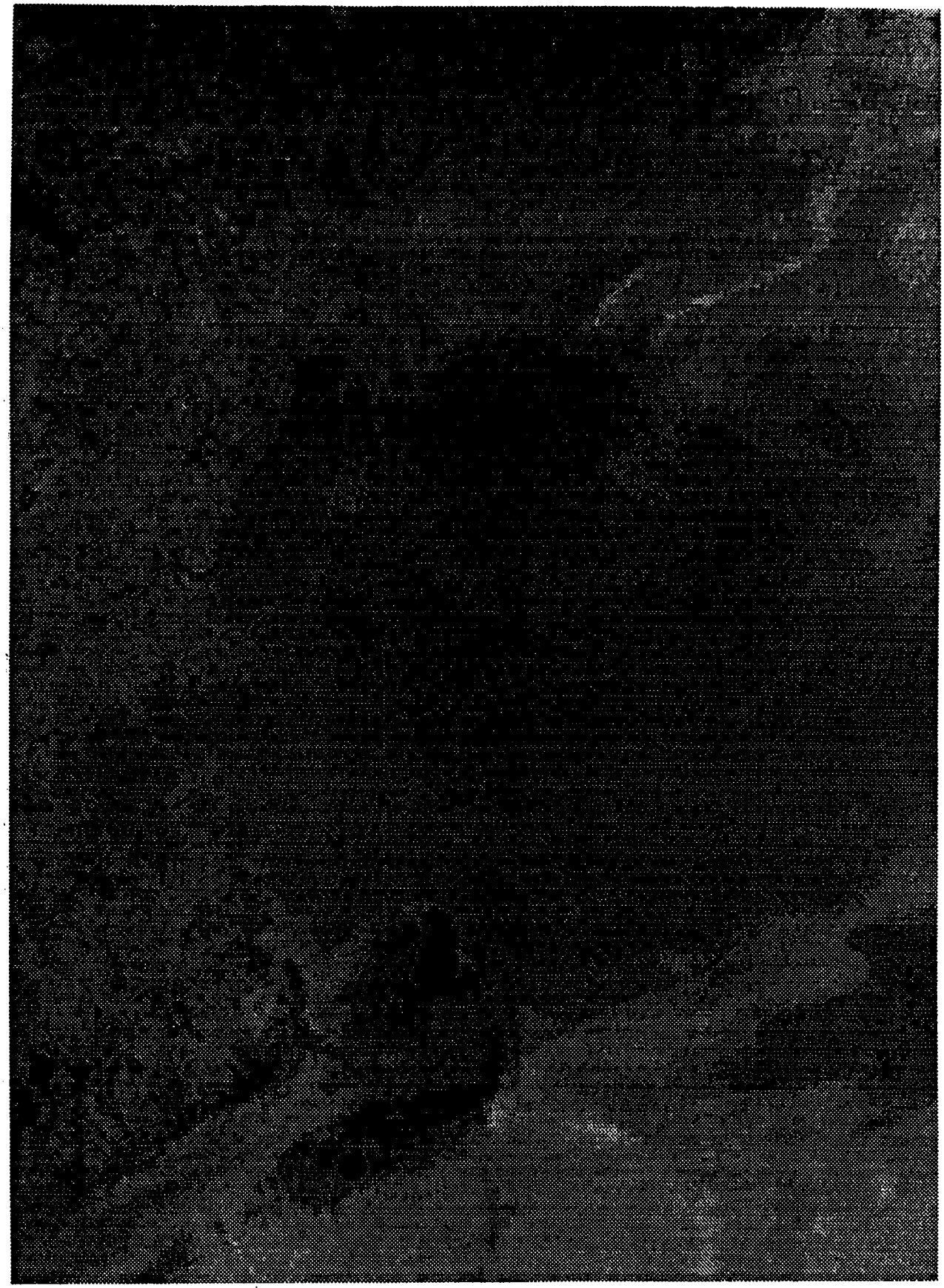

Figure 2.6-14a 8/13/90. SW and W winds. Upwelling, particularly in Cape Cod Bay. Very warm water in eastern Cape Cod Bay.

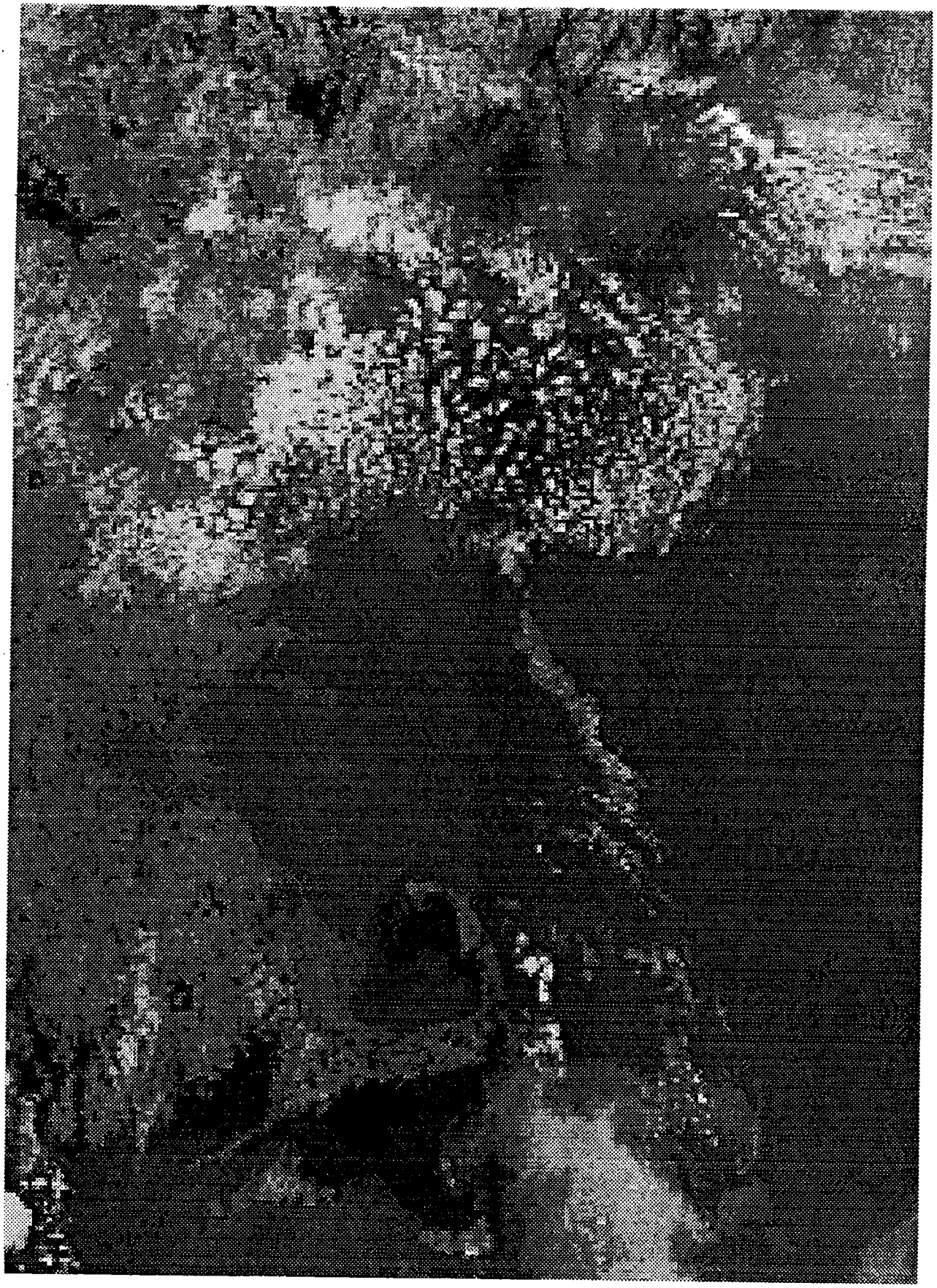

Figure 2.6-14b 8/15/90. SW and W winds.

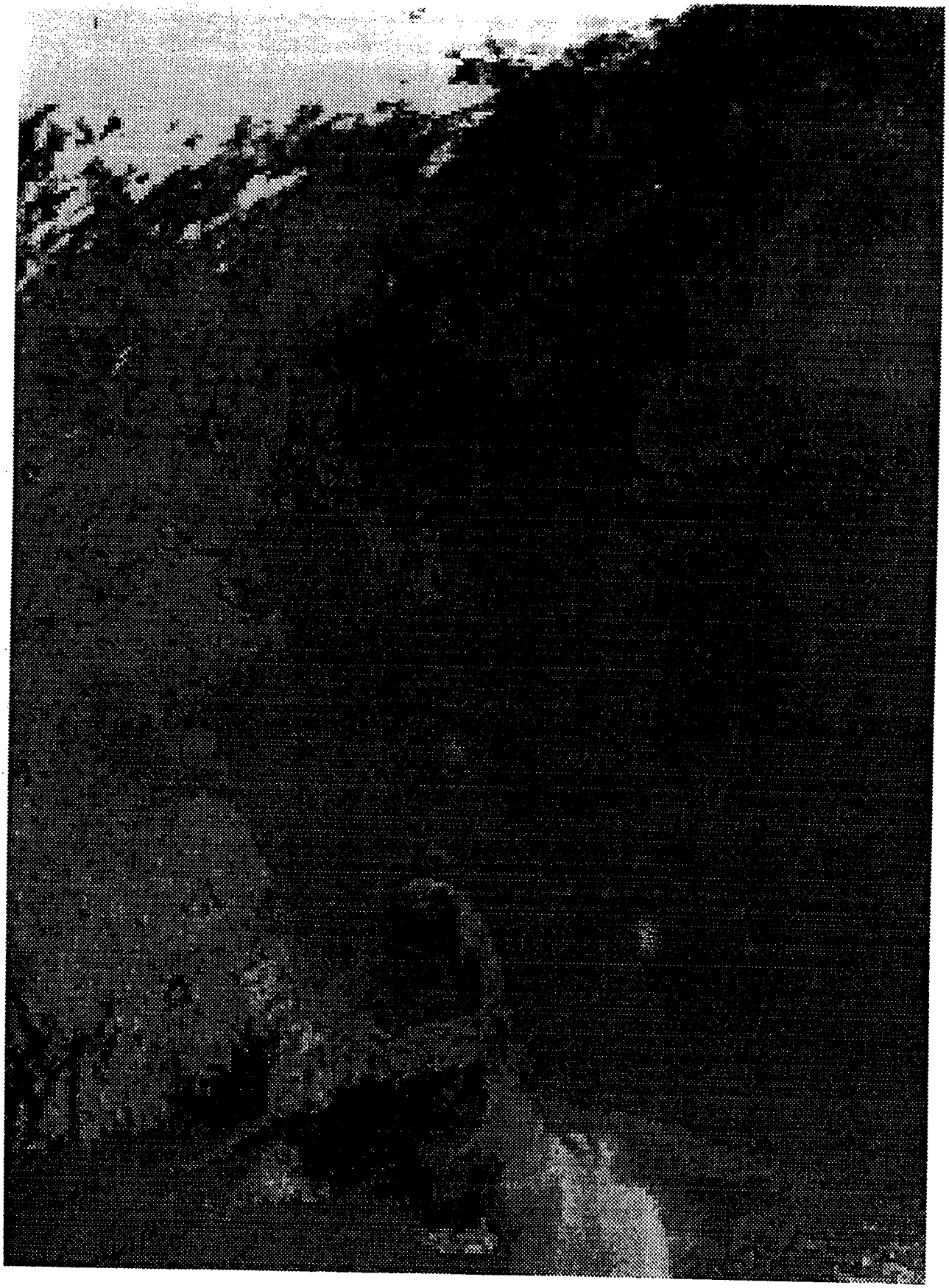

Figure 2.6-14c 8/16/90. SW and W winds.

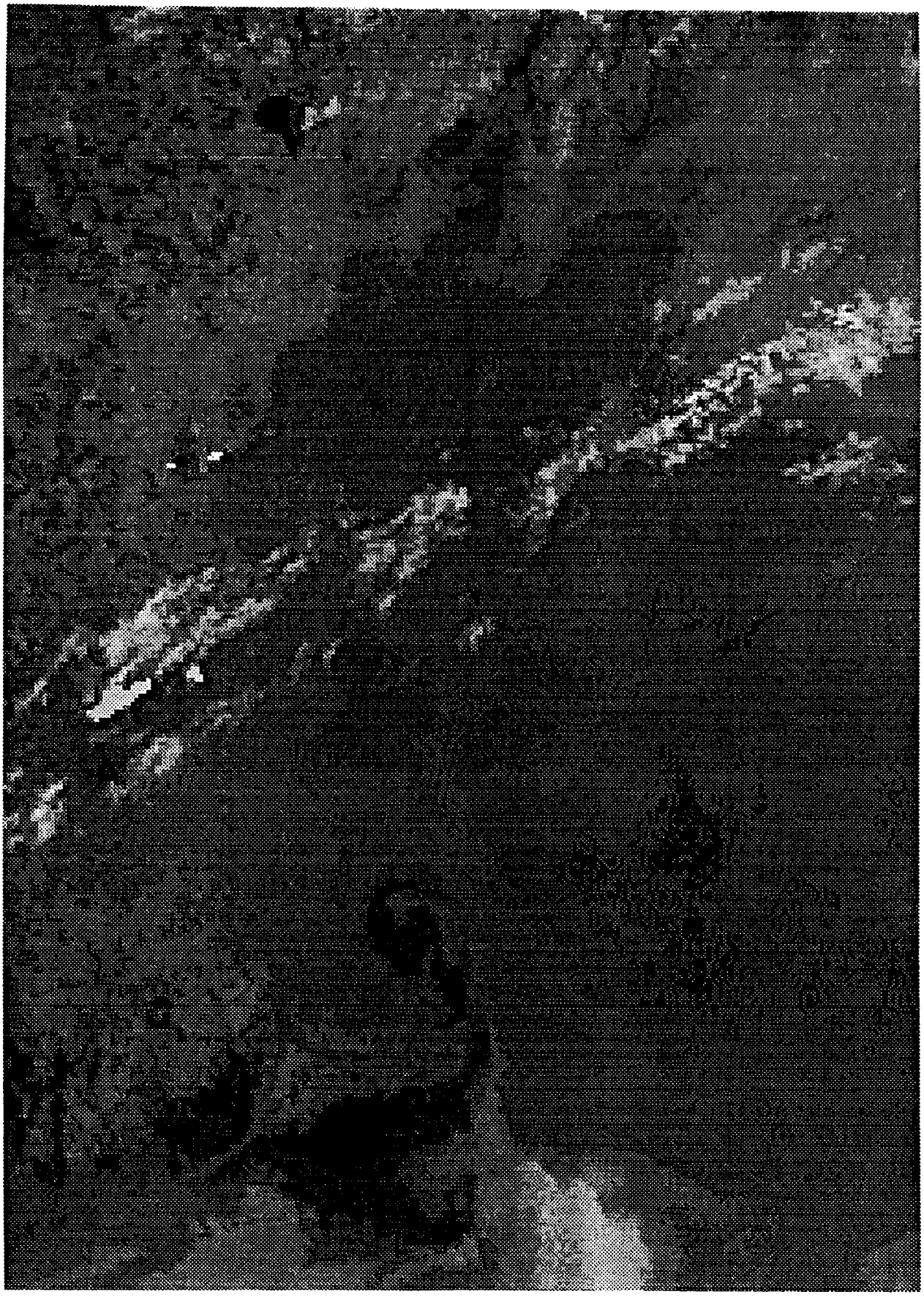

Figure 2.6-14d 8/17/90. SW and W winds.

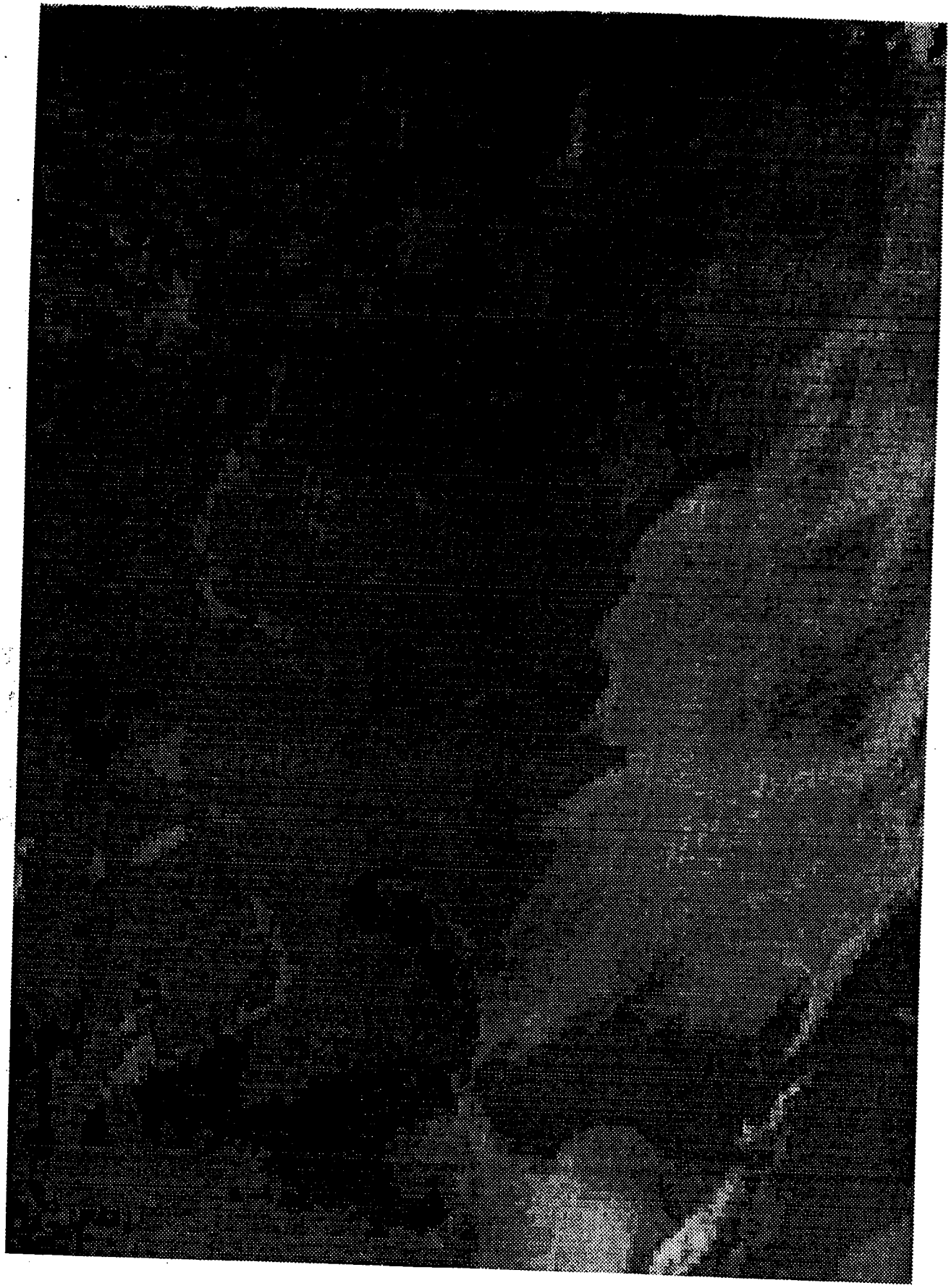

Figure 2.6-14e 8/18/90. SW and W winds.

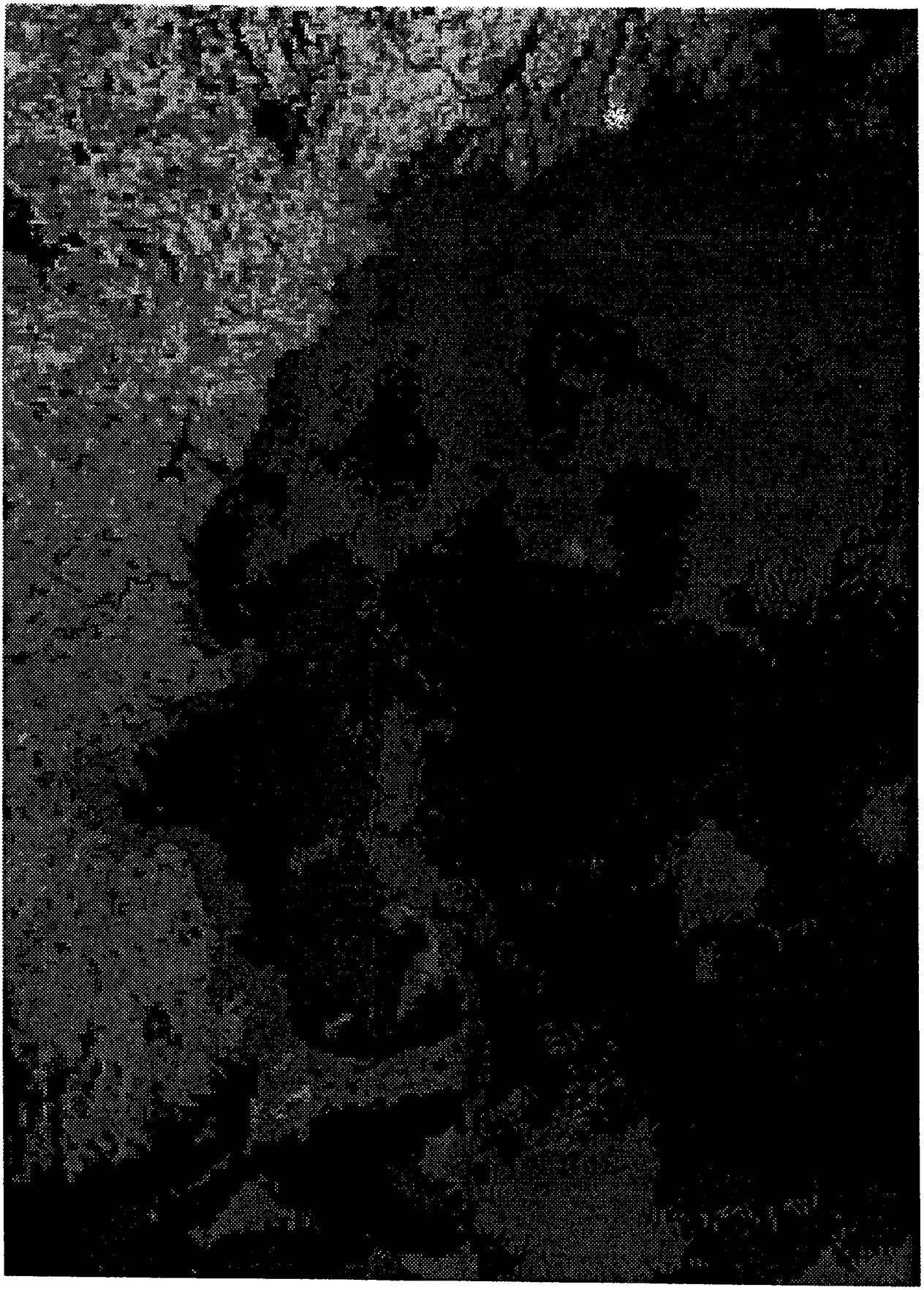

Figure 2.6-15 9/4/90. Strong NE winds. Warm water throughout Bays, particularly in southern Cape Cod Bay and along coast south of Boston.

2.7 Nutrients and Total Suspended Solids

2.7.1 Methods for Nutrients and Suspended Solids

Field Component

Samples for nutrient analysis and total suspended solids (TSS) analysis were collected at stations within Massachusetts and Cape Cod Bays on the ten cruises run by University of Massachusetts at Boston and/or Woods Hole Oceanographic Institution. The stations selected for sampling were chosen to be representative of the Massachusetts Bays system and were a subset of the UMB/WHOI hydrographic stations (figs. 1.4 and 2.4-2). The nutrient/TSS stations chosen at the ends and in the middle of the transects were intended to provide representative samples of both the near coastal and mid-Bays areas.

The number of depths sampled at each station depended on the season and the water depth at that station. Fewer depths were sampled in the winter months when the water column was not stratified and thus vertically mixed, and more depths were sampled at deeper stations and during seasons when the water column was well stratified. The depths chosen were determined in consultation with the physical oceanographers in order to obtain representative samples of the waters masses during each cruise and at each station and to characterize the nutrients and suspended solids above, below, and within the pycnocline. Niskin bottles were then used to collect water at the chosen depths. Water samples for nutrient analysis were drawn directly from the Niskin bottles into acid-washed sample-rinsed plastic vials and frozen on dry ice. Water samples for TSS were stored in plastic bottles and filtered (by suction) through tared 47-m Gleman GFC filters within one-half hour after collection.

Laboratory Analysis

Determination of the total suspended solids (TSS) and volatile suspended solids (VSS) was done using a slight modification of the methods of Strickland and Parsons (1972).

All inorganic nutrient samples were analyzed utilizing a computerized 3-channel Technicon AutoAnalyzer system using methods for sea water nutrient chemistry described by Technicon and summarized by Glibert and Loder (1977) and Loder and Glibert (1977). All samples were quantified against working standards prepared by diluting stock standards in low nutrient sea water. The stock standards were made with dried and carefully weighed reagent-grade primary standard reagents. New stock standards were always compared to old stock standards to ensure that there was continuity between analyses made over long periods of time. The salinity of the low nutrient sea water (36.5 psu) was adjusted to approximate the salinity of the samples (32 psu) by dilution with small amounts of nutrient-free deionized water. Working

standards were made daily by diluting the stock standards with calibrated Eppendorf microliter pipets and glass volumetrics except for silicate standards, which were prepared in plastic volumetrics.

All standards were run in quadruplicate and blanks were run in triplicate. A working calibration curve based on a single standard addition technique with the low nutrient sea water was used for determining the concentration of the nutrients in the samples. This worked well because the nutrient chemistries are linear in the range of concentrations normally found in these coastal waters.

2.7.2 Nutrients and Total Suspended Solids: Observations

This subsection describes the results of the nutrient and total suspended solids measurements for the six baywide surveys (see Section 2.4.1). The nutrient (ammonium, nitrate & nitrite, phosphate and silicate) and TSS data from the baywide cruises are discussed and presented in this section in a series of contour plots. The horizontal contour plot represents the surface (1 m) values. The vertical plots represent longitudinal N–S sections (looking E) for a series of sections moving away from the coast (fig. 2.7-1). Nutrient vs. nutrient plots are also presented to help in interpreting relative changes of one nutrient vs. another. Ratio lines such as the observed 8:1 line shown in fig. 2.7-7 are drawn to help in determining these relative changes.

April 27–28, 1990

There are a number of prominent features noticeable in horizontal contour plots of near-surface nutrient distributions for this cruise (figs. 2.7-2 to 2.7-5). All nutrients were low in south-central area of the Bays. There were high ammonium, nitrate plus nitrite (hereafter referred to as nitrate), and silicate concentrations in the northern section of the Bays just outside Boston Harbor in Broad Sound. There were also high concentrations of nitrate, phosphate, and silicate observed just south of Cape Ann. In both locations, the high nutrient concentrations were associated with lower salinity water (fig. 2.4-6), suggesting that the high surface-nutrient concentrations were associated with incoming fresh water from Boston Harbor and the Gulf of Maine. The river discharge data seem to support this conclusion. There was a maximum in river discharge for the Maine rivers and the Charles River just prior to this cruise. TSS showed a pronounced mid-depth maximum, with values up to 3 mg l^{-1} (fig. 2.7-6). The TSS peak occurred at the same location as the fluorescence maximum (fig. 2.4-12), suggesting that the TSS was mostly biogenic at this level.

Inner-Bays N–S Section

The ammonium and phosphate concentrations were somewhat scattered (figs. 2.7-2 and 2.7-4) with high surface concentrations in the northern section of the Bays.

The nitrate and silicate concentrations (figs. 2.7-3 and 2.7-5) were low in the surface waters and increased with depth. The low nitrate and silicate concentrations found in the surface waters extended farther down the water column in the central area of the Bays. The TSS values were low in the surface waters and increased with depth (fig. 2.7-6).

Mid-Bays N–S Section

All nutrients had higher surface concentrations in the northern section of the Bays although the higher silicate concentrations extended father south than the other nutrients (figs. 2.7-2—2.7-5). The nitrate and ammonium concentrations were low even at depths below the mixed layer in the southern section of the Bays. This was not the case for the other nutrients. The nutrient gradients were much steeper at stations in the southern section of the Bays with higher nutrient concentrations at relatively shallow depths. The highest nutrient concentrations were observed at depth in Stellwagen Basin.

Nutrient/Nutrient Plots

Nutrient vs. nutrient plots such as the nitrate vs. phosphate plot (fig. 2.7-7) are useful for determining relative changes of one nutrient vs. another. The ratio for N:P:Si (where N = nitrate + nitrite) of approximately 8:1:8 for the furthermost offshore and deepest waters in Massachusetts Bays represents ratios for the assumed GOM source water to Massachusetts Bays during the April cruise. These ratio lines were drawn on all cruise nutrient/nutrient plots for easy comparison between cruises. Although nitrate, phosphate, and silicate were all depleted in surface waters and in the southern sections as described above, the relative amounts of depletion of these nutrients were different. Nitrate (as well as DIN = nitrate + nitrite + ammonium) was depleted more rapidly than either phosphate or silicate, so that when the nitrate (or DIN) concentration was essentially zero there was still 0.1–0.4 μM phosphate and 1–2 μM silicate remaining in the water column. This suggests that nitrogen could be the limiting nutrient. Silicate was also depleted relative to phosphate in the southern section of the Bays but followed the 8:1 ratio in the northern section of the Bays.

July 24–26, 1990

The horizontal contours indicate that all nutrient concentrations and TSS values were relatively high in the northern section of the Bays just outside of Boston Harbor in Broad Sound, although ammonium and nitrate were lower and phosphate and silicate were higher than observed in April (figs. 2.7-8—2.7-12). The rest of the Bays had low surface ammonium and nitrate concentrations (less than 1 μM). Phosphate and silicate concentrations and TSS values were also high along the coast in the northern section near Cape Ann as well as in the southern section along the coast of Cape Cod Bay. The high nutrient concentrations and TSS values in the northern

section along the coast of Cape Ann and along the coast down into Cape Cod Bay were associated with high salinity water (fig. 2.4-13) and low temperature water (fig. 2.4-12), suggesting an upwelling event.

N-S Sections

All N–S sections show the same general trends with nutrient concentrations generally low at the surface and higher at depth, especially in Stellwagen Basin (figs. 2.7-8—2.7-11). However, there were specific interesting features in some of the profiles. Ammonium concentrations were low throughout most of the water column while phosphate and silicate had high surface concentrations in the northern section of the Bays as was seen in the horizontal contour plots. Phosphate and silicate had upward sloping contour lines in the southern section of the Bays where it is much shallower while ammonium and nitrate remained low throughout the whole water column in the southern section. In a general sense, phosphate and especially silicate reflect trends in salinity in the Mid-Bays section with higher silicate following higher salinity (fig. 2.4-16). High concentrations of silicate were found in Stellwagen Basin near the bottom. However, even higher concentrations were found in near bottom but relatively shallow water (16–26 m) at stations MA3 and MA6 (fig. 2.4-2). All nutrients were found to he high there suggesting this was an area of major nutrient regeneration. The source of the organic matter for regeneration to nutrients in this area is unknown at this time and warrants further study. This area also appears to be an area of denitrification which is discussed in the summary.

Nutrient/Nutrient Plots

Nutrient–nutrient plots (fig. 2.7-13) include the 8:1:8 ratio lines for comparison with the April data set (fig. 2.7-7). Nitrate was depleted relative to phosphate in the southern section of the Bays and the surface waters of the northern section. Nitrate was depleted with respect to silicate in both the northern and southern sections of the Bays. In sections of the water column where all the nitrate had been removed there was still 0.1–0.5 μM phosphate and 1–6 μM silicate left in the water column. Phosphate and silicate follow each other and the ratio of 1:8 much more closely than nitrate, except at high concentrations where the silicate concentrations were relatively higher.

October 16–18, 1990

Some distribution trends observed during the spring and summer were also present during the fall. All of the nutrient concentrations and the TSS values were high in the northern section of the Bays just outside of Boston Harbor in Broad Sound (figs. 2.7-14—2.7-18). Nitrate concentrations were also high in the southwest corner of Cape Cod Bay. Phosphate and silicate concentrations were high along the coast down into Cape Cod Bay as well. The regions of high surface phosphate

and silicate concentrations in Cape Cod Bay were associated with higher salinities, lower temperatures, and higher densities (figs. 2.4-19—2.4-21), characteristic of an upwelling event or vertical mixing. The area south of Cape Ann and the shallow southeast corner of Cape Cod Bay and the station farthest off shore into the GOM had relatively high TSS values (fig. 2.7-18).

N-S Sections

The surface phosphate and silicate concentrations in the southern section of the Bays on the Inner-Bays and Outer-Bays transects were somewhat higher than the surface concentrations in the northern sections of the Bays. This is the reverse of what was observed during the spring and summer cruises. Ammonium surface concentrations were high in the northern section of the Bays on the Inner-Bays transect but in the south the concentrations were low throughout the water column. The Mid-Bays transects show the same general trends. High surface phosphate and silicate were not observed in the south on the Mid-Bays section although there was high surface phosphate at one station in the northern part of the Bays. The nutrient gradients in the southern section of the Bays were steep and shallow on the Mid-Bays transect. High nutrient concentrations for the October cruise were observed at depth in Stellwagen Basin on the Mid-Bays section while the highest concentrations of silicate and phosphate were found in shallow bottom waters of Cape Cod Bay (especially at SW3, MA3, and PL4). These high concentrations of nutrients suggest that this area is a site of major nutrient regeneration. Phosphate, silicate, and nitrate concentrations build up during the summer and fall months and reach a maximum prior to fall cooling and destruction of the pycnocline with subsequent vertical mixing.

Nutrient/Nutrient Plots

Nutrient-nutrient plots indicate that nitrate was depleted with respect to phosphate in the surface waters of both the north and south sections of the Bays, but generally nitrate followed the 8:1 relationship in the deeper waters of the Bays (fig. 2.7-19). This was not the case in the deep waters of the southern sections for the April and July cruises (figs. 2.7-7 and 2.7-13) and could be due to a source of Gulf of Maine water to the southern deep waters at this time of the year. There was some indication of a strong influx of Gulf of Maine water at depth through the south passage (see Section 2.2) in early October. Silicate was enriched with respect to nitrate in the southern section of the Bays but followed a 1:1 relationship in the northern section of the Bays as was observed on previous cruises in the incoming Gulf of Maine water. Silicate was depleted with respect to phosphate except in the deeper waters of the Bays where phosphate was depleted with respect to silicate. When nitrate concentrations were near zero there was still 0.2–0.4 μM phosphate left in the water column.

February 4–6, 1991

The number of stations was increased for the three 1991 cruises with the addition of several stations located further out into the Gulf of Maine on the eastern side of Stellwagen Bank. All of the nutrient concentrations except for ammonium had the same general distribution patterns (figs. 2.7-20, 2.7-22, 2.7-24, and 2.7-26). The ammonium concentrations were low everywhere except for the station outside of Boston Harbor in Broad Sound. The other nutrient concentrations were highest in the Gulf of Maine east of Stellwagen Bank and relatively high in the northern section of the Bays. The nutrient concentrations in the southern section of the Bays were relatively low with the lowest concentrations in the southeast corner of Cape Cod Bay. The TSS values (fig. 2.7-28) had the opposite distributions with low values in the northern section of the Bays and in the Gulf of Maine and high values in the southern section of the Bays. There was a large diatom bloom in the southern section of the Bays especially in Cape Cod Bay during this period (personal communication with E. Haugin, see also fig. 2.4-32) which may have contributed to high TSS values in the southeast corner of Cape Cod Bay.

Inner- & Mid-Bays N–S Sections

The nutrient concentrations and TSS values had the same general distributions on these two transects (figs. 2.7-20, 2.7-22, 2.7-24, 2.7-26 and 2.7-28). The ammonium concentrations were relatively uniform with slightly lower concentrations in the southern section of the Bays. The nitrate, phosphate, and silicate concentrations were also relatively uniform with gradually lower concentrations into the southern sections of the Bays. The TSS values were relatively uniform vertically but the gradient from north to south was fairly pronounced with high values in the southern section of the Bays. The nutrient concentrations at stations MA1, MA3, and SW6 (fig. 2.4-2) were lower than the surrounding stations and the TSS values here were higher, suggesting that the bloom that was seen in the southern section of the Bays was more pronounced at these stations. The nutrient concentrations and TSS values were high on the Mid-Bays transect at depth in Stellwagen Basin.

Outer-Bays N–S Section

The distribution of ammonium was the same as observed in the other vertical sections, vertically uniform with slightly higher concentrations in the northern section of the Bays (fig. 2.7-21). The nitrate, phosphate, and silicate concentrations (figs. 2.7-23, 2.7-25 and 2.7-27) were slightly reduced at the surface at the northernmost station and significantly reduced at the southernmost station at all depths. The TSS values (fig. 2.7-29) were vertically uniform with higher values at the southernmost station. The southernmost station on this transect was the only station that was near or in the bloom.

Gulf of Maine N–S Section

The ammonium and phosphate concentrations had similar distributions with vertically uniform concentrations and an anomalous feature at depth in the northern section (figs. 2.7-21 and 2.7-25). There was an area of high ammonium and phosphate concentrations at 60-100 m depths at the two northern most stations on this section. The nitrate and silicate (figs. 2.7-23 and 2.7-27) concentrations had similar distributions. The water column was slightly stratified with higher concentrations at depth in the northern section. The higher concentrations of nitrate and silicate were observed at lower depths in the southern section. The nitrate, phosphate, and silicate concentrations were low at the southernmost station where the bloom was occurring. It appears that the low nutrient water associated with the bloom in Cape Cod Bay extended around the northern tip of Cape Cod (station PL7) and along the coast to the east (station HI1).

Nutrient/Nutrient Plots

The nutrient–nutrient plots include the 8:1:8 ratio lines drawn for comparison with the previous cruises' data (fig. 2.7-30). Nitrate to phosphate ratios in the northern section and most of the southern section were between 9:1 and 14:1, higher than the 8:1 ratio, suggesting that during the late winter months, deeper Gulf of Maine water with higher N:P ratios flows into Massachusetts Bays. Lower N:P ratios were found in the southern section where the bloom occurred. The nitrate and silicate concentrations generally followed a 1:1 ratio in the south where the diatom bloom occurred, while in the northern section nitrate was slightly depleted relative to silicate. In the area of the bloom, silicate was depleted relative to phosphate suggesting that silicate was the limiting nutrient in the bloom.

March 21–23, 1991

The ammonium concentrations were low throughout the Bays except for outside of Boston Harbor in Broad Sound (fig. 2.7-31). Nitrate, phosphate, and silicate concentrations had similar distributions (figs. 2.7-33, 2.7-35 and 2.7-37) with the highest concentrations in the Gulf of Maine and southeast of Cape Ann and the lowest in Cape Cod Bay. The stations just south of Cape Ann had unusually high silicate concentrations and somewhat higher nitrate concentrations associated with lower salinities (fig. 2.4-34), similar to what was observed on the April 1990 cruise. The values were much higher than those found at the stations to the east in the Gulf of Maine even coming into the Bays from the Maine rivers via the Gulf of Maine coastal plume. The TSS data for this cruise appeared to be very scattered making interpretation difficult. The data were not plotted.

Inner- & Mid-Bays N–S Sections

The same general nutrient concentration distributions were observed for both

of these transects (figs. 2.7-31, 2.7-33, 2.7-35 and 2.7-37). Ammonium surface concentrations were low in the northern and southern sections of the Bays but higher in the center of the Bays. Nitrate, phosphate, and silicate concentrations were relatively uniform vertically with lower concentrations in the southern section of the Bays. The nutrient concentrations on the Mid-Bays transect were high at depth in Stellwagen Basin.

Outer-Bays N–S Section

All of the nutrients had the same general distribution patterns (figs. 2.7-32, 2.7-34, 2.7-36, and 2.7-38). The water column was not well stratified and had high concentrations at all of the stations except for the southernmost station on this transect (PL7) where the nutrient concentrations were low. The surface silicate concentrations were high in the northern section of the Bays.

Gulf of Maine N–S Section

The ammonium concentrations were universally low (fig. 2.7-32). Nitrate, phosphate, and silicate concentrations were high throughout the water column on the transect except for the southernmost station (HI3) where the concentrations were lower (figs. 2.7-34, 2.7-36 and 2.7-38).

Nutrient/Nutrient Plots

The 8:1:8 ratio lines were drawn for comparisons with the previous cruises data (fig. 2.7-39), although nitrate to phosphate and silicate to phosphate ratios were slightly higher than those observed during the February cruise. However, at low nitrate concentrations, the N:P ratios were less than 8:1, so that nitrate was depleted with respect to phosphate. The nitrate and silicate concentrations were very close to the 1:1 ratio but silicate was slightly depleted with respect to nitrate. The exception to this was a set of stations just south of Cape Ann where the lower salinity water was characterized by the highest silicate concentrations and only high nitrate concentrations, resulting in a N:Si ratio much lower than 1:1. In areas of low overall nutrient concentrations, the ratios for both nitrate and silicate to phosphate became lower as was observed during all the previous cruises.

April 29 – May 2, 1991

As observed for previous cruises, nutrient concentrations were generally high just outside of Boston Harbor in Broad Sound and low in the southern section of the Bays. The nitrate and silicate concentrations were high in the Gulf of Maine as well as in Broad Sound while ammonium concentrations were low throughout all of the Bays except in Broad Sound. The high silicate concentrations in the northern section in the Gulf of Maine and the very high area around station SC4 were associated with low salinities (fig. 2.4-41).

Inner- & Mid-Bays N–S Sections

The ammonium concentrations were stratified with slightly higher concentrations at the surface in the center of the sections and at depth. The highest values were found in Stellwagen Basin. Nitrate concentrations were generally low throughout the Bays and even at the bottom of Stellwagen Basin they were only 60–70% of the value observed in February and March. There were slightly higher concentrations of nitrate at depth in the northern section of the Bays while the low concentrations extended throughout the water column in the southern section. The water column was not strongly stratified with respect to phosphate for the Inner-Bays section, but was for the Mid-Bays section with the highest values found in Stellwagen Basin. Phosphate did not have relatively high surface concentrations in the center of the transect as did ammonium and nitrate. For the Inner-Bays section, silicate had slightly higher concentrations at depth. For the Mid-Bays section, silicate values were generally low in the southern area with slight increase from top to bottom. In the northern area, however, the lowest values were found at mid depths. There were high values associated with the low salinity water near the surface, while the highest values were found at the bottom at the northern end of Stellwagen Basin. These values were higher than those in the bottom waters off Cape Ann (possible source water) suggesting that the high silicates observed were due to local remineralization. The TSS values were slightly stratified with surface values higher near shore and near bottom values higher in the mid-bays area. The lowest values were observed at mid depths.

Outer-Bays N–S Section

Ammonium and nitrate concentrations were stratified with higher concentrations at depth. There was an area of slightly higher nitrate concentrations at the surface in the center of the transect. Phosphate concentrations on this transect were weakly stratified with the highest concentrations in Stellwagen Basin. Silicate concentrations were low throughout the most of the water column for this transect except at depth in the Basin and at the northern end of the transect. The TSS values were not stratified for this transect although higher values were found at the surface.

Gulf of Maine N–S Section

Ammonium concentrations were stratified with slightly higher concentrations at depth at the southern end of this section. Nitrate concentrations were also stratified with a gradually increasing gradient from surface to bottom. The low surface concentrations of nitrate extended further down the water column at the southern end of this transect. Phosphate concentrations had the same basic distribution as nitrate. There was a patch of low phosphate concentration water at the surface in the center of the transect. Silicate concentrations were somewhat scattered with relatively high surface concentrations at the northernmost station of this transect (station R06). The highest concentrations of silicate on this transect were found at the bottom.

Nutrient/Nutrient Plots

The 8:1:8 ratio lines were drawn for comparisons with the previous cruises' data (fig. 2.7-50). The southern section and the surface waters of the northern section were depleted in nitrate with respect to both phosphate and silicate. The deeper waters in the northern sections tended to follow the 8:1:8 relationship, except for a few samples from the GOM area at high concentrations that were enriched in nitrate with respect to phosphate and silicate. Here N:P ratios were 10–12:1. In the Stellwagen Basin, however, nitrate was low relative to the enriched silicate with N:Si ratios of much less than 1:1. Although the data for the Si:P ratio fell around the 8:1 ratio, there was some scatter around the line. The samples from the northern part of the bays appeared to be enriched in silicate relative to phosphate while there appeared to be a loss silicate relative to phosphate in the southern section.

Summary of Nutrient Findings

Nutrient sources to Massachusetts Bays are different for different nutrients and different seasons. In a broad sense, nutrients do not track salinity very well, suggesting multiple sources and processes, especially in the surface waters of the Bays once the water is in Massachusetts Bays. However, lower salinity plumes associated with river runoff such as those observed in April 1990 and March 1991 are characterized by relatively high silicate and nitrate concentrations. Based on the distribution of the various nutrients, it appears that silicate and nitrate come into the Bays from the northeast around Cape Ann when the physical oceanographic conditions are right. Ammonium and phosphate are always high in the Boston Harbor/Broad Sound area and have their source at the area of the existing sewage discharge. All nutrients, but especially phosphate and silicate are upwelled in summer months along the west coast of the Bays. The relative importance of each of these sources has not yet been determined. This question is being addressed as part of Susan Becker's Master's thesis research at UNH.

The distribution of nutrients in Massachusetts Bays is controlled by a combination of both physical and biological processes. There are wide variations in nutrient concentrations especially during the seasons when Massachusetts Bays is relatively well stratified (i.e., spring, summer and fall). Even during February, when the water column was not stratified, a diatom bloom in Cape Cod Bay depleted nutrients so that there was a strong N–S gradient in the Bays. Areas of low nutrient concentrations are almost always those where biological processes, mainly phytoplankton nutrient uptake, have occurred. These processes are most prominent during the spring months, so that by late spring (April, May) all nutrients are very low in the surface waters throughout the Bays. It is during this period that even waters in the deeper parts of the Bays (Stellwagen Basin) have reduced nutrient concentrations. For example, in April 1991, the concentration of nitrate in the deep water, was only 60–70% of the values found in February and March. Whether this is due to in situ nitrate removal

or replacement of the deep water by relatively nutrient depleted water from the Gulf of Main is uncertain.

During the stratified seasons, certain areas of the Massachusetts Bays system almost always have relatively higher nutrients than other areas. Different areas are enriched for a variety of both physical and biological reasons including:

- Cape Ann area: input of Gulf of Maine water and river-sourced coastal plume nutrients;
- Boston Harbor and Broad Sound area: input of nutrients from the MWRA outfall;
- Western Cape Cod Bay area: nearshore upwelling caused by SW winds;
- Southeastern Cape Cod Bay area: vertical mixing in shallow waters;
- Stellwagen Basin and Central Cape Cod Bay areas: nutrient regeneration in the bottom waters.

Because many of the above processes are localized, nutrient distributions in Massachusetts Bays tend to be rather patchy and variable depending on the season and nutrient type. For example, high values of nutrients were found in the sub-pycnocline layers in Stellwagen Basin and in central Cape Cod Bay in July and October most likely due to bottom water and benthic regeneration of nutrients from organic matter. Although, all the nutrient concentrations were relatively high, the very highest silicate concentrations observed in Massachusetts Bays were found during July in relatively shallow water in central Cape Cod Bay. Both high silicate and phosphate were found in the same area in October. The mechanisms for the concentration of organic matter for regeneration of nutrients in this area are unknown and warrant further study. Although nitrate was also high at this same location, higher values were found during February associated with the saltier Gulf of Maine water brought into Massachusetts Bays during the winter months. What was observed is that the different nutrients behave differently with different seasons and at different locations so that nutrient ratios can be helpful in interpreting these processes.

The inorganic nitrogen nutrients (nitrate, nitrite and ammonium) typically are found in ratios to phosphate far lower than the classic Redfield ratios of about 16:1. The source waters to Massachusetts Bays have an N:P:Si ratio (based on NO3:PO4:SiO4) of about 8:1:8 during the spring, summer, and fall months of the year. During the winter, however, when deeper Gulf of Maine water mixes upwards and gets carried into the Bays, the ratios are higher in nitrogen and silicate relative to phosphate, but still not close to the Redfield ratios. Since the source waters into the Bays are depleted in nitrogen relative to both phosphate and silicate, it would

appear that nitrogen may play the limiting nutrient role in the Bays. Often when concentrations of nitrate and/or ammonium are near zero, there is still significant phosphate and silicate left in the water. For example, for surface waters in April, July and October in areas where nitrate and ammonium values were near zero, there was still 0.2–0.4 μM of phosphate and 1–6 μM of silicate left in the water column. This suggests that the Bays system as a whole is nitrogen limited, but the pools of organic nitrogen and nitrogen recycling rates would have to examined before any definite conclusions can be reached. Silicate tends to covary with phosphate during some months in the northern part of the bays while in February during the diatom bloom it covaried with nitrate with a ratio of 1:1. When silicate values were near zero for surface waters in February, phosphate values were still about 0.3 μM suggesting that silicate could also be limiting during certain times.

It appears that north and south sections of the Bays behave differently with respect to their nutrient distributions and relative nutrient ratios during most, and maybe all of the year. The various sources of water and nutrients typically enter the Bays from the north and northwest. This is a physically more dynamic area with deeper water and deeper ties to the Gulf of Maine. Water just south of Cape Ann and in the north part of Stellwagen Basin seems to be influenced by the coastal current and Gulf of Maine water flowing into Massachusetts Bay. However, in the southern part of Massachusetts Bays, especially during the stratified seasons, water in Cape Cod Bay, further away from the sources to the north, tends to remain static for relatively long periods of time. The surface waters in the central region are west of the tip of Cape Cod tend to become highly impoverished in nutrients during late spring and summer months with nitrogen nutrients generally depleted before the phosphate and silicate. In diatom blooms silicate can also become depleted. The deeper water in that area, however has some of the highest concentrations of nutrients as a result of nutrient regeneration. Here the nutrient ratios suggest that the processes are slightly different than in the deeper waters of Stellwagen Basin. Whereas the dissolved inorganic N (DIN = nitrate + nitrate + ammonium) ratios to phosphate and silicate waters of Stellwagen Basin, they are: DIN:P = 6:1 and DIN:Si = 0.44:1 at Station MA3. This indicates that there is a reduced amount of nitrogen relative to both phosphorus and silicate in the central Cape Cod Bays area relative to further north. Nitrogen is not returned to the inorganic pool as completely as phosphorus and silicate and is either transformed to organic nitrogen or denitrified. The same trends in ratios are found along the southwest coast of Cape Cod Bay in the area of upwelling where water with relatively low nitrogen is found during the summer months. The importance of nutrient regeneration in Cape Cod Bay relative to the overall budget of nutrient recycling in Massachusetts Bay is unknown at this time and warrants further work. Also unknown is the mechanism of apparent organic matter buildup in that area. The buildup of nutrients in the deep waters of Massachusetts Bays ends abruptly in late October or early November when surface cooling and wind mixing causes the Bays to mix vertically, essentially diluting the deep water nutrients with low nutrient surface

waters.

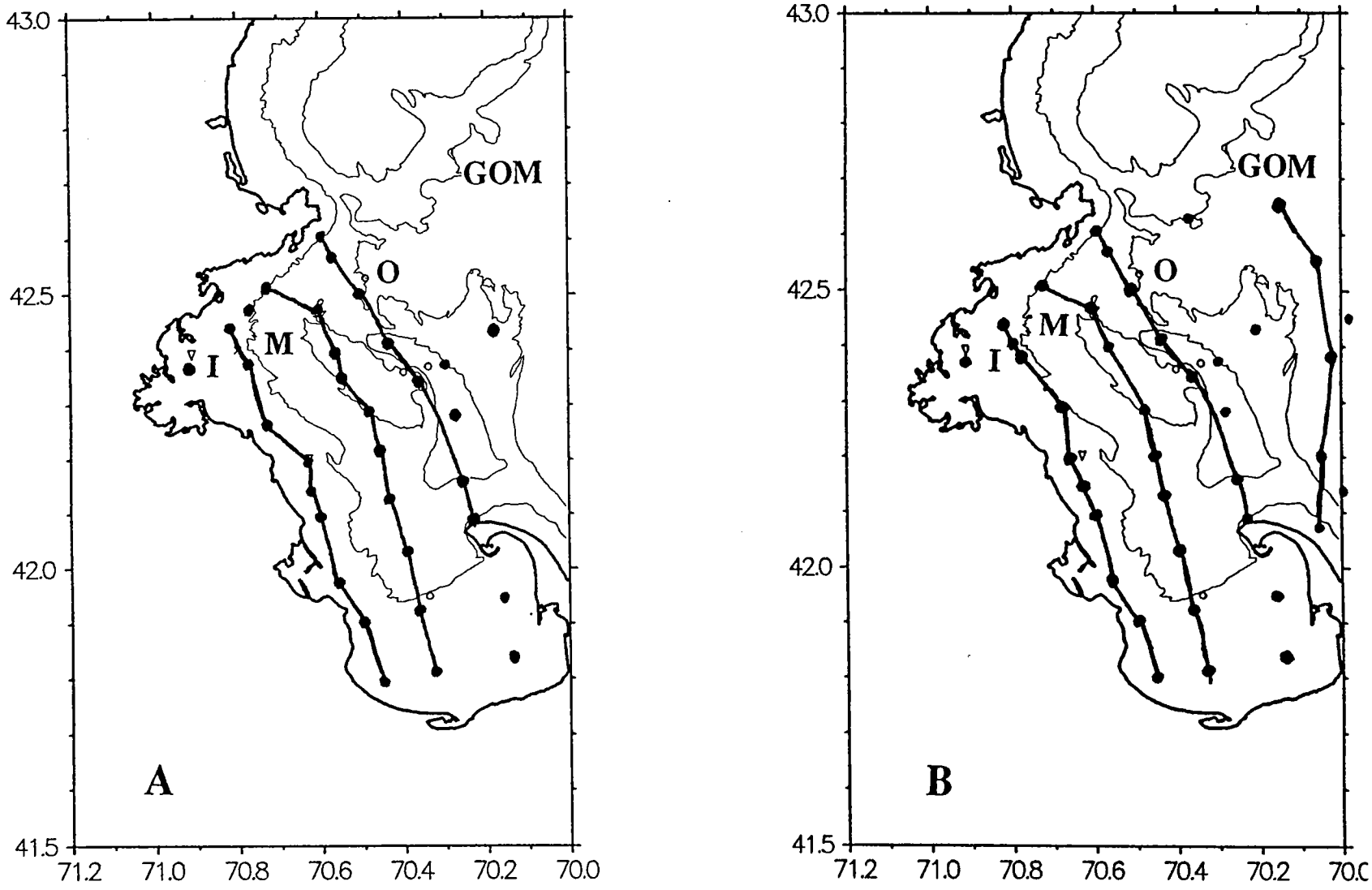

Figure 2.7-1 Vertical section location maps for Massachusetts Bays. Fig. A sections are for cruises in 1991. Fig. B sections are for cruises in 1992. Sections are labeled as follows: I: Inner-Bays; M: Mid-Bays; O: Outer-Bays; GOM: Gulf of Maine.

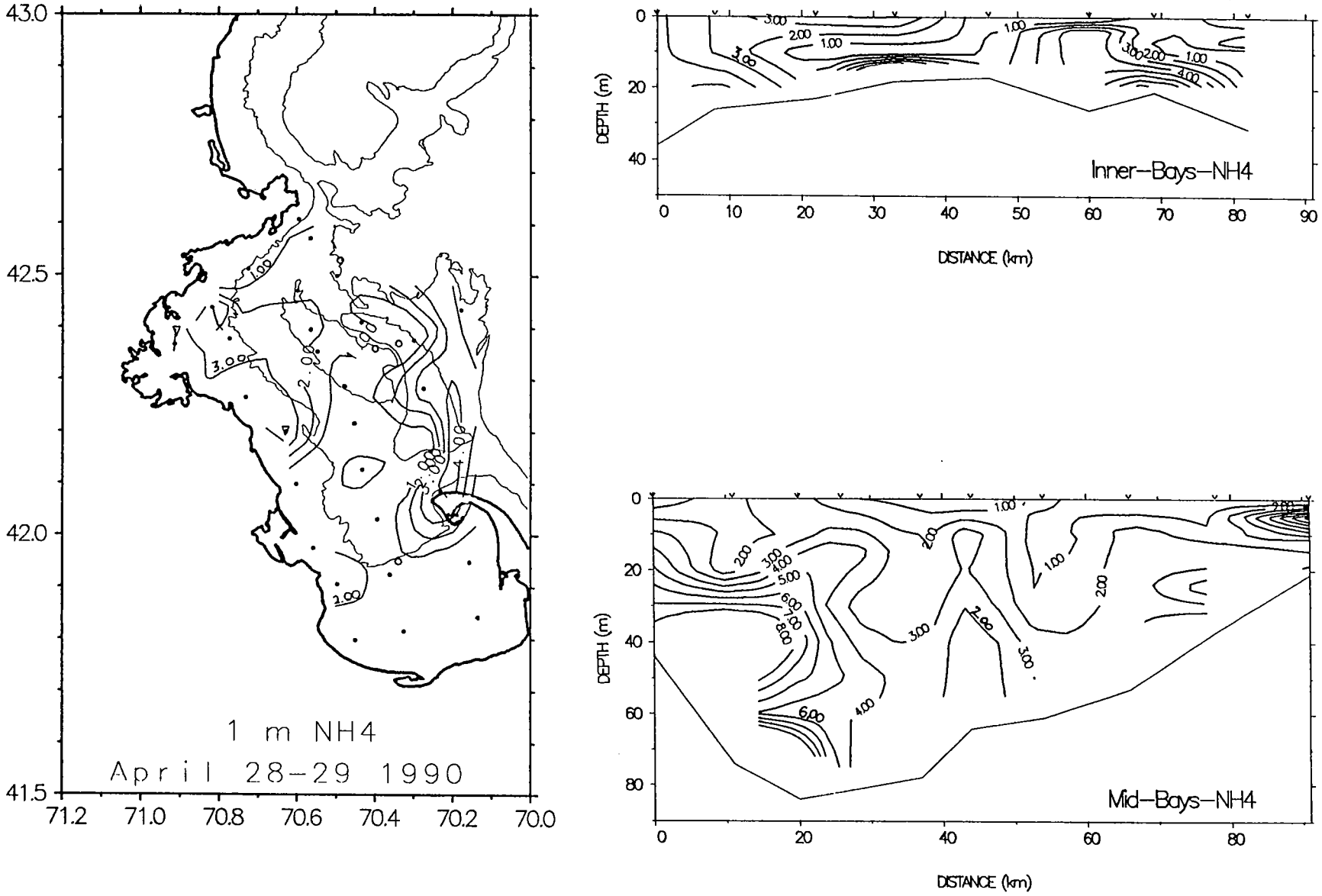

Figure 2.7-2 April 28–29, 1990 ammonium contour plots. The units are μM and the contour interval is 1 μM.

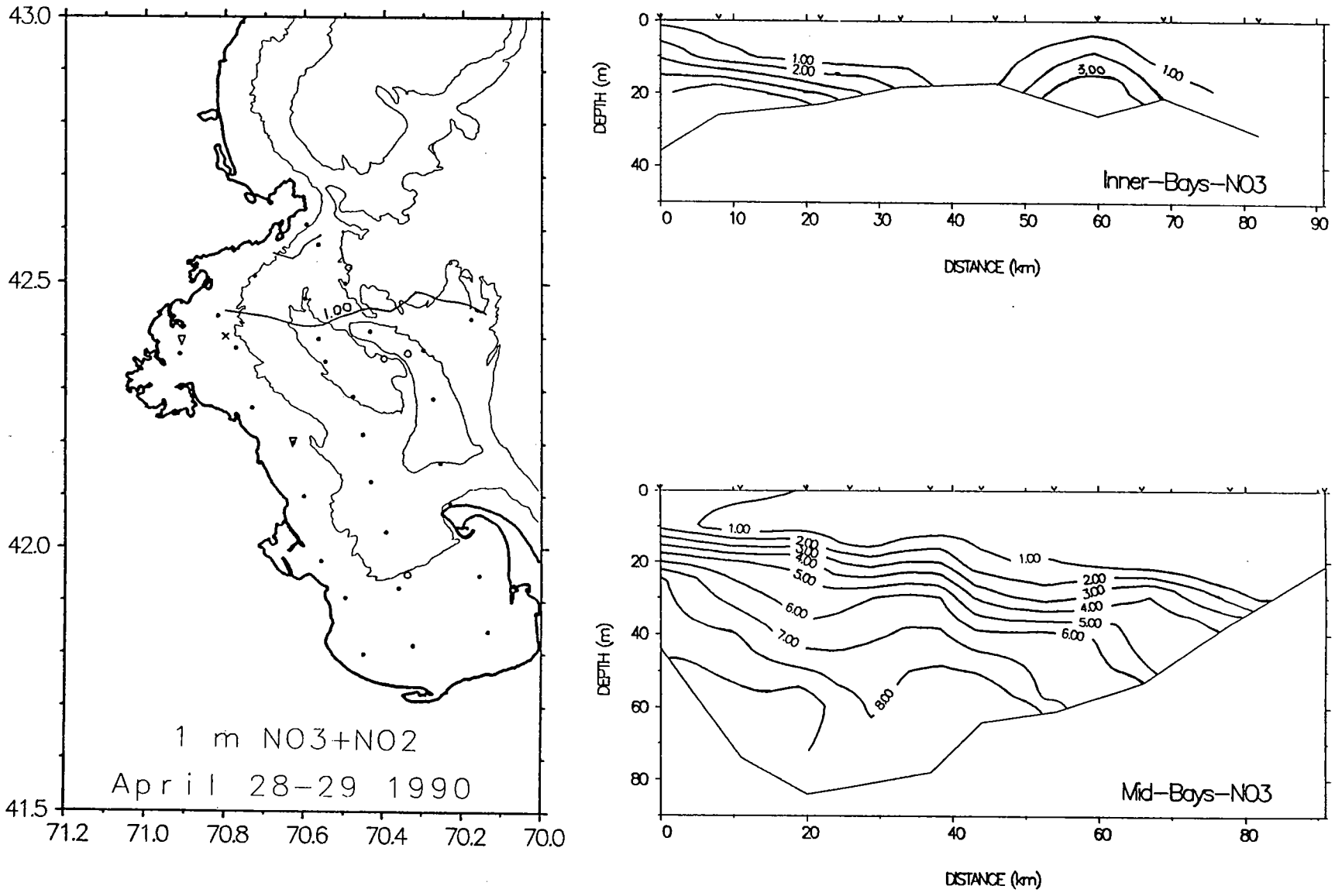

Figure 2.7-3 April 28–29, 1990 nitrate contour plots. The units are μM and the contour interval is 1 μM.

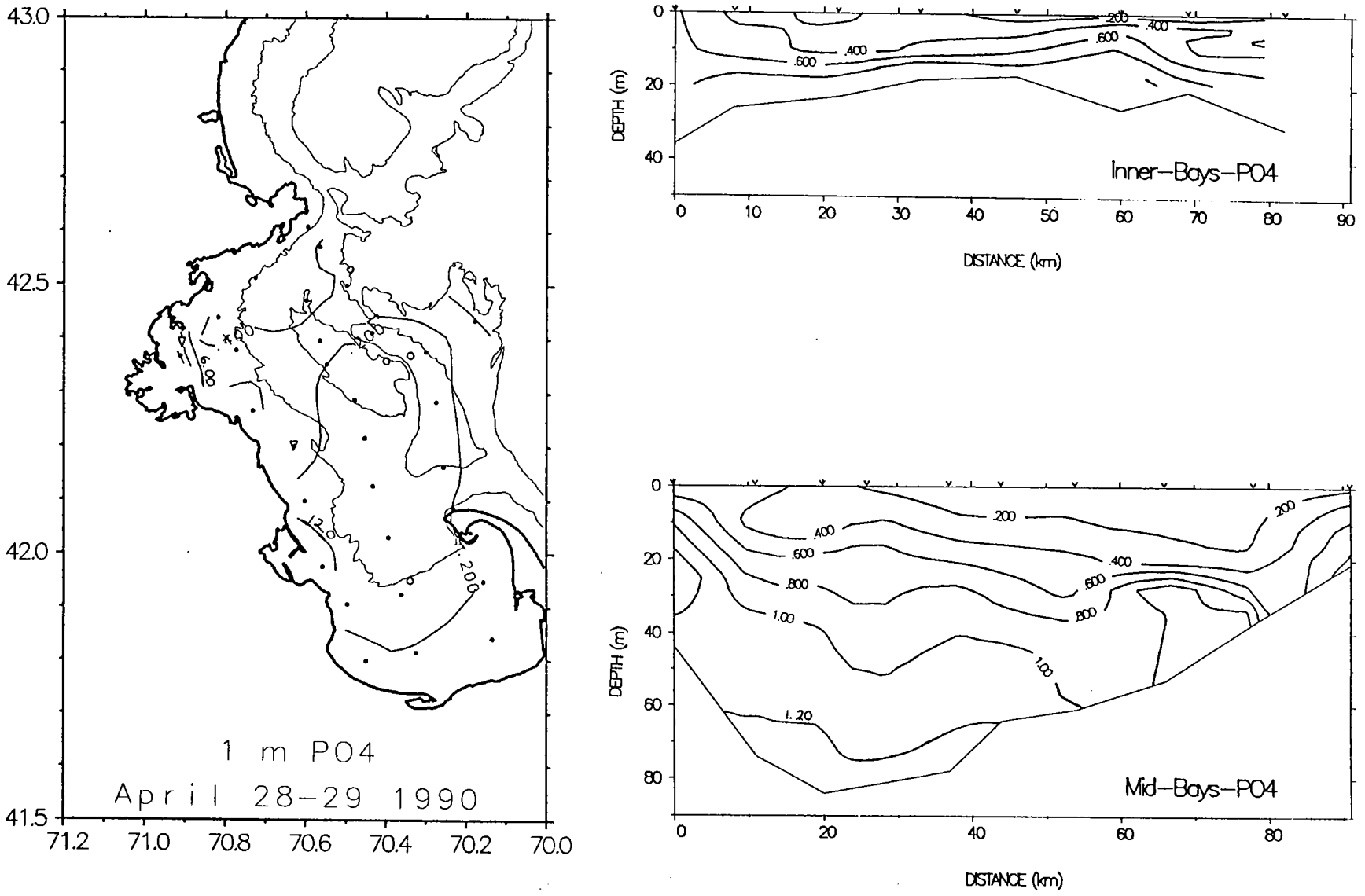

Figure 2.7-4 April 28–29, 1990 phosphate contour plots. The units are μM and the contour interval is 0.2 μM.

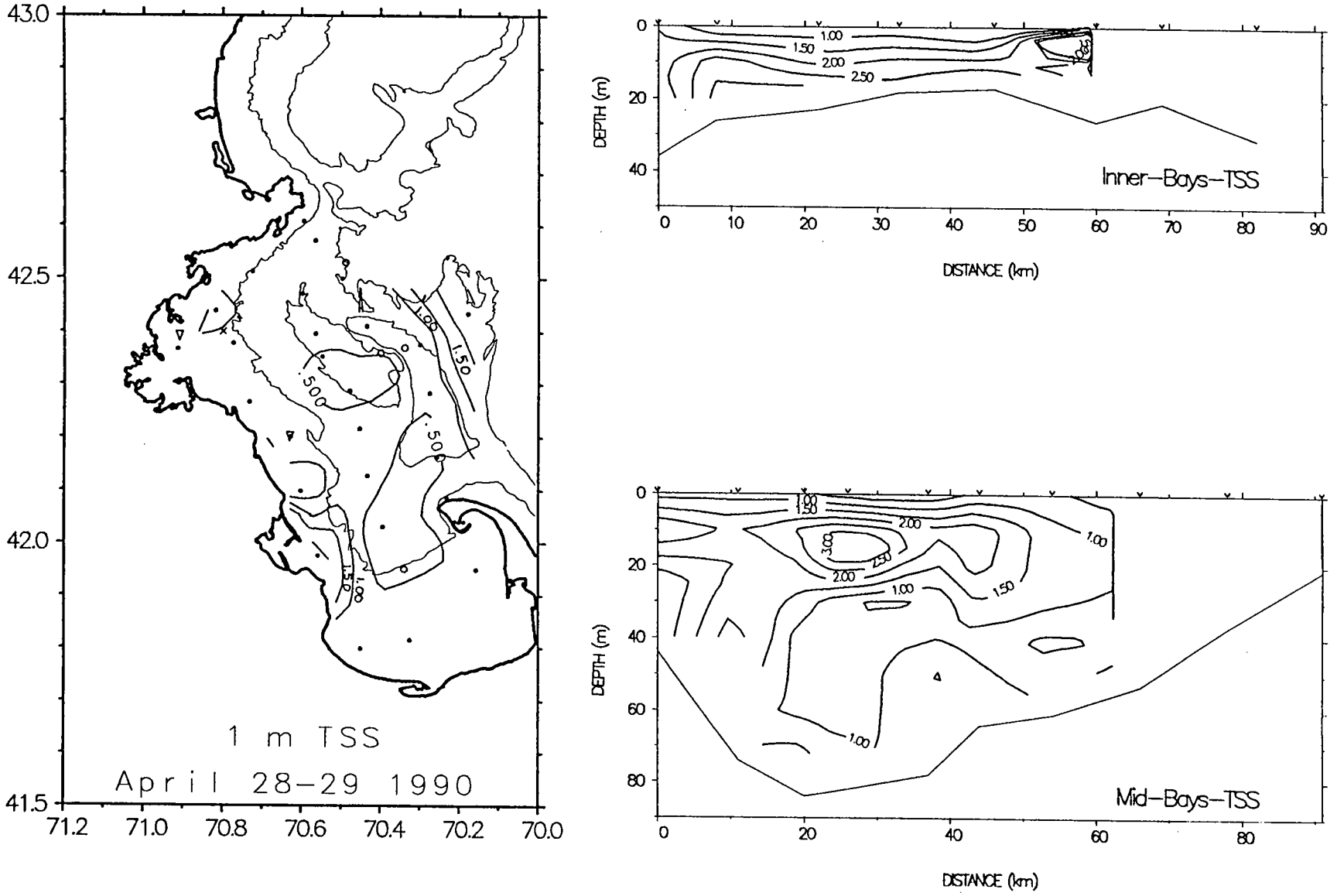

Figure 2.7-6 April 28–29, 1990 TSS contour plots. The units are mg/L and the contour interval is 0.5 mg/L. There was some missing data at depth in the southern section of the Bays.

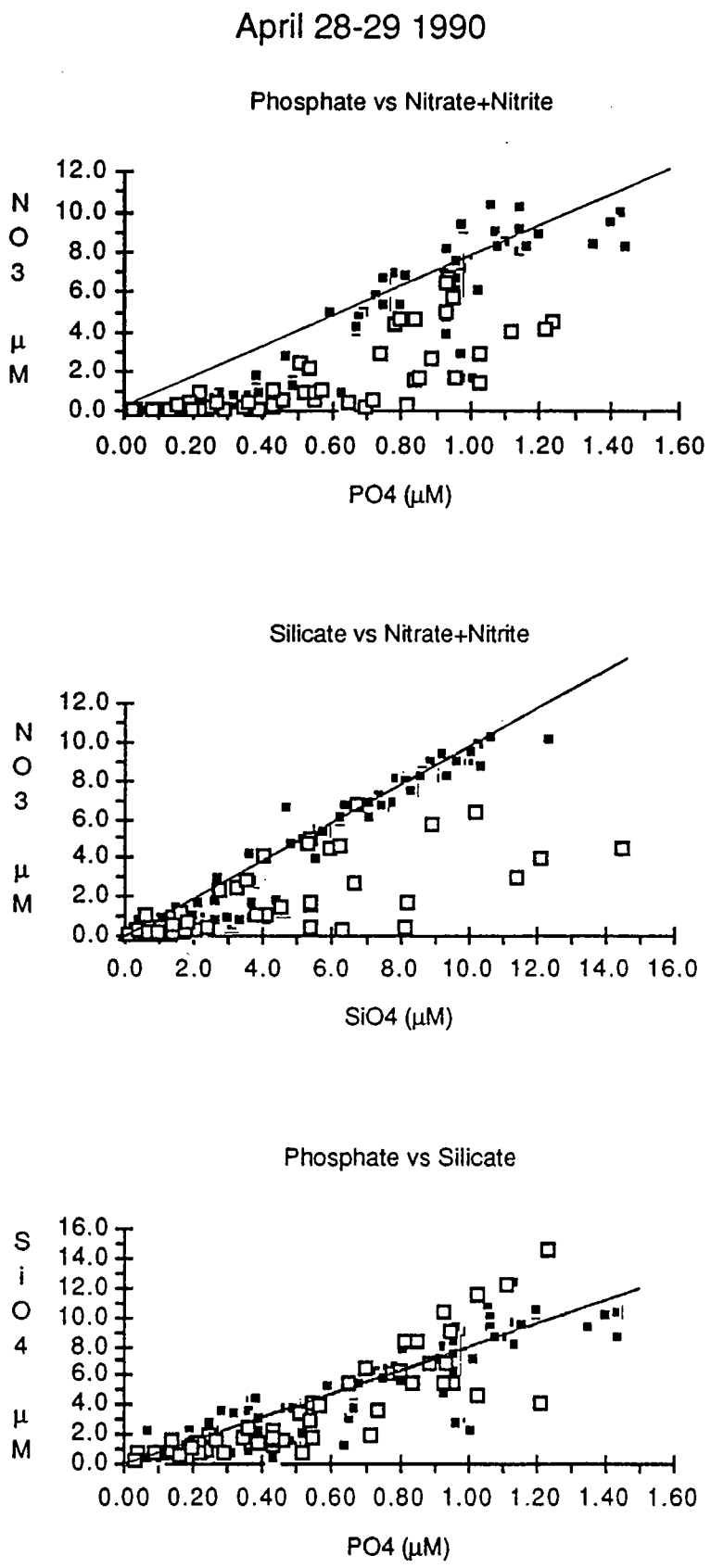

Figure 2.7-7 April 28–29, 1990 nutrient-nutrient plots. The lines are N:P:Si ratio of 8:1:8. The open squares represent the southern section of the Bays and the closed squares the northern section.

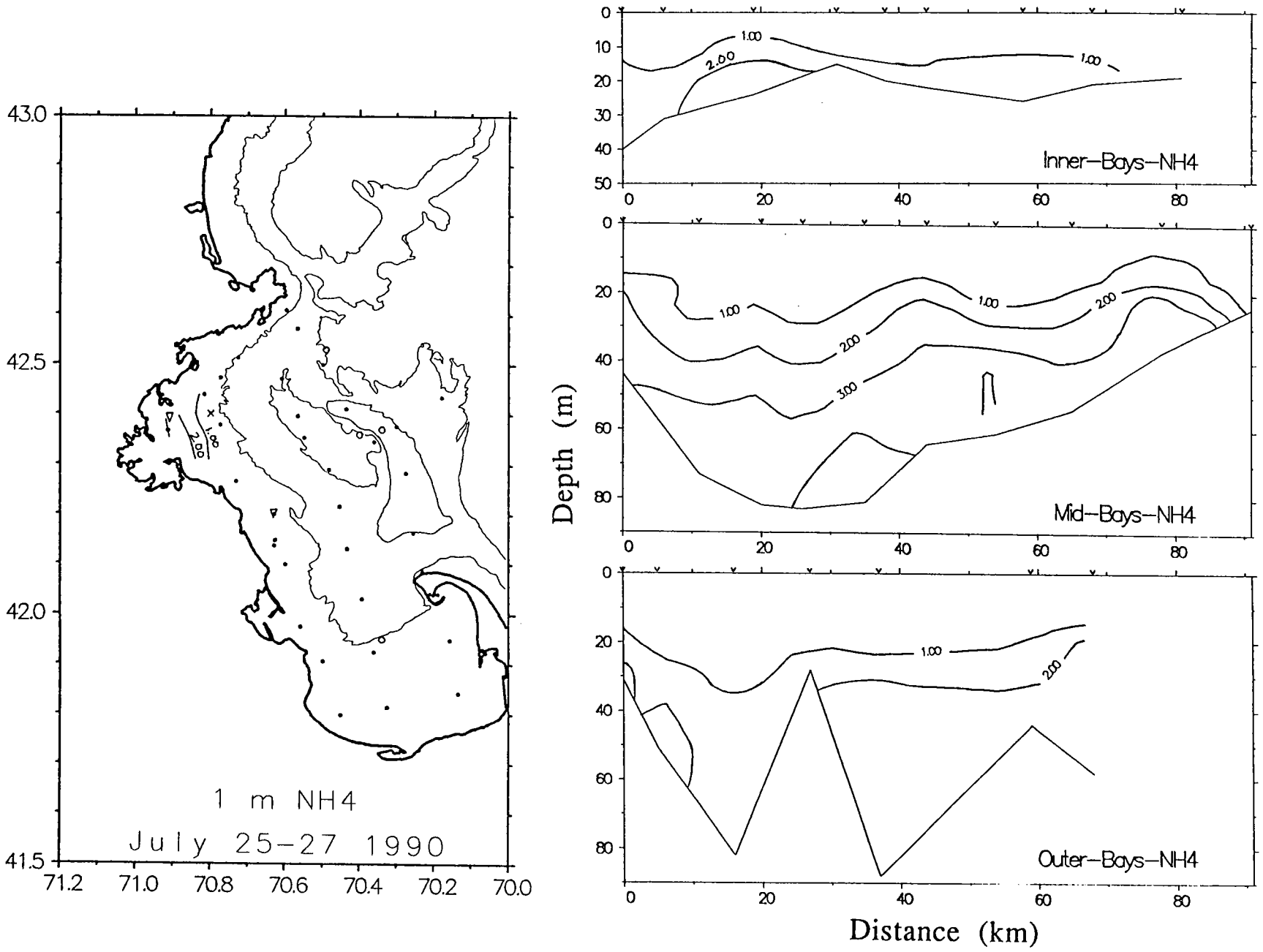

Figure 2.7-8 July 25–27, 1990 ammonium contour plots. The units are μM and the contour interval is 1 μM.

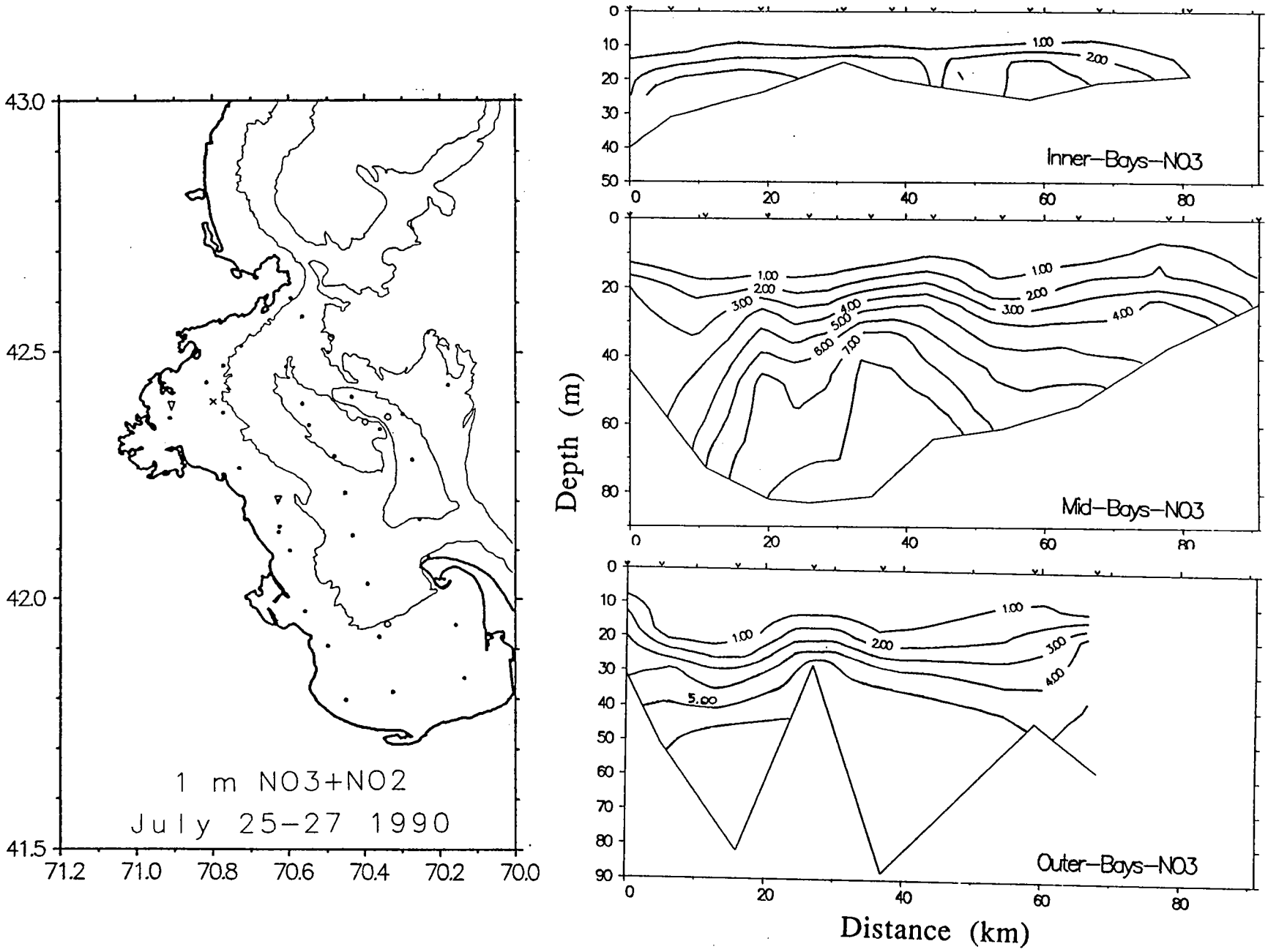

Figure 2.7-9 July 25–27, 1990 nitrate contour plots. The units are μM and the contour interval is 1 μM.

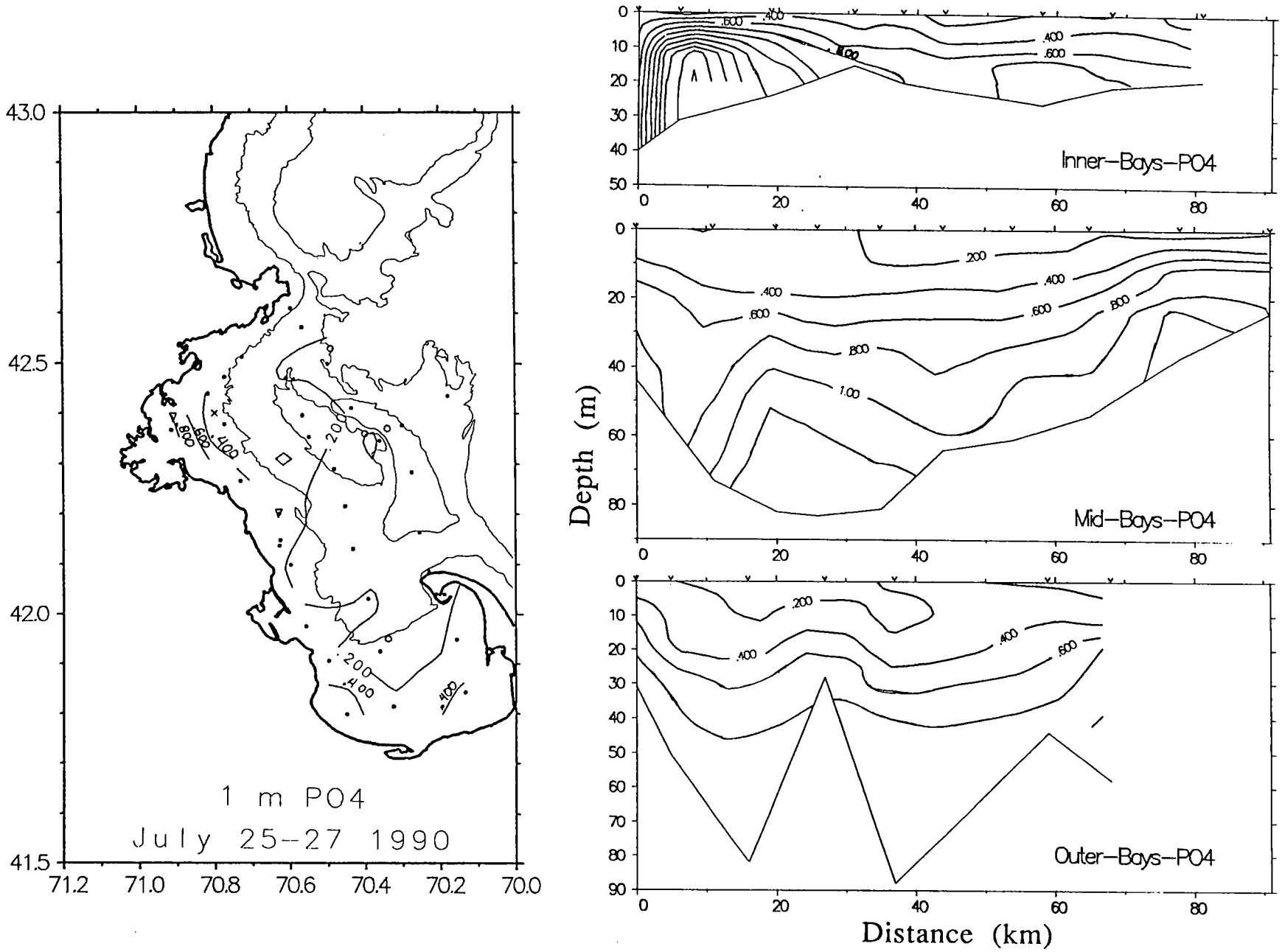

Figure 2.7-10 July 25–27, 1990 phosphate contour plots. The units are μM and the contour interval is 0.2 μM.

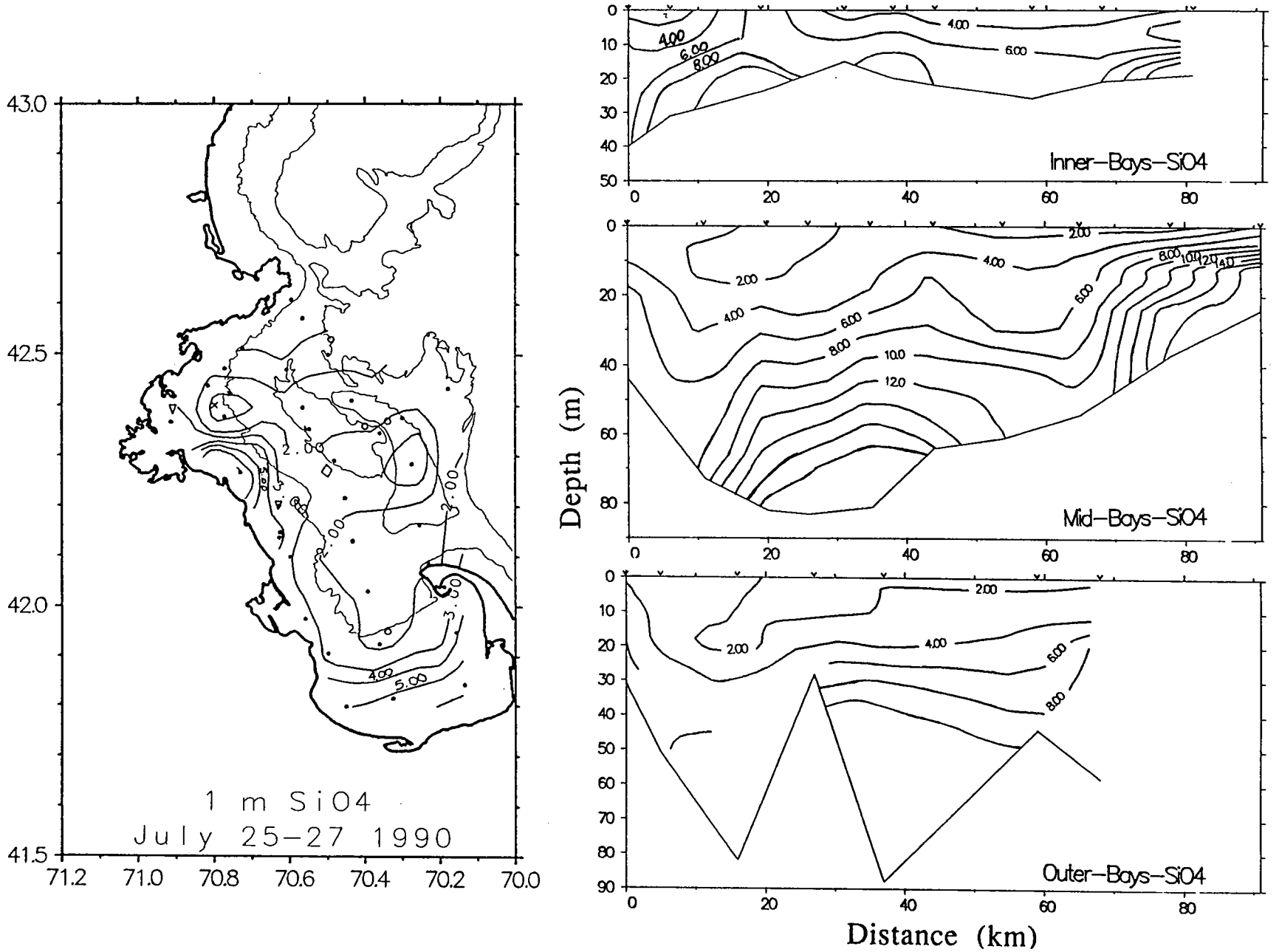

Figure 2.7-11 July 25–27, 1990 silicate contour plots. The units are μM and the contour interval is 2 μM for the vertical sections and 1 μM for the horizontal contour plot.

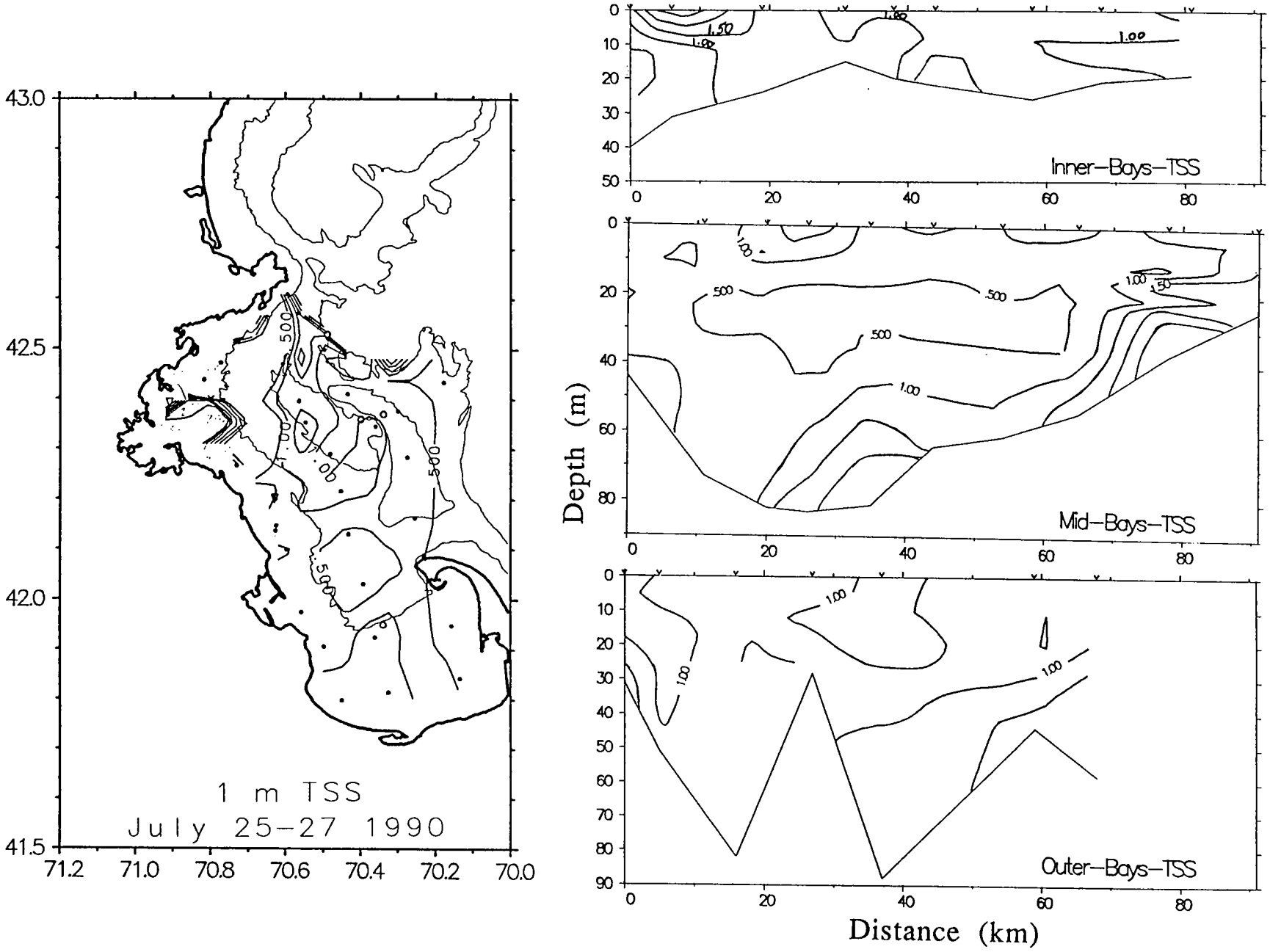

Figure 2.7-12 July 25–27, 1990 TSS contour plots. The units are mg/L and the contour interval is 0.5 mg/L.

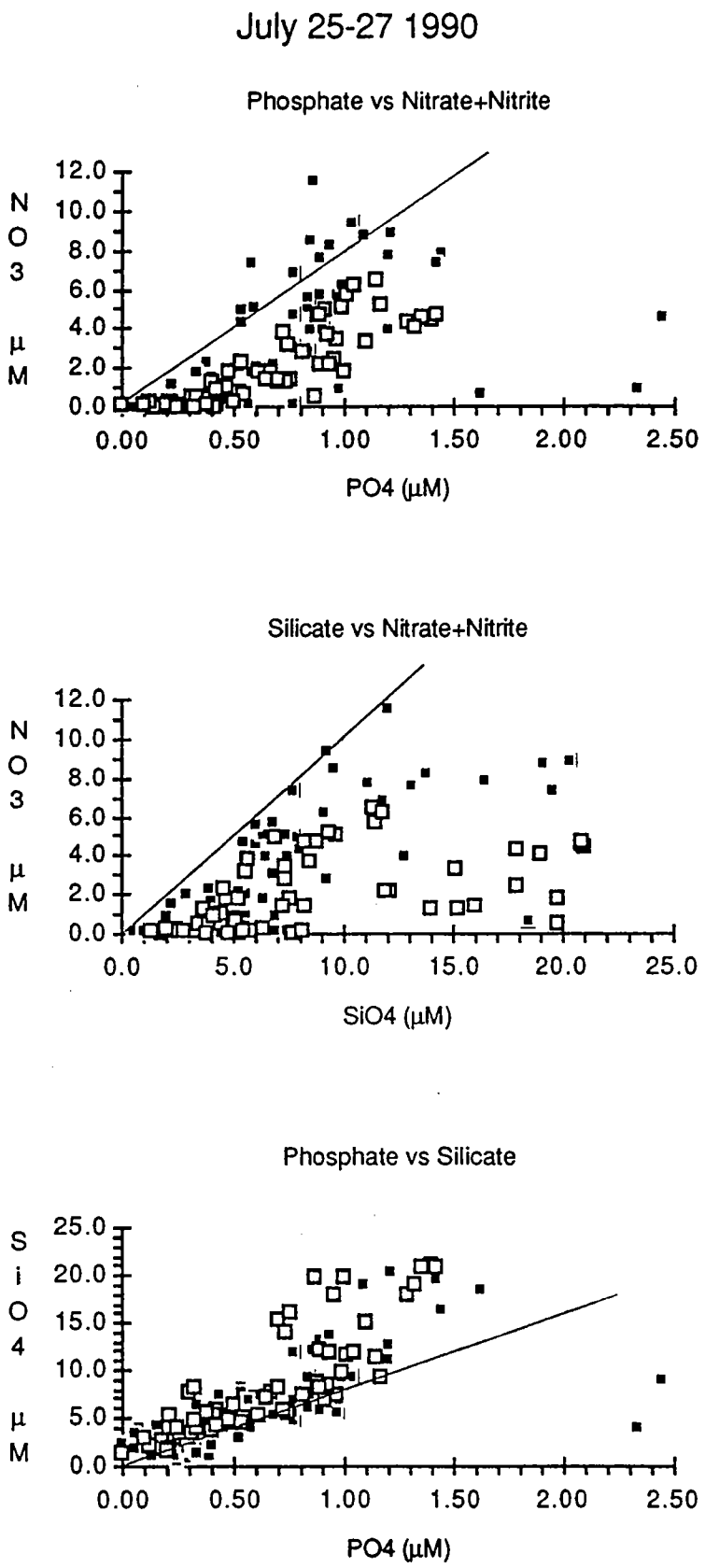

Figure 2.7-13 July 25–27, 1990 nutrient-nutrient plots. The lines are N:P:Si ratio of 8:1:8. The open squares represent the southern section of the Bays and the closed squares the northern section.

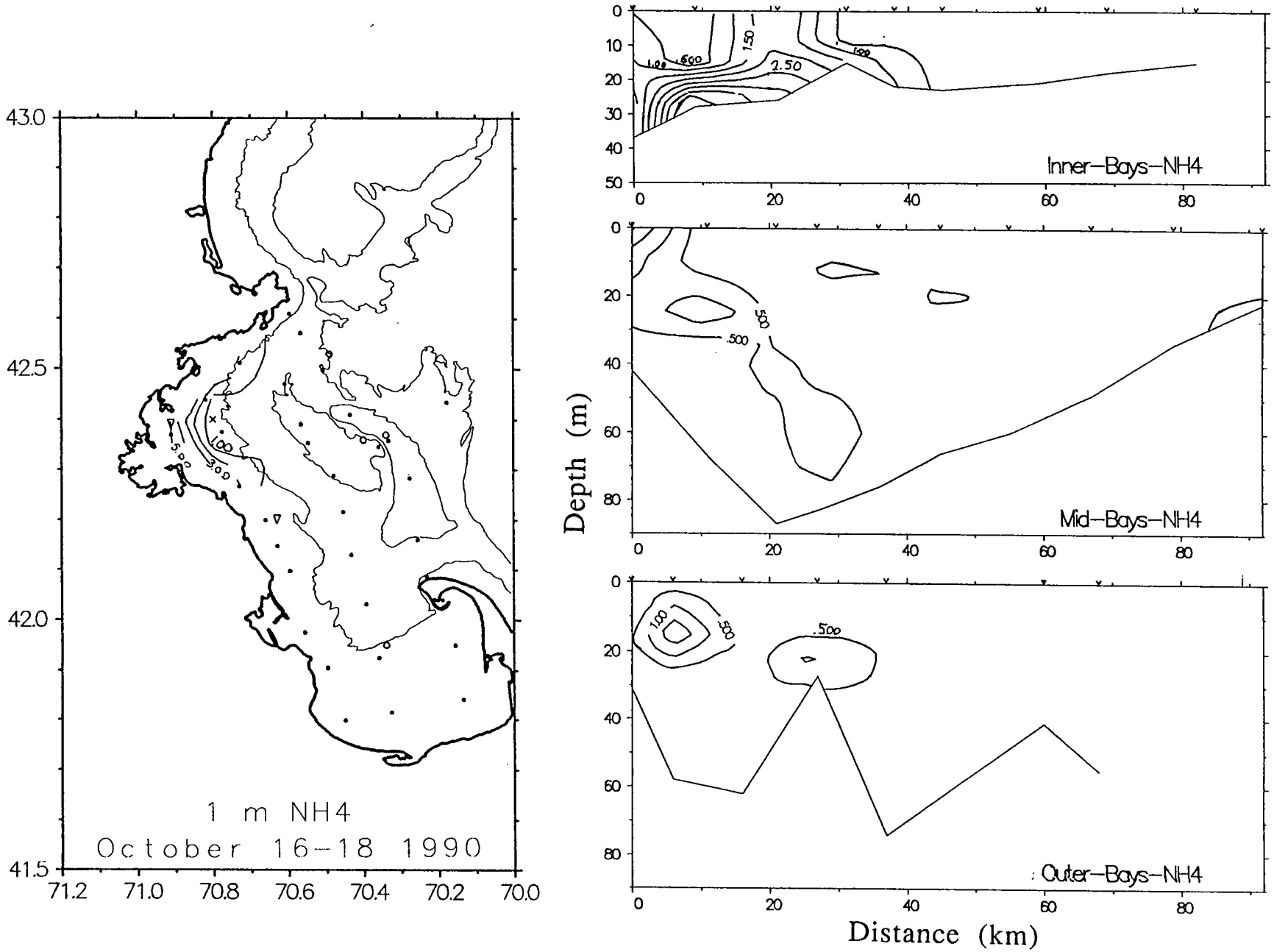

Figure 2.7-14 October 16–18, 1990 ammonium contour plots. The units are μM and the contour interval is 1 μM.

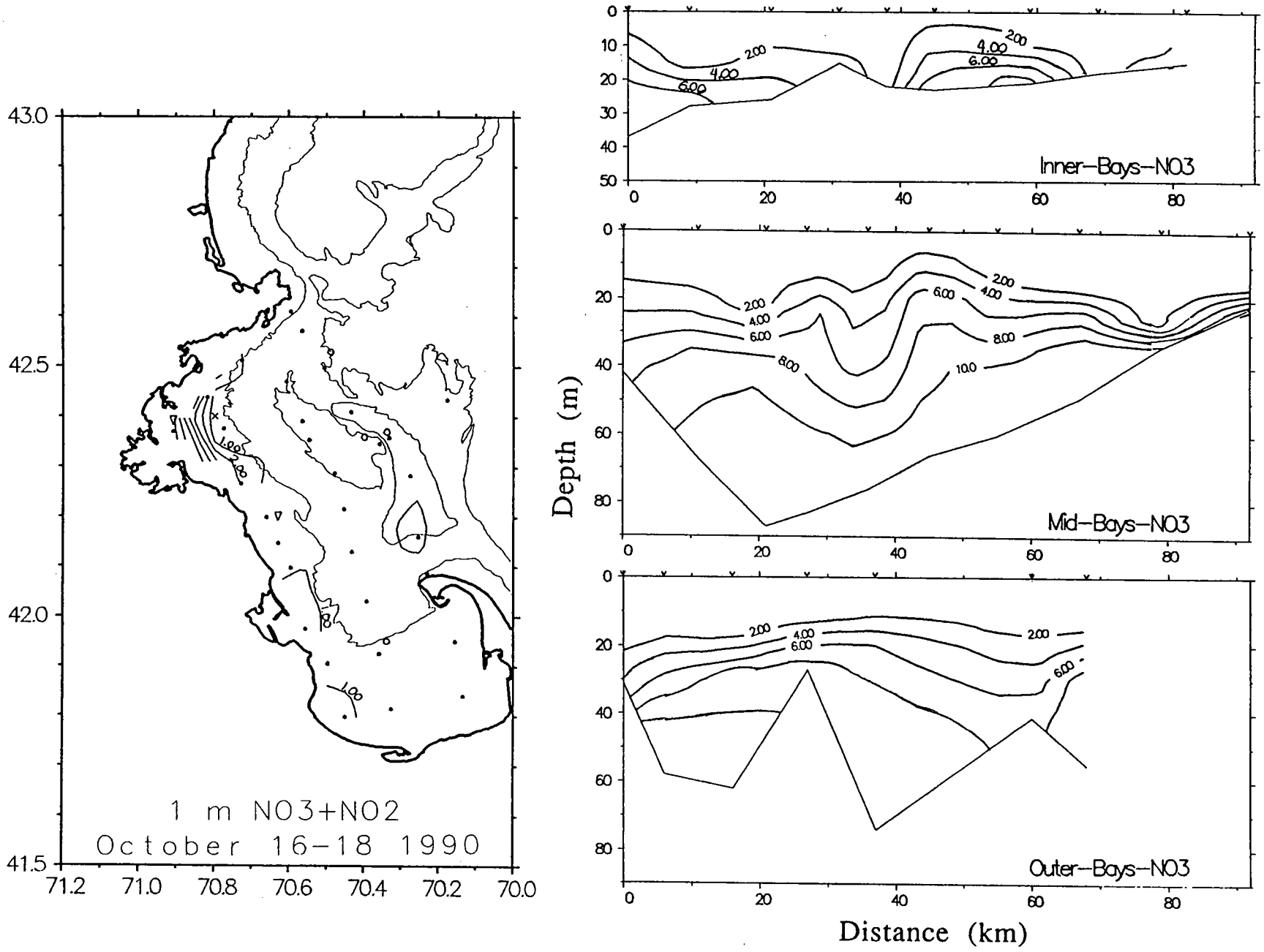

Figure 2.7-15 October 16–18, 1990 nitrate contour plots. The units are μM and the contour interval is 2 μM for the vertical sections and 1 μM for the horizontal contour plot.

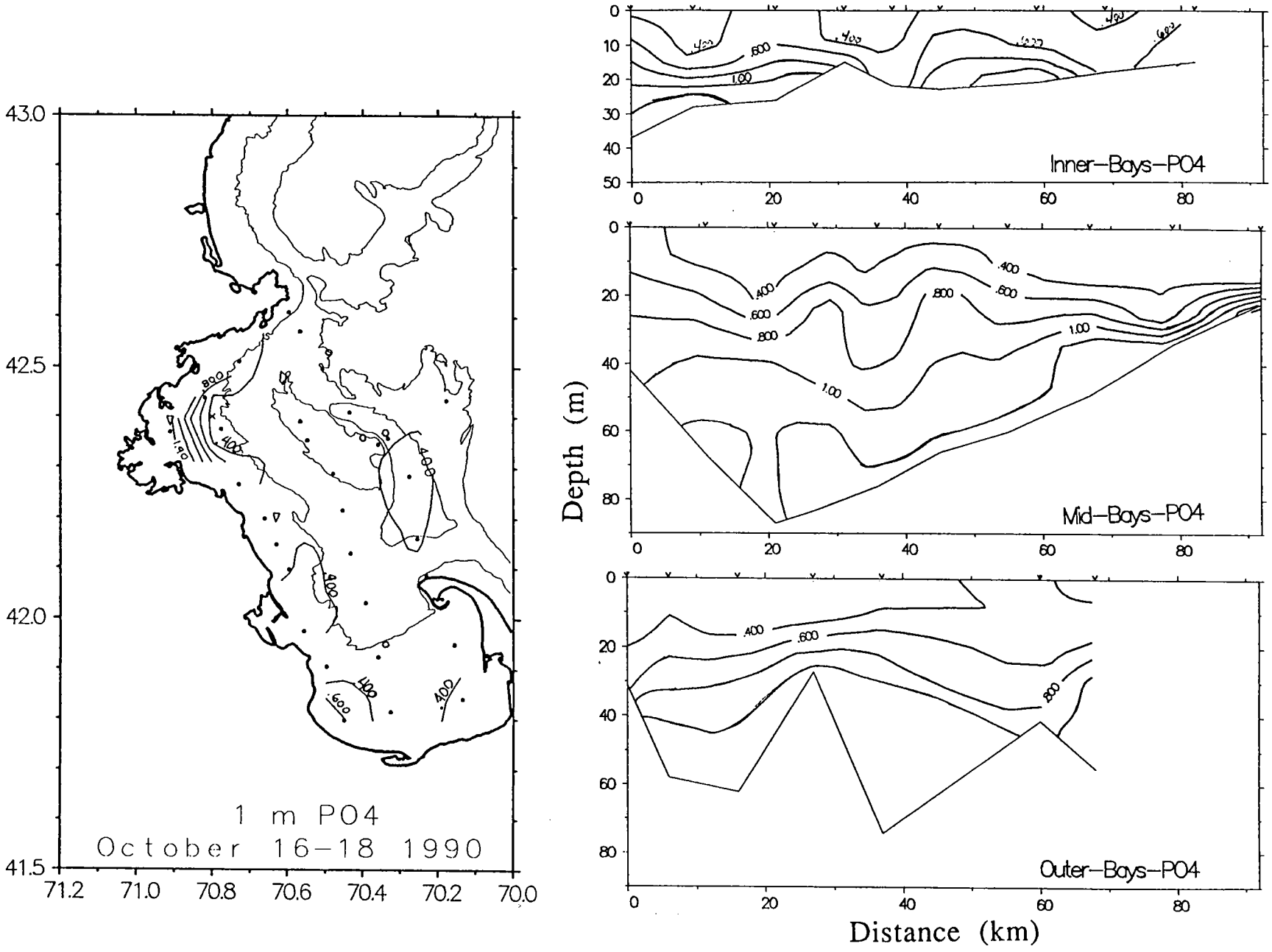

Figure 2.7-16 October 16–18, 1990 phosphate contour plots. The units are μM and the contour interval is 0.2 μM.

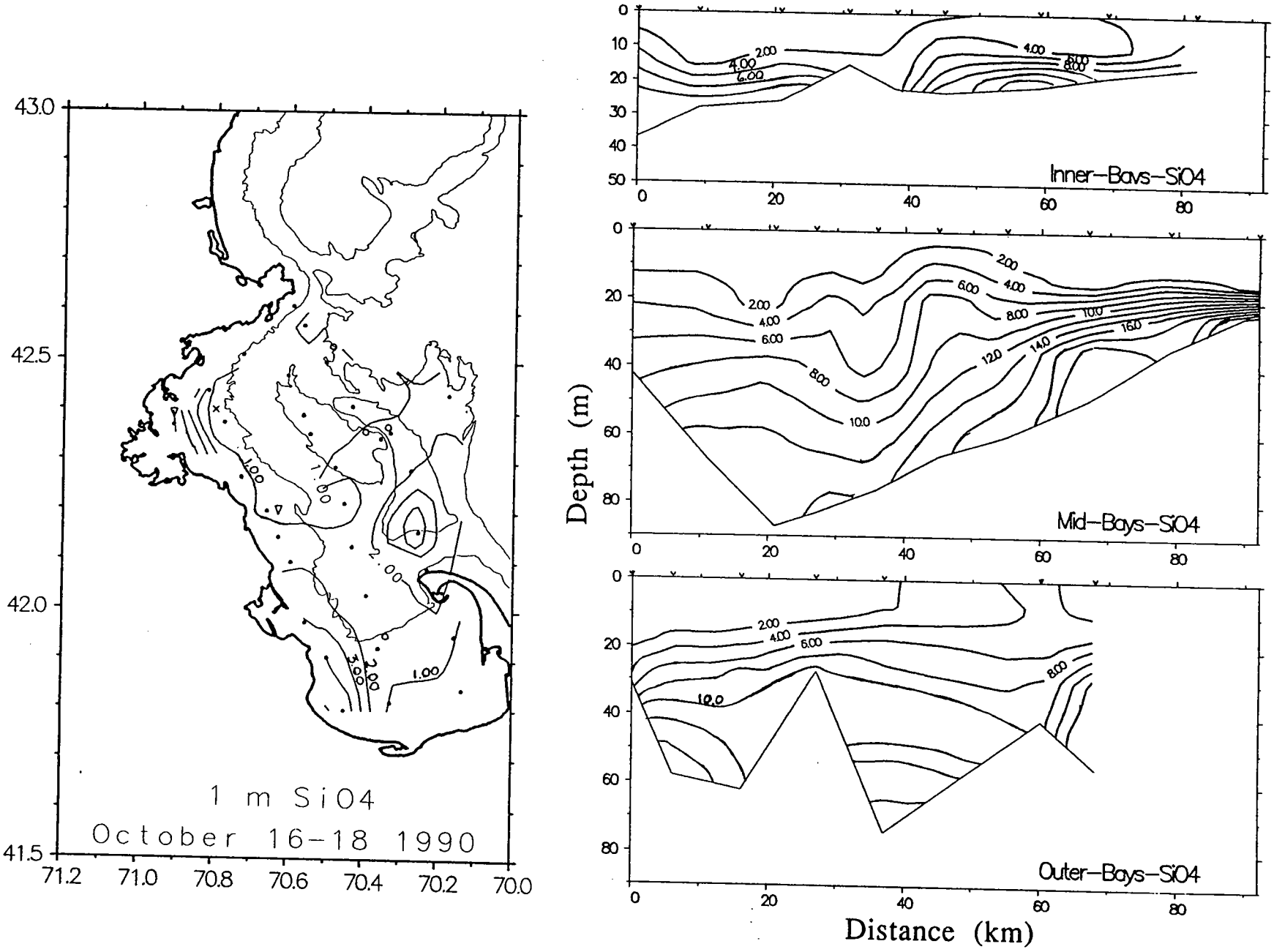

Figure 2.7-17 October 16–18, 1990 silicate contour plots. The units are μM and the contour interval is 2 μM for the vertical sections and 1 μM for the horizontal contour plot.

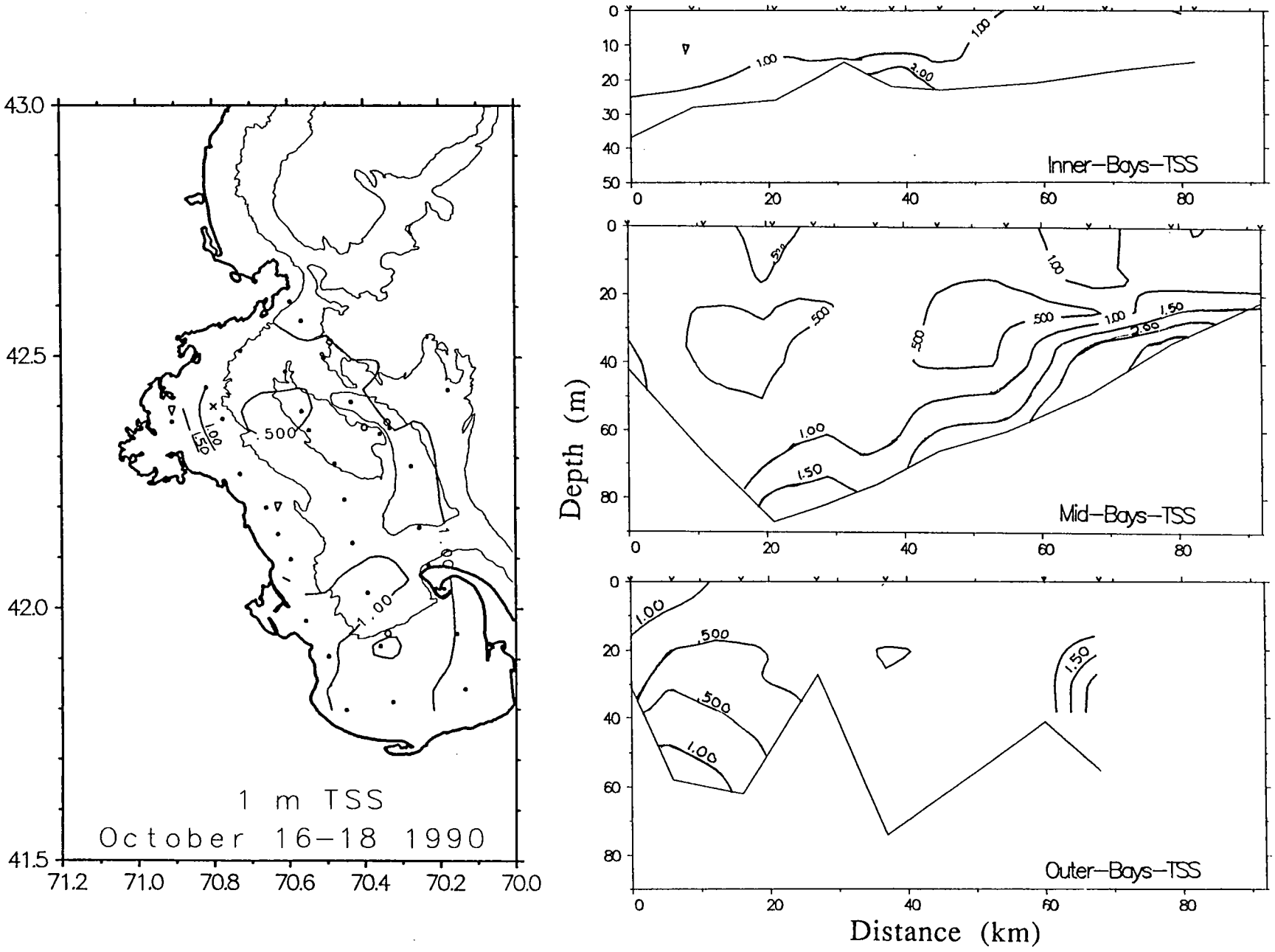

Figure 2.7-18 October 16–18, 1990 TSS contour plots. The units are mg/L and the contour interval is 0.5 mg/L.

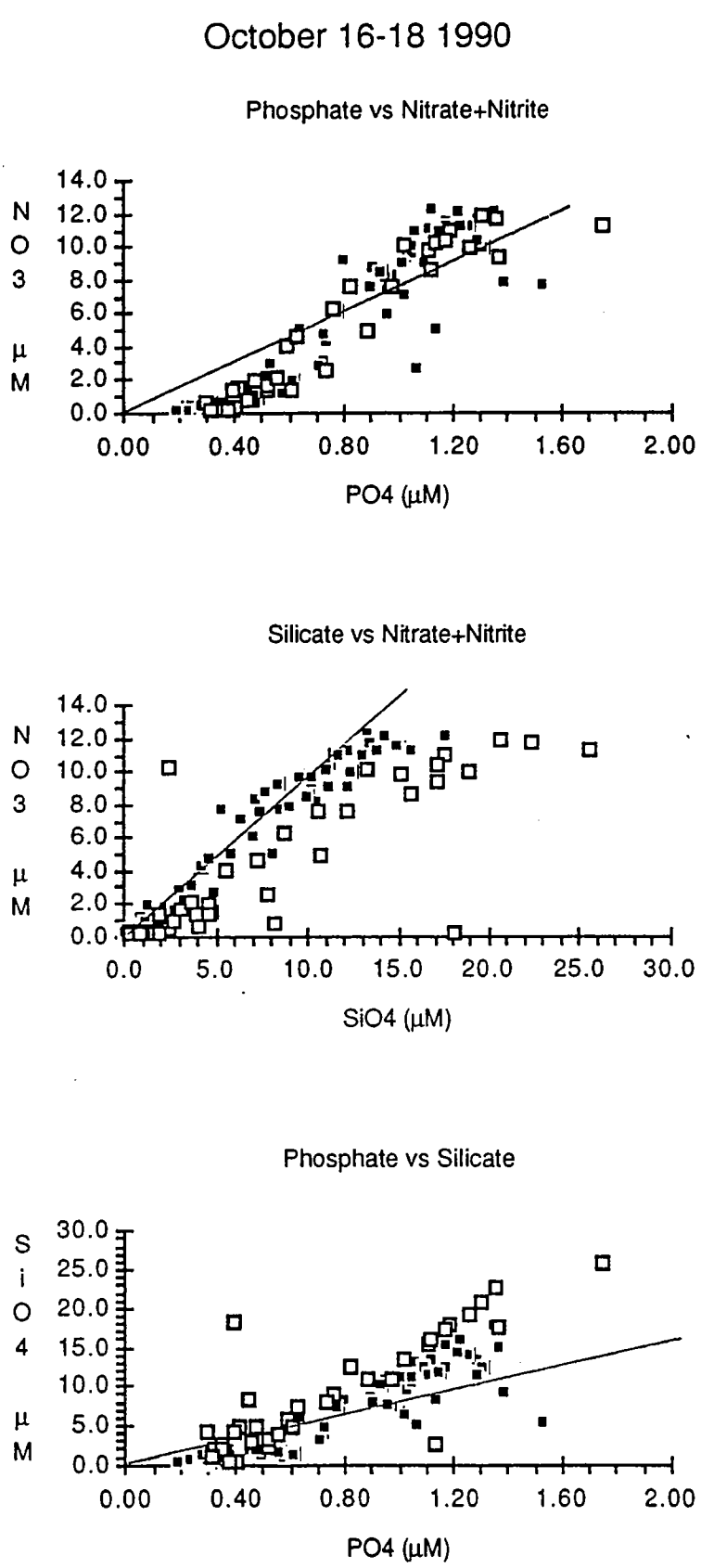

Figure 2.7-19 October 16–18, 1990 nutrient-nutrient plots. The lines are N:P:Si ratio of 8:1:8. The open squares represent the southern section of the Bays and the closed squares the northern section.

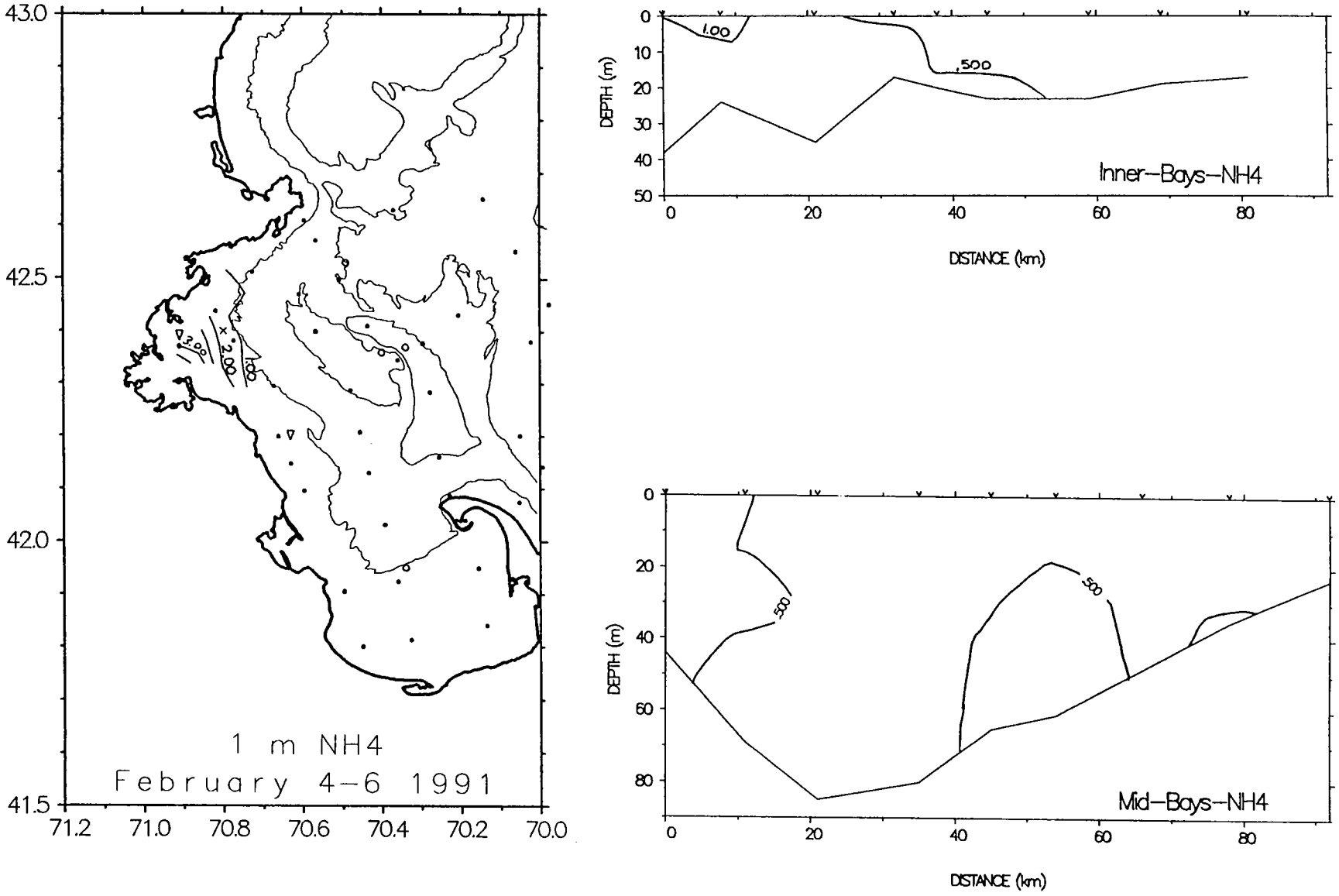

Figure 2.7-20 February 4–6, 1991 ammonium surface, Inner, and Mid-Bays contour plots. The units are μM and the contour interval is 0.5 μM for the vertical sections and 1 μM for the horizontal contour plot.

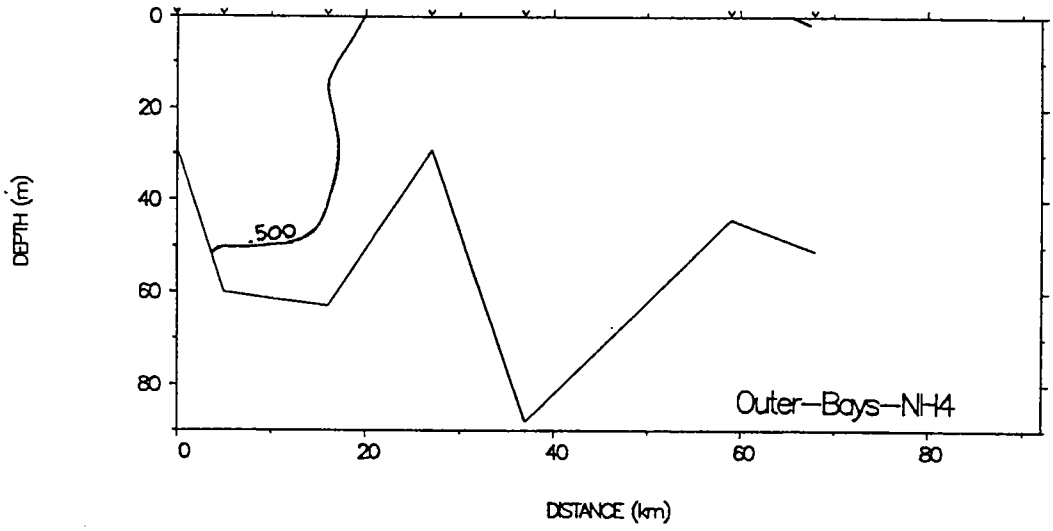

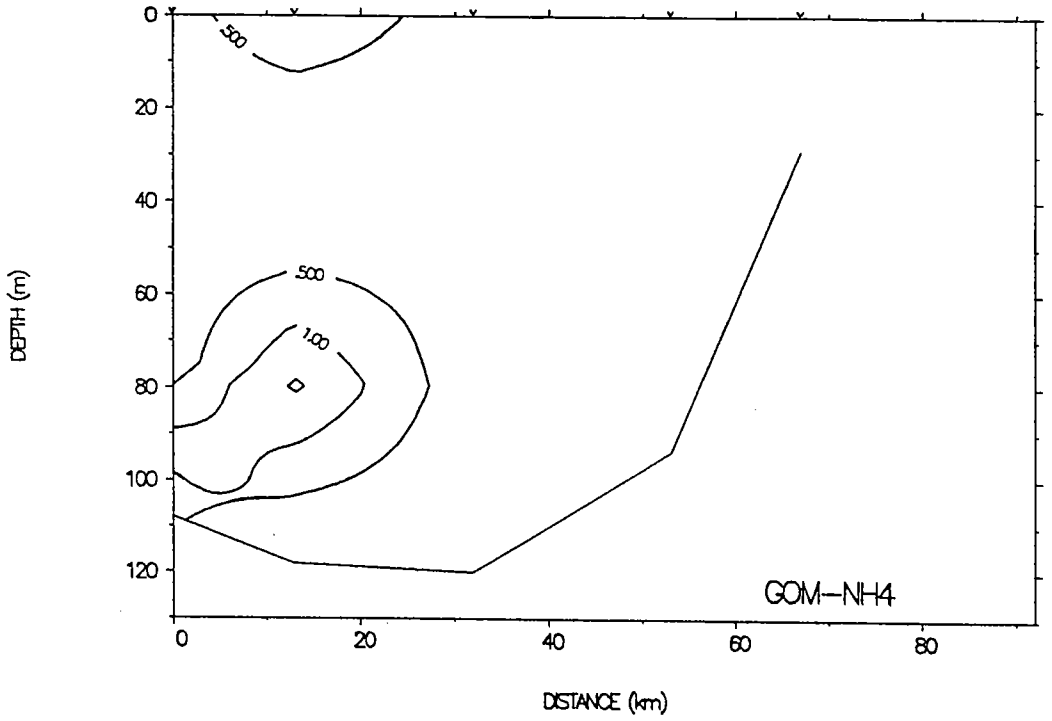

Figure 2.7-21 February 4–6, 1991 ammonium Outer-Bays and GOM vertical contour sections. The units are μM and the contour interval is 0.5 μM.

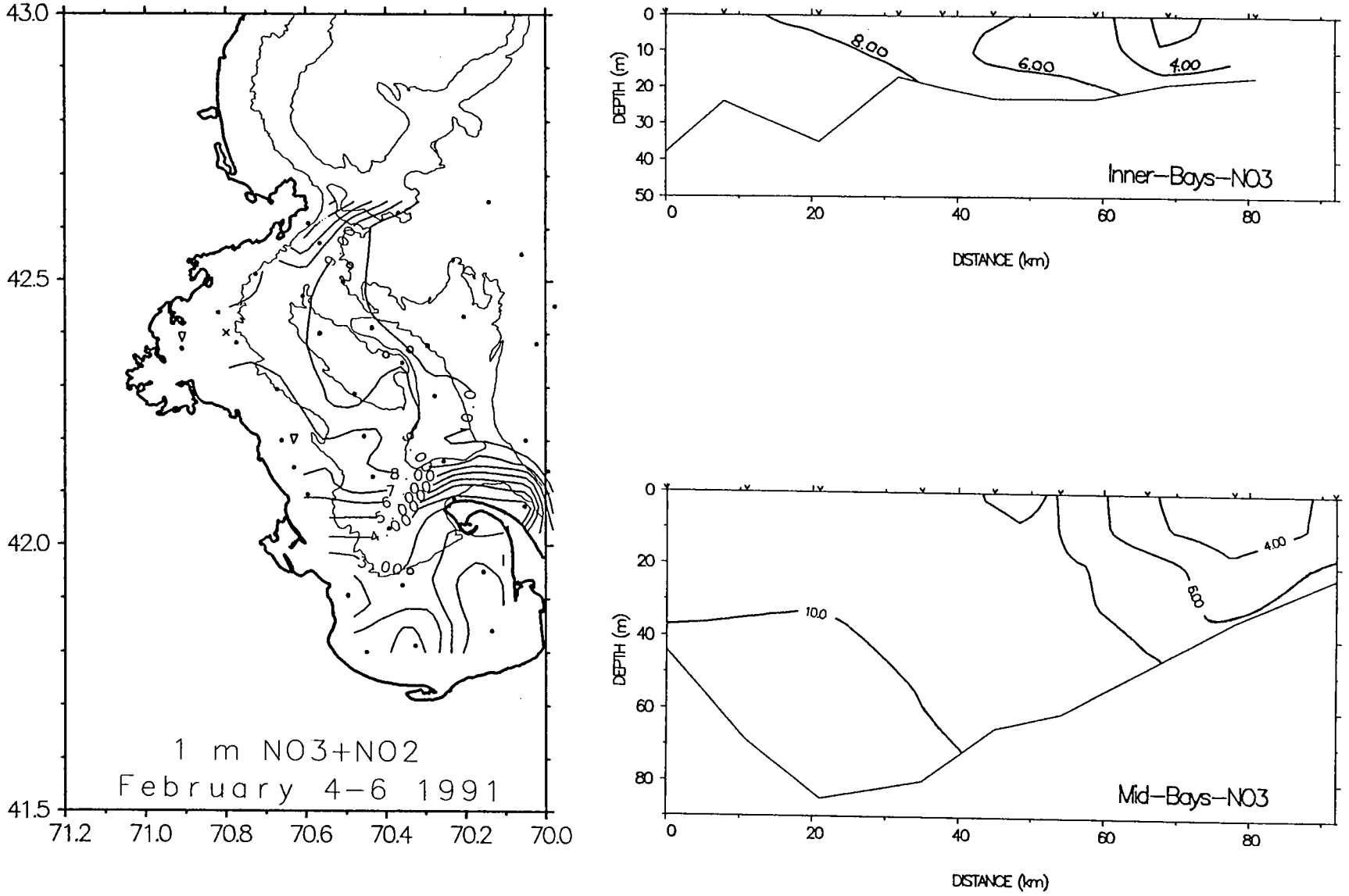

Figure 2.7-22 February 4–6, 1991 nitrate surface, Inner, and Mid-Bays contour plots. The units are μM and the contour interval is 2 μM for the vertical sections and 1 μM for the horizontal contour plot.

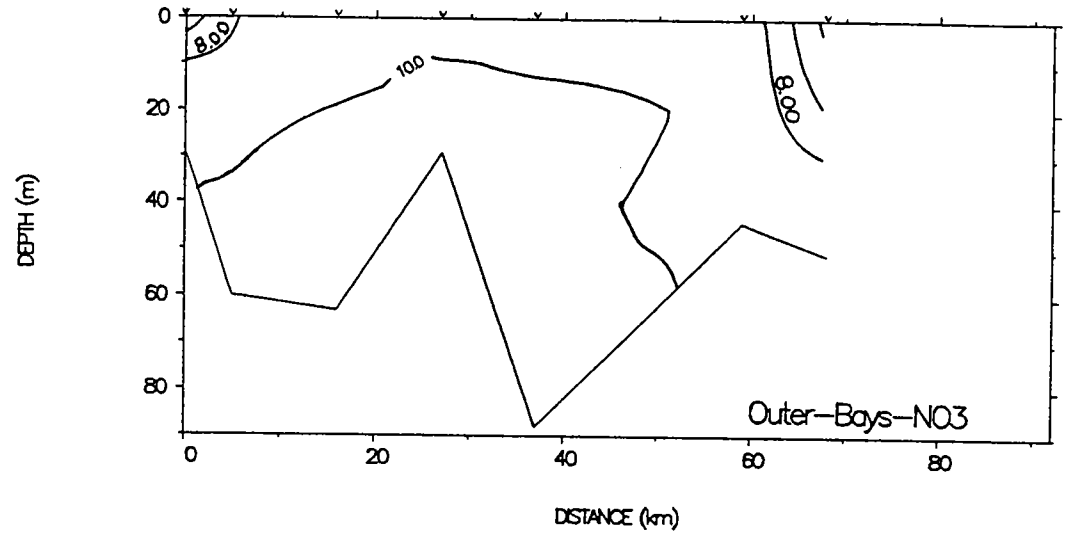

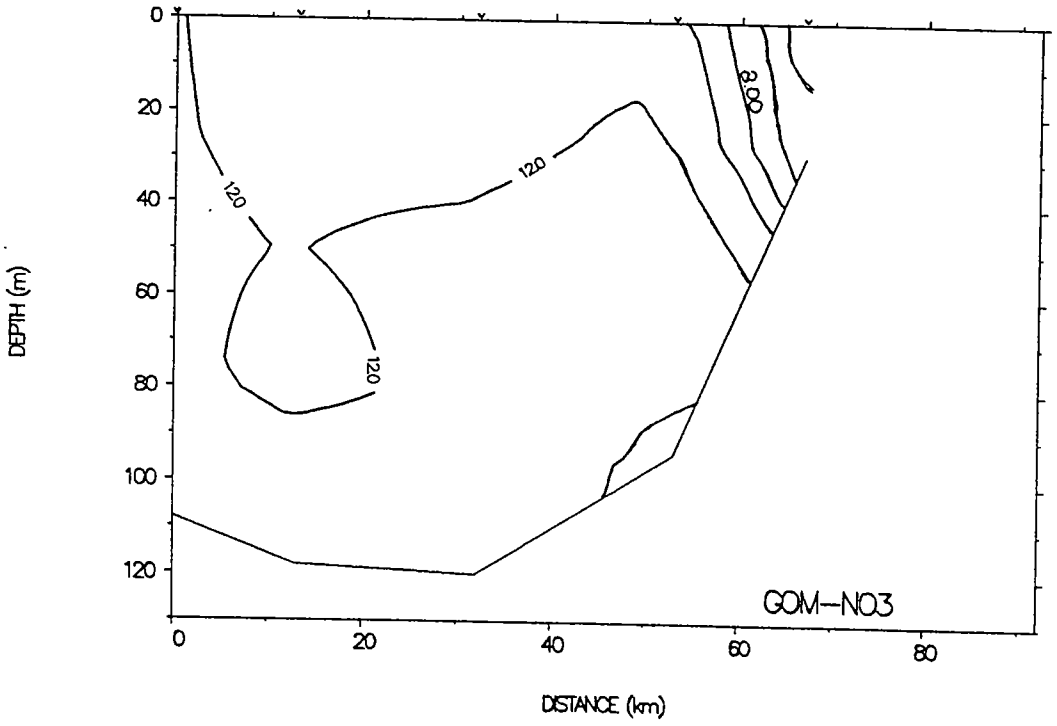

Figure 2.7-23 February 4–6, 1991 nitrate Outer-Bays and GOM vertical contour sections. The units are μM and the contour interval is 2 μM.

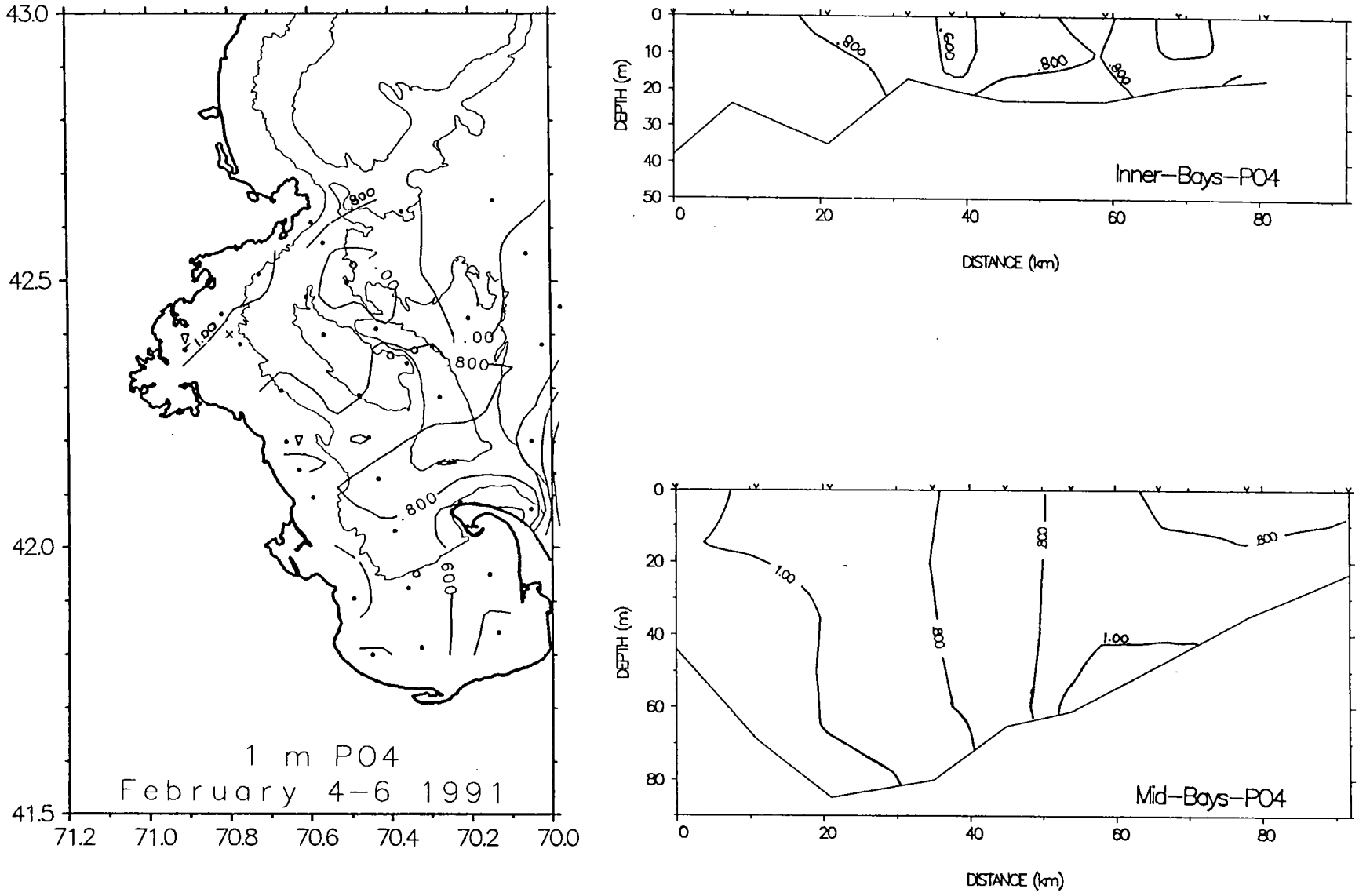

Figure 2.7-24 February 4–6, 1991 phosphate surface, Inner, and Mid-Bays contour plots. The units are μM and the contour interval is 0.2 μM.

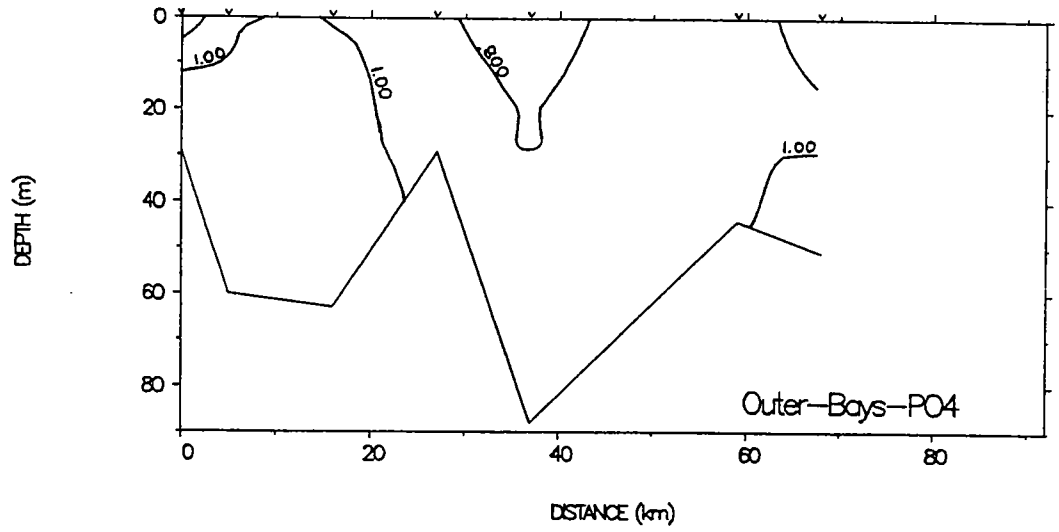

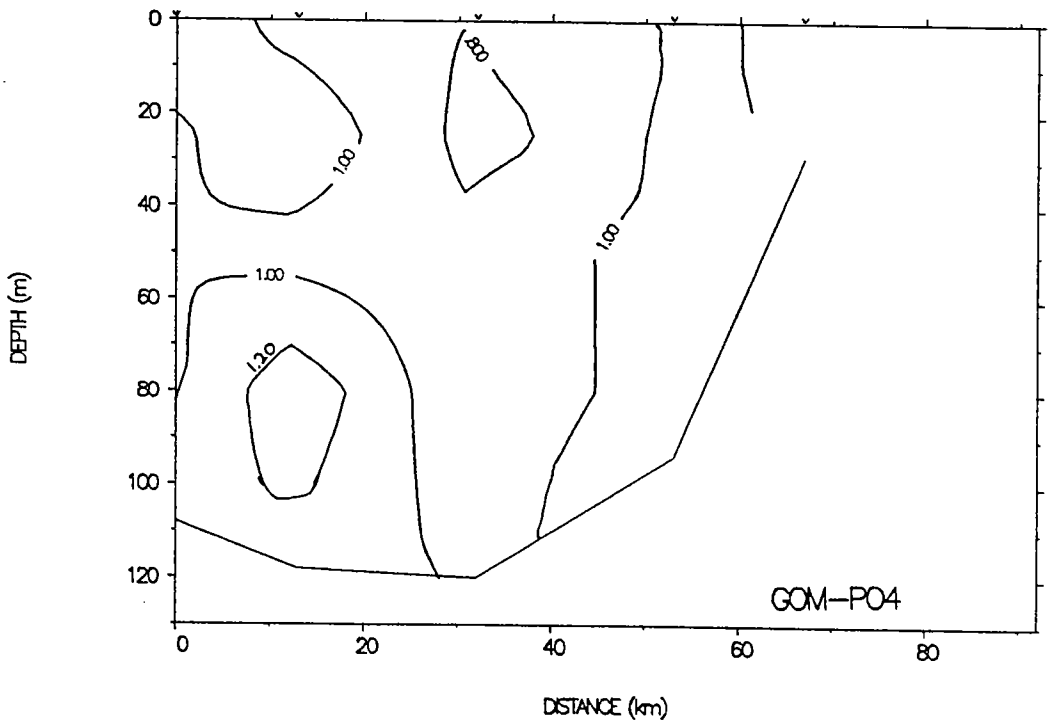

Figure 2.7-25 February 4–6, 1991 phosphate Outer-Bays and GOM vertical contour sections. The units are μM and the contour interval is 0.2 μM.

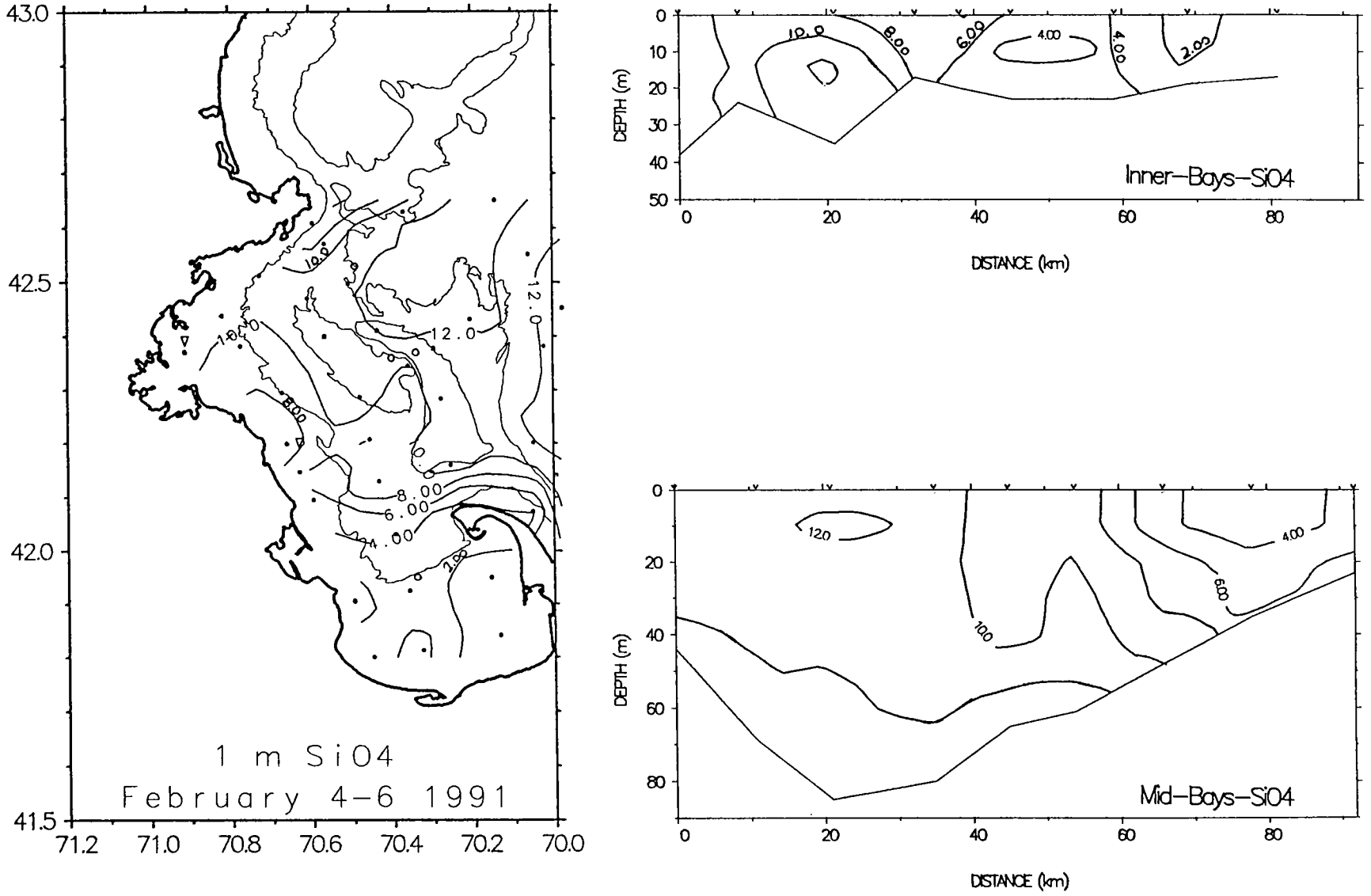

Figure 2.7-26 February 4–6, 1991 silicate surface, Inner, and Mid-Bays contour plots. The units are μM and the contour interval is 2 μM.

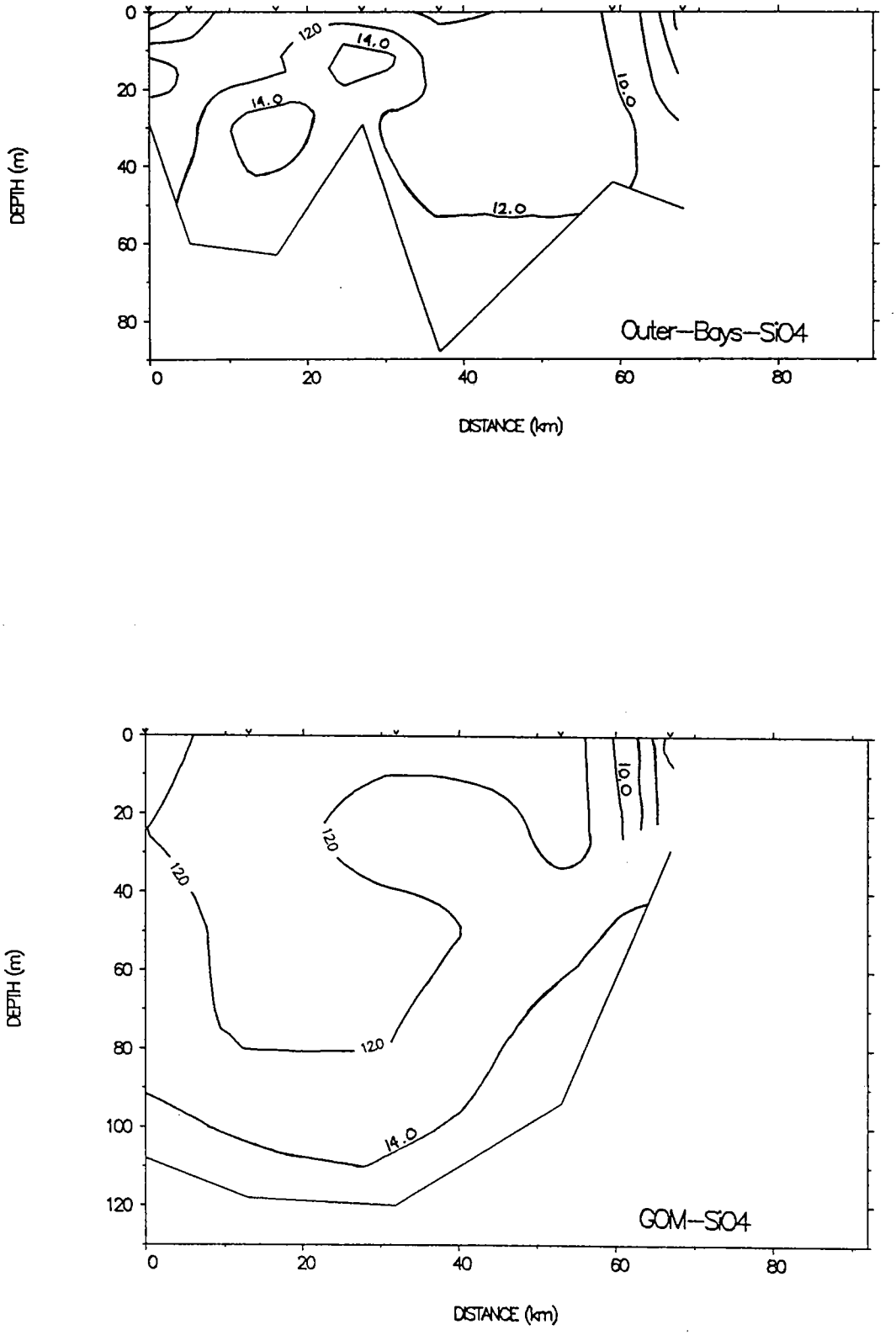

Figure 2.7-27 February 4–6, 1991 silicate Outer-Bays and GOM vertical contour sections. The units are μM and the contour interval is 2 μM.

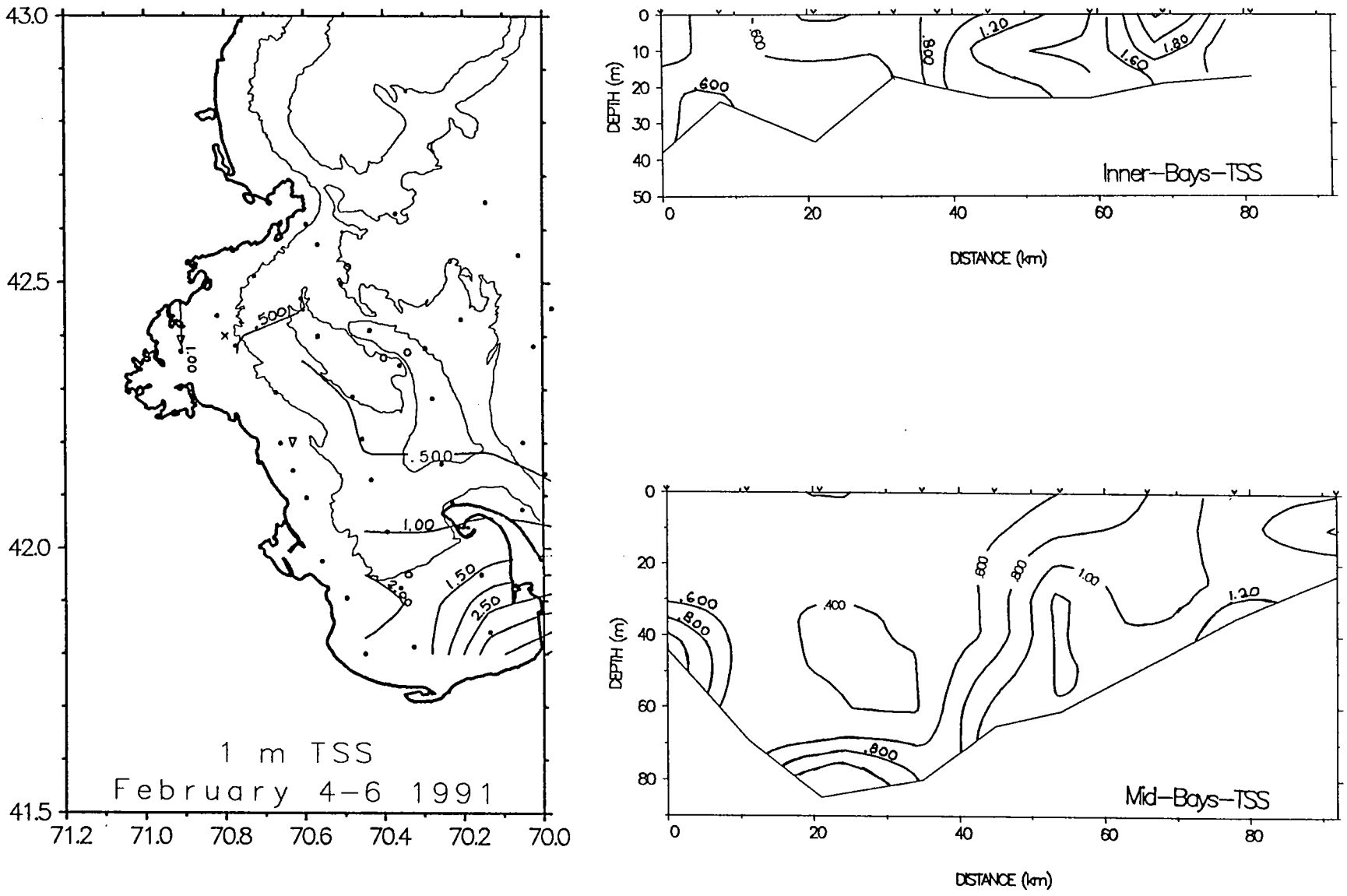

Figure 2.7-28 February 4–6, 1991 TSS surface, Inner, and Mid-Bays contour plots. The units are mg/L and the contour interval is 0.2 mg/L for the vertical sections and 0.5 mg/L for the horizontal contour plot.

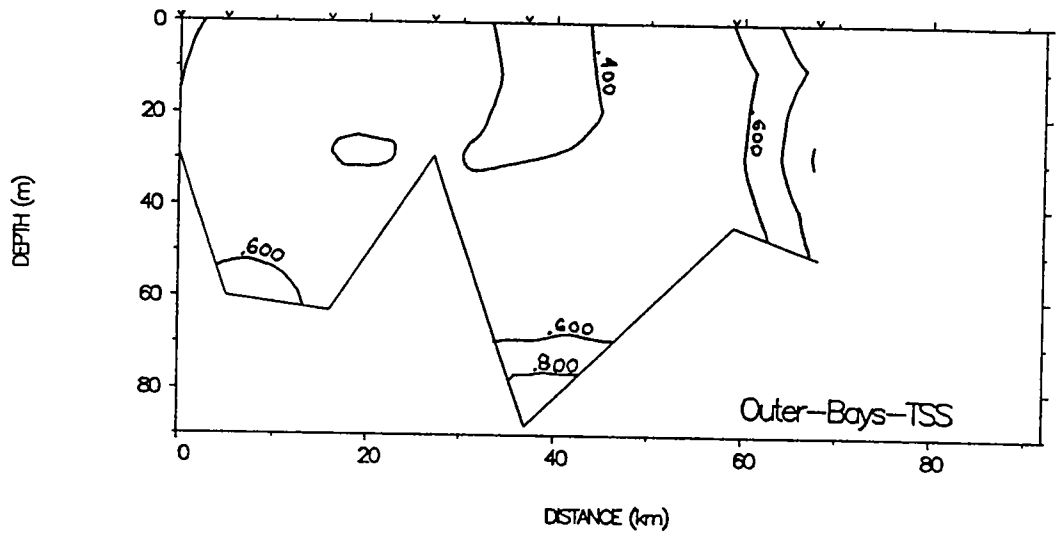

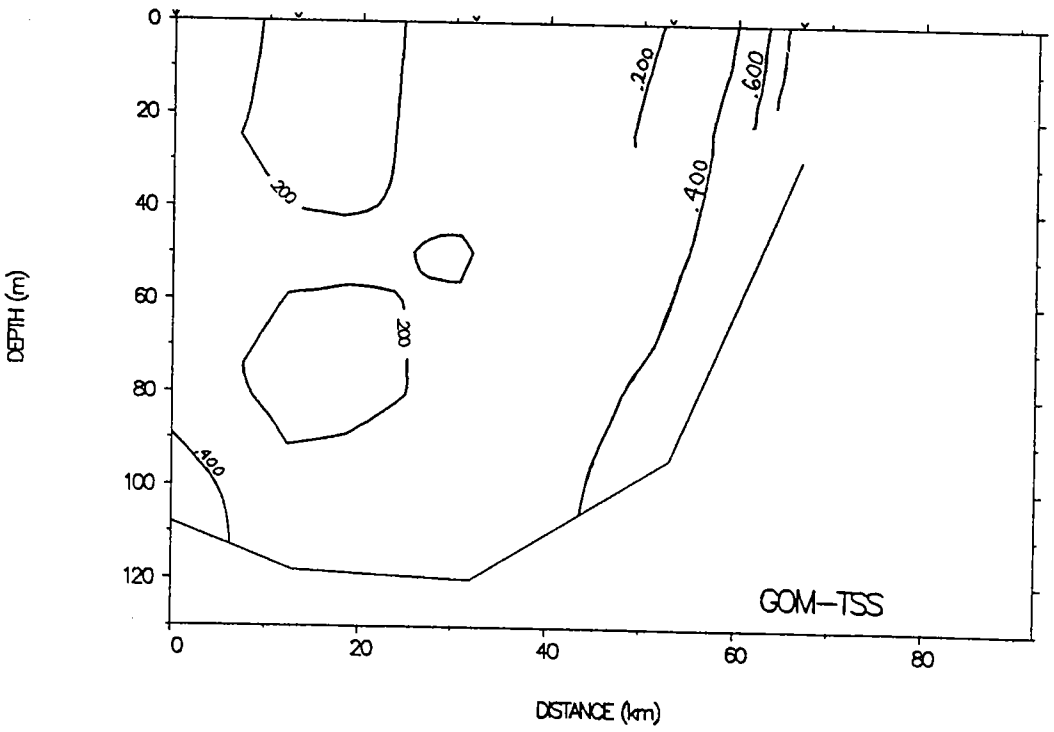

Figure 2.7-29 February 4–6, 1991 TSS Outer-Bays and GOM vertical contour sections. The units are mg/L and the contour interval is 0.2 mg/L.

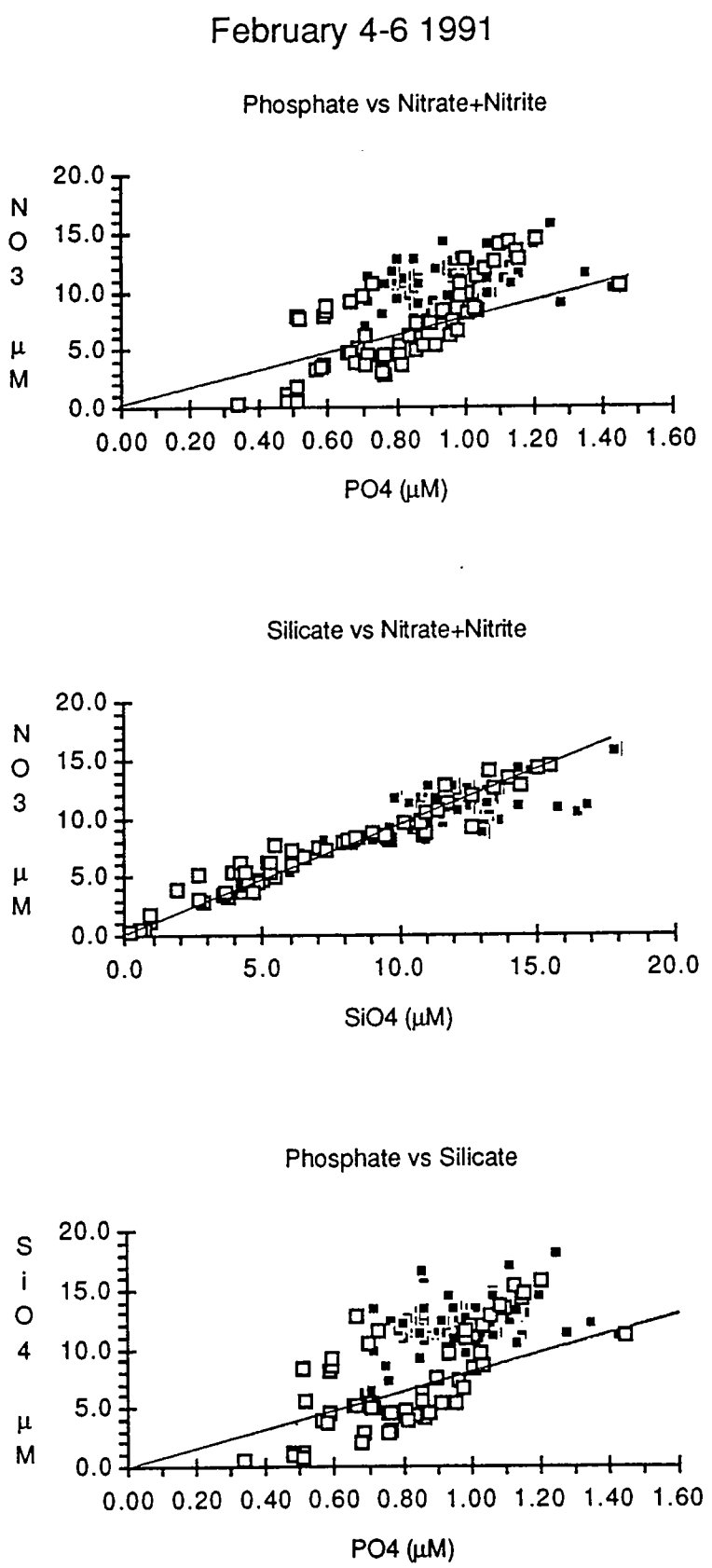

Figure 2.7-30 February 4–6, 1991 nutrient-nutrient plots. The lines are N:P:Si ratio of 8:1:8. The open squares represent the southern section of the Bays and the closed squares the northern section.

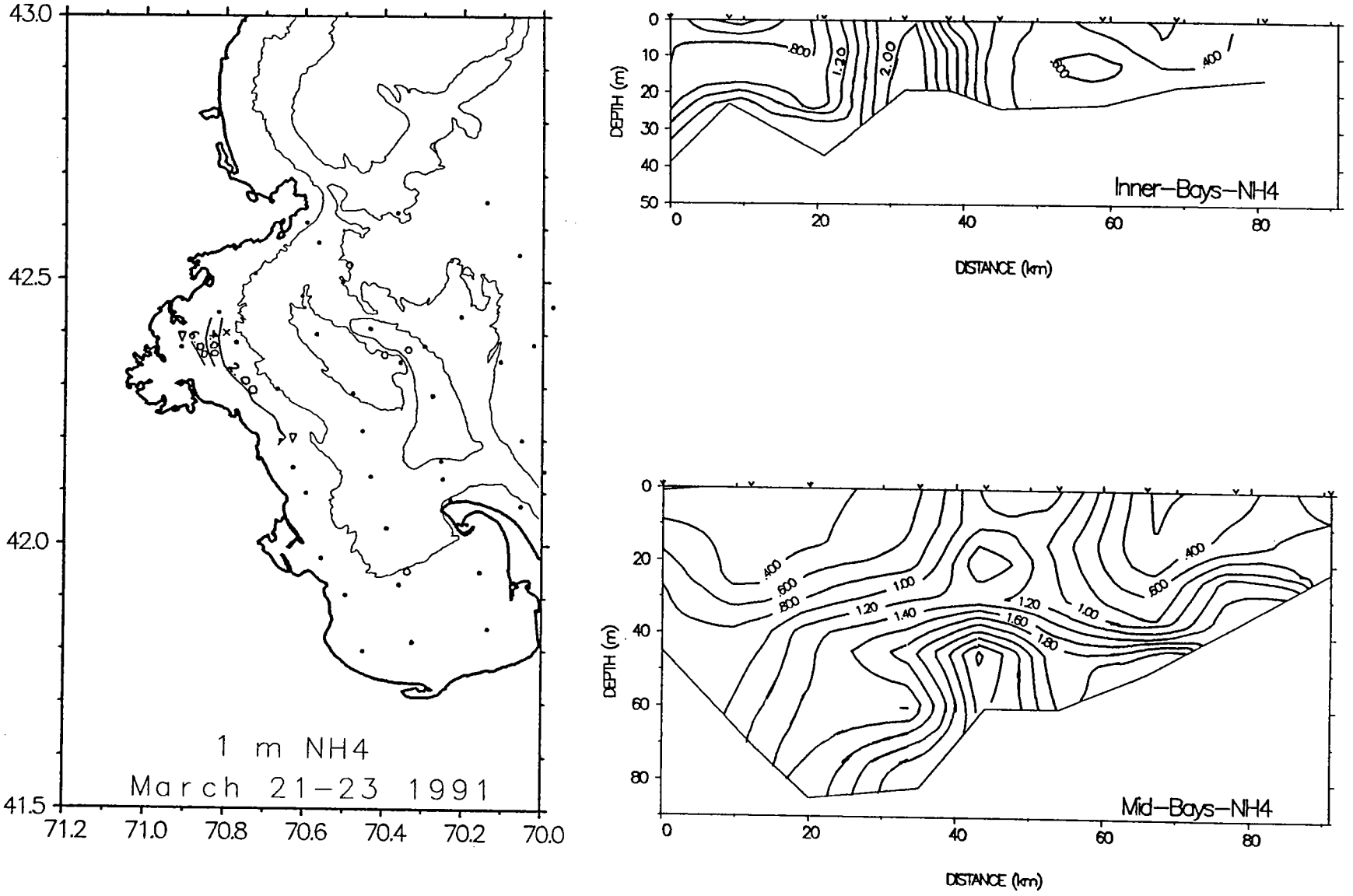

Figure 2.7-31 March 21–23, 1991 ammonium surface, Inner, and Mid-Bays contour plots. The units are μM and the contour interval is 0.2 μM for the vertical sections and 2 μM for the horizontal contour plot.

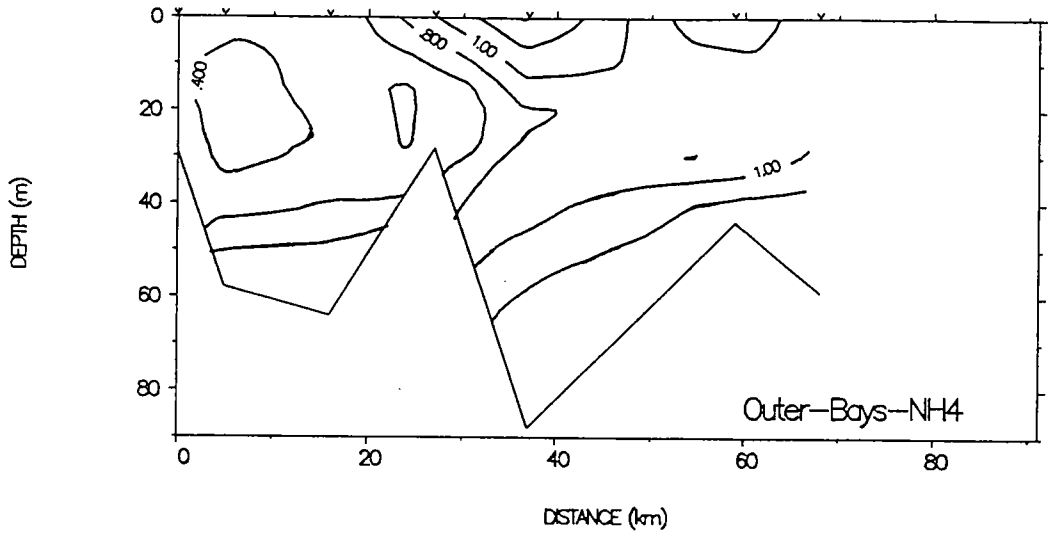

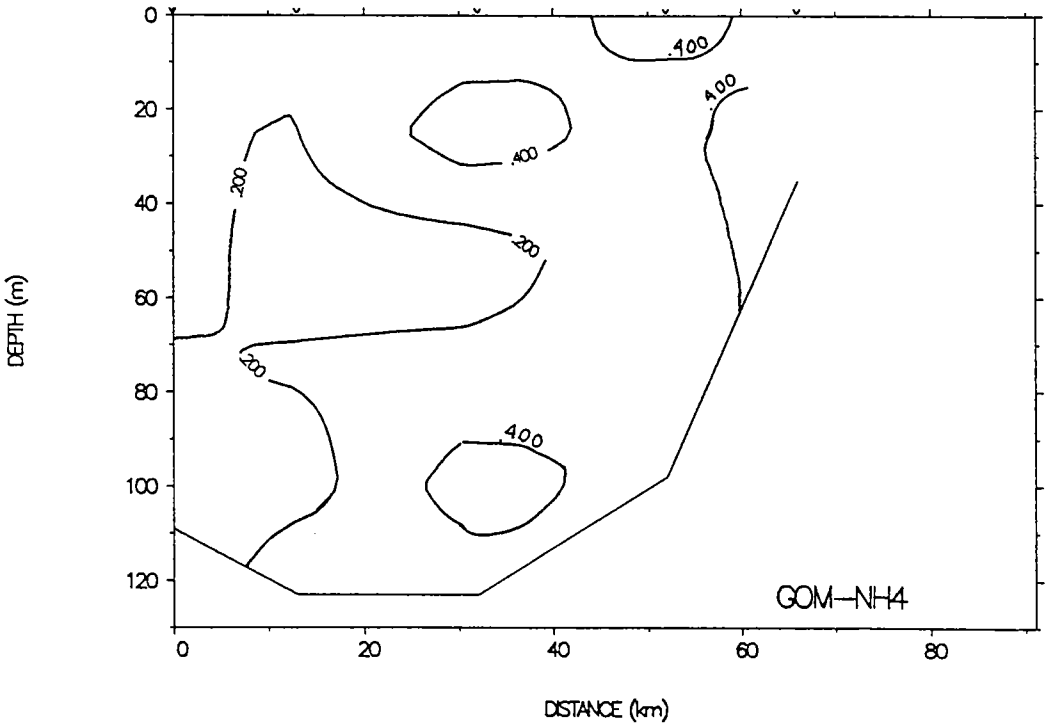

Figure 2.7-32 March 21–23, 1991 ammonium Outer-Bays and GOM vertical contour sections. The units are μM and the contour interval is 0.5 μM.

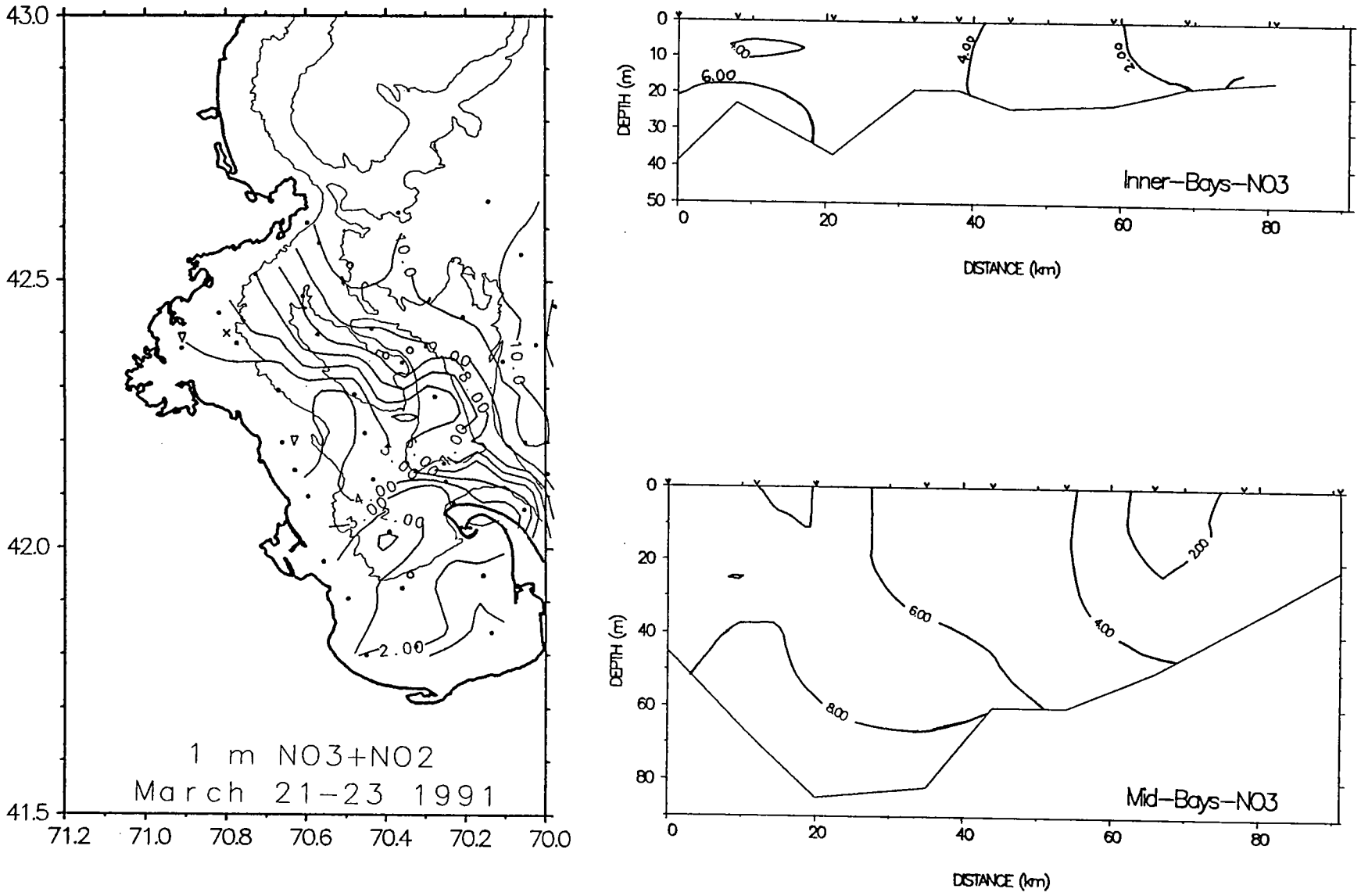

Figure 2.7-33 March 21–23, 1991 nitrate surface, Inner, and Mid-Bays contour plots. The units are μM and the contour interval is 2 μM for the vertical sections and 1 μM for the horizontal contour plot.

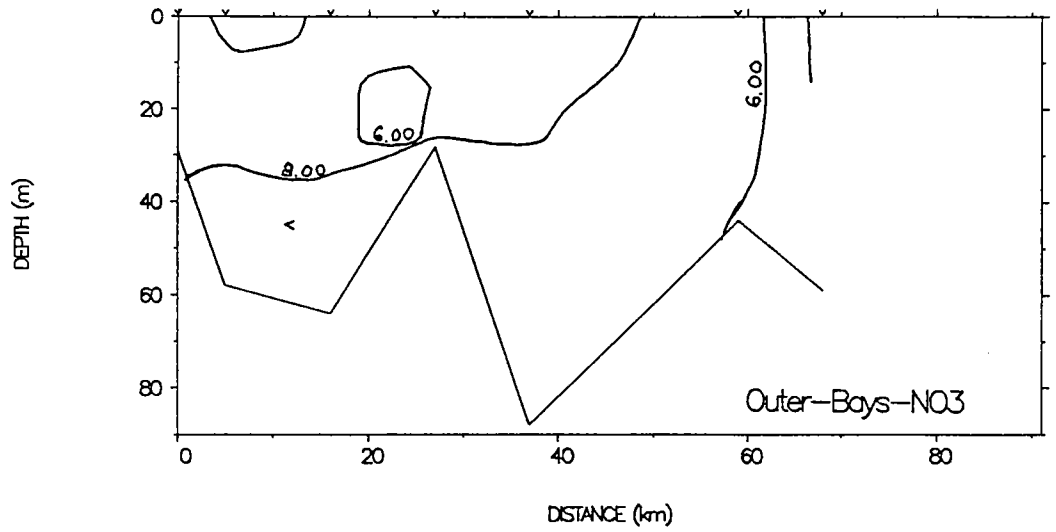

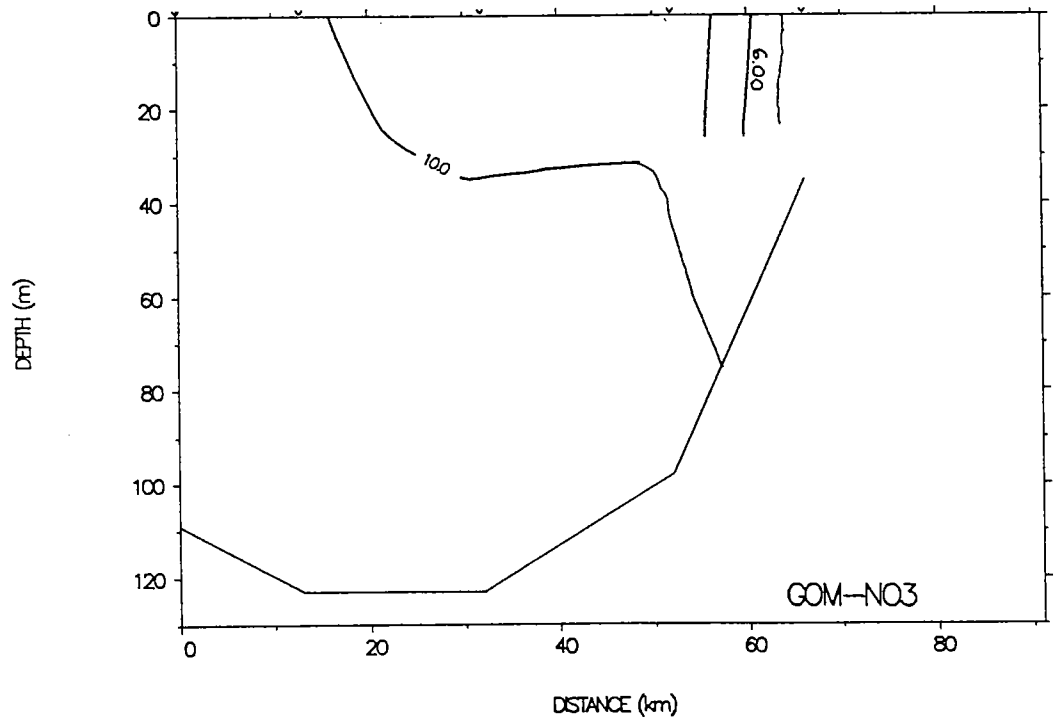

Figure 2.7-34 March 21–23, 1991 nitrate Outer-Bays and GOM vertical contour sections. The units are μM and the contour interval is 2 μM.

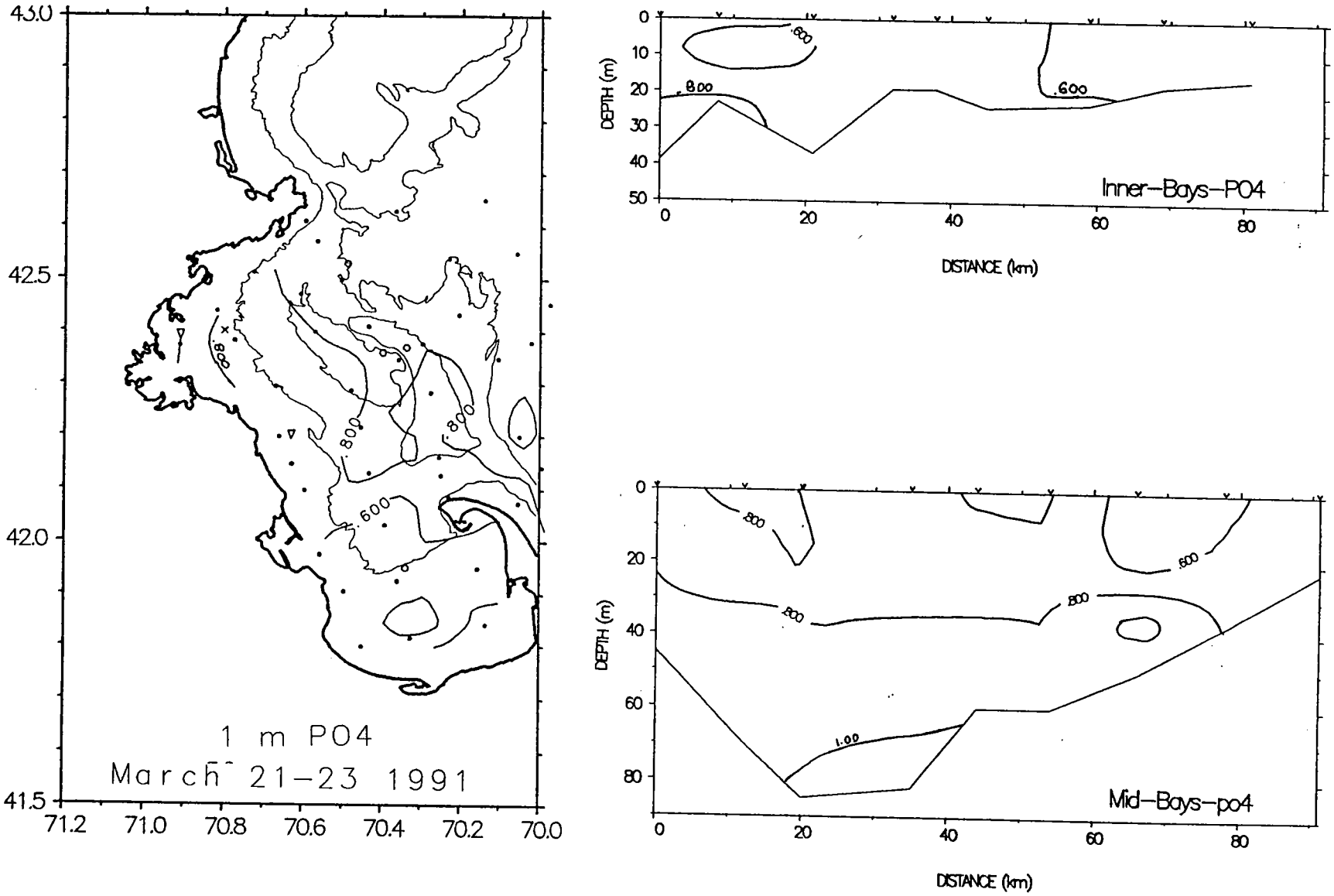

Figure 2.7-35 March 21–23, 1991 phosphate surface, Inner, and Mid-Bays contour plots. The units are μM and the contour interval is 0.2 μM.

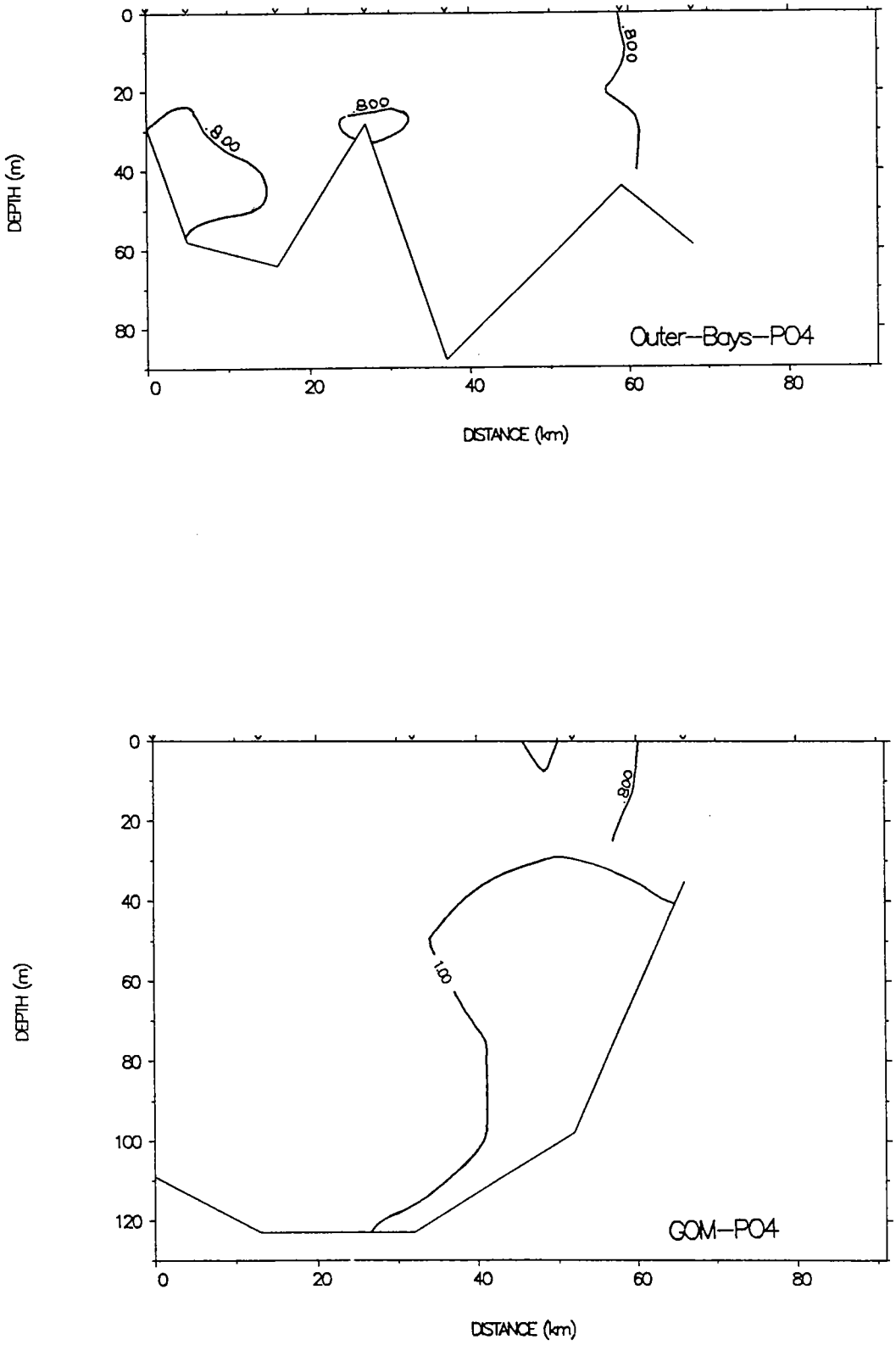

Figure 2.7-36 March 21–23, 1991 phosphate Outer-Bays and GOM vertical contour sections. The units are μM and the contour interval is 0.2 μM.

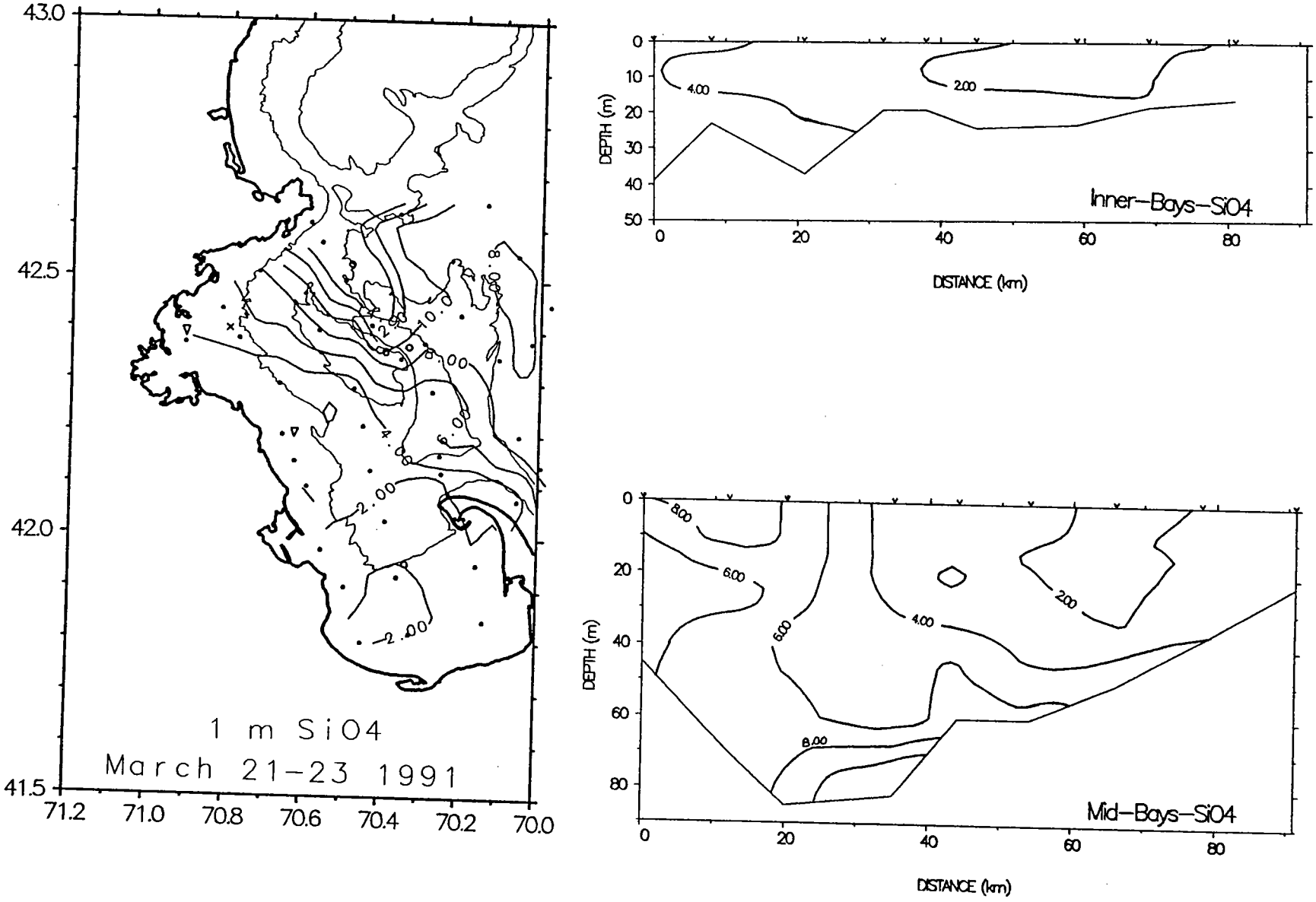

Figure 2.7-37 March 21–23, 1991 silicate surface, Inner, and Mid-Bays contour plots. The units are μM and the contour interval is 2 μM.

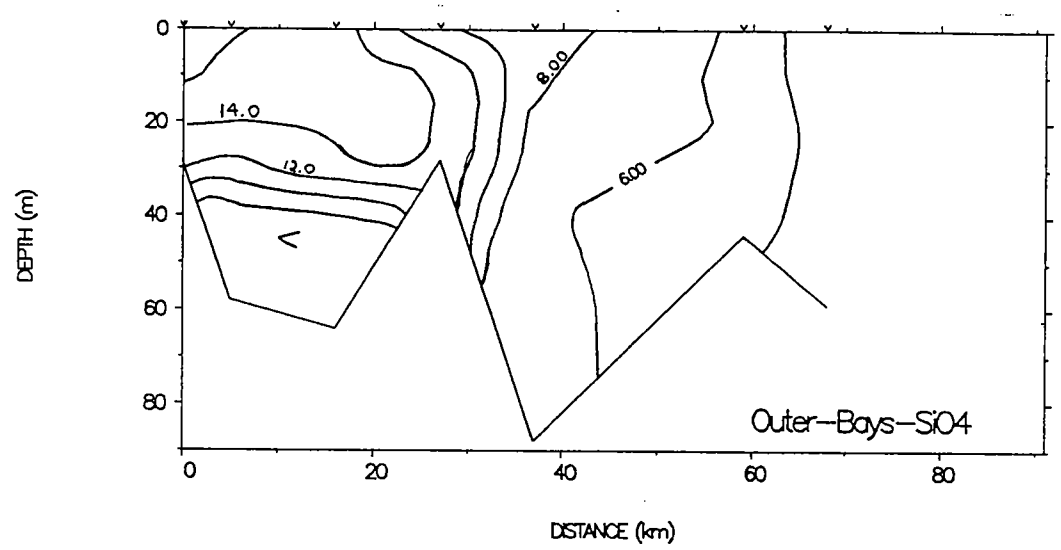

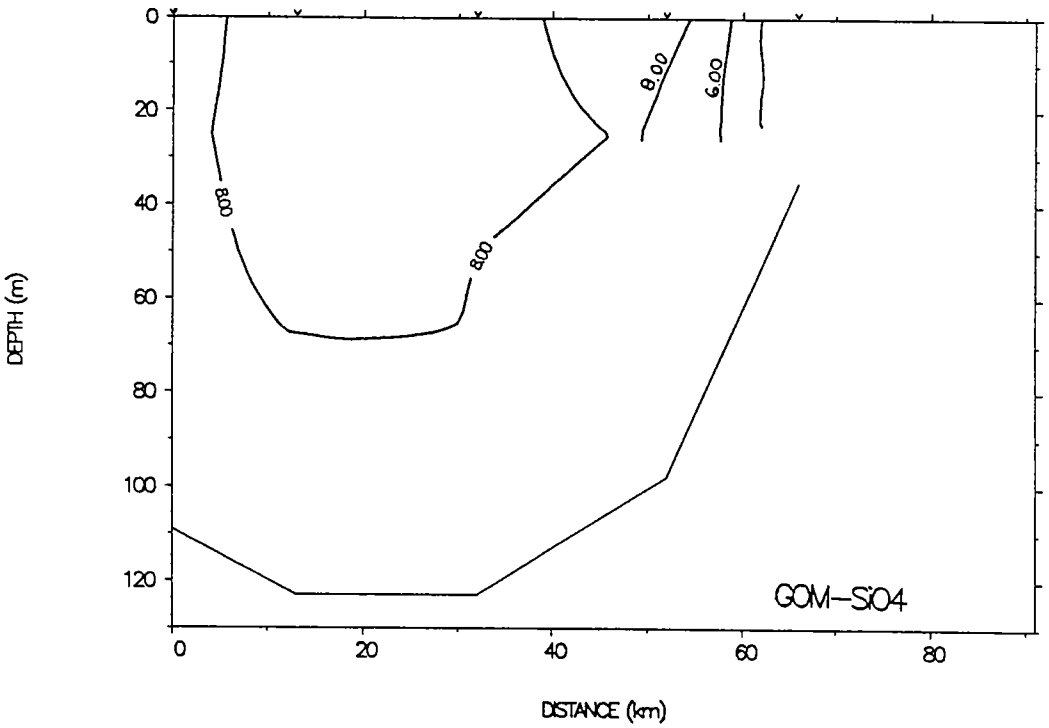

Figure 2.7-38 March 21–23, 1991 silicate Outer-Bays and GOM vertical contour sections. The units are μM and the contour interval is 2 μM.

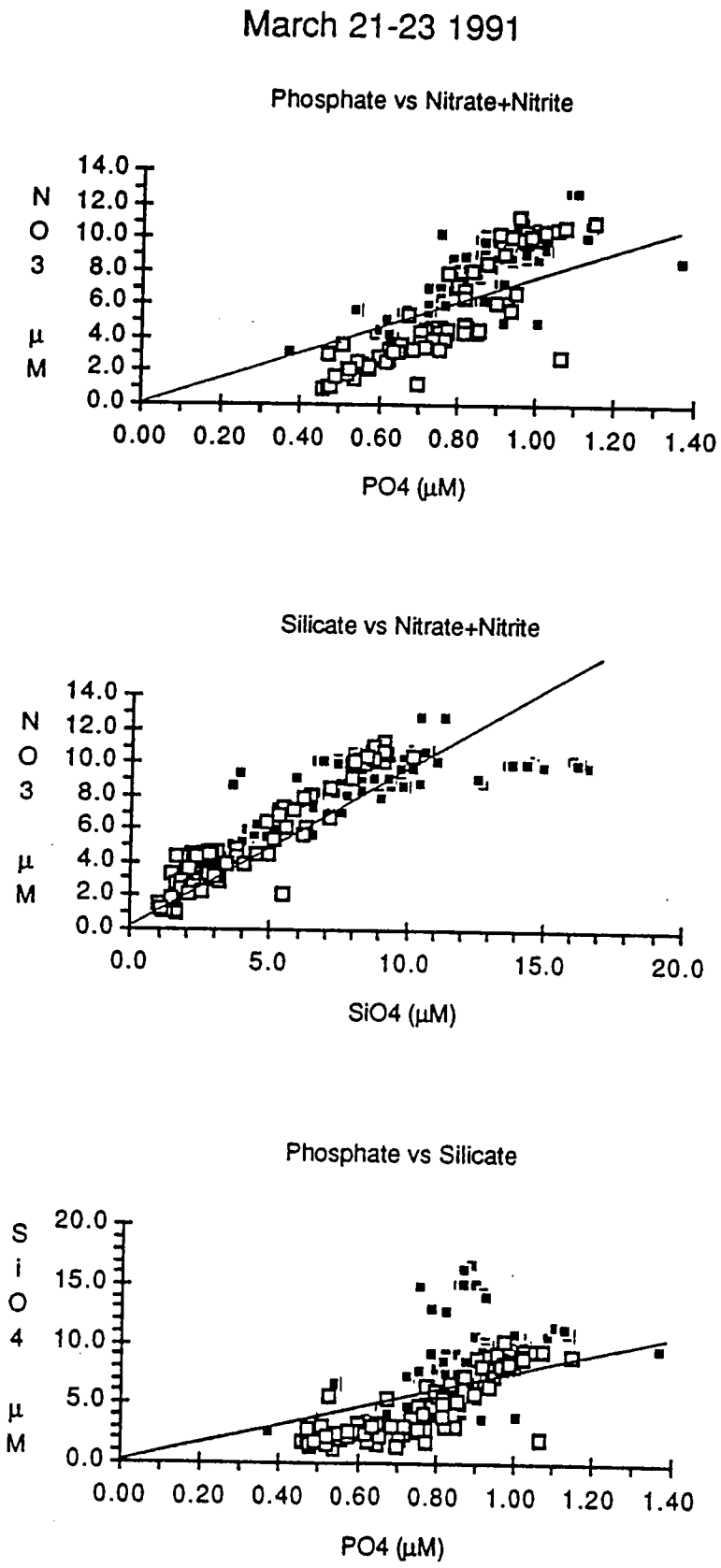

Figure 2.7-39 March 21–23, 1991 nutrient-nutrient plots. The lines are N:P:Si ratio of 8:1:8. The open squares represent the southern section of the Bays and the closed squares the northern section.

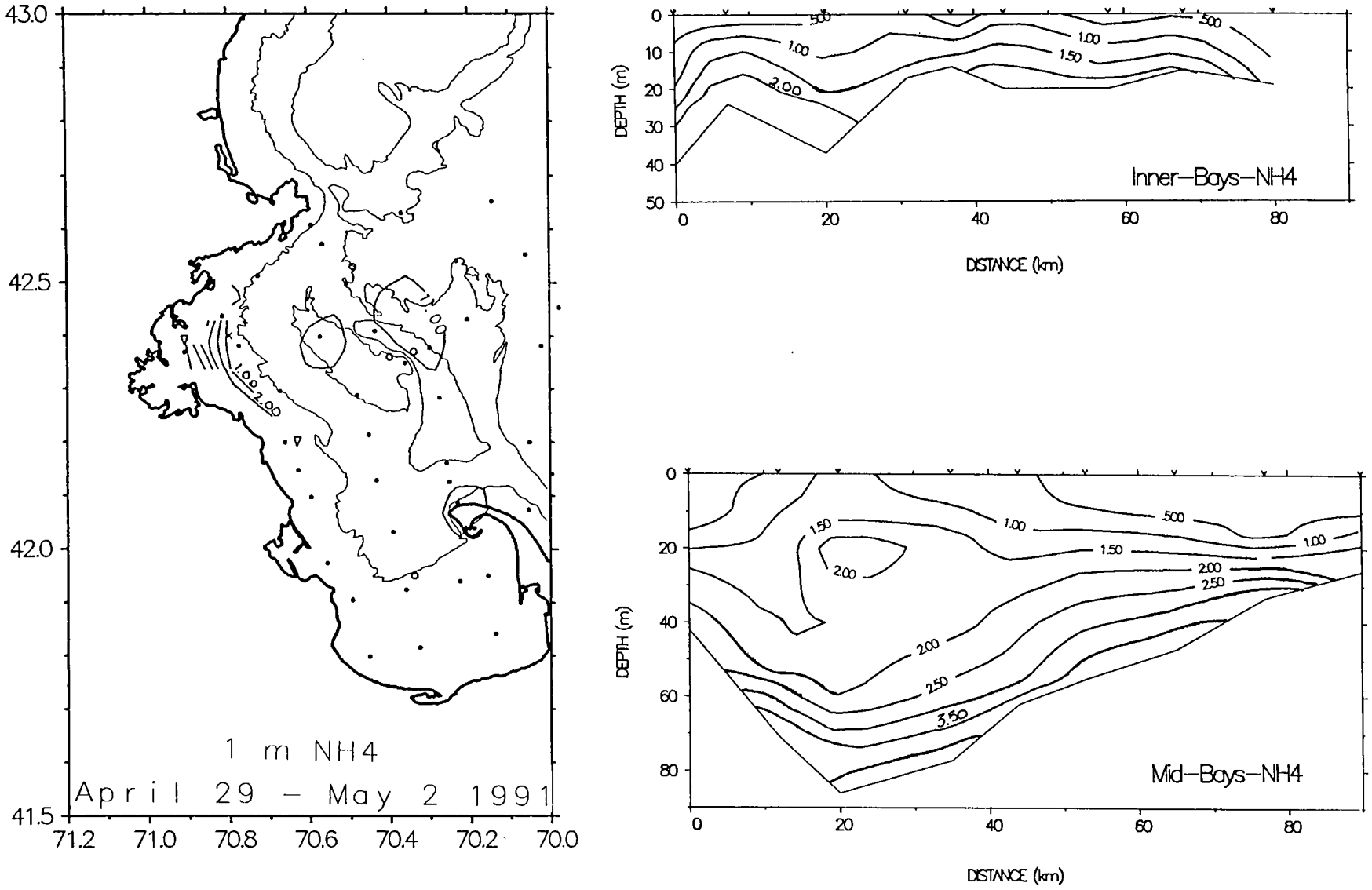

Figure 2.7-40 April 29 - May 2, 1991 ammonium surface, Inner, and Mid-Bays contour plots. The units are μM and the contour interval is 0.5 μM for the vertical sections and 1 μM for the horizontal contour plot.

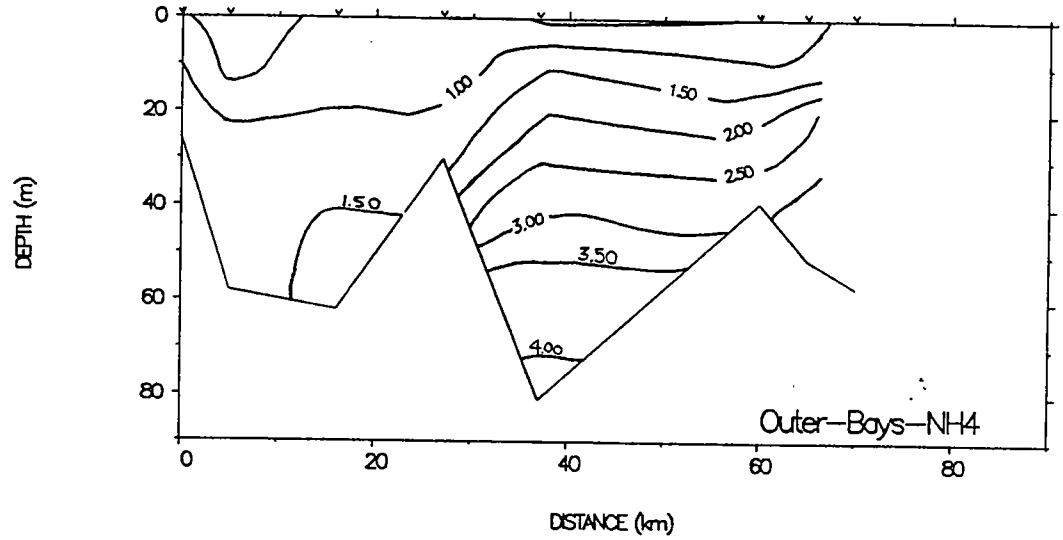

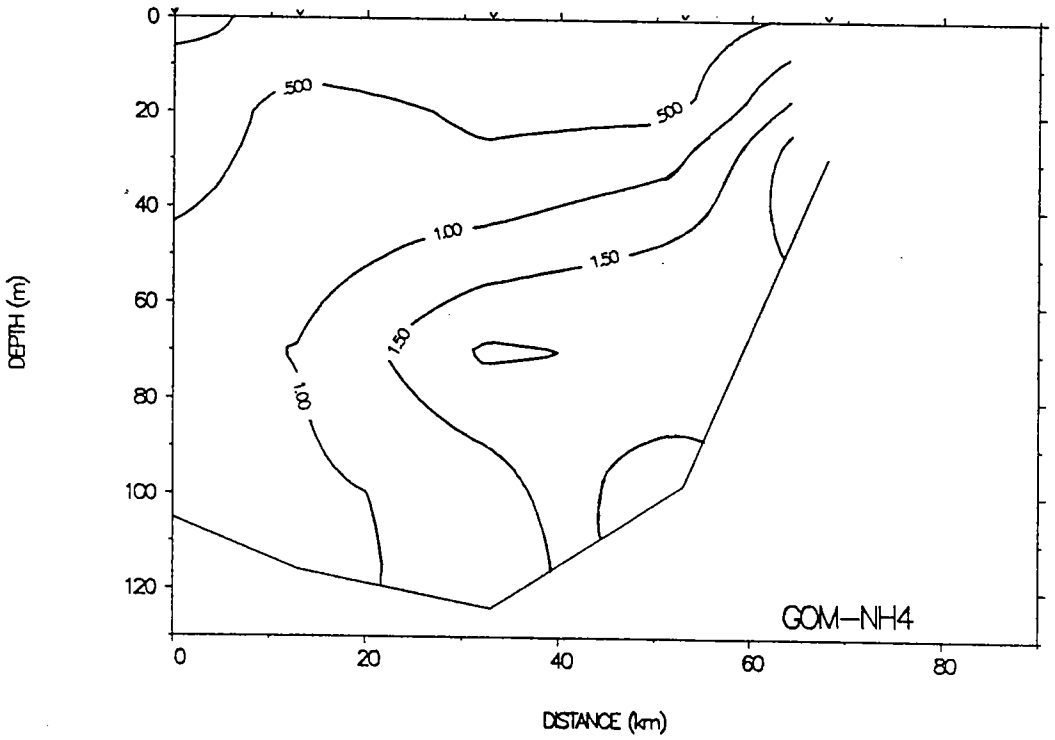

Figure 2.7-41 April 29 – May 2, 1991 ammonium Outer-Bays and GOM vertical contour sections. The units are μM and the contour interval is 0.2 μM.

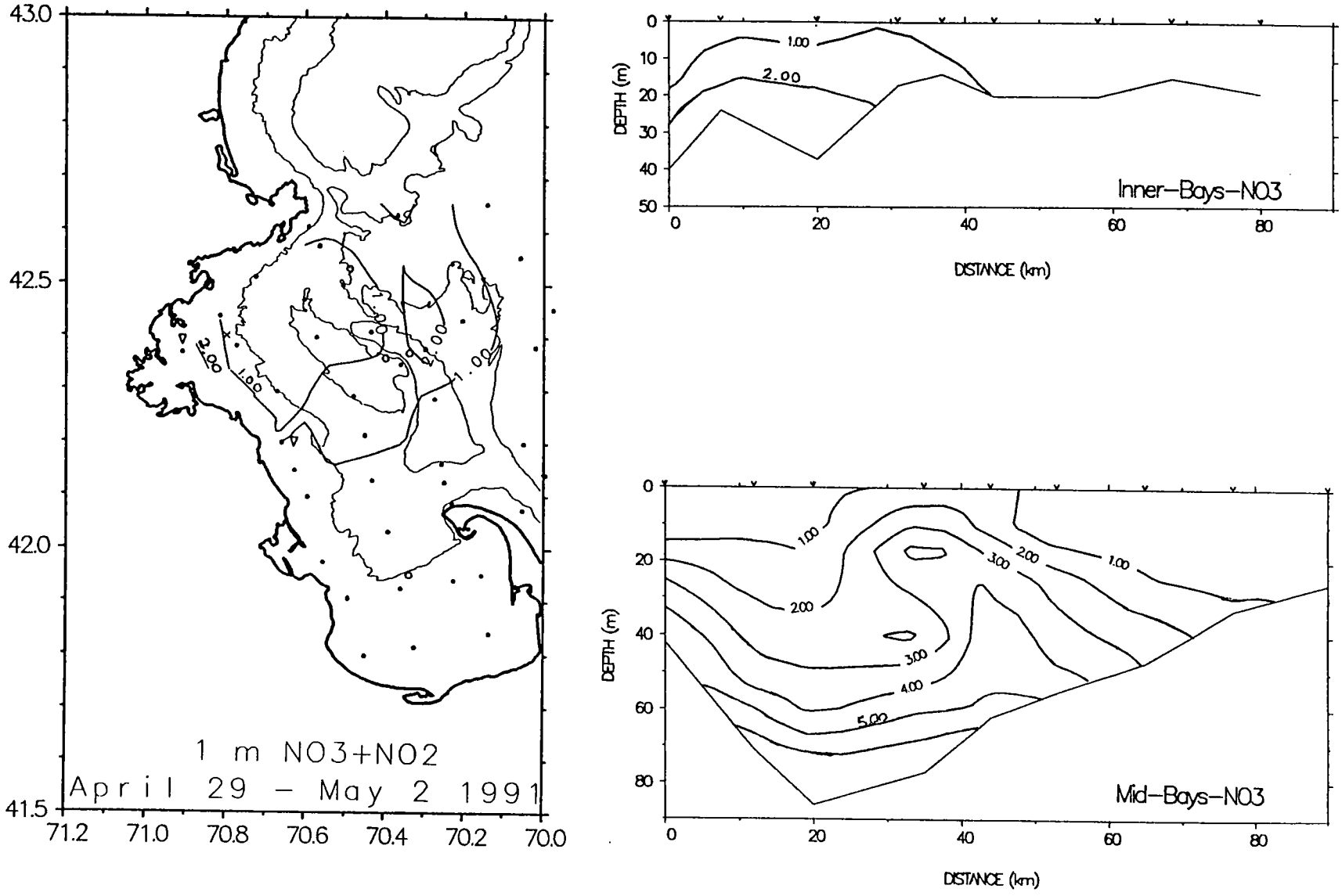

Figure 2.7-42 April 29 – May 2, 1991 nitrate surface, Inner, and Mid-Bays contour plots. The units are μM and the contour interval is 2 μM.

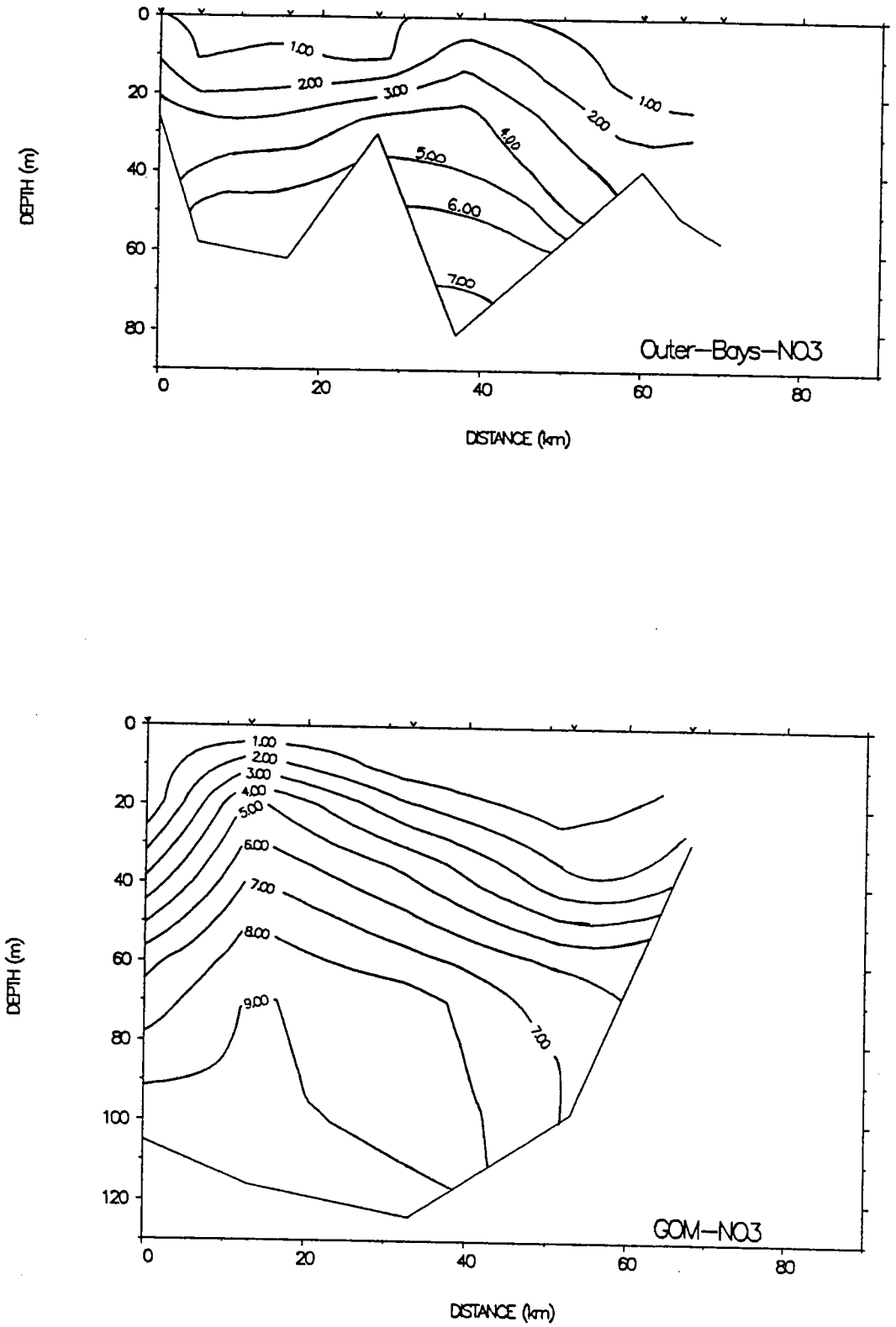

Figure 2.7-43 April 29 – May 2, 1991 nitrate Outer-Bays and GOM vertical contour sections. The units are μM and the contour interval is 1 μM.

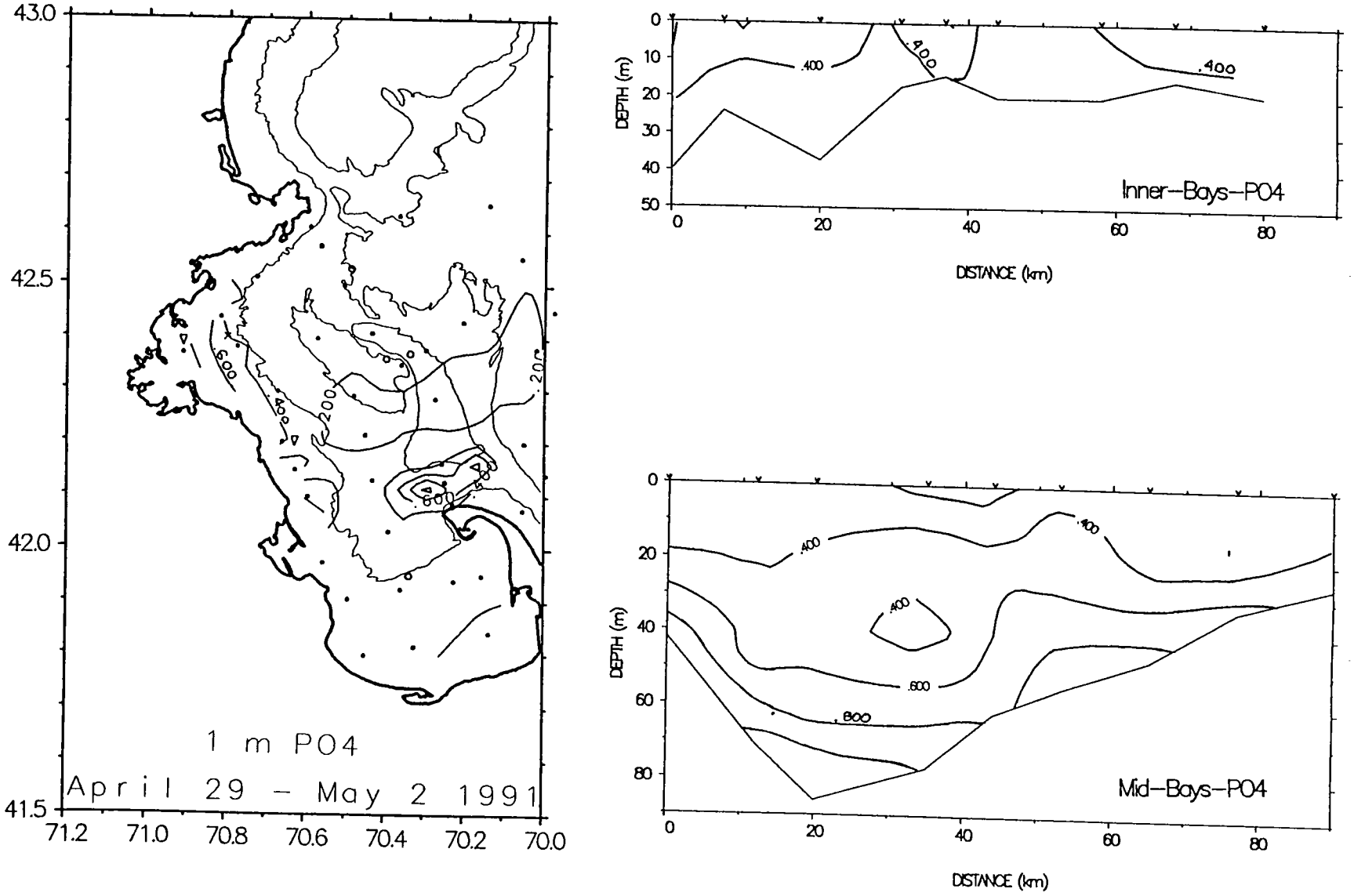

Figure 2.7-44 April 29 - May 2, 1991 phosphate surface, Inner, and Mid-Bays contour plots. The units are μM and the contour interval is 0.2 μM.

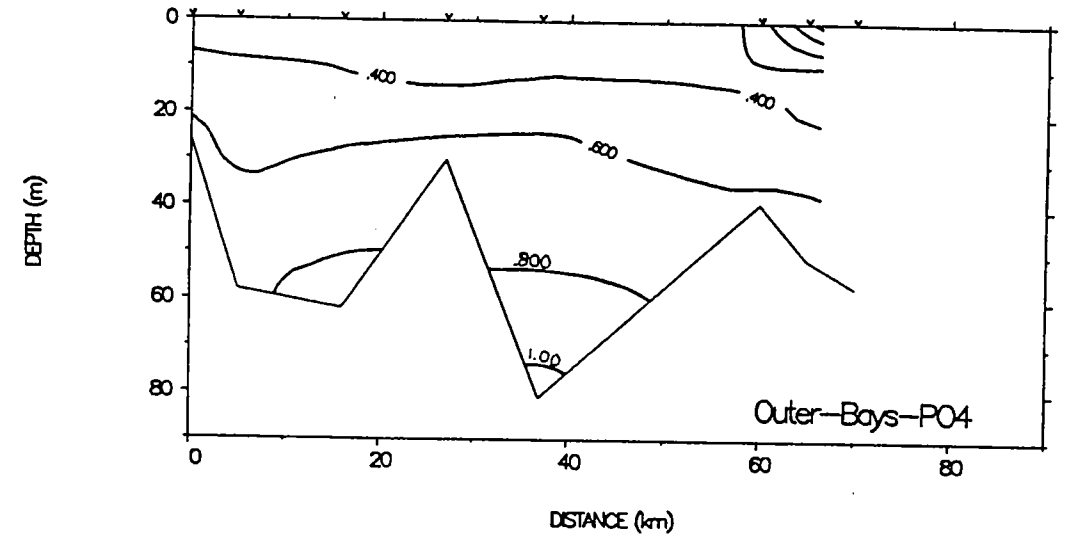

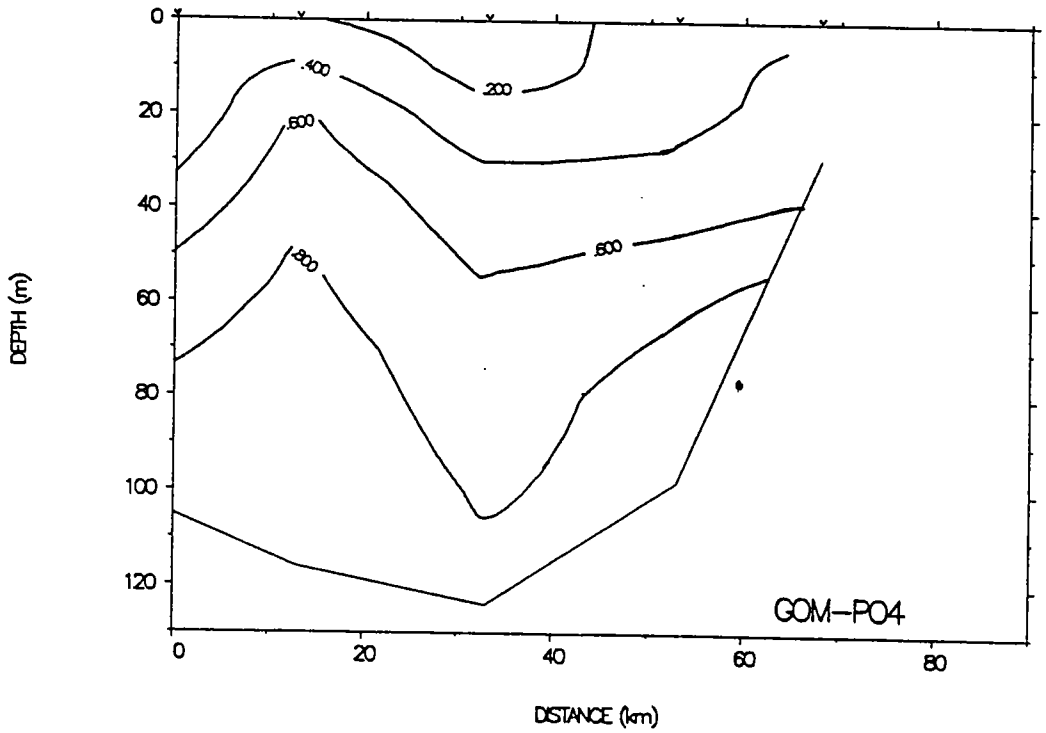

Figure 2.7-45 April 29 – May 2, 1991 phosphate Outer-Bays and GOM vertical contour sections. The units are μM and the contour interval is 0.2 μM.

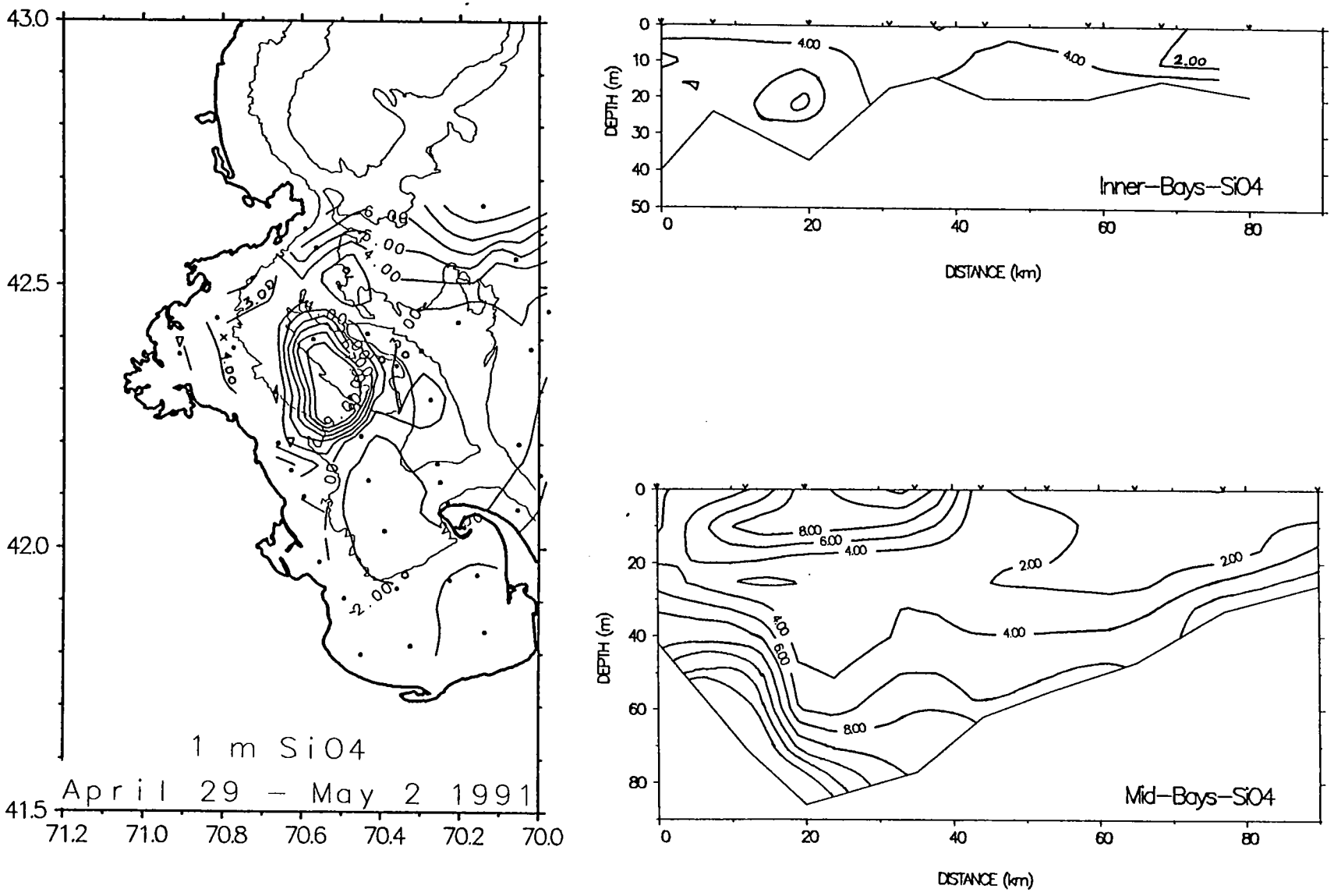

Figure 2.7-46 April 29 – May 2, 1991 silicate surface, Inner, and Mid-Bays contour plots. The units are μM and the contour interval is 2 μM for the vertical sections and 1 μM for the horizontal contour plot.

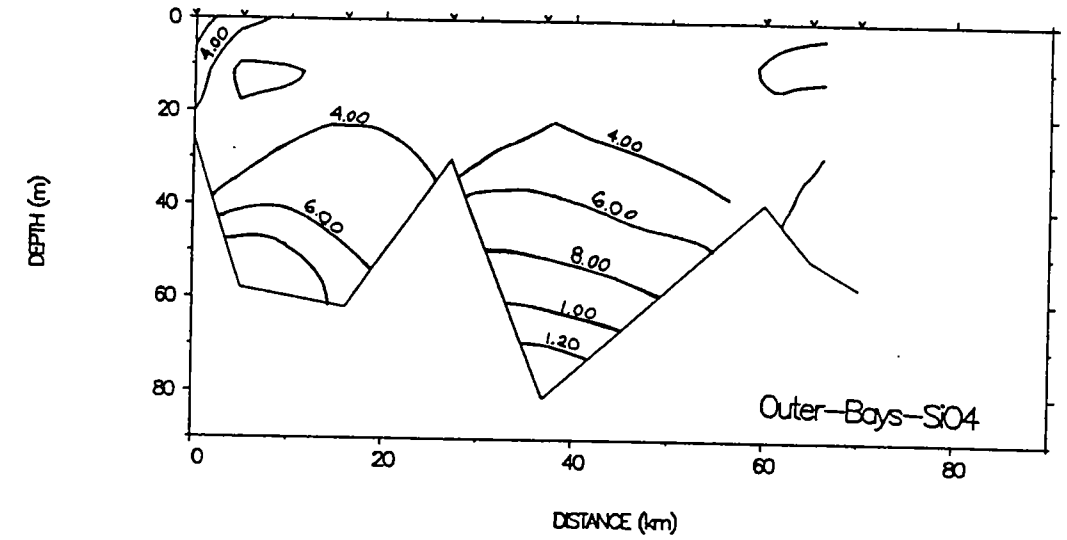

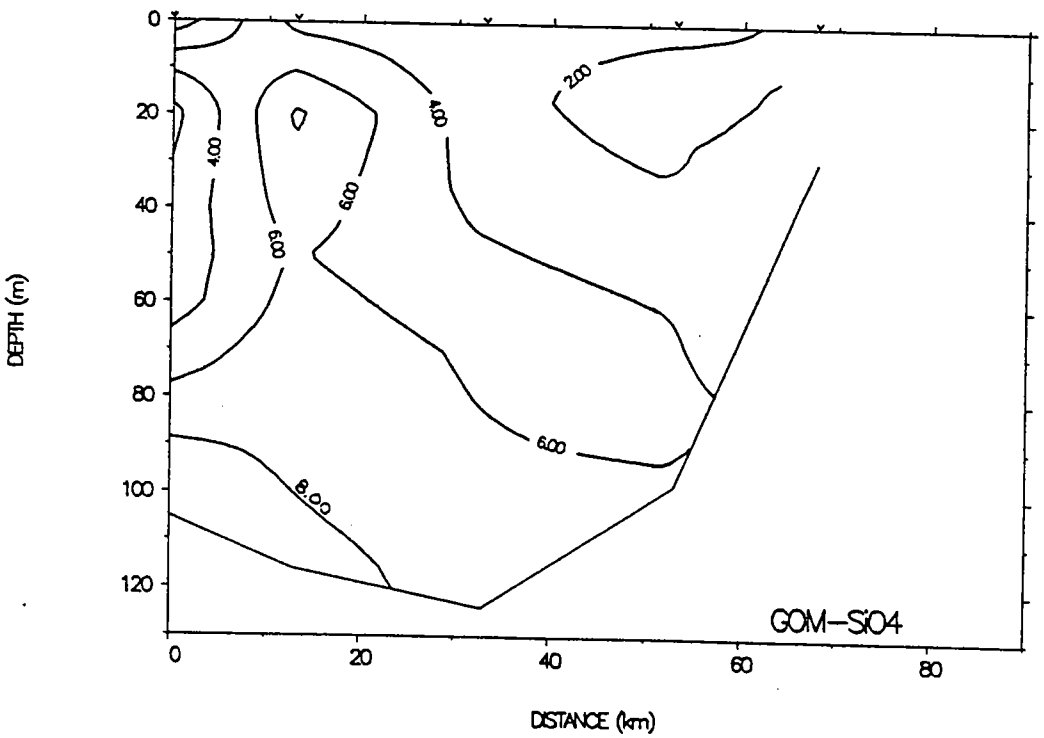

Figure 2.7-47 April 29 – May 2, 1991 silicate Outer-Bays and GOM vertical contour sections. The units are μM and the contour interval is 2 μM.

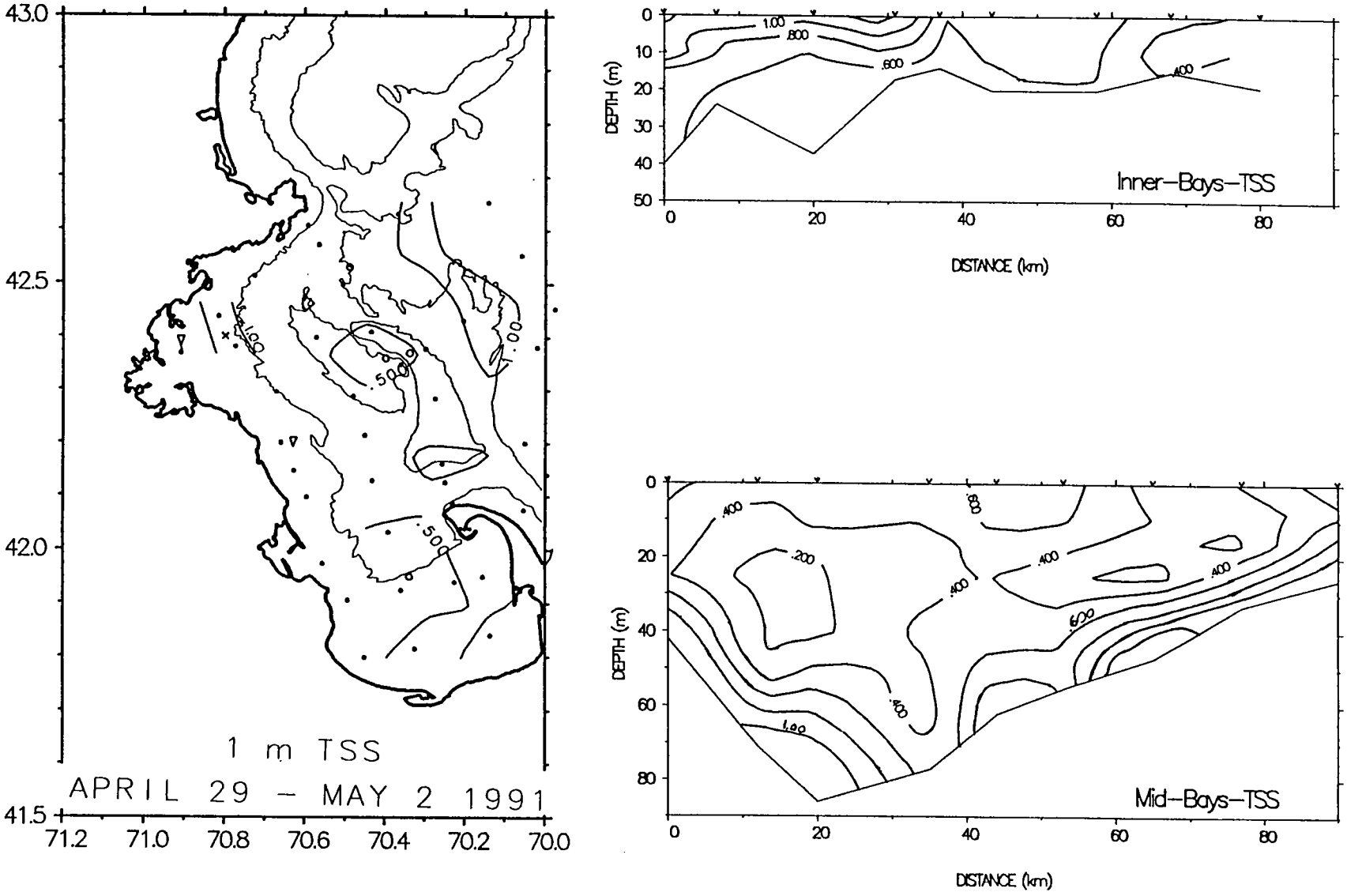

Figure 2.7-48 April 29 – May 2, 1991 TSS surface, Inner, and Mid-Bays contour plots. The units are mg/L and the contour interval is 0.2 mg/L for the vertical sections and 0.5 mg/L for the horizontal contour plot.

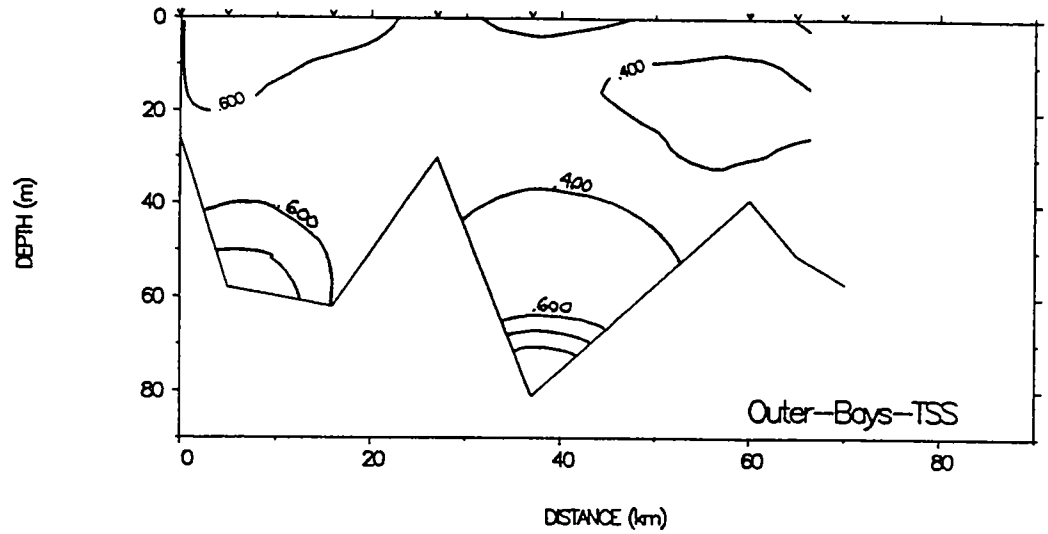

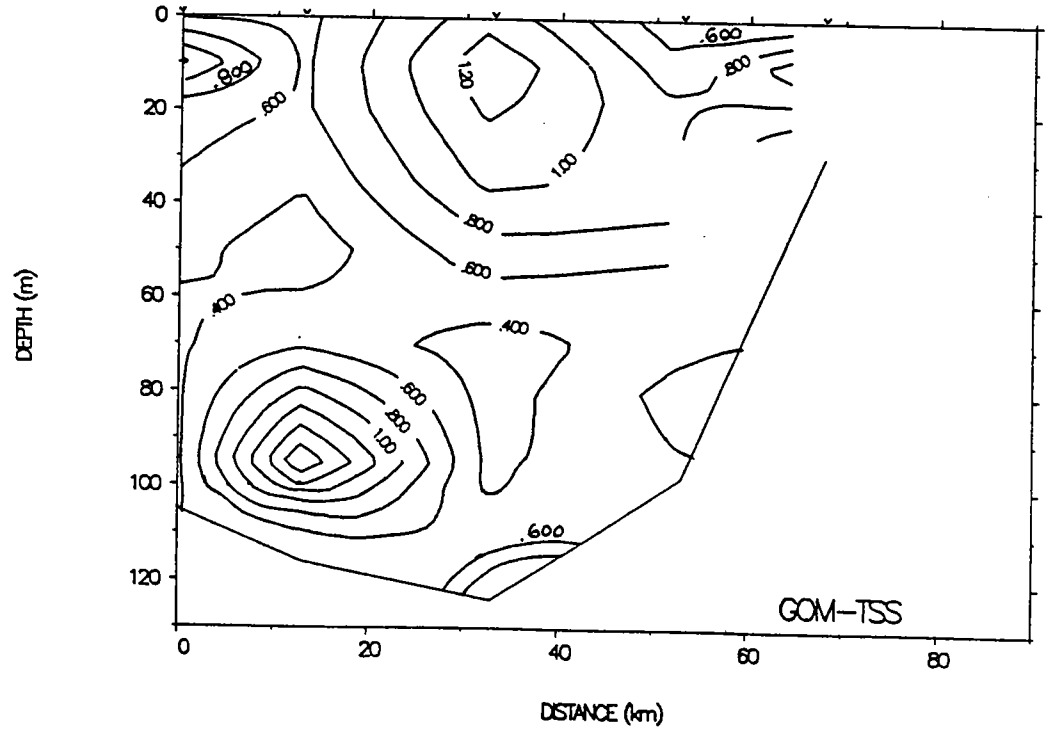

Figure 2.7-49 April 29 - May 2, 1991 TSS Outer-Bays and GOM vertical contour sections. The units are mg/L and the contour interval is 0.2 mg/L.

April 29 - May 2 1991

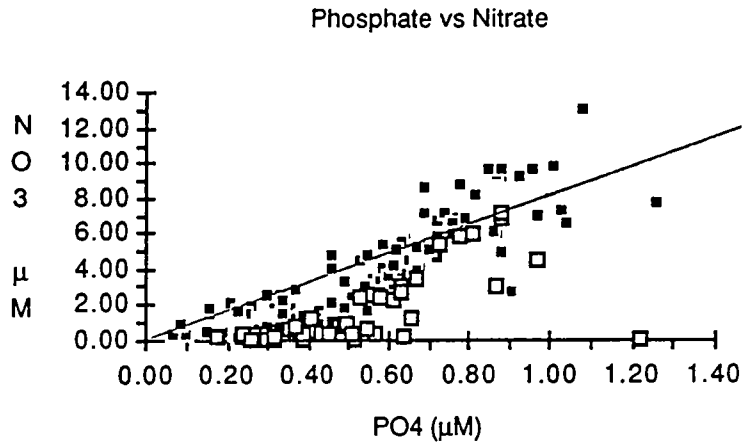

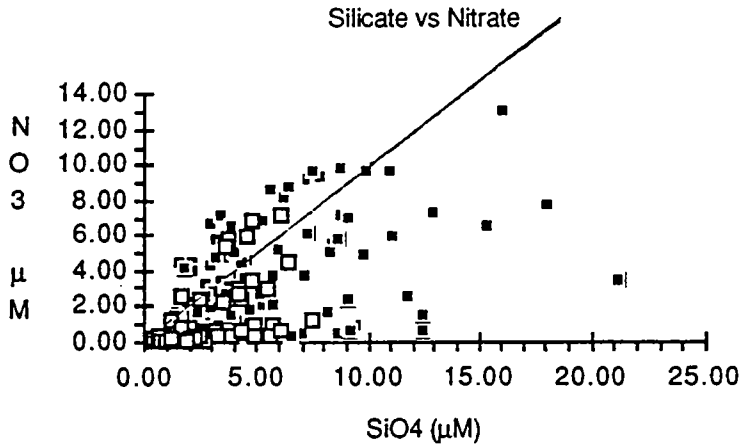

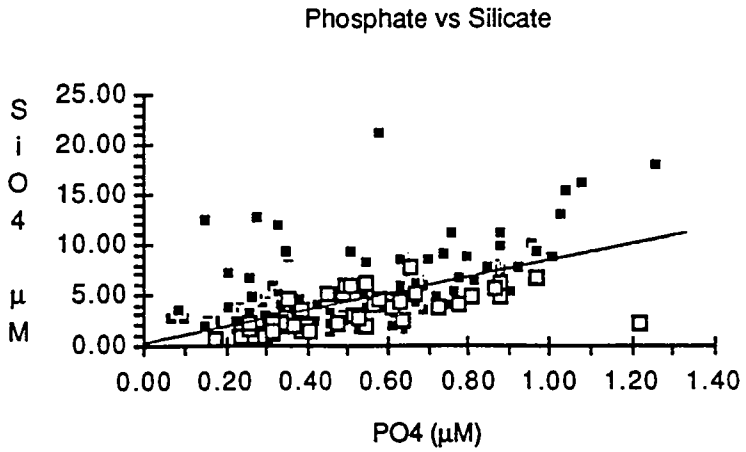

Figure 2.7-50 April 29 – May 2, 1991 nutrient-nutrient plots. The lines are N:P:Si ratio of 8:1:8. The open squares represent the southern section of the Bays and the closed squares the northern section.

2.8 Long-Term Current and Sediment Transport Observations

The objective of the long-term observations is to document seasonal and inter-annual variability in currents, hydrography, and suspended-matter concentration and composition in western Massachusetts Bay. The measurements are also designed to investigate the importance of infrequent catastrophic events, such as major storms or hurricanes, to sediment resuspension and transport. The observations provide a context for the year-long measurements made between April 1990 and June 1991 by the Bays program.

The long-term observations were made at station BB at the U.S. Coast Guard's Large Navigational Buoy (LNB, 42° 22.6'N 70° 47.1'W, Station BB, see figure 1.3) in western Massachusetts Bay. Observations of current, temperature, salinity and light transmission were made at 5 m from the surface, above the seasonal thermocline, by means of a VMCM and Seacat suspended from the LNB and at 23 m, typically below the seasonal thermocline, by similar instrumentation on a subsurface mooring (figure 2.2-2b). Bottom observations of current, temperature, salinity, light transmission and pressure were obtained by means of a bottom tripod system (Butman and Folger (1979) and Martini and Strahle (1992)). A time-series sediment trap collected material from the water column sequentially over 9-day intervals. Instrumentation is recovered and deployed three times each year with logistical support provided by the U.S. Coast Guard. Observations began in December 1989 and are continuing.

The mean flow (the vector average of all the observations over several months) at the long-term site is typically less than 1 cm/s and is generally not statistically different from zero given the strength of the low-frequency fluctuations. The long-term site is apparently to the west of the counterclockwise residual flow pattern suggested by the moored array and Lagrangian drifter observations. Thus water and material in this northwestern portion of the bay are not swept away in a consistent direction by a well-defined steady current but are mixed and transported by a variety of processes, including tides, winds, and river inflow. Based on the strength of the low frequency fluctuations, one day particle excursions from the long-term site are typically 10 km. These excursions are probably sufficient to mix water into the residual flow pattern on a regular basis, consistent with the results of the Lagrangian drifter observations.

Although the vector mean of the current over any one deployment is small, there is a suggestion of a weak offshore flow in the surface layers and onshore flow at the bottom that is consistent with analysis of historical current observations in western Massachusetts Bay. This weak onshore/offshore flow is probably driven by the mean eastward winds that drive the surface water offshore, requiring a return flow at depth.

The amplitude of the low-frequency currents (fig. 2.8-1) are typically stronger near the surface (4 to 6 cm/s at 5 m) than at depth (2 to 4 cm/s at 23 m). At 5 m, the low-frequency currents are strongest and most variable in the spring and summer due to the horizontal and vertical density gradients associated with the runoff of freshwater from Boston Harbor and the Merrimack River and the development of a strong seasonal thermocline that reduces the influence of bottom friction on the currents. At 23 m, the weak low-frequency current speeds are more or less constant with season. Winds are strongest in winter and are the major forcing agent of the weak currents in winter.

The strength and orientation of the low-frequency currents on a seasonal basis is illustrated by the current ellipses (fig. 2.8-2). At 5 m, the low-frequency ellipse is nearly circular. At 23 m, the low-frequency ellipse is oriented northwest-southeast. This orientation may reflect the enhanced bay-wide response to wind along the major axis (northwest-southeast) of the bay. The long-term mooring is located on the southern side of a east-west trending submarine ridge or drumlin with about 10 m of relief that probably orients the near-bottom low-frequency currents in an east-west direction. The orientation of the low frequency ellipses is similar from season to season and from year to year for the two years of data available.

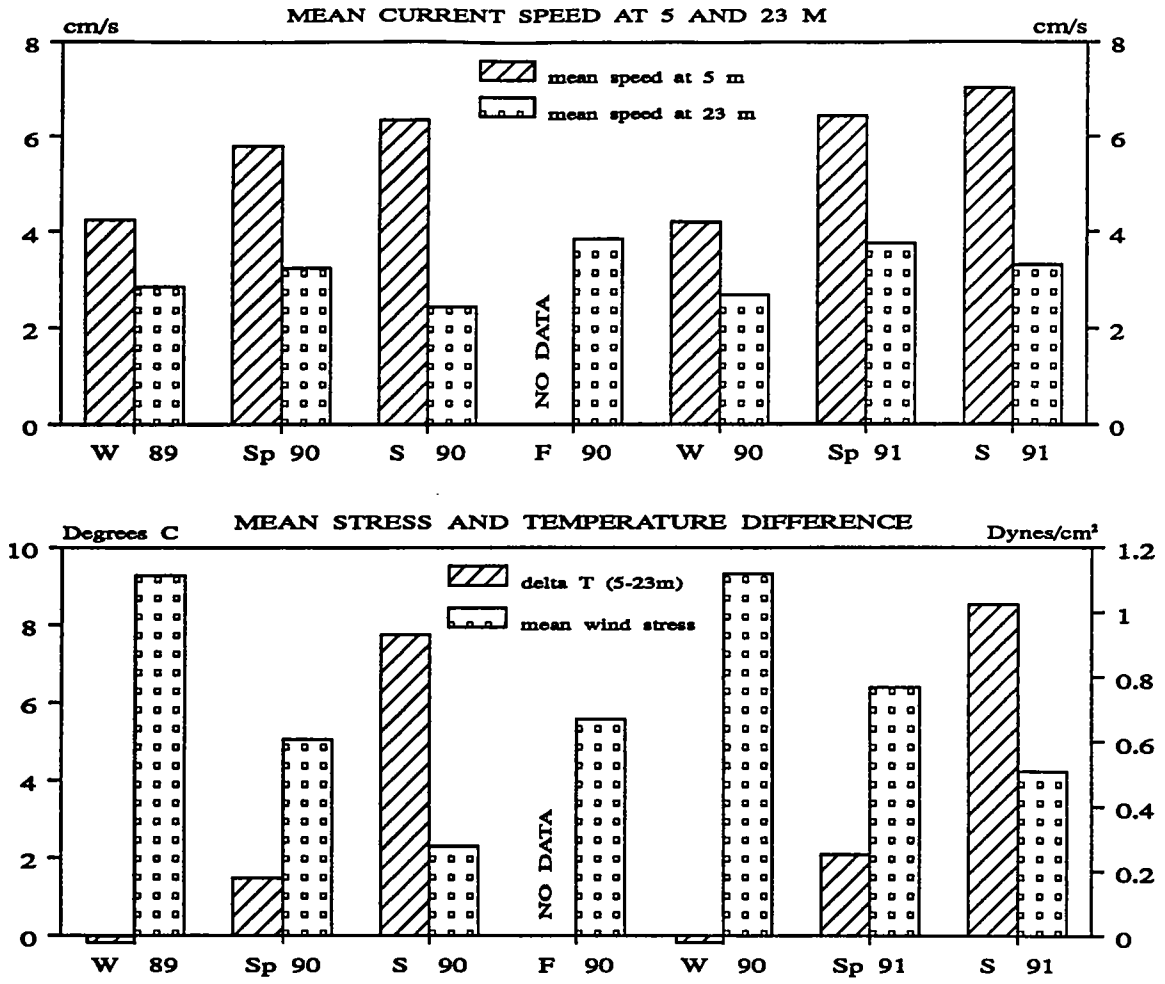

Figure 2.8-1 Top: Mean daily vector-averaged current speed at 5 and 23 m water depth obtained at the USGS long-term monitoring station (winter, November through February; spring, March through May; summer, June through August; fall, September and October). These current speeds can be used to estimate daily water-particle travel distances (approximately 0.9 km/day for each centimeter per second of speed). Bottom: Mean daily averaged wind stress amplitude at the Large Navigational Buoy and temperature difference between 5 and 23 m water depth at the long-term monitoring site. Wind stress is strongest in winter and weakest in summer; stratification (as indicated by the temperature difference between 5 and 23 m) is weakest in winter and strongest in summer. At 5 m, the current speeds increase from about 4 cm/s in winter to 6 cm/s in summer even though the winds are stronger in the winter. This suggests that stratification is more important than wind in determining the strength of the near-surface current at the new outfall site. Current speeds at 23 m remain between 2 and 4 cm/s and do not show a seasonal trend. No data was obtained in fall 1990.

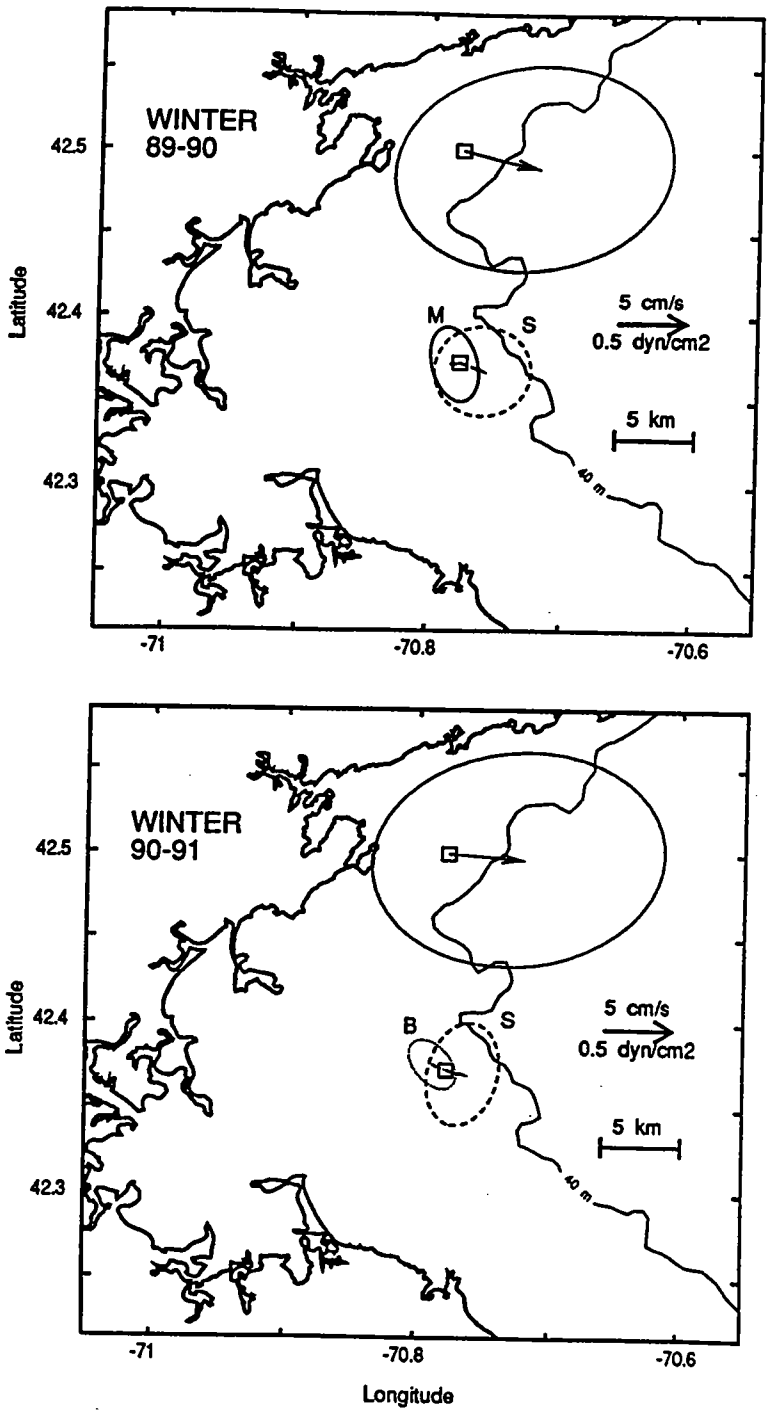

Figure 2.8-2a Map showing the mean flow (solid arrow) and the low-frequency variability (shown as ellipses centered around the tip of the mean flow) for observations at 5, 23 and 32 m at the long-term station for Winter, November 1 – March 1 (S corresponds to surface, M to mid-depth, and B for bottom). Wind stress measured at the LNB is also shown. Typically, the daily-averaged current originates at the station symbol and flows toward any location within the ellipse. The arrows and ellipses have been scaled to correspond to the distance a particle moving with that current would travel in one day. The fluctuations are larger than the mean. The area of the new ocean outfall is an area of weak flow compared to the outer bay and there is no strong preferred direction of flow; it is apparently located to the west of the stronger residual coastal current system.

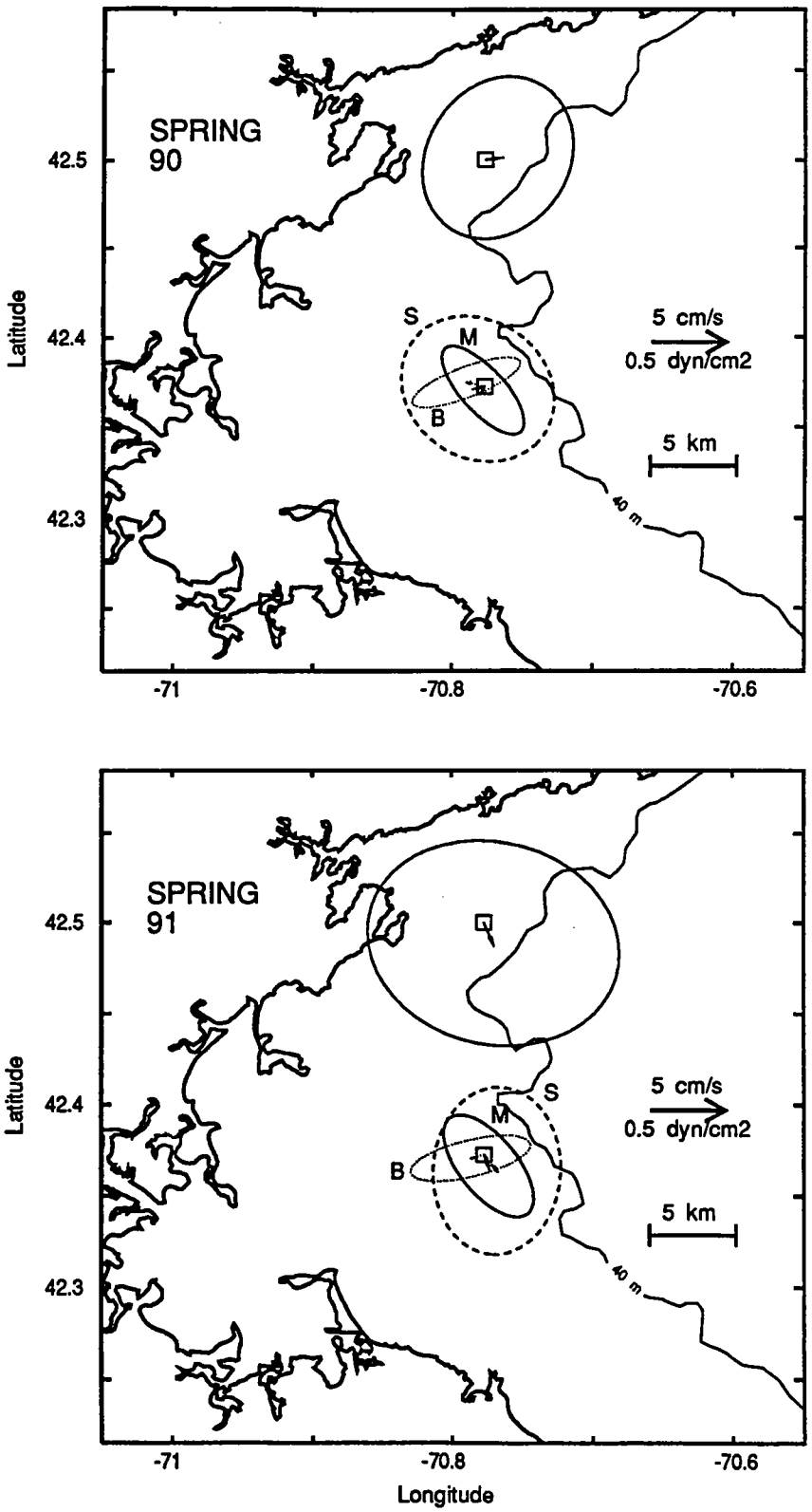

Figure 2.8-2b Map showing the mean flow (solid arrow) and the low-frequency variability (shown as ellipses centered around the tip of the mean flow) for observations at 5, 23 and 32 m at the long-term station for spring (March 1 – June 1). See figure 2.8-2a for explanation.

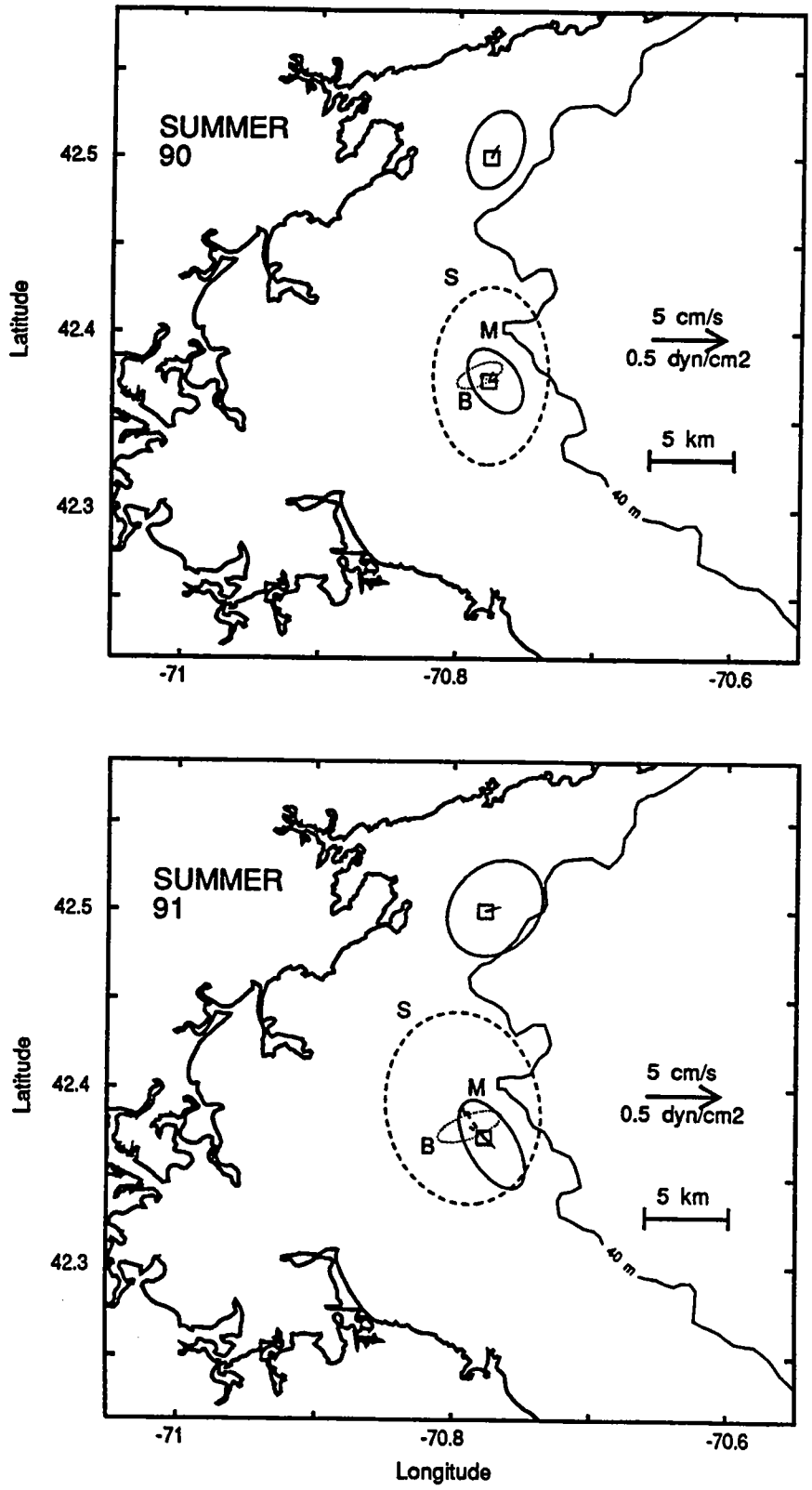

Figure 2.8-2c Map showing the mean flow (solid arrow) and the low-frequency variability (shown as ellipses centered around the tip of the mean flow) for observations at 5, 23 and 32 m at the long-term station for summer (June 1 – September 1). See figure 2.8-2a for explanation.

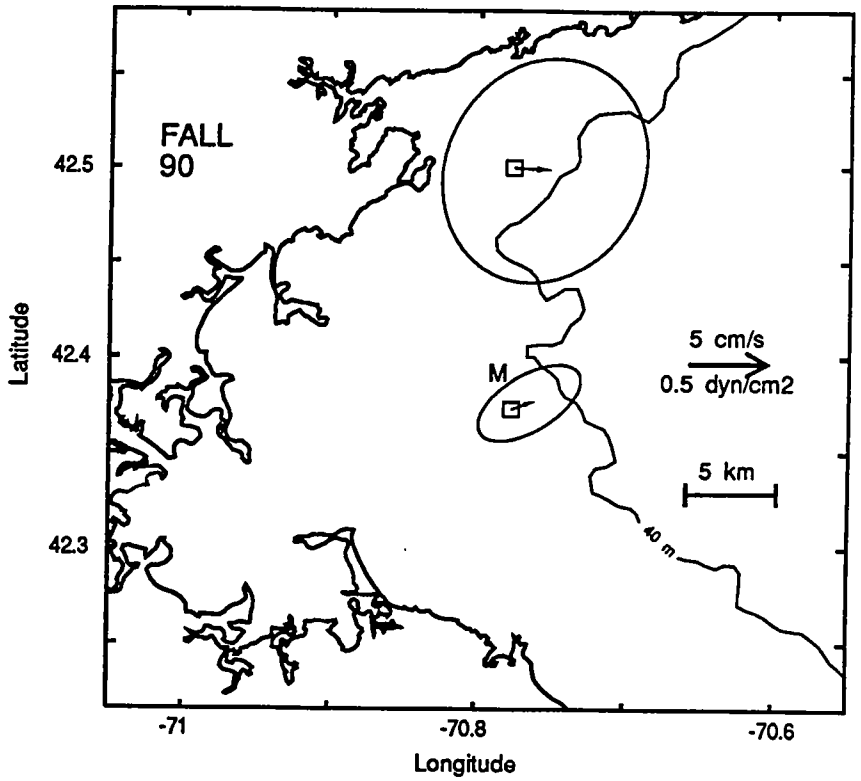

Figure 2.8-2d Map showing the mean flow (solid arrow) and the low-frequency variability (shown as ellipses centered around the tip of the mean flow) for observations at 5, 23 and 32 m at the long-term station for fall (September 1 – November 1). See figure 2.8-2a for explanation.

3 Analysis of Physical Processes

3.1 Tidal Processes

Tides in the Bays are forced by the tides in the Gulf of Maine which are in turn are forced primarily by the tides of the North Atlantic. The tides in the North Atlantic are the ocean's response to the gravitational forcing by the sun and the moon. These tides are "long waves" (wavelengths of order 9,000 km which are much greater than the water depth of 4 to 6 km) with the periods of about the response in the of North Atlantic basin are once-a-day (diurnal) and twice a day (semidiurnal) edge waves rotating counter-clockwise around an amphidromic point (no elevation change) in the center of the North Atlantic. Along the east coast of the United States, the tidal wave propagates from northeast to southwest along the coast, passing the mouth of the Gulf of Maine. The deep ocean tidal elevation changes cause the tides in the Gulf of Maine and Bay of Fundy system. The Gulf of Maine tides are a results of its near-resonance (in the open organ pipe sense) at about the semidiurnal frequency (Garrett, 1972, 1974).

The tidal current structure in the Bays is more complicated than the tidal sea level structure because of the bathymetry. Not only are surface tidal currents deflected by such features as Stellwagen Bank, but internal tidal currents associated with vertical density stratification are generated. In order isolate the part of the tidal currents due to surface tides, a least squares tidal analysis of winter currents was performed.

The highly polarized M_2 surface tidal current ellipses (fig. 3.1-1) depict a rather simple pattern of oscillating across-isobath tidal flow throughout the Bays. The corresponding subsurface tidal current ellipses are very similar to the surface tides in amplitude and orientation (Table 3.1-1) as expected for the weakly stratified winter conditions. The largest M_2 tidal currents are clearly off of Race Point (U4) with some enhancement in the Stellwagen Bank and Broad Sound tidal currents.

The dominant semidiurnal surface tidal current interacts with Stellwagen Bank bathymetry to generate semidiurnal internal tidal oscillations which propagate from the Bank towards western Massachusetts Bay. The internal tide in Stellwagen Basin was examined using the high resolution current and isopycnal displacement measurements on the U6 mooring. The internal tidal current component Figure 3.1-2 was isolated by subtracting the predicted surface tidal currents from the observed tidal currents during spring 1991. The internal tidal current ellipses are oriented generally east/west and show amplitude maximal near the surface and near the bottom; the upper and lower level currents are about 180° out of phase.

The water column vertical displacement was inferred by tracking isopycnal

movement inferred two ways; (1) by spatial interpolation between adjacent density time series measurements (DIS) and (2) by dividing density time series with the instantaneous density gradient (ISO). The two different approaches gave the consistent vertical displacement structure results which is presented in terms of harmonic constant distributions (Figure 3.1-3).

The vertical displacement and current results were consistent with each other in defining a first mode internal tide structure. The relative phases between the eastward surface tidal current and the vertical internal tidal displacement indicates that the Stellwagen Basin mooring site was situated within the generation zone of a first mode internal tidal wave. The internal tide appears to propagate westward where it induced strong internal tidal motion at the Scituate Mooring.

3.1.1 Influence of Tidal Processes on Transport and Mixing

Generally speaking, tidal transport processes are most important at spatial scales comparable or smaller than the tidal excursion distance, which is the horizontal distance that water is carried within a tidal cycle. For the 10 cm s^{-1} semidiurnal currents that typify the Bays, the corresponding tidal excursion is 1.4 km. This distance is quite small in comparison with the dimensions of the Bays; hence generally the horizontal motion due to the tides is not an important transport mechanism. The stronger tidal currents in the vicinity of Race Point have correspondingly larger tidal excursions: approximately 5.6 km based on velocities of 40 cm s^{-1}. These motions may be responsible for localized exchange between Cape Cod Bay and the nearby offshore waters. Another region where horizontal tidal transport is important is the mouth of Boston Harbor, where the tidal excursion distance is comparable to the dimensions of the entrance region. Tidal exchange appears to be a dominant mechanism for exchange between Boston Harbor and western Massachusetts Bay (Signell, 1992).

Although the tidal currents have limited influence on horizontal exchange, they are usually the dominant contributors to kinetic energy of flow. Thus, they influence the strength of the bottom-generated turbulence during non-storm conditions. During storms, the motions due to surface gravity waves may exceed those due to the tides and increase the bottom-generated turbulence.

Internal tides have two potentially important effects on mixing. First, they enhance the near-bottom tidal currents by as much as a factor of two over the barotropic tidal velocities, increasing the turbulence level in the bottom boundary layer. Second, they provide a source of shear to the thermocline region, which can lead to vertical mixing in this important region of strong nutrient gradients (Haury, Briscoe, and Orr, 1979).

Analysis of the tidal data showed marked increases in the tidal amplitudes at

some of the mooring locations during the stratified periods, when internal tides were present (see Appendix T, Table T11). Interestingly there were no clear examples of near-bottom tidal currents increasing due to internal tides. Still, the possibility should be considered that internal tidal motions can increase the near-bottom turbulence, possibly leading to sediment resuspension, in the deep waters of the Bays.

There was some evidence of strong vertical shears associated with internal tidal motions which may have lead to mixing within the thermocline. During the ADCP survey at Scituate in August, 1990, velocity differences of as much as 40 cm/s^{-1} were observed across the thermocline due to internal tidal fluctuations. The ratio of shear to stratification during this period indicated that the flow was marginally unstable, i.e., it is possible that small-scale shear instability was occurring. This observation is consistent with the direct observations of shear instabilities by Haury et al., (1979). Shear-induced mixing due to the internal tidal fluctuations may be an important mechanism for transporting nutrients across the thermocline. It could be enhanced by an ambient shear, such as that associated with the buoyancy-driven or wind-driven currents.

See Appendix T for more detailed analysis of the tidal processes.

Table 3.1-1. - Bays M_2 Currents principal axes determined for the winter period from 1 November 1990 to 1 March 1991 by the Least Squares Method. The winter 1989 results are identified.

Station	Depth (m)	Major (cm/sec)	Minor (cm/sec)	Tilt (rel N)	Phase (G)	
Broad Sound	5	16.11	1.41	49.7	219.8	
	18	9.96	1.26	65.9	188.6	
Boston Buoy	5	9.43	-0.66	77.1	204.0	
(1989)	5	9.85	-0.98	76.9	203.9	
(1989)	23	9.10	-0.30	87.1	196.6	
	23	7.71	0.55	-82.0	6.7	(Short)
	33	6.69	0.59	77.0	185.1	
Manomet Point	5	11.26	0.03	-4.9	211.1	
	29	10.61	0.64	-1.3	207.3	
Race Point	5	40.81	3.28	54.3	200.2	
	23	43.47	-1.07	53.1	201.4	
	55	42.64	0.37	62.0	189.1	
	60	30.11	0.46	67.9	184.0	
Scituate	5	7.80	1.21	45.6	202.9	
Stellwagen Basin	75	13.49	0.88	-88.3	8.6	(Short)
	84	7.94	1.64	-84.6	356.9	
North Channel	4	8.28	1.46	78.6	232.5	
	25	13.90	2.08	-89.5	50.1	
	60	11.21	2.86	84.3	237.4	
Stellwagen Bank	4	15.36	-1.27	68.6	231.7	
	25	13.92	-0.16	61.3	42.7	
Cape Cod Bay	4	13.45	-0.24	-4.3	222.6	

Negative minor axis indicates clockwise current rotation. Tilt is the orientation of major axis clockwise from North. Records labeled "short" are less than one month long.

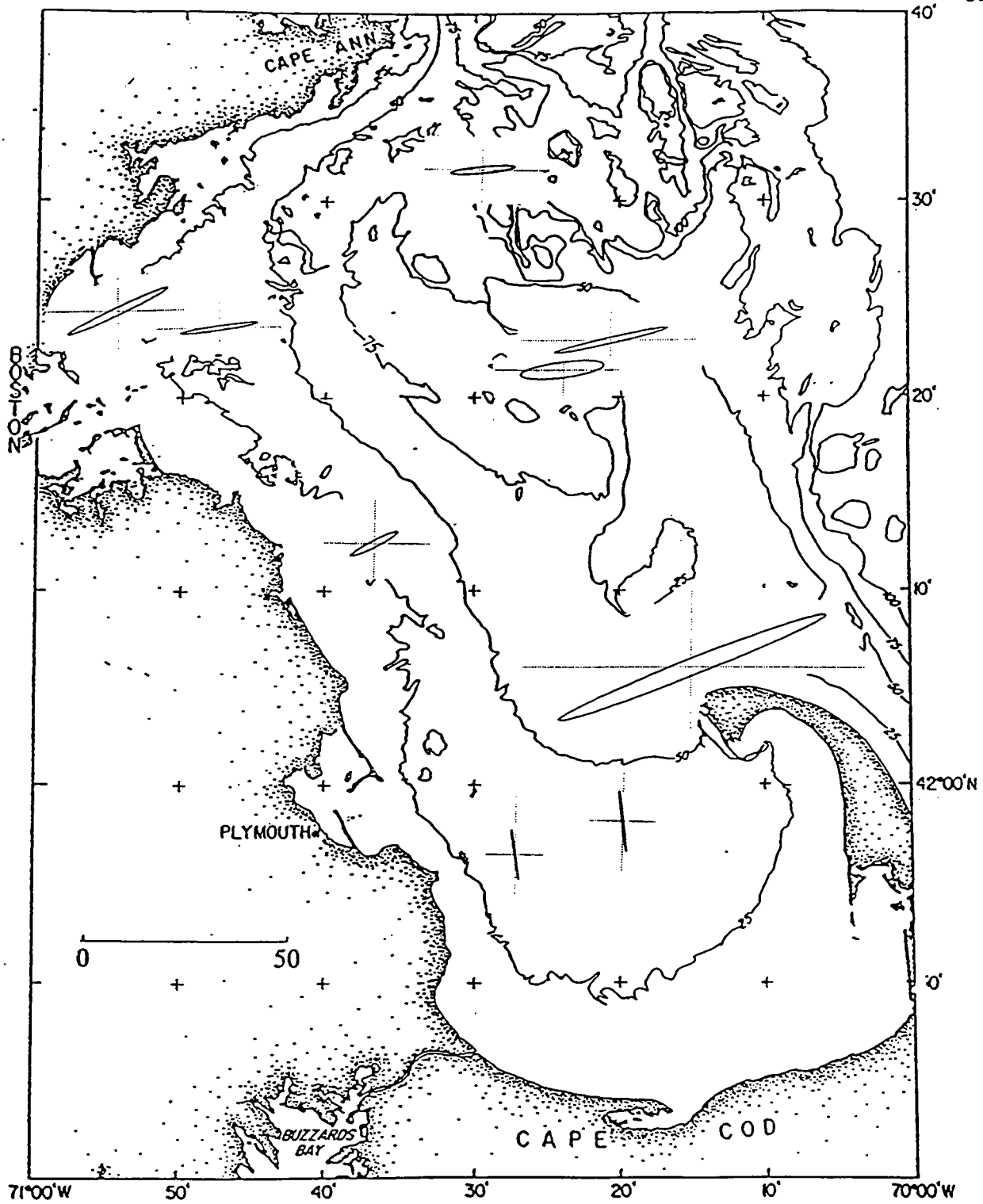

Figure 3.1-1 The M_2 tidal current ellipses for the surface (4 to 8 meters depth) currents based on a least squares tidal analysis of the winter currents (see Table 3.1-1). The center of the ellipse is the mooring location. The scale for 50 cm/sec is shown on the right margin. The current ellipses are shown scaled to about 3.3 times the magnitude of the tidal excursion calculated by integrating the observed currents at the location.

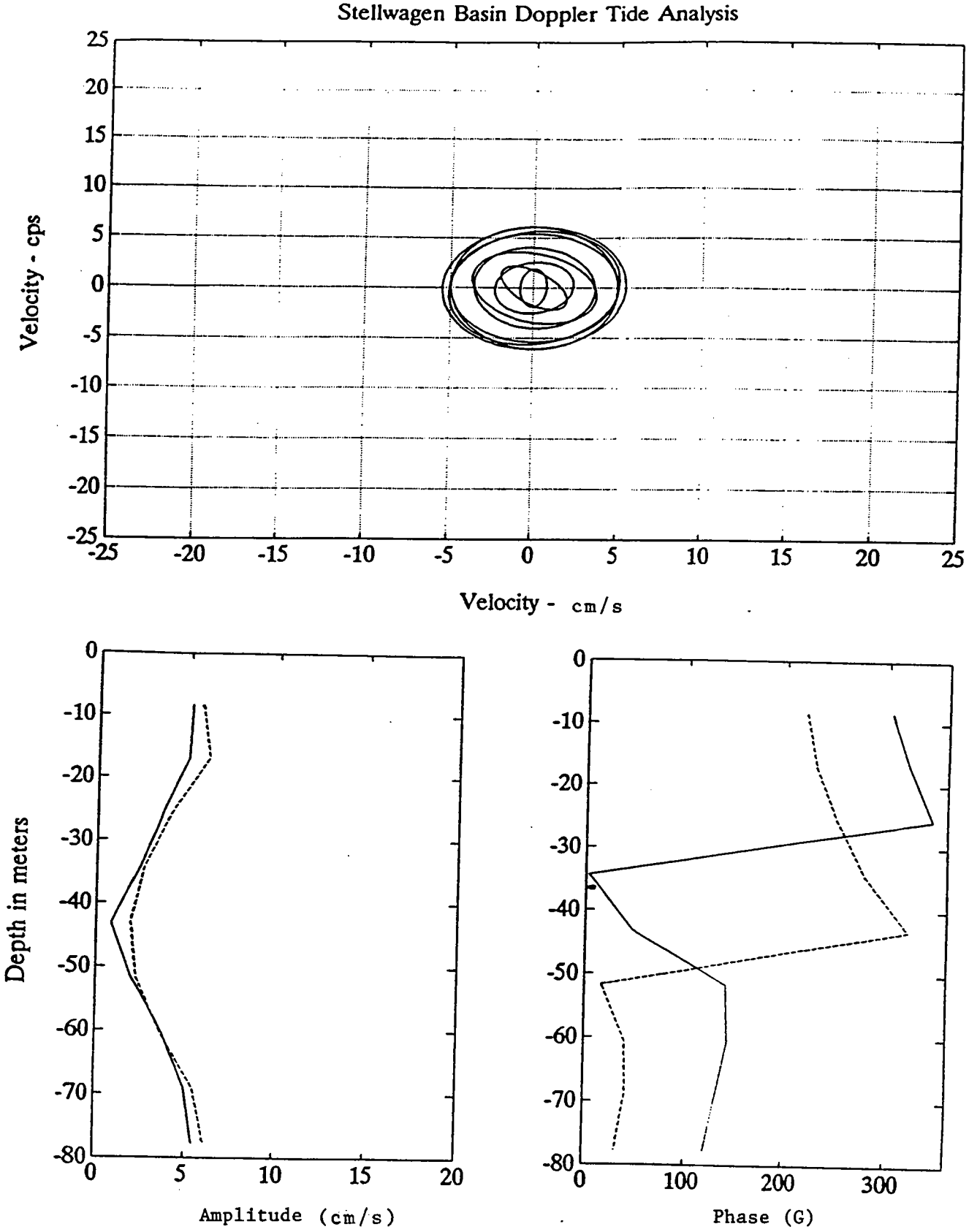

Figure 3.1-2 The semidiurnal (M_2) internal wave current structure in Stellwagen Basin for spring 1991. The internal tidal current ellipses in the top panel show maximum amplitudes at the surface and bottom and a minimum at about 40 meters depth. Note that the bottom and the surface currents are about 180 degrees out of phase; consistent with a classic first mode internal wave structure.

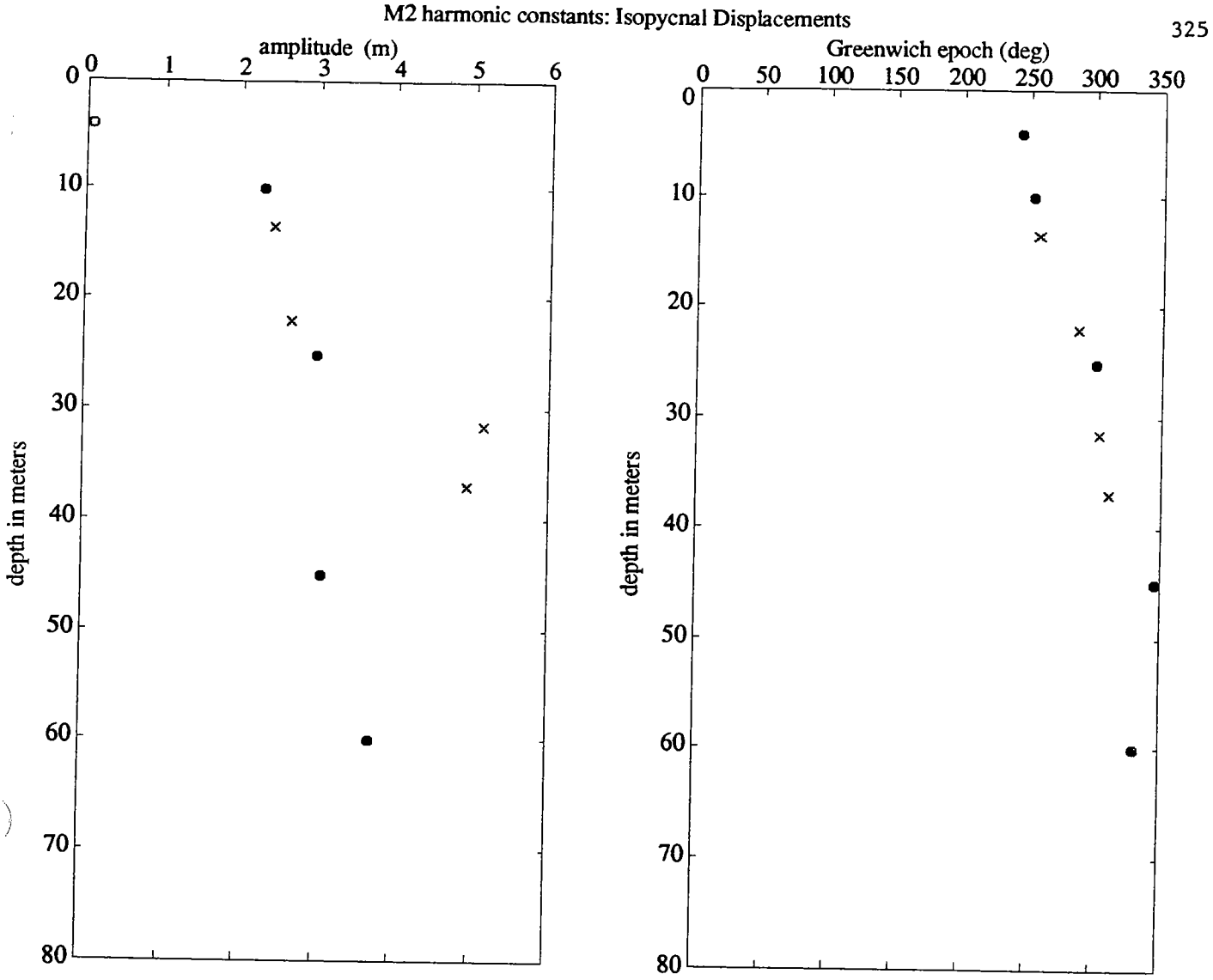

Figure 3.1-3 M_2 harmonic constants for isopycnal displacements at the Stellwagen Basin mooring. The harmonic constants for the ISO (solid circles) and DIS (x) analyses are distinguished (see text).

3.2 Density-Driven Flow

3.2.1 Introduction

The Gulf of Maine is part of the northeast American continental shelf/slope ocean. The general southwestward mean alongshelf flow is thought to be driven by fresh-water-related buoyancy inflow from the north (Chapman and Beardsley, 1989). The alongshelf buoyancy-driven flow enters the Gulf and creates a tendency for cyclonic counterclockwise flow around the Gulf of Maine. Superimposed on the gulf-scale cyclonic flow tendency is a basin-scale flow variability due to water mass structure associated with Georges, Jordan and Wilkinson Basins. The water mass distributions evolve due to seasonally varying of buoyant (relatively fresh) inflows from the Scotian Shelf, relatively salty inflows at depth through the Northeast Channel, winter water mass formation in the interior Gulf, and fresh water runoff around the perimeter of the interior Gulf.

The variability of the basin-scale flow pattern is related to the seasonal evolution of the water masses within the Gulf. During May the large amounts of winter water in Wilkinson and Jordan Basins (Brown and Irish, 1992) are partitioned into warm Maine Surface Water and cold Maine Intermediate Water by the developing temperature-induced thermocline. The density-induced pressure gradients associated with these evolving water mass distributions are responsible for the basin-scale circulation patterns in the western Gulf (i.e., Wilkinson Basin) — as well as forcing Intermediate Water out of southern Wilkinson Basin at mid-depth. In addition, wind-forcing modulates the Gulf-scale buoyancy-driven flows. For example, Ramp et al., (1985) have shown that Gulf-scale wind-forcing is responsible episodic indrafts of deep Slope Water through the Northeast Channel — a process which has its analogue in the Bays.

At different times the Basin-scale flows can reinforce and/or counteract the Gulf-scale cyclonic flow tendency. For example, the maximum intensity of the well known Gulf of Maine cyclonic gyre in spring/early summer is in part related to augmentation by the western Gulf of Maine coastal current(s) which form in response to the large springtime river discharges. The results of Brooks and Townsend (1989) suggest that the eastern Gulf of Maine coastal current is frequently deflected off shore in the region of Penobscot Bay by the shoreward arm of a cyclonic gyre in Jordan Basin. In the western Gulf, the springtime discharges from the rivers help to intensify a coastal current which flows southwestward towards Massachusetts Bay (Franks, 1990).

Thus the southward flow in the western Gulf just seaward of the Massachusetts Bay entrance is part of a general gulf-scale buoyancy-driven circulation pattern which is augmented by a coastal current fed by the episodic river discharges. Franks' (1990)

work suggests that more local wind-forcing will affect the speed and configuration of the western Gulf of Maine coastal current. Wind could have a crucial influence in whether the plume enters Massachusetts Bay or not during a particular time period.

Butman (1975, 1976) found that the density field associated with the river runoff dominated the low-frequency current variability in northern Massachusetts Bay during spring 1973. The source of the majority of the fresh water entering the Bays the during this study was thought to be from the Merrimack River. Thus the dynamics of the buoyant coastal plumes formed by river discharge is a pertinent issue in the study of the Massachusetts Bays system.

Various studies of the dynamics of buoyant coastal plumes (Chao and Boicourt, 1986; Chao, 1987 & 1988; and Garvine, 1987) describe their effects on local circulation. The response of coastal regions to a nearshore low density i.e., buoyant flux has been studied by Csanady (1974), using an analytical model which incorporated either a wedge-shaped or a lens-shaped pycnocline. The model currents circulated anticyclonically around the buoyant water features, whose scales were given by the internal Rossby radius.

The effect of the local wind stress on the development and movement of coastal buoyant plumes is documented by Chao's (1987, 1988) three-dimensional primitive equation model. Downwelling favorable winds produce a downwind coastal jet which elongates and accelerates as it is pressed against the shore. Upwelling favorable winds separate the plume from the coast and retard the plume progression along the coast. An across-shelf, seaward wind accelerates the plume and begins to separate it from the coastline.

Observational evidence is consistent with theoretical and numerical results. For example, Peter Franks (1990), in his study of toxic dinoflagellates distributions, examined the influence and progression of the buoyant coastal plume in the western Gulf of Maine. Franks estimates of the alongshore velocity of the buoyant plume, based on Margules's relation, agreed with the modelled results of Chao (1988). Franks further found that toxic shellfish poisoning occurred more frequently during periods of downwelling-favorable winds and less frequently during periods of upwelling-favorable winds.

The theoretical and observational reviewed above sets a framework for the dynamics of the western Gulf of Maine coastal current which at times enters northern Massachusetts Bay. The following describes the Bays circulation variability during late spring/early summer 1990 when the inflow of the coastal current appears to have had considerable influence on the flow variability in the Bays.

3.2.2 Density-Driven Flow: Spring/Summer 1990

The study described here focuses on the subtidal variability of the Bays currents associated with the density field changes during late spring/early summer; 30 April 1990 and 19 July 1990. The questions addressed include:

- What were the primary forcing agents of the late spring subtidal current variability in the Bays?
- What were the local and remote sources of the buoyancy variability which affected the Bays circulation and stratification?
- How did the changes in the buoyancy field affect the currents in the Bays?
- How did wind forcing modify the density-driven flow?

Vertical density stratification is a major factor in controlling circulation variability. Thus it is important to know the relative importance in temperature and salinity change on density structure change. The measured water properties in the Bays changed significantly during the study period. The combined moored and ship survey observations show that the Bays were noticeably warmer and fresher in July than in late April. The increase in temperature in the Bays was due to the solar warming of the water above the seasonal pycnocline. The decrease in the Bays salinity was due primarily the inflow of relatively fresh water from outside the Bays — some from the coastal current and some from the Gulf of Maine itself.

Despite the freshening of the Bays, the principal increase in stratification strength during the late spring and early summer was due to the general seasonal warming of the upper 20–30 meters (fig. 3.2-1). Stellwagen Basin water property observations show that the general warming-induced stratification increase was augmented on occasion by episodic surface freshening. For example the effects of one such buoyancy inflow are seen near the end of May (fig. 3.2-2).

The variability in the subtidal Bays currents (fig. 3.2-3) in response to buoyancy and wind forcing varies significantly from station to station. (A summary of the statistics for the current variability for this period is shown in Table 3.2-1). The lack of any clear relationship between currents and winds suggests that buoyancy forcing dominates the current variability during late spring/early summer.

Table 3.2-1. Statistics for hourly and subtidal spring/summer eastward and northward subtidal current (cm/s) and wind stress (dyne/cm^2) series for 00:00 30 April 1990 to 00:00 19 July 1990 (UTC).

Station ID	Sensor Depth	Component	Hourly MEAN	Hourly VAR	Subtidal MEAN	Subtidal VAR
BB	40 m	East	0.07	0.17	0.06	0.10
		North	0.10	0.28	0.10	0.18
BS	16 m	East	0.90	56.98	0.92	3.63
		North	-0.28	20.79	-0.28	2.02
SC	16 m	East	-1.24	16.19	-1.24	1.72
		North	0.25	9.01	0.26	1.05
U2	25 m	East	-0.73	97.54	-0.71	11.58
		North	13.26	63.98	-13.24	41.04
U6	14 m	East	-2.00	135.03	-1.99	21.08
		North	-0.49	90.41	-0.46	13.43
	25 m	East	-3.75	94.09	-3.74	16.14
		North	-0.13	62.10	-0.12	10.79
	46 m	East	-3.83	109.52	-3.81	12.42
		North	0.14	28.87	0.14	0.76
	62 m	East	-1.69	162.61	-1.66	0.60
		North	-0.56	27.53	-0.56	3.24
U7	4 m	East	4.45	98.65	4.46	44.85
		North	3.43	239.12	3.46	40.63

The time-averaged currents during this period (fig. 3.2-4) were characterized by the large southward flow into the northern Bays (U2), modest westward flow in the Stellwagen Bank/Basin region (U3, U6), and northeastward flow in northern Cape Cod Bay (U7). The former two suggest inflow and the latter suggests outflow around Race Point. The nearshore stations, Broad Sound (BS) and Scituate (SC), did not have near-surface instruments during this time period. The near-bottom currents, which are quite weak, are offshore and on shore, respectively.

The current variability also differs considerably from site to site. For example, the current variability in Cape Cod Bays (U7) (fig. 3.2-5) is largest and relatively unpolarized in contrast to the significantly polarized current variability in the northern Bays (U2). Although there was generally significant statistical coherence between currents at different depths on the same mooring — even across the pycnocline — there was no significant statistical coherence between subtidal currents at different sites. It appears that during this time of the year, the wind was not a major organizing agent of the spring/summer flow field, except for occasional upwelling along the coast. The flow field had a significant mesoscale (10–20 km) component which was

partially responsible for the low spatial coherence in the flow. As we will show, the mesoscale structure of the spring/summer Mass Bays flow field was due primarily to the patchiness in the density field.

The mean moored current pattern suggests a Bays-scale flow pattern. This pattern is characterized by inflow into northern Massachusetts Bay and outflow around the tip of Cape Cod. Corroborating evidence includes a surface drifter trajectory from 24–29 May 1991 (fig. 3.2-6), which shows that there can be inflow around Cape Ann into the Bays. Although the latter flow episode actually occurred in May 1991, a satellite sea surface temperature (SST) image from 27 May 1990 during the study period (fig. 3.2-7) shows that a warm band of water extended from the coast north of Massachusetts Bay southward into the Bays. Franks (1990) showed that fresher water was generally warmer water and thus could be tracked during spring and early summer using satellite SST images. Thus we conclude that in spring/early summer 1990 the coastal current, fed by episodic river discharge, flowed around Cape Ann and entered the Bays through the passage north of Stellwagen Bank.

The north to south flow through the Bays was convincingly demonstrated by the May 1990 drifter trajectories (fig. 3.2-8). A drifter launched 15 May 1990 (fig. 3.2-9) also moved southward, before becoming entrained in what was a baroclinic eddy, associated with a warm, fresh patch of water located in Cape Cod Bay. The drifter remained in the eddy for 30 days(!!) before escaping from the Bays around Race Point.

The Bays mesoscale velocity structure, seen in some of the drifter trajectories, was in many cases associated with the low density patchiness as revealed by the CTD-derived dynamic height field. For example, the dynamic height field in the northern portion of the Bays, during the 28–29 April 1990 cruise (fig. 3.2-10) exhibits a nearshore dynamic high about 30–35 km east-northeast of Boston. The high was related to a patch of warmer, fresher water ($T \geq 7.0°C$; $S \leq 32.0$ psu). The map also reveals a dynamic low on the eastward side of the channel north of Stellwagen Bank, directly east of a high, which is related to a saltier, cooler patch of water ($T \leq 7.0°C$; $S \geq 32.1$ psu). The geostrophic flow section between Cape Ann to Race Point (fig. 3.2-11a), clearly shows the lateral structure of the geostrophic shear associated with the inflow through the North Passage. While many of the mesoscale features in the dynamic height maps are real, some near Stellwagen Bank are due to aliasing by internal wave variability.

The geostrophic shear field during the 24–26 July 1990 survey was stronger than that during the April survey. The dominant feature during this survey (fig. 3.2-12) was the relatively strong dynamic high in Cape Cod Bay. The high was related to a patch of relatively warm, fresh water. Another very strong geostrophic shear feature over northern Stellwagen Bank is also present. The structure of the more robust eddy in Cape Cod Bay is depicted in the Figure 3.2-13 geostrophic shear flow

sections.

The primary mechanism affecting salinity during spring/summer was the inflow of relatively freshwater from the Gulf of Maine into the northern half of the Bays. Some of the inflow water was from the Wilkinson Basin portion of the Gulf of Maine and some was from the coastal current. Local and remote rivers are the primary sources of the episodic freshening which contributed to the surface-intensified smaller scale current variability in the Bays. Of the major rivers which discharge into the Gulf of Maine, the nearest are a combination of the smaller Charles River/MWRA treatment plant and the larger Merrimack river discharges. The volume of freshwater in the Bays increased by about 12 percent between the April to July surveys (see Section 3.4).

Because of the importance of the freshwater portion of the buoyancy input, (the other component of buoyancy being temperature) we focus the discussion on freshwater distributions rather than salinity. In particular, a freshwater index was calculated for each CTD station, according to

$$F = \frac{S_o - S}{S_o} ,$$

where the selected reference salinity S_o was 34.3 psu; the maximum salinity measured in the Bays during this time period. Therefore, this analysis focuses on the total volume of freshwater which had mixed with deep Gulf of Maine water. The freshwater is from the local region, possibly from eastern Gulf of Maine, and surely from outside the Gulf.

In order to emphasize the influence of local river discharge on upper water column buoyancy distribution, the freshwater index was integrated over the upper 30m thus yielding the thickness of 100% freshwater. The map of freshwater thickness in the upper 30m for the April 1990 survey (fig. 3.2-14a) probably shows the influence of a recent Charles River/MWRA discharge pulse. The July 1990 map (fig. 3.2-14b) documents a large concentration of freshwater in Cape Cod Bay and an apparent recent inflow of a relatively salty patch over Stellwagen Bank.

Influence of Winds on Buoyancy Driven Flow

The wind stress during the study period was generally weak (<0.5 dynes/cm^2). Thus with the exception of some wind-induced upwelling (and downwelling) observed at the coastal stations (see next section), the subtidal current variability due to the wind stress, i.e. wind-forced flow, was generally weak relative to the density-related flow. However there were a few occasions where wind-forced response could be detected.

The response of the (Stellwagen Basin U6) currents to wind was normally minimal with the exception of several events. For example, a southward wind event, with stress in excess of 1 dyne/cm^2, occurred on 4–5 May, 28–29 May and 9–10 June 1990 (fig. 3.2-3). During the 28–29 May event, the 14 and 26 meter observations showed a noticeable increase in the southward currents. In this particular case there was a sharp drop in the salinity at 4, 10 and 25 meters at U6, suggesting that a patch of fresher water from an earlier river discharge event was advected into the region of the mooring. On occasion in the Cape Cod (U7) 4 meter current measurements exhibited flow events which exhibited Ekman-like current responses (fig. 3.2-3).

Conceptual Model

We summarize our conclusions in terms of a conceptual model for the nontidal circulation in Massachusetts and Cape Cod Bays during the spring and early summer 1990. The Bays-scale and mesoscale flow components are highlighted.

Bays-scale Flow:

The general north to south mean flow through the Bays, order 5 cm s^{-1} during the period from 30 April 1990 to 19 July 1990 is associated with the western Gulf of Maine coastal current and the larger-scale Gulf of Maine circulation in Wilkinson Basin. The Bays-scale flow is induced by the westward deflection of generally southward Gulf of Maine flow into the northern Bays. Within the Bays the general flow appears to miss the Broad Sound region before moving southward along the western coast of Massachusetts Bay toward Cape Cod Bay. The flow enters Cape Cod Bay to the extent that hydrographic and wind conditions permit before exiting the Bays around Race Point.

Mesoscale Flow Variability:

The near surface, low density water inflow to the Bays results in the formation of small scale (5–10 kilometer), density-related (i.e. baroclinic) currents within the Bays. The episodic nature of the river discharge, combined with the wind effects, are probably responsible for the formation of the small-scale, low-density patches which influence the subtidal circulation of the Bays. The sources of freshwater, which contribute to the small-scale baroclinic flows in the Bays, come from the Charles River, the Massachusetts Water Resource Authority (MWRA) treatment plant discharge, and inflow from the Gulf of Maine (which itself includes water from the northern rivers).

The relatively small Charles River and MWRA freshwater sources can be important locally (northwestern portion of the Bays) in the early stages of the evolution of the seasonal pycnocline (and during winter). Satellite imagery and drogued drifter trajectories show the pathway by which Merrimack River discharge enters the Bays. We estimate that the plume from the Merrimack moves down the coast with a speeds

in the range of 5–15 cm s^{-1} (without accounting for wind effects) as is evidenced by drifter, satellite and water property data. These velocities are consistent with those found by Franks (1990) and the model results of Chao (1987). Therefore our estimates indicate that would take about 15–20 days for a water parcel to travel from the mouth of the Merrimack to reach the central part of Massachusetts Bay.

The episodic river discharge results in the formation of patches of relatively fresh water which are advected through the Bays by the Bays-scale flow. The increased surface warming during the summer months also helps to increase the density contrast of the patchy low density features in the Bays (especially in Cape Cod Bay during July). These patches of low density water have an associated baroclinic circulation which disrupts the general Bays-scale circulation in the vicinity of the features. The geostrophic circulation associated with these eddies is one of the principal sources of the subtidal variability in the Bays. So while the density-related flow variability dominates during this part of the year, the winds do appear to modulate the movement of the low-density patches and associated currents.

Further study into the influence of the low-density input in the Bays during other seasons may help to distinguish between the influences of the freshening due to the Gulf of Maine inflow and the smaller magnitude river discharge from both local and remote sources. By using the current data at Race Point and Cape Ann during spring 1991, a more accurate time calculation should be possible. Continued analyses of the complete data set should provide insight into the relation of the general Bays circulation with the general circulation of the Gulf of Maine as well as what effect any local perturbations may have on the Massachusetts and Cape Cod Bays system.

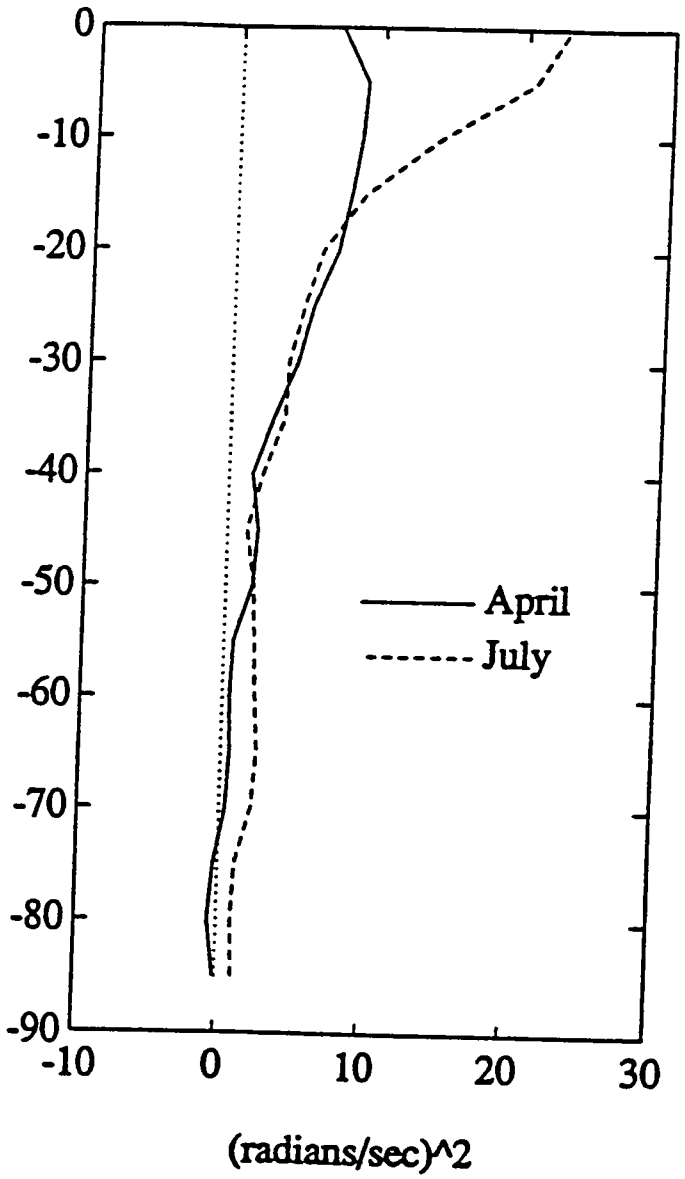

Figure 3.2-1. Basin-averaged Brunt-Väisälä frequency squared from the April 1990 and July 1990 hydrographic cruises. The profiles have been depth-averaged over 5 meter intervals to reduce the noise.

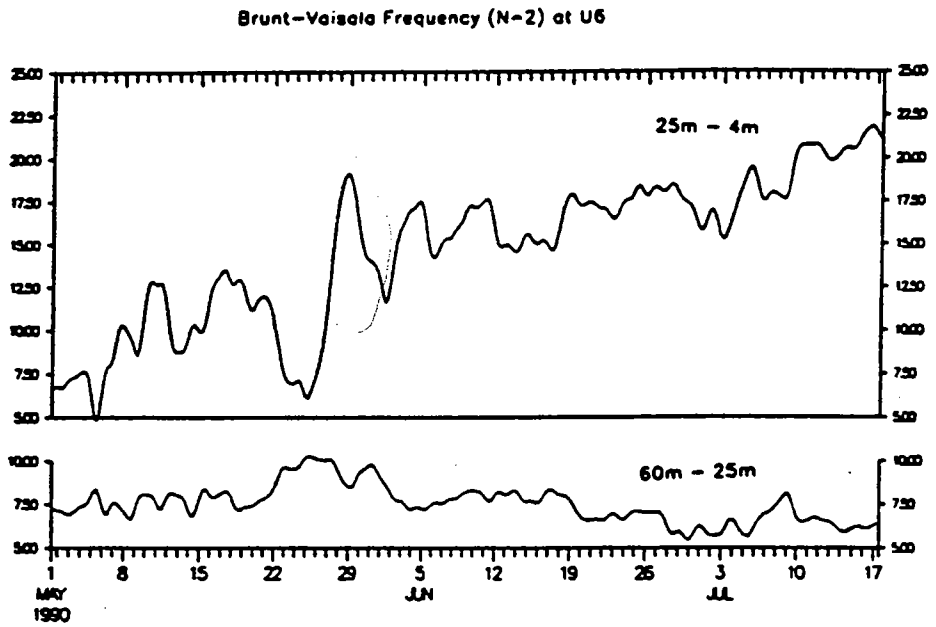

Figure 3.2-2. Subtidal Brunt-Väisälä frequency squared (stratification) based on time series measurements in Stellwagen Basin (U6). The upper series represents an average over the 4m and 25m depth range. The lower series is an average over the 25m and 60m depth range. The sharp increase in stratification of the upper water column in late May was due to freshwater inflow.

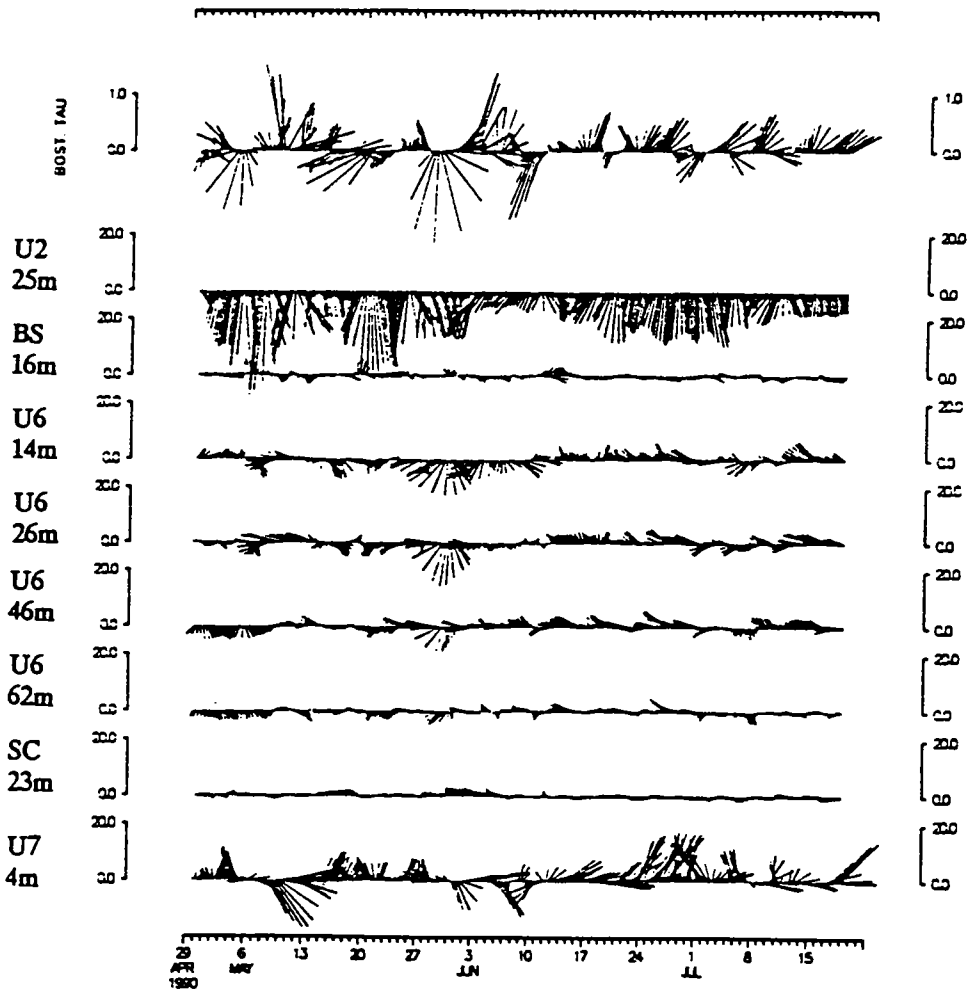

Figure 3.2-3. Six-hourly vectors of the subtidal currents and windstress between 30 April 1990 and 19 July 1990. True north is towards the top of the page; currents are in cm/s; windstress is in dynes/cm^2.

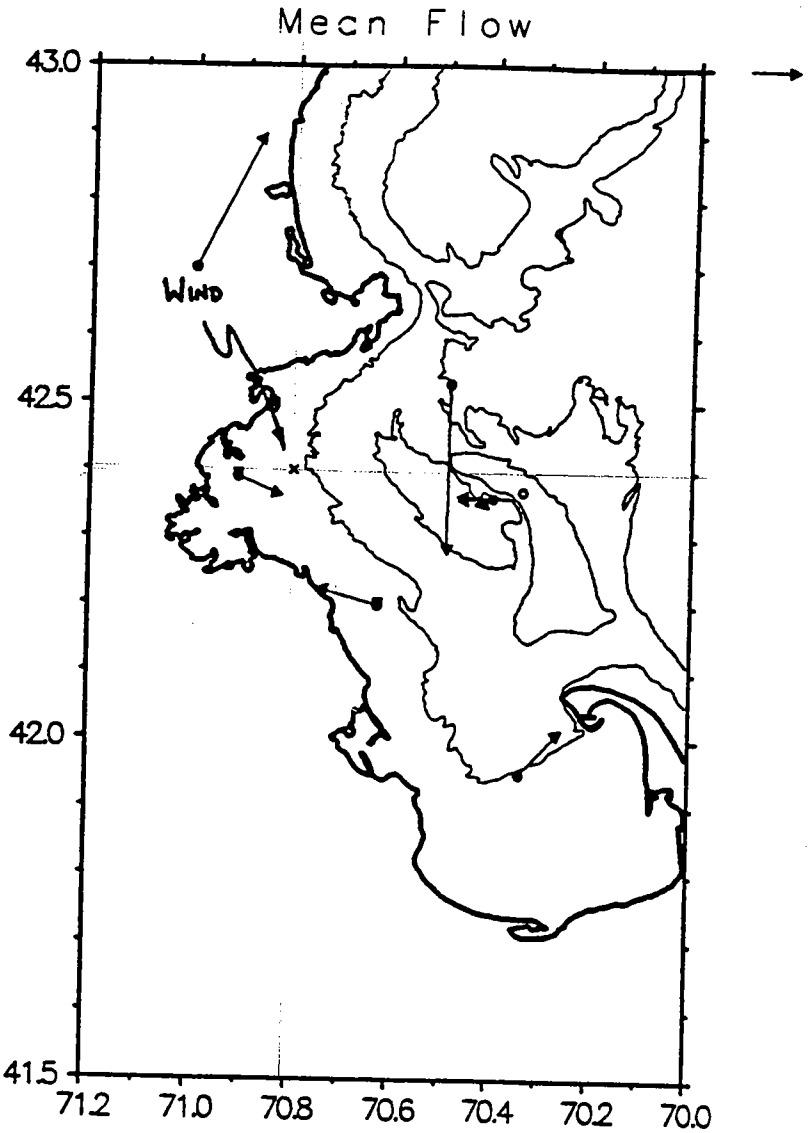

Figure 3.2-4. Mean currents and windstress for the period 30 April–19 July 1990. The amplitudes of Broad Sound and Scituate mean currents have been amplified five times for clarity. The arrow in the upper right corner is the 5 cm/s and 0.05 dynes/cm^2 scale for current and windstress respectively.

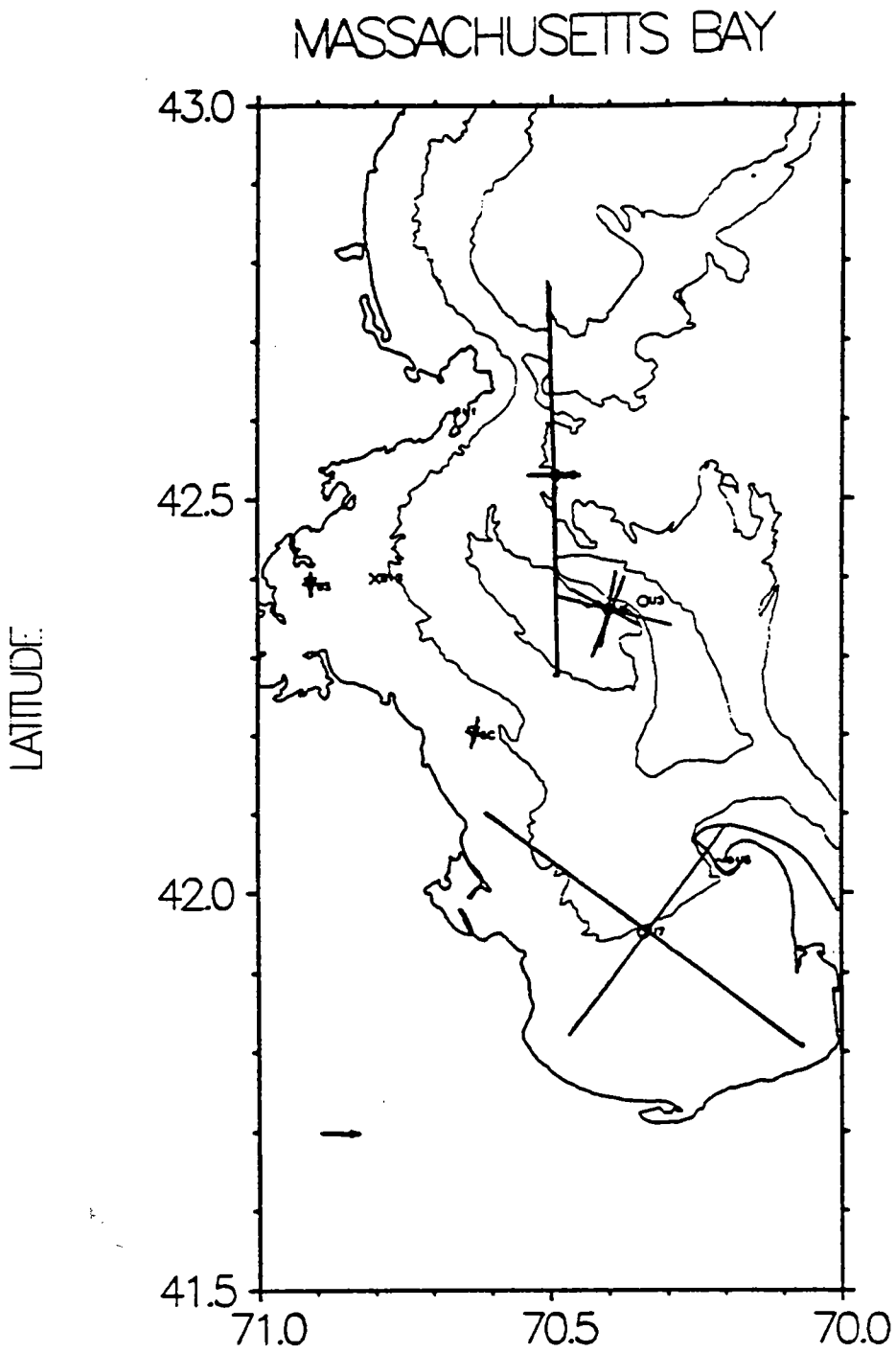

Figure 3.2-5. Principal axes of subtidal current variances for the period 30 April–19 July 1990. Broad Sound and Scituate current variances have been amplified five times for clarity.

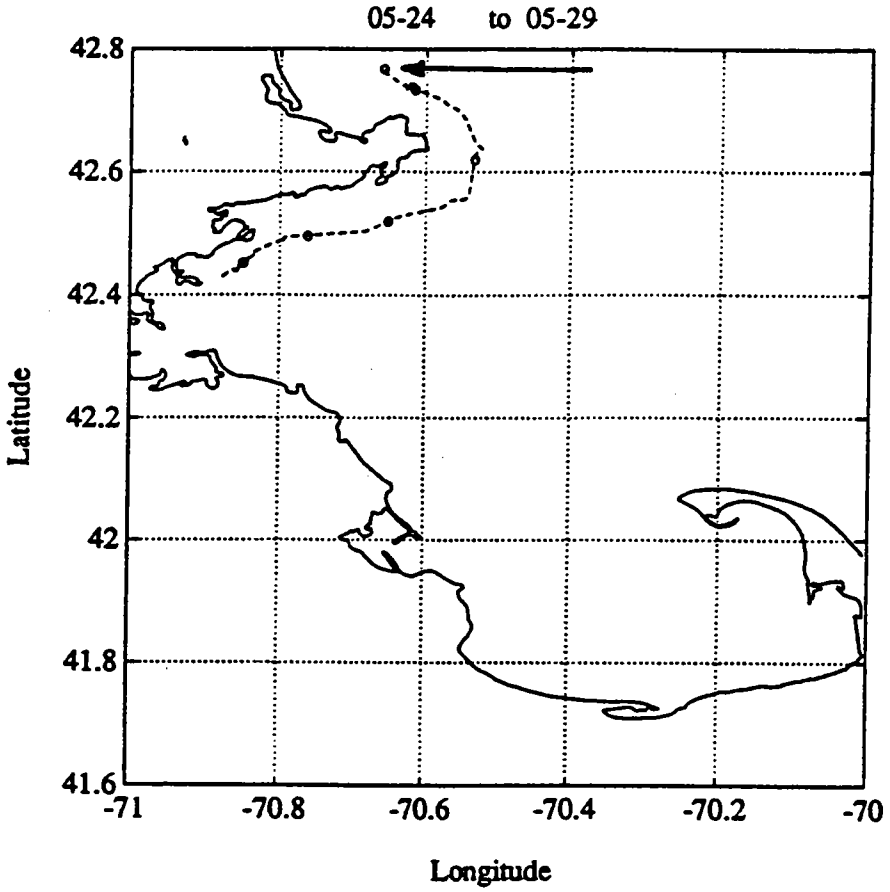

Figure 3.2-6. Surface drifter trajectory for 24–29 May 1991. Drifters were drogued at 10 meters. The launch point is indicated by the arrow and dots locate daily positions.

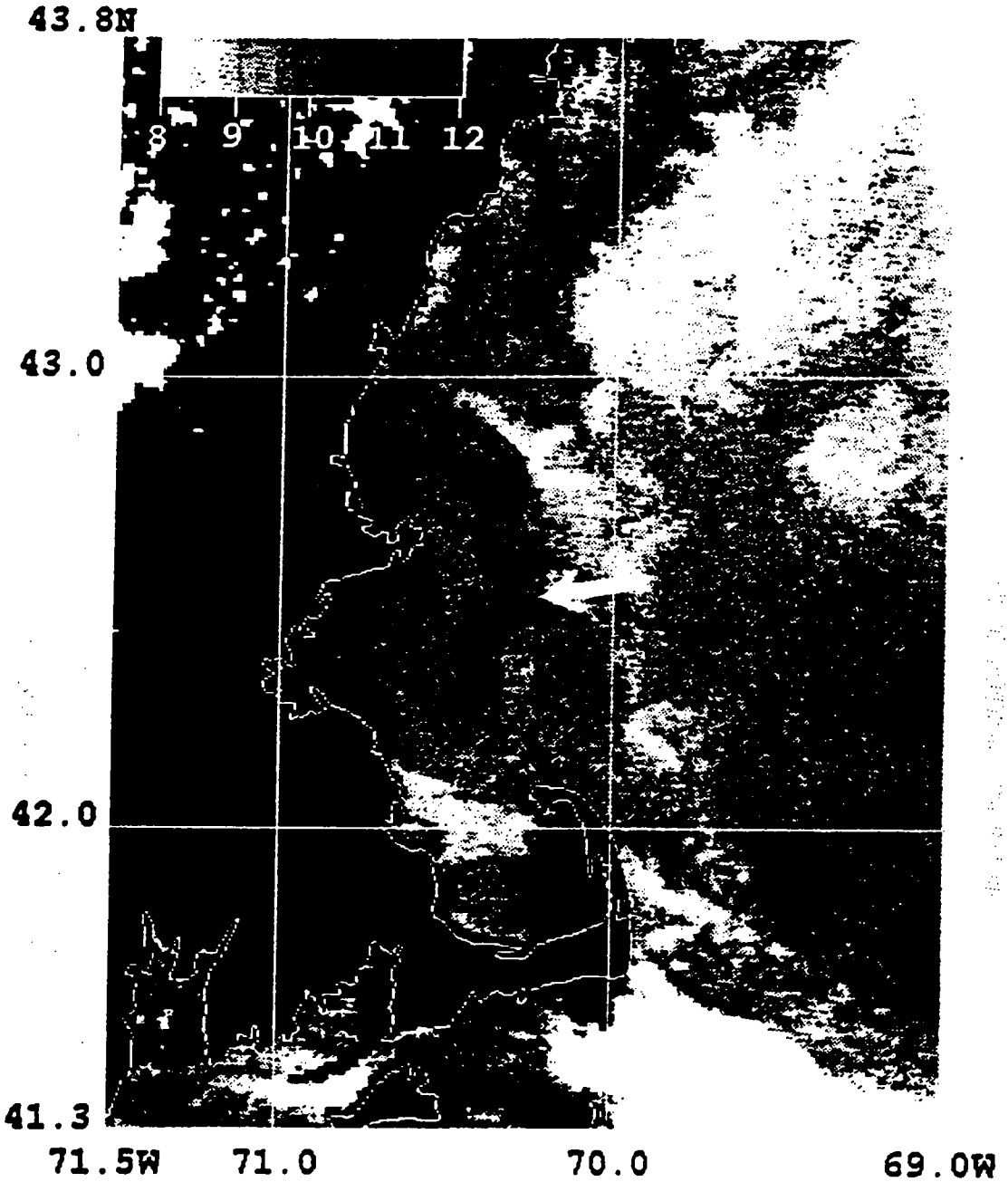

Figure 3.2-7. Satellite infrared sea surface temperature image from 27 May 1990. Temperature scale is nonlinear and indicated on the image.

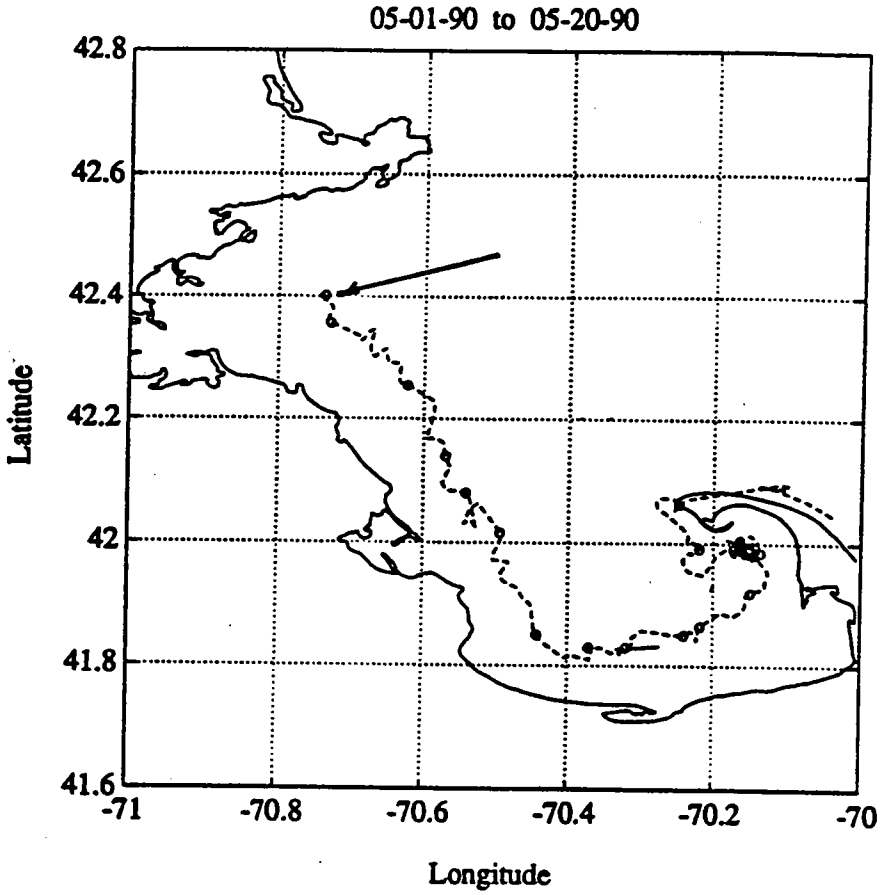

Figure 3.2-8. Surface drifter trajectory for 1–20 May 1990. Drifters were drogued at 10 meters. The launch point is indicated by the arrow and dots locate daily positions (0000 UTC).

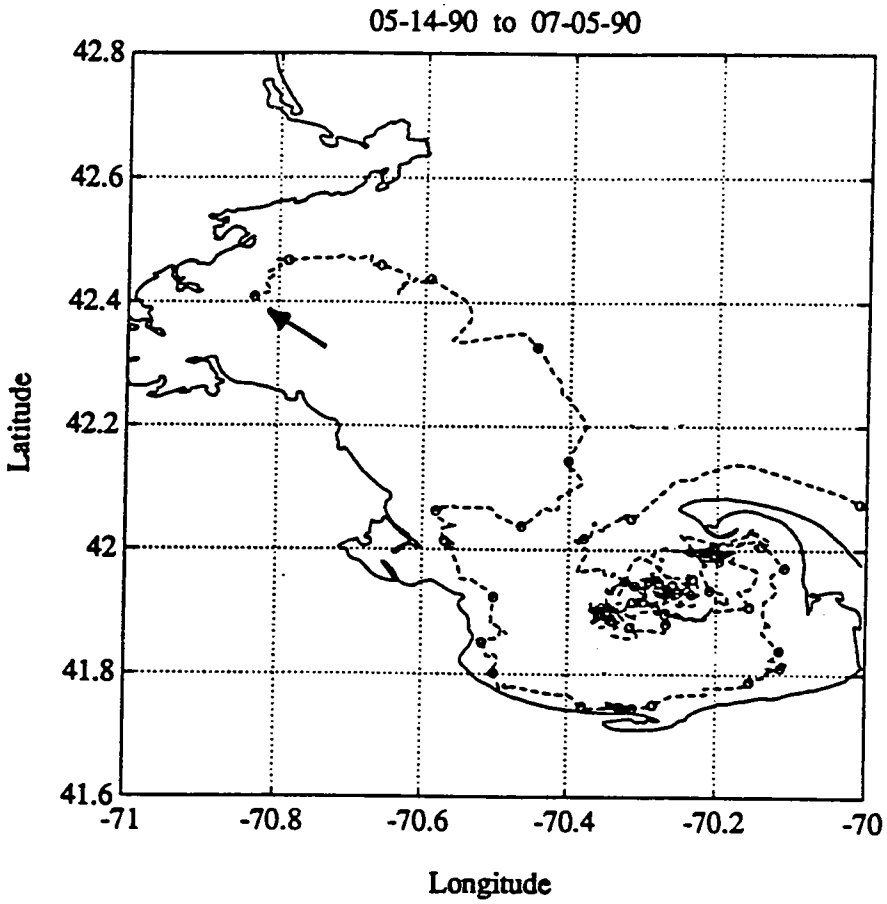

Figure 3.2-9. Surface drifter trajectory for 14 May–5 July 1990. Drifters were drogued at 10 meters. The launch point is indicated by the arrow and dots locate daily positions (0000 UTC).

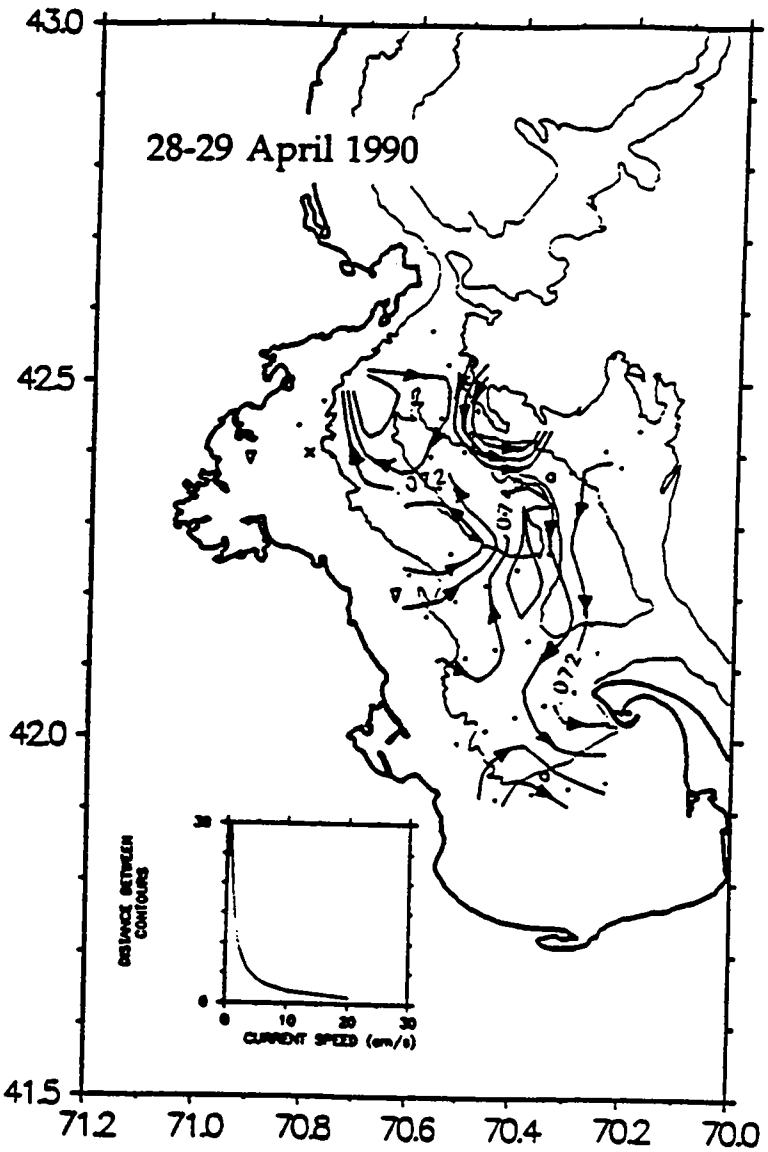

Figure 3.2-10. Surface dynamic heights relative to 30m for 27–28 April 1990. Units are in dynamic centimeters; contour interval is 0.2 dyn. cm. The direction of the geostrophic flow is indicated by the arrows; the flow speed can be inferred from the graph in lower left.

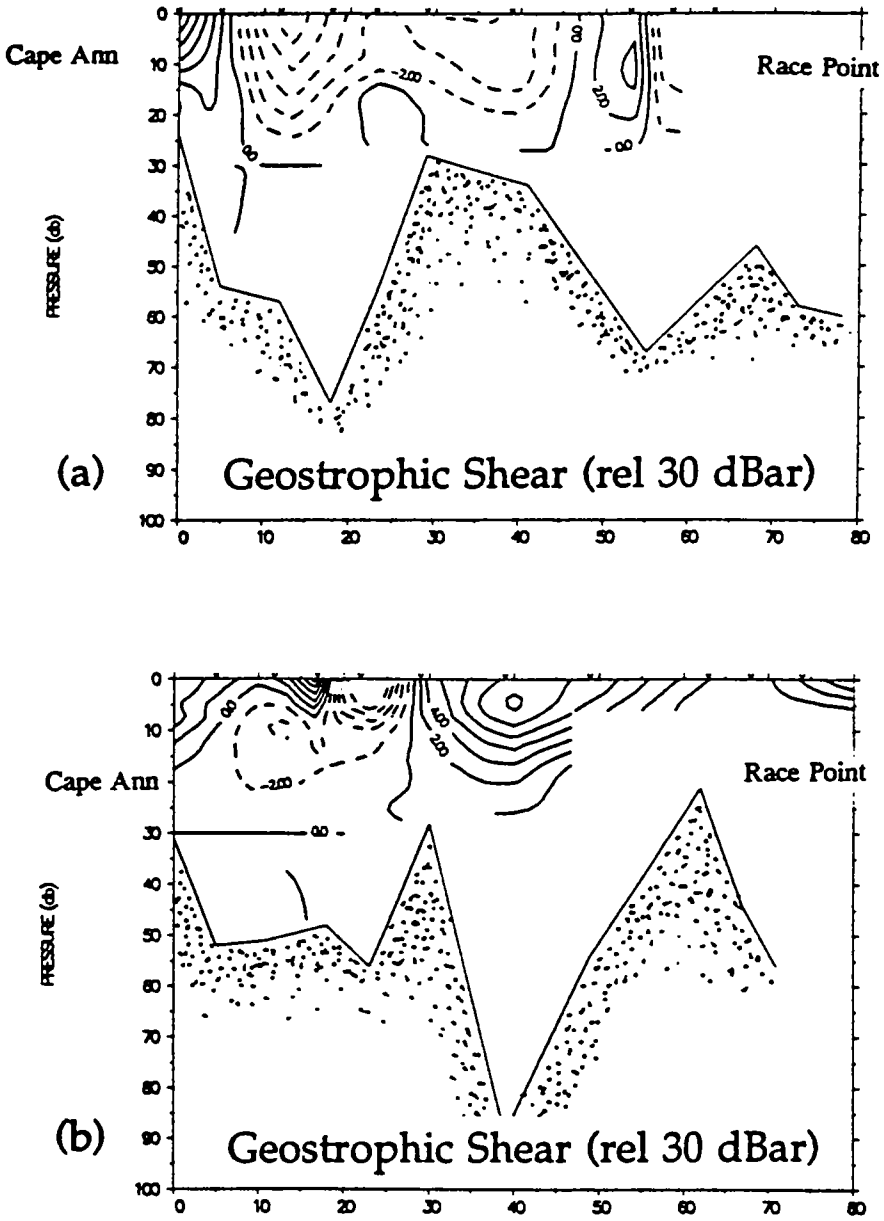

Figure 3.2-11. Vertical section of geostrophic shear (relative to 30m) from Cape Ann to Race Point for (a) 28–29 April 1990 and (b) 24–26 July 1990. The contour interval is 2.0 cm/s. The dotted lines (negative values) indicate flow out of the page.

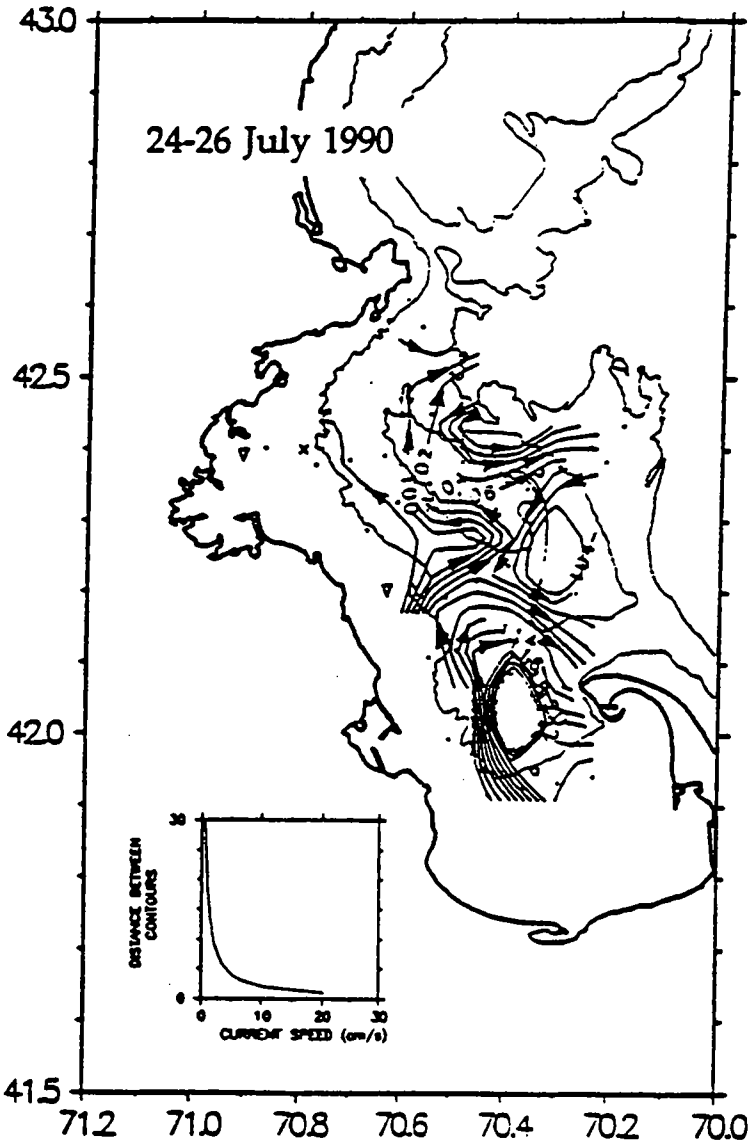

Figure 3.2-12. Surface dynamic heights relative to 30m for 24–26 July 1990. Contour interval is 0.2 dyn. cm. The direction of the geostrophic flow is shown by the arrows; the flow speed can be inferred from the graph in lower left.

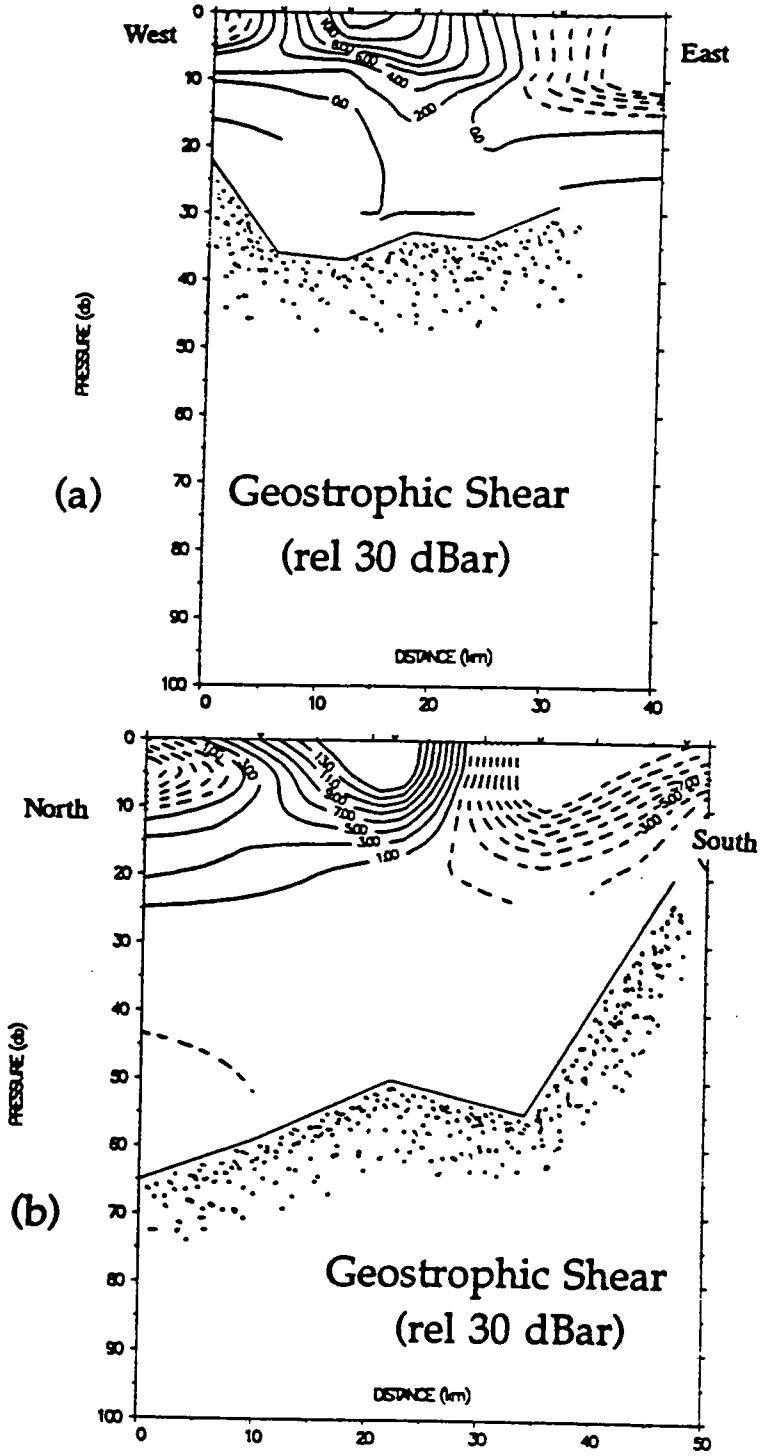

Figure 3.2-13. Vertical sections of geostrophic shear (relative to 30m) in Cape Cod Bay for 24–26 July 1990. (a) East-west section; (b) North-south section. The dotted lines (negative values) represent flow out of the page.

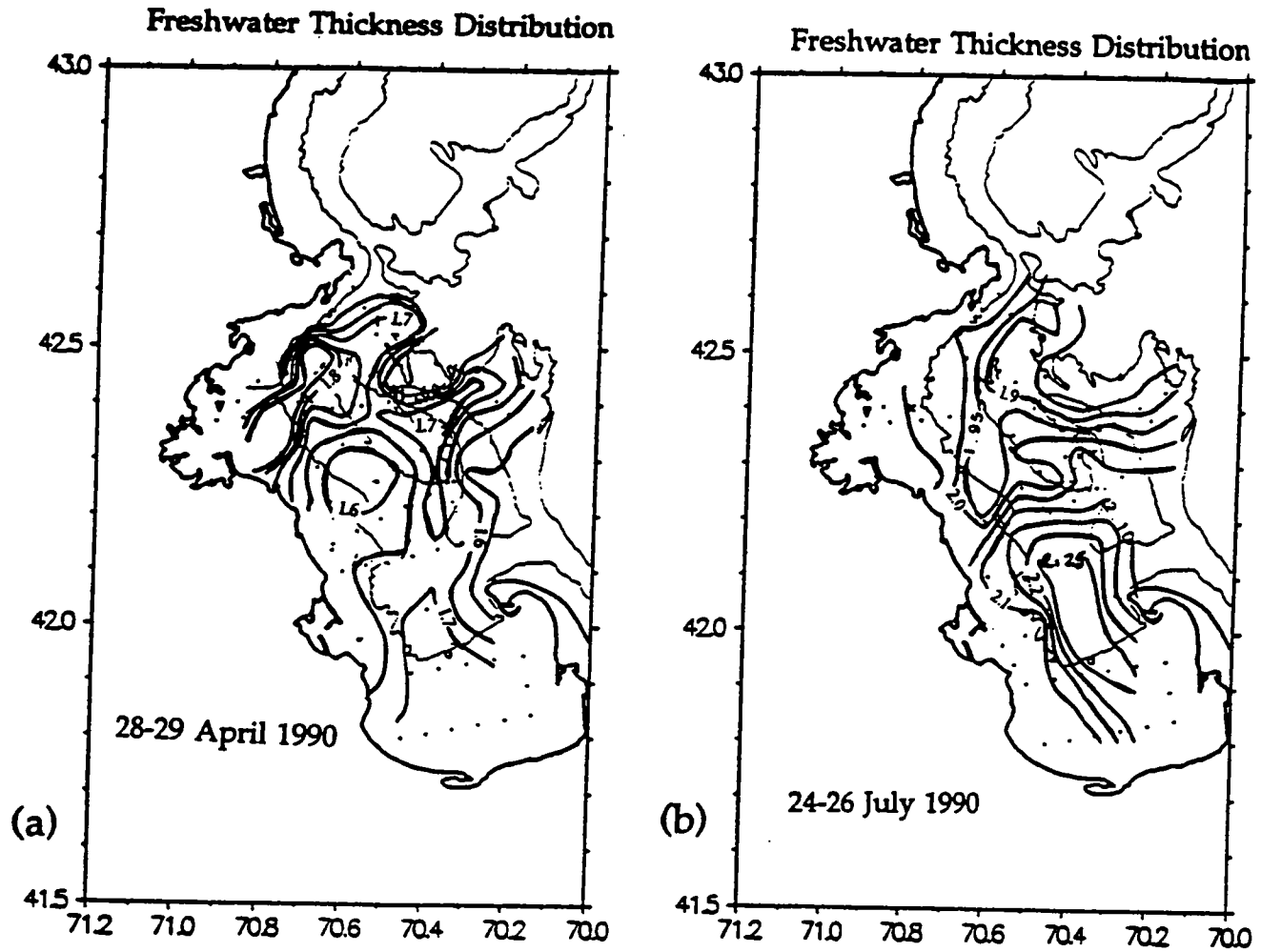

Figure 3.2-14. The distribution of freshwater thickness in the upper 30m for (a) 28–29 April 1990 and (b) 24–26 July 1990. Contour interval is 0.05 meters.

3.3 Wind-Driven Response

Wind-stress is an important driving force for the motions in the Bays, as well has having a marked influence on water properties due to upwelling, downwelling and vertical mixing. Previous work by Butman (1975) indicates a significant response of the sea level to along-bay (NW–SE) winds, and model results by Wright et al. (1986) indicate significant along-bay currents in response to along-bay winds. One of the important objectives of the field program was to document the along-bay response, and to determine whether it has an important influence on transport and exchange in the Bays. The measurements did indeed reveal an energetic response to along-bay winds, largely consistent with predictions based on earlier studies.

Less was known about the response to cross-bay winds at the outset of the field program. The model results of Wright et al. (1986) indicate a weak response in the Bays to SW wind forcing, although there is a large response of the Gulf of Maine as a whole. The measurement program did show a significant influence of cross-bay wind stress, particularly with respect to upwelling and downwelling in the coastal regions.

The spatial scales of winds in this region tend to be large relative to the size of Massachusetts Bay. However differences in wind stress were observed between sensors at Logan Airport, the Boston Buoy and Otis Air Force Base on Cape Cod. Some of these differences are due to measurement errors and/or local effects. But some may be due to significant spatial variations in the wind stress that could influence circulation. We did not resolve those variations well-enough to consider their effects. Thus, for the purpose of this discussion it will be assumed that the winds are uniform, using the winds measured at Logan Airport or the Boston Buoy to characterize the Baywide wind field.

Wind records at Logan and the Boston Buoy indicate that the dominant wind directions are NW and SW, with SW winds being more frequent in the summer and NW winds in the winter (fig. 2.1-1). There are occasional strong winds from the NE associated with storms. The winds tend to be stronger in the winter, with the magnitude of stress averaging 0.8–1.2 dyn cm^{-2} compared to summertime averages of 0.2–0.4 dyn cm^{-2}. The correlation timescale of the winds is quite short, estimated at 0.7–1.1 days, with slightly longer timescales during the summer. The persistence timescale, estimated by the zero crossing of the autocorrelation function, is 1–4 days, the larger values occurring during the summer. The short timescale of wind events means that although the response may be energetic, the excursions accomplished by those motions will not be large. For example, a strong wind-driven current of 10 cm s^{-1} that persists for 1 day will result in an excursion of 9 km. Such a displacement is significantly less than the 50–100 km scales of the Bays. Thus these wind-driven displacements are usually insufficient to cause large-scale exchange be-

tween the Bays and the adjacent Gulf of Maine. The wind-driven motions are most effective in redistributing the water within the Bays.

The following describes the wind-driven response of the Bays as seen in the pressure and current observations during times when the density-related flow variability was less important.

3.3.1 Baywide Response to Wind Forcing — Pressure Measurements

A statistical analysis of the Bays pressure and pressure difference fields is based on observations from late autumn-early winter period of 26 October 1990 through 14 January 1991 when there was particularly detailed coverage of the Bays pressure field. During this time of the year, the density stratification is relatively weak (see fig. 2.2-7) and the wind-forced response of the Bays was stronger than at other times in the year. This can be seen in the relatively large amplitudes of the pressures (fig. 2.2-12). For this analysis, a linear trend was removed from each pressure record to emphasize the wind driven variability and minimize contamination from drift in the pressure measurements.

The visual similarity of the pressure records is very obvious in the time series comparison (fig. 2.2-12). Closer inspection reveals that the more western and northern stations have larger fluctuations. This spatial similarity is quantified in terms of an empirical orthogonal function (EOF) analysis of the pressure field variations (see Appendix P). This analysis extracts that part of the pressure field that moves in unison (i.e., is correlated). The amplitudes of the pressure variations, associated with the primary pattern (i.e., mode-1), are contoured in Fig. 3.3-1. Based on the strong visual similarity of the records, it is not surprising that the primary EOF mode explains 94.6% of the total pressure variance. Thus in this case, sea level in the Bays is heaving up and down in unison with an amplitude of about 10 cm. The temporal variation of the mode looks very much like the pressure time series themselves (fig. 2.2-7). The primary pressure EOF is most highly correlated (0.86) with the across-Bays windstress. It has been shown that the large scale Gulf of Maine pressure field is also more strongly coupled to the across-Bays (i.e., along-Gulf) component of the windstress than to the along-Bays (i.e., across-Gulf) windstress component. Thus we find that the Bays pressure field variability is an integral part of the larger scale Gulf of Maine response to windstress.

Despite the similarity, there are measurable differences in the pressures (fig. 3.3-2). Pressure differences are a proxy for "geostrophic" ocean currents; those currents for which earth rotation is important. The temporal variability in the pressure differences is largest at periods between 2 and 5 days. A selected set of pressure difference time series (fig. 3.3-2) have been subjected to a statistical analysis similar

to that of the pressures. The pressure difference EOF analysis shows that the first and second EOF modes (57.7%, 29.2%) explain nearly 90% of the pressure difference variance. The first EOF mode inflow (or outflow) pattern (fig. 3.3-3) involves more of the bays than the second EOF mode which appears to be localized around Stellwagen Bank. The first EOF mode is more highly correlated (0.91) with local wind stress than the second EOF mode (0.60). Therefore, about 59% of the geostrophic flow (i.e., pressure difference) variance is wind-forced — a result somewhat larger than a similar analysis of measured currents.

3.3.2 Baywide Response to Wind Forcing—Moored Current Measurements

The influence of the winds on the currents is best exemplified by the wintertime conditions at Scituate (fig. 3.3-4), where the along-bay flow is highly correlated with along-bay winds. The correlation coefficient between along-bay winds and along-bay currents at Scituate is 0.75 for this period. Although this location shows the highest correlation with the wind, the moored records tend to show significant correlations throughout the year, indicating an important although not always dominant role of the wind in driving the flow in the Bays.

A simple statistical representation of the wind-driven currents is obtained by covariance analysis between the winds and currents. The analysis is based on the model $u_{\text{water}} = \alpha u_{\text{wind}}$, where α is the transfer function. Using complex covariance analysis, α includes the magnitude and direction of response. It was found that the character of the response depends sensitively on the wind direction, so separate analyses were done for the across-bay (SW–NE) and along-bay (NW–SE) directions. Due to seasonal variations in the response of the Bays to winds due to changes in stratification, the response was analyzed separately for the individual seasons, (as defined in Section 2.2). The results of this analysis are presented in Table 3.3-1 and figures 3.1-5 and 3.1-6.

Response to along-bay winds (NW–SE)

It was found, not surprisingly, that there was a more energetic response to along-bay winds than across-bay winds. Fluctuations in this direction were generally associated with northwesterlies, so the plots of the transfer function represent a "typical" northwesterly event of 1 dyn cm^{-2} or roughly 14 knots (fig. 3.3-5). The response was stronger during the summer and fall than the winter and spring, presumably because stratification reduced the influence of friction on the wind-driven flow. The response was largest during the summer, when the NW winds were found to produce a large response in the surface waters at the Boston Buoy, Scituate and U2. The maximum response was at Scituate, with a transfer coefficient of 14.4 cm s^{-1}

per dyn cm^{-2}. The large response at U2 may be spurious, since the correlation with winds was not high at that location.

The general character of the response to NW winds persisted through the rest of the year, with the exception of the flow at U2, which showed no significant response during the fall and winter periods. (There were no data at the U2 surface instrument during the spring of 1991). By continuity, water still must have been entering Massachusetts Bay during these periods, but apparently the inflow was confined more closely to Cape Ann. The addition of instruments at Race Point and Manomet allowed the response there to be observed during the fall, winter and spring periods. Of particular interest are the Race Point data, which show deep outflow and surface inflow in the fall, switching to outflow through the whole water column during the winter and spring periods.

A downwelling response was suggested by the currents at the Boston Buoy and Manomet during all seasons except for the winter. During the winter, the near-surface and near-bottom flow followed the isobaths along the coast.

Response to across-bay winds (SW - NE)

Across-bay winds generally corresponded to southwesterlies, although there were occasional strong northeasterly storms. For the purpose of illustrating the response to across-bay winds, the response to a 1 dyn cm^{-2} wind stress from the SW was plotted (fig. 3.3-6). During the summer of 1990, there was a strong response in the near-surface water at the North Passage (U2) as well as Cape Cod Bay (U7), but weak response elsewhere. The deep coastal instruments indicated an upwelling response to SW winds, with a magnitude of 1–3 cm s^{-1}. Although it was weak, the correlation coefficients were high (0.45–0.6; see Table 3.3-1), indicating that a significant fraction of the variance was explained by the upwelling response. A stronger upwelling response was evident during the fall period, during which near-bottom currents at Manomet reached 5 cm s^{-1} per dyn cm^{-2}, and near-surface currents of comparable magnitude were directed offshore at Manomet and Scituate. During the fall period, SW winds forced strong inflow in the deep water at Race Point (12 cm s^{-1} per dyn cm^{-2}). During the winter and spring the same general pattern persisted, although the magnitude of the inflow at Race Point was greatly reduced.

Table 3.3-1: Correlation between Wind and Currents
Units of the transfer function are cm s^{-1} per dyn cm^{-2}.
Orientation theta is degrees True.

Summer 1990

	NW - SE			SW - NE		
	corr	transfn	theta	corr	transfn	theta
broad_18	0.34	2.47	255.0	0.59	3.33	272.3
bb_5	0.32	8.15	222.7	0.08	1.82	114.3
bb_23	0.19	2.10	277.1	0.24	1.96	283.0
bb_33	0.07	0.45	318.2	0.19	0.92	276.5
scit_5	0.46	14.40	159.2	0.06	1.72	171.9
scit_23	0.08	0.35	234.7	0.45	1.50	277.6
u7_4	0.15	5.06	326.1	0.28	7.42	29.0
u2_4	0.25	11.18	221.2	0.39	15.65	28.3
u2_25	0.26	4.95	62.1	0.29	4.40	15.8
u2_60	0.14	1.26	48.0	0.29	2.37	245.7
u3_4	0.06	1.95	179.0	0.11	2.95	148.3
u3_25	0.24	2.56	6.4	0.38	3.27	16.5
u6_8	0.13	1.82	253.8	0.09	0.96	285.9
u6_28	0.14	1.97	280.0	0.14	1.55	238.4
u6_80	0.16	0.76	59.6	0.19	0.73	41.9

Fall 1990

	NW - SE			SW - NE		
	corr	transfn	theta	corr	transfn	theta
broad_18	0.48	2.57	309.3	0.38	2.02	252.4
bb_23	0.24	2.25	16.0	0.62	5.36	314.0
scit_5	0.57	12.17	171.5	0.20	4.22	71.4
mano_5	0.36	6.03	199.6	0.21	3.76	66.7
mano_29	0.35	3.18	41.0	0.52	5.01	298.0
u7_4	0.13	2.20	330.1	0.21	3.69	228.3
u2_4	0.08	2.07	342.4	0.15	4.10	342.3
u2_60	0.24	2.25	73.1	0.20	1.97	288.0
u3_4	0.21	4.90	309.8	0.03	0.76	52.1
u3_25	0.17	1.60	35.0	0.11	1.10	354.2
u6_8	0.15	1.55	291.1	0.15	1.59	310.1
u6_28	0.15	1.83	248.0	0.17	2.14	315.8
u6_80	0.08	0.45	151.4	0.21	1.22	37.0
u6b_75	0.52	4.30	310.6	0.35	3.04	121.4
u6b_84	0.51	2.53	299.6	0.23	1.20	111.4
race_5	0.29	6.04	178.6	0.15	3.47	29.8
race_23	0.52	8.53	57.9	0.29	5.06	242.9
race_55	0.45	8.31	55.1	0.61	12.16	235.3

Table 3.3-1 (con't) : Correlation between Wind and Currents
Units of the transfer function are cm s^{-1} per dyn cm^{-2}.
Orientation theta is degrees True.

Winter 1990 - 1991

	NW - SE			SW - NE		
	corr	transfn	theta	corr	transfn	theta
broad_18	0.31	1.14	288.6	0.57	2.57	252.5
bb_5	0.53	4.16	180.1	0.36	3.47	59.5
bb_33	0.33	1.40	197.7	0.49	2.58	294.8
scit_5	0.75	9.34	156.2	0.28	4.39	98.9
mano_5	0.46	3.81	147.8	0.12	1.25	101.7
mano_29	0.28	1.94	123.2	0.34	3.00	270.3
u7_4	0.13	0.87	85.8	0.36	3.03	163.9
u2_4	0.05	0.76	140.3	0.22	4.09	324.7
u3_25	0.26	2.00	17.9	0.28	2.62	10.7
u6_8	0.22	2.35	142.1	0.20	2.98	198.1
u6_28	0.23	2.73	144.9	0.16	2.54	192.2
u6_80	0.20	1.20	156.6	0.18	1.47	95.6
u6b_75	0.15	1.39	330.9	0.18	2.18	298.4
u6b_84	0.22	1.40	328.3	0.15	1.21	306.3
race_5	0.27	3.85	125.1	0.14	2.46	139.4
race_23	0.45	4.75	74.3	0.33	4.44	228.2
race_55	0.44	5.43	45.0	0.30	4.69	255.1

Spring 1991

	NW - SE			SW - NE		
	corr	transfn	theta	corr	transfn	theta
broad_5	0.55	3.96	188.8	0.16	1.02	152.5
bb_5	0.45	6.09	205.2	0.15	1.81	89.5
bb_23	0.22	1.92	292.3	0.53	4.05	314.3
bb_33	0.24	1.92	273.4	0.57	4.04	286.9
scit_5	0.59	8.50	165.0	0.21	2.57	109.5
mano_5	0.37	4.90	154.4	0.22	2.60	87.1
mano_29	0.28	2.36	101.2	0.35	2.56	289.1
u7_25	0.46	3.76	39.6	0.11	0.80	198.3
u2_60	0.22	2.44	51.9	0.22	2.18	323.1
u3_4	0.20	4.86	172.4	0.06	1.30	269.4
u3_25	0.25	1.90	351.2	0.11	0.77	31.9
u6_8	0.23	3.54	141.0	0.01	0.13	172.3
u6_28	0.34	4.27	122.0	0.04	0.44	140.9
u6_80	0.33	2.04	128.8	0.18	0.99	76.0
u6b_75	0.33	1.86	335.4	0.21	1.01	312.8
race_5	0.24	4.08	124.4	0.23	3.51	99.2
race_55	0.38	4.40	31.8	0.34	3.46	253.0
race_60	0.33	2.70	39.4	0.33	2.39	252.2

3.3.3 Baywide Response to Wind Forcing–Drifter Measurements

The drifter data also provide a measure of the response of the currents to winds, although since the time the drifters spend adrift in the Bays is short (10–25 days), the statistics are not very accurate on the transfer function. Table 3.3-2 indicates the correlations and transfer functions between the wind stress and drifter velocity for the five drifter deployments, again doing separate analyses for SW and NW wind directions. There was a lot of scatter in the magnitude of the transfer function, but it typically ranged from 5 to 10 cm s^{-1} per dyn cm^{-2}. Higher values were observed in the summer 1990 and spring 1991 periods, and the lower values were observed during the winter.

The average veering angle for northwesterly winds was 15° to the right of the wind, and for southwesterly winds it was 56° to the right of the wind, although with considerable scatter. The veering is likely the result of the Earth's rotation, which in the absence of bottom friction or lateral boundaries would produce a 90° veer in the current direction. The smaller veering angle for northwesterly winds is probably related to the stronger constraint of the lateral boundary, which restricts the flow in the on–offshore direction. The presence of boundaries also influences the response to across-bay winds, although it is not as pronounced. Bottom friction also reduces the veering tendency. The influence of bottom stress should vary markedly between unstratified and stratified periods, however there is no clear evidence of a marked change in veering between winter and summer periods. Again the data are noisy enough due to the short record lengths that it is difficult to make detailed comparisons.

Summary of the Baywide Response to Wind Forcing

The along-bay winds drive a coastally intensified, along-bay flow, consistent with Csanady's (1974) and Wright et al's (1986) model predictions. Based on these model studies as well as the analysis of pressure data, the wind stress sets up an along-bay pressure gradient that opposes the wind stress. In the shallow coastal regions, wind stress dominates over the pressure gradient, and there is downwind flow. In the deep regions, there is a weak return flow. This pattern is complicated by the geometry of the Bays and by the variations in stratification. More analysis should be done to determine the dynamics of the along-bay response. This analysis will be facilitated by use of a three-dimensional numerical model being applied to Massachusetts Bay by the USGS.

The dynamics of the response to cross-bay winds are more problematical. Since they relate to the upwelling regime, they will be discussed in the next subsection.

Table 3.3-2
Correlation between Winds and Drifter Velocities
(parentheses indicate insignificant correlation)
Units of the transfer function are cm s^{-1} per dyn cm^{-2}.
Orientation theta is degrees True.

Spring 1990

NW - SE			SW - NE			
corr	trans	theta	corr	trans	theta	npoints
(0.10	2.27	170)	0.34	6.49	26	144
(0.17	3.46	73)	0.32	5.23	4	74
(0.11	3.69	161)	0.43	11.24	89	61

Summer 1990

NW - SE			SW - NE			
corr	trans	theta	corr	trans	theta	npoints
not enough points						
0.38	14.94	163	0.43	21.70	39	46

Fall 1990

NW - SE			SW - NE			
corr	trans	theta	corr	trans	theta	npoints
0.53	8.26	160	0.40	5.73	71	50
0.36	5.57	150	0.36	7.04	58	104
not enough points						

Winter 1990 - 1991

NW - SE			SW - NE			
corr	trans	theta	corr	trans	theta	npoints
not enough points						
0.36	6.61	145	(0.19	3.46	72)	79
0.35	6.06	126	0.35	7.73	69	73

Spring 1991

NW - SE			SW - NE			
corr	trans	theta	corr	trans	theta	npoints
0.35	11.36	156	0.32	10.54	86	86
(0.20	5.90	360)	(0.20	4.19	100)	66
(0.13	6.75	125)	0.52	17.82	64	43

3.3.4 The Upwelling–Downwelling Regime

Upwelling occurs in coastal environments when wind stress acts in a direction that causes the near-surface, wind-driven flow to be carried away from shore. In regions deep enough that the surface and bottom Ekman layers are distinct, the near-surface transport is roughly 90° to the right of the wind, while in shallower regions where stress is transmitted through the whole water column, the angle decreases somewhat from 90°. In Massachusetts Bay, the prevailing SW winds occurring during the summertime are oriented at 45–90° to the west coast of the Bays, providing upwelling-favorable conditions. Conversely, downwelling is favored when the winds are oriented in the northerly quadrant (NW–NE). During the summertime period, northerly winds occur as brief interruptions of the prevailing southerly wind pattern (fig. 2.1-1).

The presence of upwelling was evident in the satellite data, the moored temperature data, and in the hydrographic data. The moored data provide a statistical basis for examining the upwelling process and its time-variation, while the other data provide more information about its spatial structure.

Description of the Upwelling Regime, 1990

The response of the currents to southwesterly winds (fig. 3.3-6) clearly indicates the upwelling tendency in the coastal waters. The occurrence of upwelling is also indicated in the moored records by colder temperatures observed in the surface waters at the coastal stations than offshore. This is clearly revealed in fig. 3.3-7, in which temperatures at the Broad Sound, Boston Buoy and Scituate moorings are found to drop well below the temperature at U6 in the middle of Stellwagen Basin. The Broad Sound location shows the most marked departures from the mid-bay temperatures, but the other coastal moorings also show marked drops in temperature during upwelling periods. Four major upwelling periods can be identified, as follows:

Dates			Maximum Temperature Anomaly
6/2/90	–	6/10/90	-3°
6/17/90	–	6/30/90	-3°
7/11/90	–	7/27/90	-8°
8/7/90	–	8/18/90	-4°

The upwelling periods each corresponded to periods of sustained winds with a positive component in the northeastward direction (i.e., SW winds) (fig 3.3-7, top panel). There were brief interruptions to the SW winds during some of these events, for example the wind reversal on 7/13/90, but each of these periods was dominated by southwesterlies.

There appeared to be a different time lag in the response at the different coastal moorings, which was most evident during the July event. The temperature dropped first at Broad Sound, followed several days later by a drop at the Boston Buoy. The temperature did not drop at Scituate until nearly the end of the upwelling period. The temperature at U6 also dropped slightly at the end of this period. It is conceivable that the sustained upwelling resulted in cooling all the way across Massachusetts Bay during this period (see discussion of satellite imagery, below).

The deep waters showed little response to the upwelling favorable winds, but there was a dramatic response to downwelling favorable winds. There were four pronounced downwelling-favorable wind stress events, each of which resulted in a marked increase in temperature in the deep water at Broad Sound. Downwelling events in June and mid-August caused the temperature to increase to virtually the same temperature as the near-surface waters.

Statistical Analysis of Upwelling Response

Low frequency (1.5–30 day period) temperature fluctuations among the coastal sensors were found to be positively correlated with each other (r = 0.6–0.7, based on detrended data to remove seasonal variations) during the spring–summer period, indicating that both near-surface and near-bottom temperatures varied in phase with each other. This is consistent with an upwelling–downwelling regime, as opposed to a tidal or wind-mixing regime in which the near-surface and deep temperature variations would be negatively correlated.

The temperature fluctuations were also found to be significantly correlated with the winds. Interestingly, higher correlations were obtained with Cape Cod winds than either Logan or Boston Buoy winds. The Broad Sound near-surface record has a correlation of 0.35 with a 4 day lag, while the Broad Sound deep record has a correlation of 0.58 with a 1 day lag. The orientation of the wind vector of highest correlation is 225°, with negative anomalies (i.e., upwelling) occurring with SW winds. The timeseries (fig. 3.3-7) show that the near-surface anomalies are temperature decreases associated with upwelling, while the near-bottom anomalies are temperature increases due to downwelling. The upwelling events tend to be longer lived (4–18 days) than the downwelling events (1–2 days), due to the relatively longer timescale of southwesterly wind events relative to northerlies, which tend to occur as frontal passages.

As indicated in the previous section, the currents along the western margin of the Bays clearly indicate an upwelling response to SW–NE fluctuations in winds (fig. 3.3-6), with offshore flow in the surface waters and onshore flow in the near-bottom waters. The magnitudes of the currents associated with the upwelling regime range from 1–3 cm s^{-1} per dyn cm^{-2}. While the currents are weak compared to the along-bay currents, these small cross-shore velocities result in significant vertical velocities,

on the order of 3–10 m/day, due to the small transverse distance to the shore (5–10 km). This provides a significant vertical exchange rate, as evident from the water properties data.

Satellite Imagery of Upwelling

A number of the clear satellite images obtained during the summer of 1990 indicated the presence of upwelling (see Section 2.5). This is partly due to the tendency for the weather to be clear during periods of SW winds, when upwelling occurs. Two particularly good images of upwelling are shown in figs. 3.3-8 and 3.3-9.

Figure 3.3-8 shows the surface temperature during the strongest upwelling event of the year, when surface temperatures at Broad Sound were 8° lower than those in the middle of Stellwagen Basin. This upwelling event was forced by persistent SW winds. The satellite image indicates that the coldest water extends from Broad Sound to Cape Ann, extending approximately 10 km from the coast. A smaller upwelling zone occurs in western Cape Cod Bay. A narrow band of upwelling occurs along the coast from Plymouth to the Boston area. The variations in intensity of the upwelling are likely the result of variations in orientation of the coast, which more strongly favors upwelling when it more closely parallels the prevailing SW winds. The northern portion of Massachusetts Bay and western Cape Cod Bay have the most favorable orientation to the prevailing SW winds for upwelling, and they indicate the strongest response.

Virtually all of the satellite images indicate plumes and filaments of cold water extending offshore from the coast at various places. A plume extending out across Cape Cod Bay was almost always observed. Offshore flow results from a convergence of the along-shore flow, which can occur as a result of a change in the intensity of upwelling. This probably explains the feature in Cape Cod Bay.

Figure 3.3-9 shows a period of upwelling in August, 1990, when the wind forcing was quite weak. In spite of the weak wind forcing, cold water was evident throughout the western shore of the Bays, with the most pronounced anomaly in Cape Cod Bay. This upwelling regime was apparently forced by the SW winds occurring over the previous 10 days, and the cold water remained at the surface in spite of the relaxation of the wind forcing. The temperature anomaly persisted until August 21, when a major wind reversal forced a downwelling event that homogenized the near-surface waters and caused a marked increase in the temperature of the deep waters at the coastal moorings (fig. 3.3-7).

Dynamics of Upwelling in the Bays

The dynamics of upwelling in Massachusetts and Cape Cod Bays differs from the classical upwelling regime due to the semi-enclosed geometry of the Bays. In "normal" upwelling, there is an along-coast flow that geostrophically balances the

set-down of the sea surface along the coast. Calculation of the baroclinic pressure gradients in the cross-shelf direction using the moored density data indicate that geostrophic currents of 5–15 cm s^{-1} should occur. However, there is little evidence of geostrophic flow in response to southwesterly winds, based on the covariance analysis (fig. 3.3-6). This is likely due to the variability of the orientation of the shoreline, which causes too much variability in the coastal sea-level set-down to produce a continuous coastal current. It is possible that there are limited regions in which a geostrophic flow occurs, such as the near-shore regions in western Cape Cod Bay and the north shore of Massachusetts Bay. However there were no current meters close enough to shore in these regions to detect the along-coast flow.

A detailed analysis of the upwelling regime is yet to be performed. Future investigation of the dynamics of upwelling will be performed in conjunction with the numerical modeling program being undertaken by the USGS.

Significance of the Upwelling Regime

Upwelling appears to be a major mechanism for carrying subpycnocline water into the near-surface layer of the Bays. Its influence is most pronounced in several coastal regions, notably the north shore of Massachusetts Bay and western Cape Cod Bay, but the satellite images indicate that the temperature anomalies extend across much of the Bays during periods of sustained upwelling. Based on the persistence and spatial extent of the upwelling process, it could be the most important mechanism contributing to vertical exchange in the Bays during the stratified portion of the annual cycle. However, the actual transport rate due to upwelling has not yet been quantified with precision. A crude estimate of the vertical transport due to upwelling can be obtained from the moored current meter data, suggesting a mean onshore velocity of approximately 1.0 cm/s at the Boston Buoy and Scituate (Table 2.2-5). If the vertical extent of this onshore flow is assumed to be 5 m, and it extends along 25 km of the coast, the vertical transport amounts to 1.2×10^3 m^3 s^{-1}.

Based on the volume of deep water in the Bays of approximately 8×10^{10} m^3 (see fig. 3.4-2, next section), this upwelling rate would exchange approximately one eighth of the deep water in a 3-month period. Based on the observed changes in deep temperature and salinity through the course of the summer, that may be a reasonable estimate of the total vertical exchange (see section 3.4 for more details).

The rate of vertical exchange is particularly important with respect to the primary productivity of the Bays, since the rate of phytoplankton growth is usually limited by nitrogen, and there is a large reservoir of nitrogen in the deep waters of the Bays (Townsend et al., 1990). After the near-surface nitrogen is depleted in the spring bloom, subsequent growth of phytoplankton in the Bays depends on inputs of nitrogen to the euphotic zone, either by horizontal or vertical transport. Western Massachusetts Bay receives a horizontal flux of nitrogen from the Boston sewage

outfalls, but the remainder of the Bays depends on vertical transport to support primary production. Based on these observations, the vertical transport associated with upwelling may be the primary mechanism for delivering nitrogen to the surface waters from the deep waters of the Bays. Further work is required to quantify this flux and to compare it with estimates of diffusive flux across the thermocline.

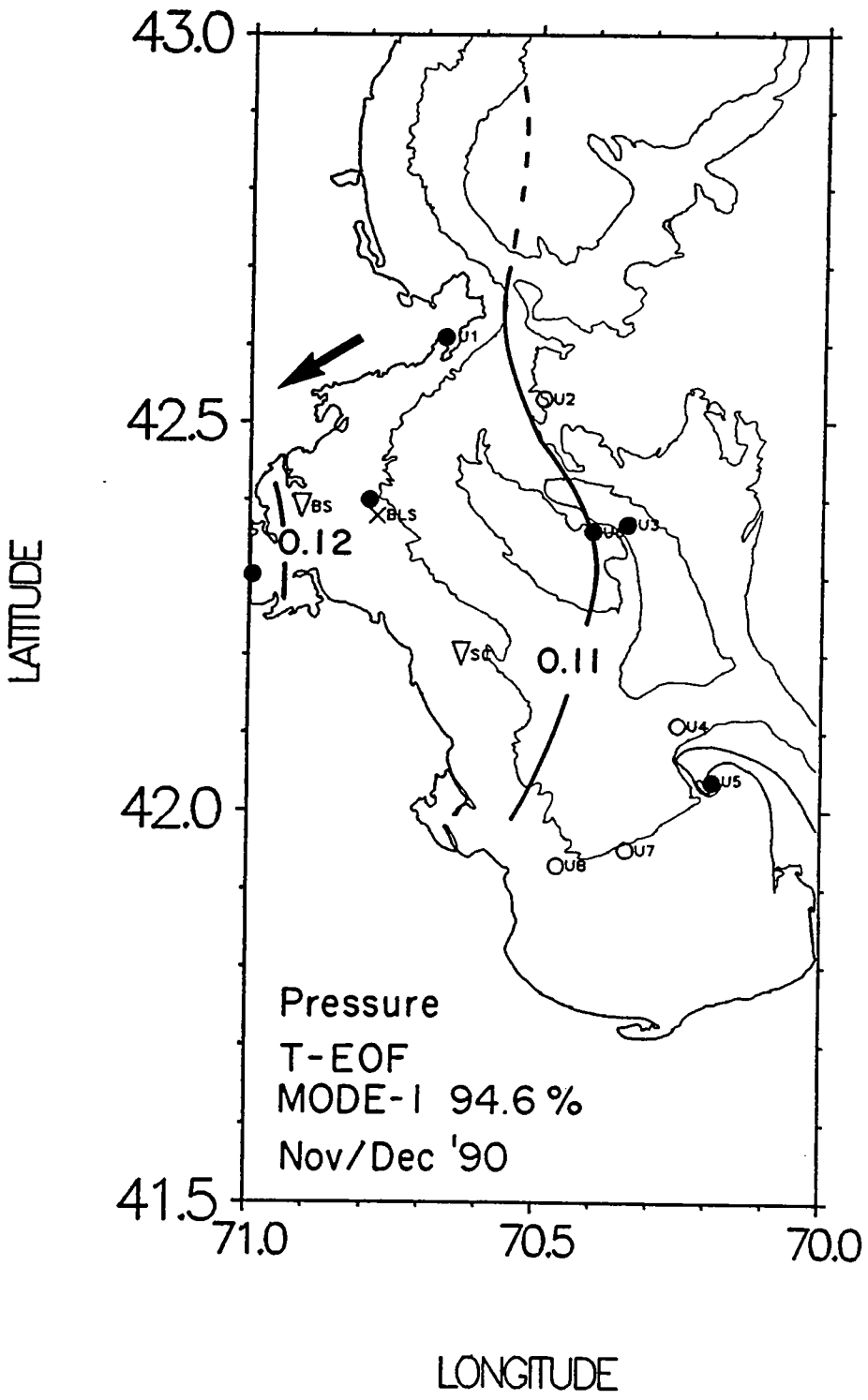

Figure 3.3-1 Primary pressure empirical orthogonal function. Amplitudes in decibars. The arrow indicates the direction of the windstress (236°T) which is most highly correlated (0.86) with this mode.

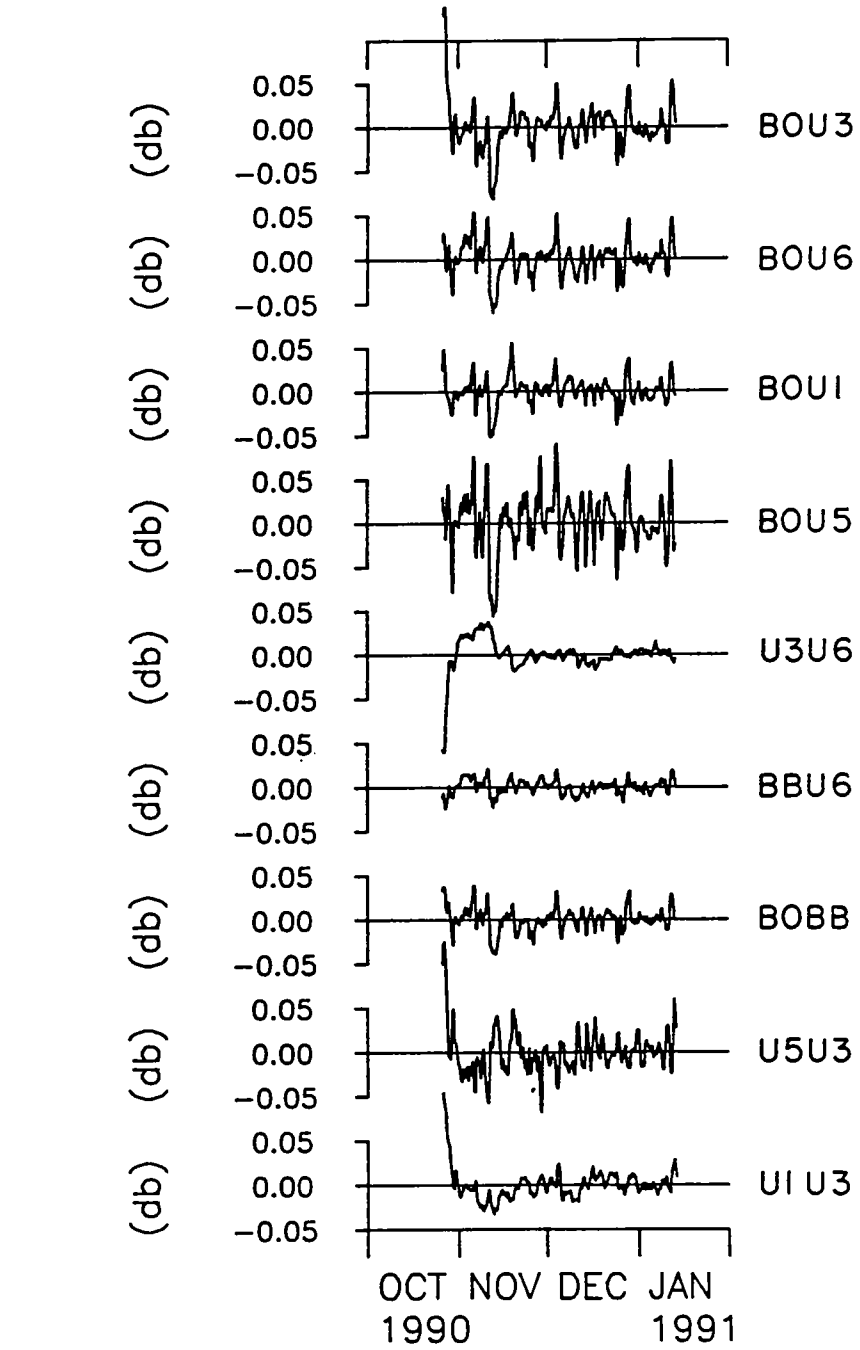

Figure 3.3-2 Pressure differences between the indicated station pairs. A linear trend has been removed from each record.

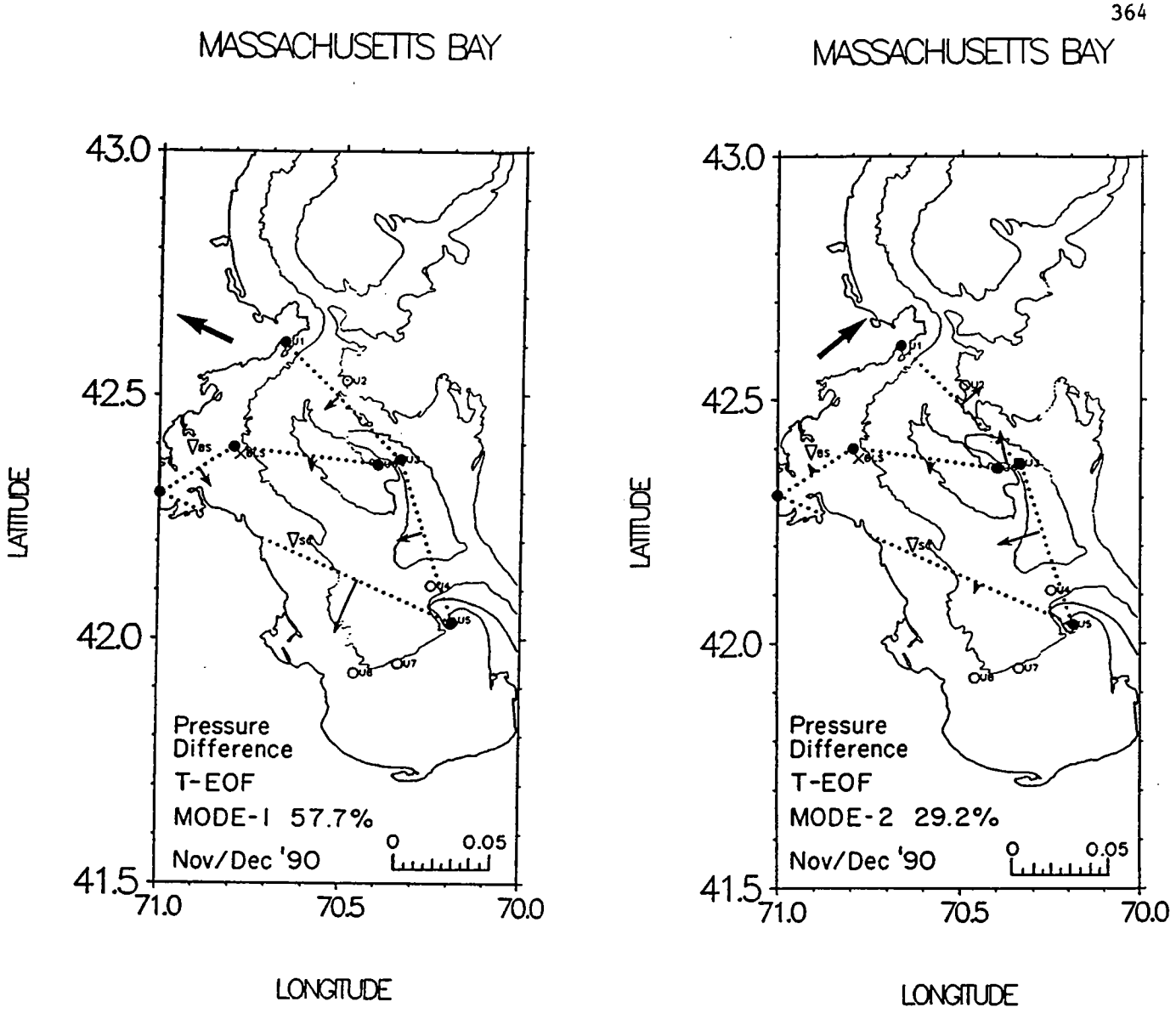

Figure 3.3-3 First and second pressure difference EOFs. The amplitudes (mb) of the pressure differences are presented so as to suggest the magnitude and sense of the inferred geostrophic transport. The arrows on land indicate the direction of the windstress (mode-1, 296°T; mode-2, 41°T) most highly correlated with mode-1 (0.91) and mode-2 (0.60) respectively.

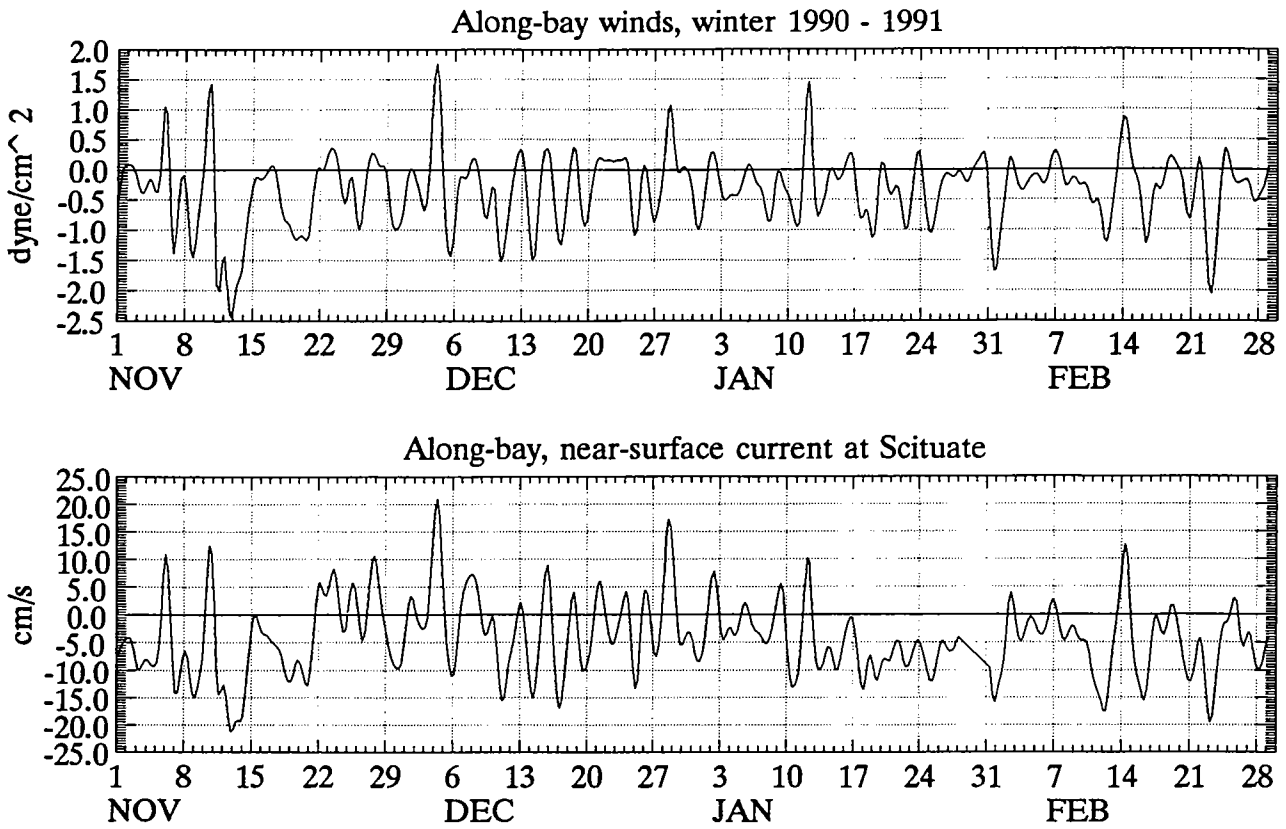

Figure 3.3-4 Along-bay (NW–SE) winds at Boston (Logan) and along-bay (-30°) currents at Scituate, 5-m depth during the winter of 1990–1991. The correlation coefficient between the wind and currents at Scituate was 0.75 for this period, with a transfer function of 9.3 cm s^{-1} per dyn cm^{-2}.

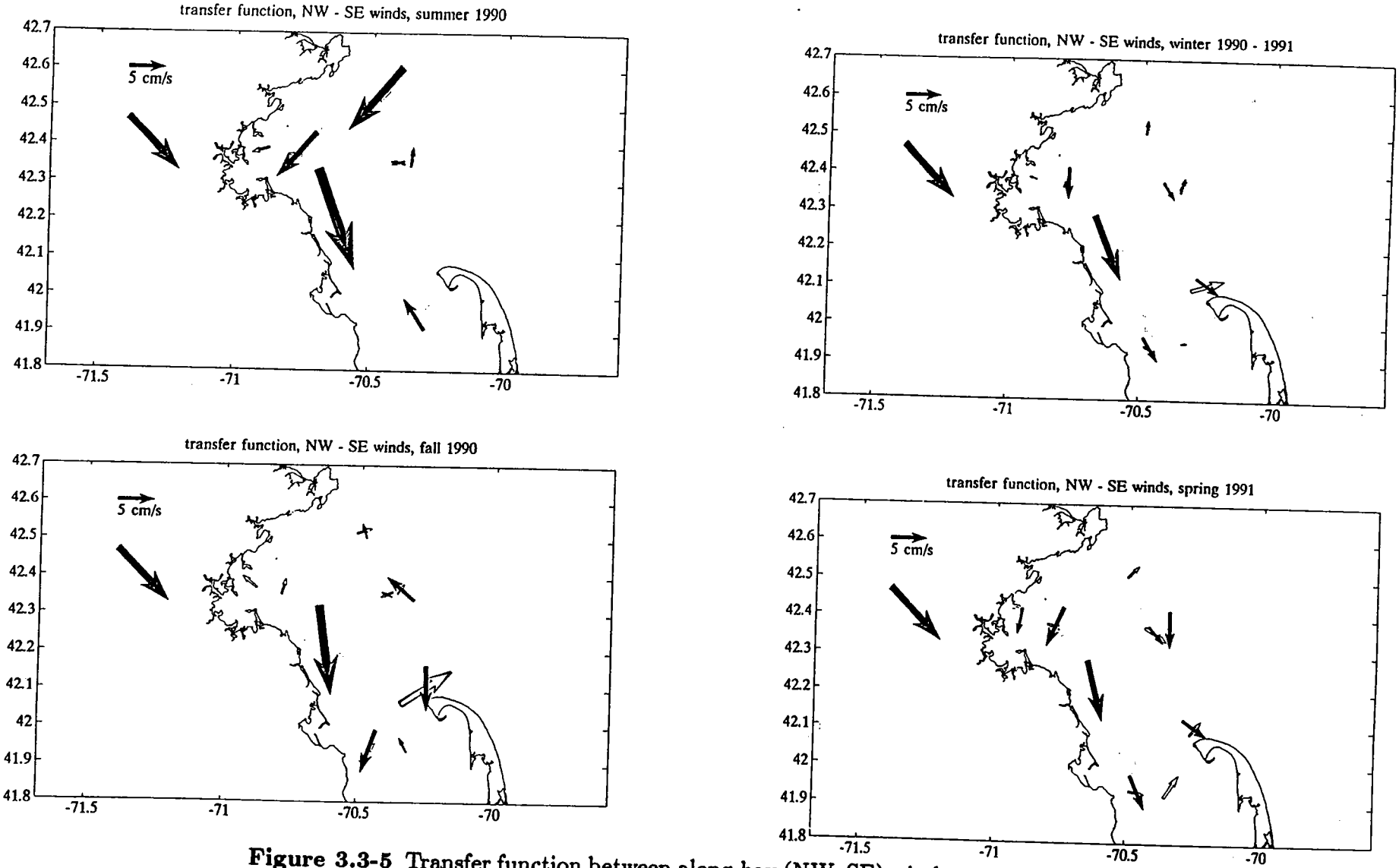

Figure 3.3-5 Transfer function between along-bay (NW–SE) winds at Boston (Logan) and the moored currents. (Solid arrows indicate near-surface currents, and hollow arrows indicate subsurface currents). The plot shows the response to 1 dyn cm^{-2} wind-stress from the NW, based on covariance analysis. A consistent pattern of along-bay flow along the coast is observed throughout the year, with the strongest response occurring at Scituate. The seaward moorings show considerable seasonal variability in their response. There is outflow in the deep water at Race Point during the three seasons for which there is data there, but the direction of the near-surface current response varies with season.

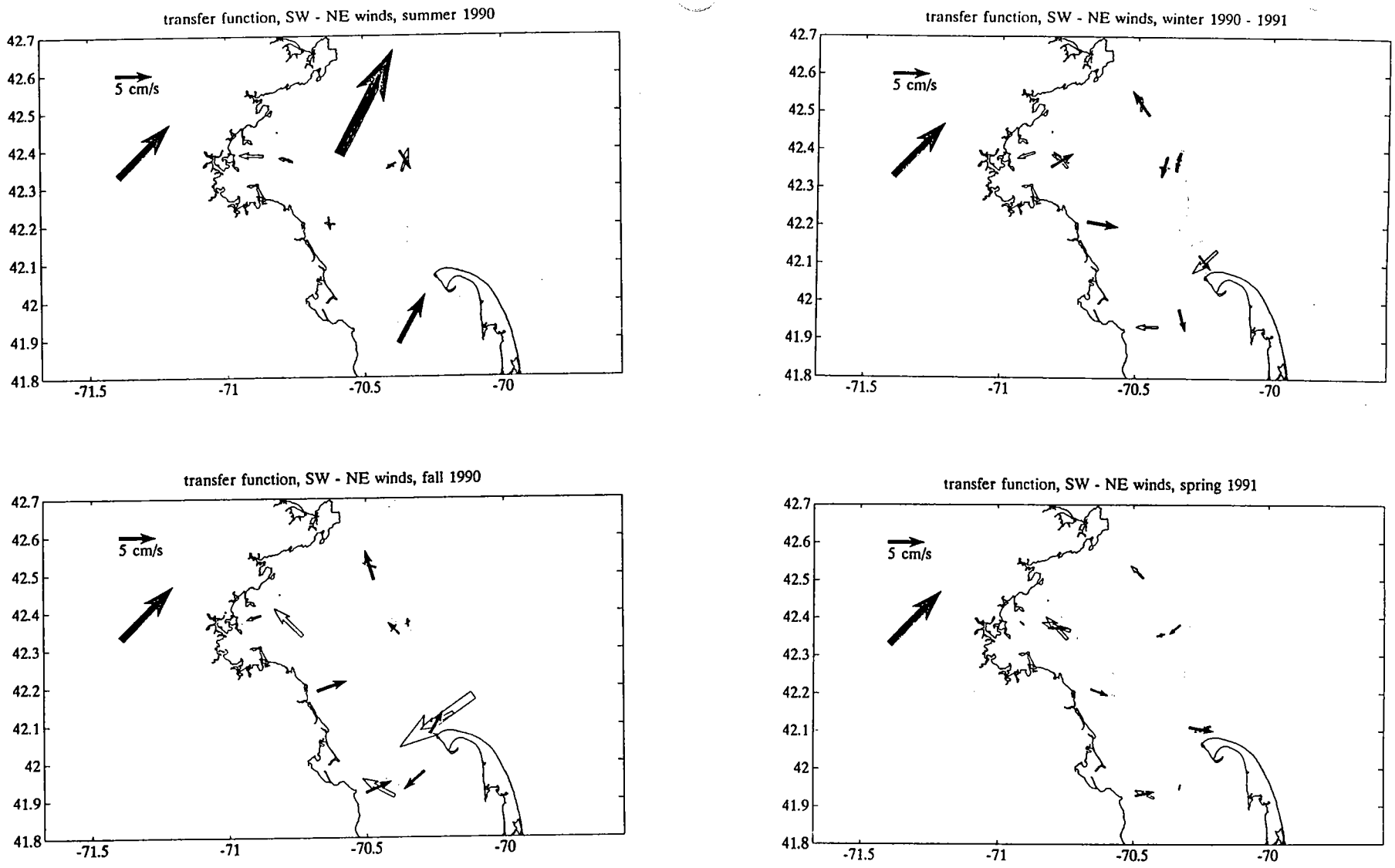

Figure 3.3-6 Transfer function between across-bay (SW–NE) winds at Boston (Logan) and the moored currents. (Solid arrows indicate near-surface currents, and hollow arrows indicate subsurface currents). The plot shows the response to 1 dyn cm^{-2} wind-stress from the SW. The most consistent feature of the response is the upwelling pattern along the coast, with offshore flow in the near-surface waters and onshore flow in the deep waters. The response at the seaward moorings appears to vary considerably from season to season, but there is a consistent tendency for deep inflow at Race Point during SW wind events.

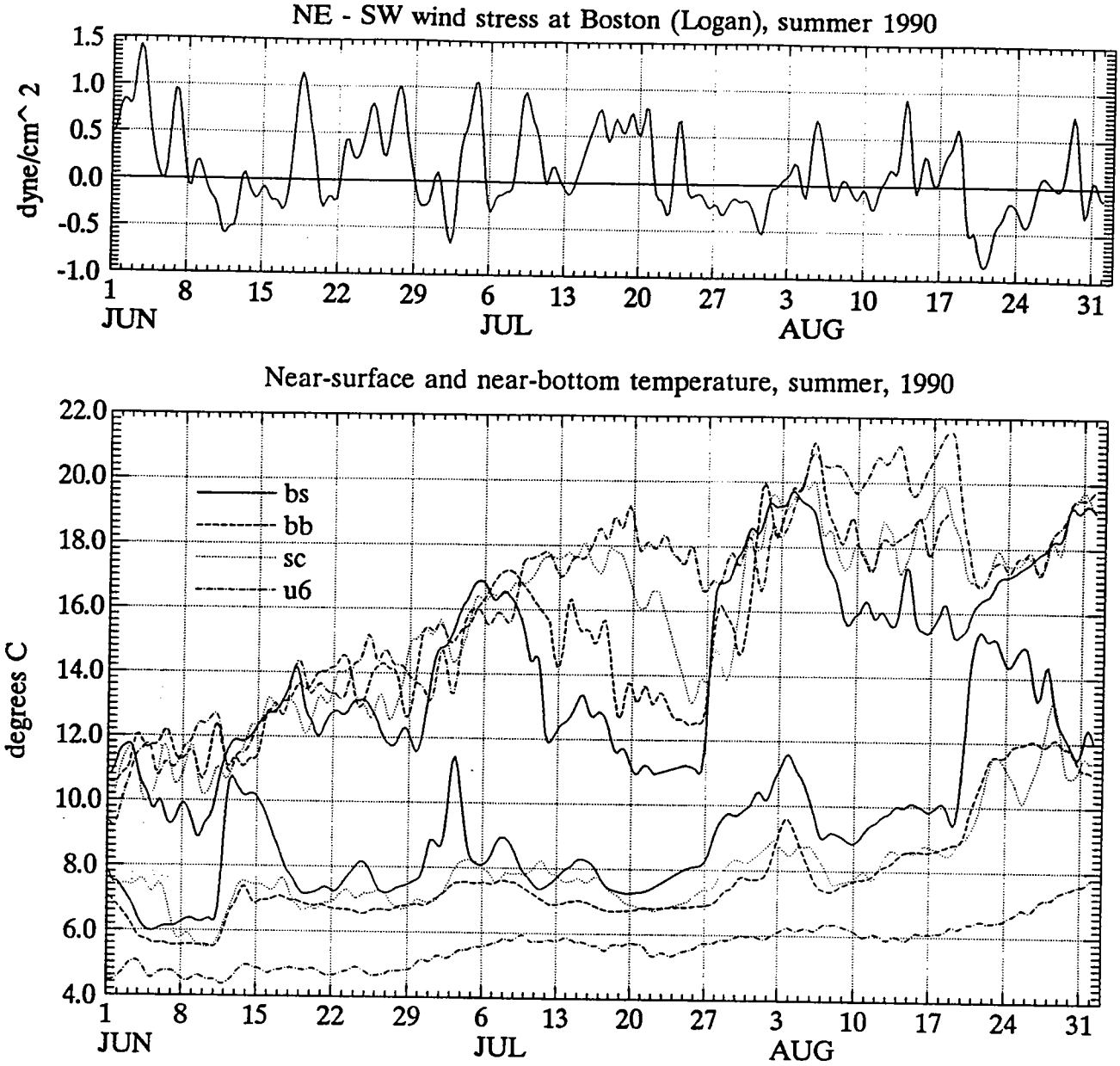

Figure 3.3-7 Across-bay wind stress at Boston (Logan) and temperatures at coastal and mid-bay locations in Massachusetts Bay. In the upper panel, positive values indicate winds toward the northeast. The temperature records include the coastal moorings at Broad Sound (bs), the Boston Buoy (bb) and Scituate (sc) and the mid-bay mooring (u6). Both near-surface (4–5 m depth) and near-bottom temperatures are plotted for each location. There are marked deviations of the coastal temperature in the near-surface waters from the mid-bay temperature, indicating periods of upwelling. The near-bottom waters at Broad Sound show episodes of sudden warming, associated with downwelling events.

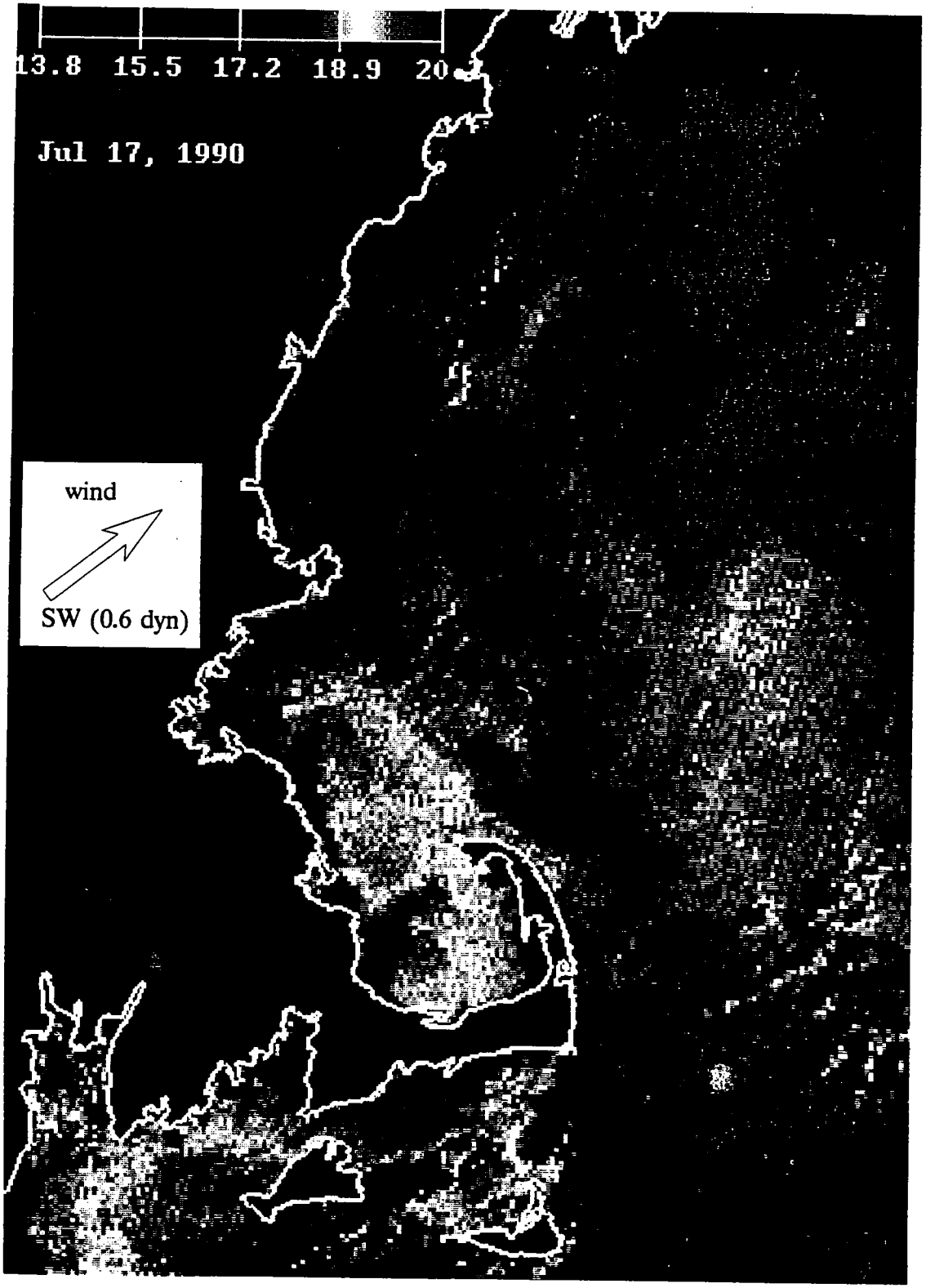

Figure 3.3-8 Satellite image of upwelling, July 17, 1990. Moderate wind forcing from the SW produced strong upwelling in northern Massachusetts Bay and western Cape Cod Bay. Based on the moored temperature data at Broad Sound, this was the strongest upwelling event of the year.

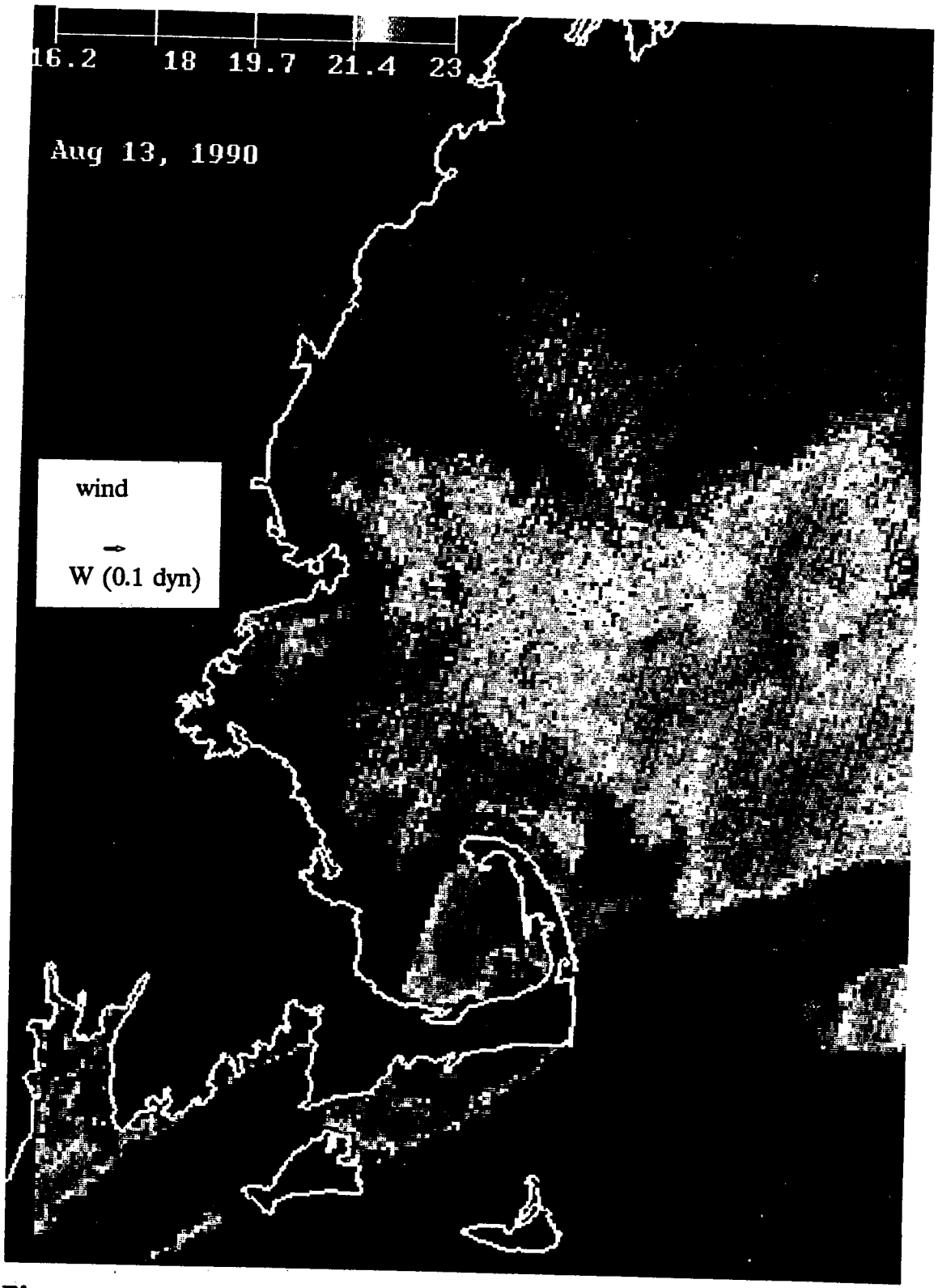

Figure 3.3-9 Satellite image of upwelling, August 13, 1990. Wind forcing is weak, but there is a pronounced temperature anomaly along the coast associated with persistent upwelling conditions. Although there was some contamination by clouds in the lower portion of the image, in situ measurements confirmed that the variations observed in Cape Cod Bay were real.

3.4 Residence Time Estimation

Residence time is usually defined as the average length of time that some substance remains in a body of water before it is removed. The concept is very valuable for assessing the relative rates of physical removal processes to biological or chemical removal. In the case of water in coastal embayments, the physical removal process due to currents is much more rapid than any other process, so the residence time of water is inherently a function of the physical oceanography. The estimation of residence time is difficult in practice, for a variety of reasons. The definition is clear in the case of a well-mixed system with well defined inputs and removals, for example a stretch of a river. However in the case of most embayments, neither is the system well-mixed nor are there well defined inputs and removals of water.

It is clear from the hydrographic data that Massachusetts and Cape Cod Bays are not well mixed, as evident by the variations in water properties in different parts of the Bays. During the warm months, the strong vertical stratification indicates that the waters above the thermocline have little exchange with the waters below the thermocline, hence these represent separate "reservoirs" which likely have different residence times. Likewise there are significant horizontal gradients between different portions of the Bays. The region near Boston Harbor tends to be fresher than the offshore water, and Cape Cod Bay tends to have different water mass characteristics than Massachusetts Bay. If there were adequate information about transport, the optimum approach would to be to divide the system into small enough subsections that the well-mixed assumption was approximately satisfied in each section, i.e., that the variations within a section was small relative to variations between sections. However, this requires knowledge of exchange rates between each section, which limits the extent to which subsections can be defined. For the purpose of residence time calculations in the Bays, the upper water is distinguished from the deep water, since there is evidence that their residence times are considerably different. However there is inadequate transport information to distinguish in a quantitative sense the residence times in different regions of the Bays. At the end of the section some qualitative comparisons will be made between different regions, based on the available data.

Estimates of input or removal of water can be accomplished in several ways. A common approach in estuarine systems, where there is a well defined input of fresh water, is to use the transport and volume of fresh water to determine the fluid residence time. The difficulty of this approach in the Bays is that a major fraction of the fresh water enters through the seaward boundary. While this flow is related to the discharge of the rivers of the Gulf of Maine, the actual amount of fresh water that enters the Bays is a complicated function of the runoff and wind forcing, hence it cannot be easily quantified. A second approach is to put a tracer in the water, and actually observe how long it takes before it is removed. The drifters deployed in this program provide such a tracer. The weakness of this approach is that the

statistical significance of the drifter residence times is difficult to determine, due to the small numbers of samples. A third approach is to use current measurements at the boundaries and within the Bays to determine the transport in or out of the Bays. In principle this is valid, but it requires that there be a well defined flow regime with distinct regions of inflow and outflow. In many systems the exchange is not the result of an organized circulation, but rather it depends on fluctuations of currents across the boundary, i.e., dispersive exchange rather than advective transport.

The current measurements in Massachusetts Bay suggest that in fact the advective transport is more important for exchange than dispersion. This is based on observations of typical mean velocities of 2–5 cm/s within the Bays and 10–20 cm/s at the seaward boundary. The general pattern of the mean flow is southward, with inflow south of Cape Ann and outflow north of Race Point. Hence the inflow and outflow are distinct, which provides for a well defined residence time if either the inflow or outflow can be quantified. While there are marked fluctuations about these means, the time scales of the fluctuations are short, on the order of 1–2 days, so they do not accomplish significant net transport. Hence the dispersive transport is not as important as the mean flow for baywide exchange. Dispersive transport is important in certain regions of the Bays, notably the region around the Boston Buoy (where the new sewage outfall is being placed), where the mean flow is weak, so the transport is accomplished by dispersion due to the fluctuations (see more detailed discussion below).

In the remainder of this section, the residence time will be estimated based on different data sources and techniques. The variation among the different estimates provides some indication of the uncertainty of the calculations, as well as the actual variation in residence time among the seasons and regions for which each method is most applicable.

3.4.1 Residence Time Based on Advective Transport

The residence time can be estimated, assuming the dominance of advective transport, by

$$T_{\text{res}} = \frac{V}{u_{\text{mean}} A}$$

where T_{res} is the residence time, V is the volume of the portion of the Bays of interest, u_{mean} is the mean inflow or outflow velocity in the direction normal to the entrance or exit section, and A is the area of that section. Based on the mean pattern of currents in the Bays, three sections can be defined that should each include roughly the same amount of mean throughflow (fig. 3.4-1). Unfortunately none of the sections have adequate current meter coverage to quantify the transport. Still, it is instructive to look at the mean flows normal to these sections based on the current meter data

to provide at least an order-of-magnitude estimate of the residence time. Considering the record-average data, the mean flow at the North Passage section tends to be at an angle to the section, but there is a significant mean inflow. At the other sections the mean flow of the near-surface water is nearly normal to the section. The component of velocity normal to each section, based on the record-length data, is shown in Table 3.4-1.

Table 3.4-1: Mean velocities at North Passage, Mid-Bay and South Passage Sections, based on data over the entire deployment period. The section width is very approximate, based on an estimate of the breadth over which the mean inflow or outflow occurs. The transport estimates are in $m^3\ s^{-1}$ for 20-m depth increments: 0–20, 20–40 and 40–60 m.

Location	Inst. Depth (m)	Section Width (≈km)	Mean Velocity (cm s^{-1})	Transport ($m^3 s^{-1}$)
North Passage	5	20	4 (inflow)	16000
(U2)	25	14	9 (inflow)	25200
	60	0.5	4 (inflow)	400
Mid Bay	5	30	3 (down-bay)	18000
(SC)	23	20	0	0
South Passage	5	10	8 (outflow)	16000
(RP)	23	7	0	0
	60	0	0	0

The results, albeit crude, show a consistent throughflow for the near-surface mean transport of 16000–18000 $m^3\ s^{-1}$. This agreement is largely fortuitous, given the weak assumption of spatial uniformity required to make these calculations. The main weakness of the calculation is the poor spatial resolution of the moorings. Additionally, seasonal variations in transport are not accounted for. It should be noted here that the drifters typically indicated higher throughflow velocities than did the moored instruments (Section 2.3). How much of this difference is related to undersampling in space of the moored instruments vs undersampling in time of the drifters is not known, but for the present either estimate of the throughflow is plausible.

The deeper transport shows considerable inconsistency between the North Passage and other sections. This discrepancy is most likely due to spatial variation in the southward flow around U2 due to complex topographic variation. Based on the orientation of the isobaths, the deeper flow would be expected to curve eastward rather than continuing straight into Massachusetts Bay; hence it is reasonable to discount the large inflow values from the deeper instruments. There probably is some throughflow at depths below 20 m, but its magnitude is probably a small fraction of the near-surface throughflow.

The volume of the Bays was calculated by numerical integration of bathymetric data. The horizontal area of the Bays was also calculated as a function of depth. The resulting hypsometric curve and area vs. depth curve are shown in fig. 3.4-2. The total volume of the Bays is 1.45×10^{11} m^3, with roughly half that volume above and below 20 m depth. The area at the surface is 4.05×10^9 m^2.

Residence time can be estimated for the waters in the top 20-m, based on the above transport estimates and the hypsometric data, yielding a residence time of 47–52 days. The residence time of the entire water column will tend to be longer, but it depends on what value of deep through flow is assigned. There is some evidence from hydrography that the deep water exchange is weak or negligible during the summer months (see Section 3.4.4). This is not inconsistent with the moored velocity data.

3.4.2 Residence Time Based on Drifter Transit Times

Transit times of drifters suggest quite short residence times of the near-surface waters. Results from Section 2.3 indicate that the average transit time of drifters between western Massachusetts Bay and South Passage, where they exit, 18 days $\pm$ 13 days, based on 9 drifter trajectories. This may be a biased estimate, since it neglects drifters that grounded. In addition, the statistics of the drifter motion are not as solid as the moored data, due to the limited number of deployments. The transit time is somewhat analogous to a residence time, although the portion of the transit getting into western Massachusetts Bay should be included as well. That may add another 10 days to the total, yielding a residence time in the top 10-m of approximately 28 days. This is approximately half of the value estimated from the moored data, which is consistent with the analysis that shows mean velocities of the drifters roughly twice the moored values.

3.4.3 Residence Time Based on Fresh Water Replacement

If the volume of fresh water within the Bays (V_{fw}) is known and the flux of fresh water into the Bays (Q_{fw}) can be estimated, a residence time can be calculated by dividing the former value by the latter: $\tau_{fw} = V_{fw}/Q_{fw}$. The fresh water volumes were calculated for each major cruise by calculating the fresh water fraction relative to a specified reference salinity for each 0.5m sample at each station. This was multiplied by the depth interval and summed over each station to obtain the fresh water volume per unit area at that station. These values were then interpolated onto a grid, the interpolated values at each grid multiplied by the grid area and the results summed to obtain bay-wide estimates of fresh water volume. A variety of reference salinities were used, and displayed in the table below. For the present purpose, a value of 33.2 psu is taken as representative of western Gulf of Maine water into which river water

mixes.

Table 3.4-2

Fresh Water Volume/($m^3 \times 10^9$)										
	Reference Salinity									
Date	32.2	32.4	32.6	32.8	33.0	**33.2**	33.4	33.6	33.8	34.0
4/27-28/90	0.064	0.27	0.69	1.24	1.90	**2.74**	3.60	4.44	5.27	6.10
7/24-25/90	0.84	1.37	2.11	2.91	3.71	**4.50**	5.28	6.06	6.82	7.58
10/16-18/90	0.58	1.07	1.75	2.61	3.47	**4.32**	5.15	5.98	6.77	7.60
2/4-6/91	0.040	0.19	0.52	1.26	2.14	**3.02**	3.90	4.76	5.61	6.45
3/20-23/91	0.12	0.41	1.04	1.91	2.81	**3.70**	4.58	5.45	6.31	7.16
4/29-5/2/91	2.63	3.43	4.28	5.14	5.98	**6.82**	7.65	8.46	9.27	10.06

Combining the river flow data (fig. 2.1-3) with the estimates of fresh water volume yields residence times ranging from 14 days in April, 1990 to 104 days in July, 1990. The 104 day estimate used river flows during the period immediately preceding the cruise. However it makes sense to consider flows over a longer period when the residence time is this long, and using a higher value based on flows in June yields a value of 37 days. It should also be noted that during the stratified conditions of spring through early fall, only the upper layer will be significantly influenced by the flow of fresh water, so the estimates may be high by a factor of two. However, this is offset, and other estimates increased by the fact that the coastal current carrying the river flow from the north does not penetrate the bay continuously. It is not possible to determine the fraction of northern river water which actually transits the Bays, but a value of 50% is probably not greatly in error, resulting in residence times in the range of 28 to 100 days based on fresh water replacement.

3.4.4 Residence Time Based on Cross-Pycnocline Diffusion

During the warmer months (approximately April-October), the bay is sufficiently stratified to restrict vertical mixing across the pycnocline. Examination of the temperature-salinity characteristics in the deep water of the Bays (Stellwagen Basin) and those in the adjacent region of the Gulf of Maine suggest that relatively little lateral advection of Gulf of Maine water into the deep waters of Stellwagen Basin, presumably due to the relatively shallow sills at the northern and southern ends of Stellwagen Bank. The renewal of the deep waters during this period may thus be modeled as a one dimensional vertical mixing process. The water properties in the basin and in the Gulf are compared in figure 3.4-3. T-S curves for station BO7, in Stellwagen Basin (SB) and station SC9, the furthest offshore station in Gulf of Maine (GM) during the early cruises, are shown for all cruises from April, 27 through October 16, 1990. For the

bay-wide cruises, open symbols represent SB conditions and closed symbols represent GM conditions. Northern bay cruise samples in SB are represented by '+' and 'x' symbols. In April, 1990, the deep waters were very similar in the two locations. By late June, the SB water had warmed and freshened, particularly at shallower depths. The deepest water is very similar to conditions which could have been achieved by mixing of the earlier profile, suggesting that as the upper layer warmed, some heat diffused downward, but that the warming had not penetrated to the bottom. From late June to late July the data indicates an evolution of the deep water in SB due entirely to mixing. Note, however that the deep water in GM was considerably warmer and/or saltier than that in SB, while the T-S curve in SB tended to converge towards the GM curve at shallower depths. This is consistent with the hypothesis that the GM water was advecting through the bays in the upper layers, but that interaction between this water and the deep water in SB was strictly through vertical mixing.

The September 28 northern bay cruise found a rather different T-S relation in the deep water. The deepest water lay on the GM curve for July 24. This water could have been formed either by mixing of the July GM water or by mixing of SB water assuming additional warming of the shallower water. In either case, the September T-S curve suggests considerable warming of the shallower water. Between September 28 and October 16, the water at SB changed significantly, suggesting that during this period advection was important. This is supported by the similarity between the deepest waters in SB and GM.

It is clear from figure 3.4-3 that the waters in both SB and GM were steadily warming during the spring-fall period. For this reason, advection through the Bays from north to south would be expected to result in a horizontal gradient of water properties, while local mixing would yield relatively uniform conditions in SB. Figure 3.4-4 shows the T-S curves for the Salem, Boston, Cohasset and Scituate stations in the deepest portions of SB for the July 24, 1990 cruise. Note that through the deep water, the curves are essentially coincident, supporting the mixing hypothesis over advection for the period prior to the July cruise. In contrast, figure 3.4-5, which shows T-S curves for the same four stations in October, 1990 clearly indicate an advective event. The Scituate station, which is the furthest south of the four is distinct from the other three, suggesting that the advected water had not yet reached that location.

The T-S curves provide sufficient confidence in the vertical mixing hypothesis to make calculations based on it, useful at least through July 24. The variation in temperature and salinity in the deep water was therefore used to estimate a vertical diffusion coefficient in the pycnocline, and the residence time of the deep water. The diffusion coefficient was estimated using one dimensional diffusion equations for the salt and heat content of the lower layer. Horizontal diffusion and advection were ignored. Temperature and salinity data were used to derive independent estimates of the diffusion coefficient, allowing some verification of the assumptions. If horizontal

processes were dominant, the two estimates might differ significantly. Horizontal variations in the T-S characteristics of laterally transported water would cause different errors in estimates based on heat or salt. The diffusion equations used are:

$$\frac{\partial T_l V_l}{\partial t} = K_z A_i \frac{\partial T}{\partial z}$$
$$\frac{\partial S_l V_l}{\partial t} = K_z A_i \frac{\partial S}{\partial z}$$

where T_L, S_L and V_L are the temperature, salinity in the lower layer and the volume of the lower layer respectively and K_z is the vertical turbulent diffusivity. Note that the temperature equation should use heat ($\rho C_p T$) and the salinity equation should use salt (ρS). However the variations in ρ and C_p are small enough to be reasonably neglected for these calculations.

Examination of the temperature and salinity data at station BO7 gave the following values for the lower layer temperature and salinity, the temperature and salinity gradients in the pycnocline, the horizontal area at the top of the lower mixed layer and volume of the lower mixed layer. The lower mixed layer was defined as being below 40 m. Water properties are not completely uniform in the deep layer, and it is difficult to define an upper boundary to the layer precisely. The volume and area of the layer below 40 m are 3.48×10^{10} m^3 and 1.61×10^9 m^2 respectively.

Table 3.4-3

Date	T_l	S_l	$\partial T/\partial z$	$\partial S/\partial z$
4/13/90	3.50	33.01	0.025	-0.047
4/28/90	3.25	33.08	0.241	-0.055
6/29/90	4.75	32.67	1.100	-0.100
7/25/90	5.30	32.54	1.080	-0.088
9/28/90	7.60	32.51	0.194	-0.021
10/17/90	8.40	32.63	0.241	-0.035

There is some variation in the time derivatives of temperature and salinity, but a clear trend towards increasing temperature and decreasing salinity in the lower layer is consistent with diffusion from above the pycnocline. An estimate of the diffusion coefficient in the pycnocline was obtained by averaging the vertical gradients from the 4/28 through the 9/28 cruises, and using the changes in temperature and salinity over that period to estimate the time derivatives. Substituting these values, plus the volume and area, into the diffusion equations results in equations containing only the coefficients as unknowns. This results in: $K_z^H = 0.11$ cm^2/s and $K_z^S = 0.14$ cm^2/s, where K_z^H is the diffusion coefficient derived from temperature and K_z^S is derived from salinity. These values are reasonable for a strongly stratified water column. While they are not identical, they are sufficiently similar to suggest that vertical diffusion is important during this period.

The importance of diffusion in determining deep water characteristics in the Bays suggests that a mean residence time for the bottom water during the summer can be calculated from the ratios of the difference in temperature and salinity between the surface and deep water and the time derivative of those properties:

$$\tau_H = (T_s - T_b)/\frac{\partial T}{\partial t} \tag{1}$$

where τ_H is the residence time based on temperature variation, T_s is the surface temperature and T_b is the bottom temperature. A similar formula applies to the salinity data, substituting S for T. The data at station BO6 indicate that the averaged over the April to September period, $T_s - T_b = 8.6°C$ and $S_s - S_b = -1.11$ PSU. Using these values and time derivatives derived from the above table, residence times are found to be: $\tau_H = 301$ days and $\tau_S = 298$ days. Clearly these are longer than the period during which the conditions on which they are based persist. Therefore these values should be used as an indication of the rate of renewal by vertical diffusion during the summer months, and not as actual residence times. The deep water is renewed more rapidly than this by complete vertical mixing in late fall and winter. The importance of this result is that the deep water in the Bays will remain relatively stagnant during this period, and may accumulate introduced nutrients or contaminants. The estimates of the vertical diffusion coefficient will be useful in estimating the flux of nutrients to the upper layers during the summer in studying the phytoplankton ecology of the Bays.

3.4.5 Summary of Residence Time Estimates

The residence time estimates for different portions of the Bays, for different time periods and by different methods are summarized in Table 3.4-4.

Table 3.4-4: Massachusetts/Cape Cod Bays residence time estimates

Method	Time Period	Region	Residence Time
Advective Transport	Year	Top 20 M	47–52 days
Drifter Transit	Year	Top 10 M	≈28 days
Fresh Water Replacement	4/26–28/90	Upper mixed layer	14 days
Fresh Water Replacement	7/24–25/90	Upper mixed layer	104 days
Fresh Water Replacement	10/16–18/90	Upper mixed layer	63 days
Fresh Water Replacement	2/4–6/91	Upper mixed layer	29 days
Fresh Water Replacement	3/20–23/91	Upper mixed layer	30 days
Fresh Water Replacement	4/29–5/2/91	Upper mixed layer	26 days
Diffusion	Spring–Fall	≥40 M	≈300 days

These estimates indicate that the waters above the thermocline have short residence times, most likely in the range of 20 to 50 days. The longer estimates of residence times are probably not realistic; the shorter estimates may be valid for short, energetic periods. The residence time of the waters in the thermocline and of the deep waters are not known with confidence. It is plausible that the deep waters of Stellwagen Basin have limited exchange with the overlying water or with the Gulf of Maine waters during the period of strong stratification in the summertime.

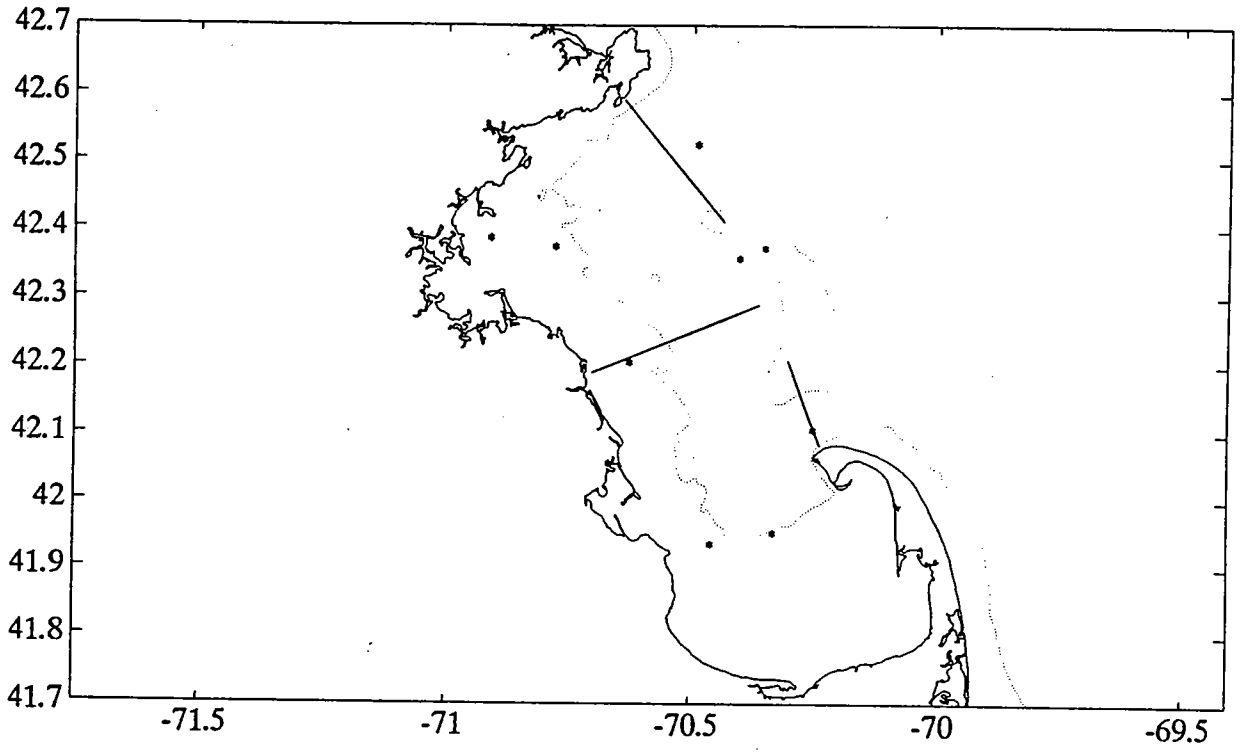

Figure 3.4-1 Sections for calculating mean throughflow in the Bays. The mooring locations are indicated by asterisks.

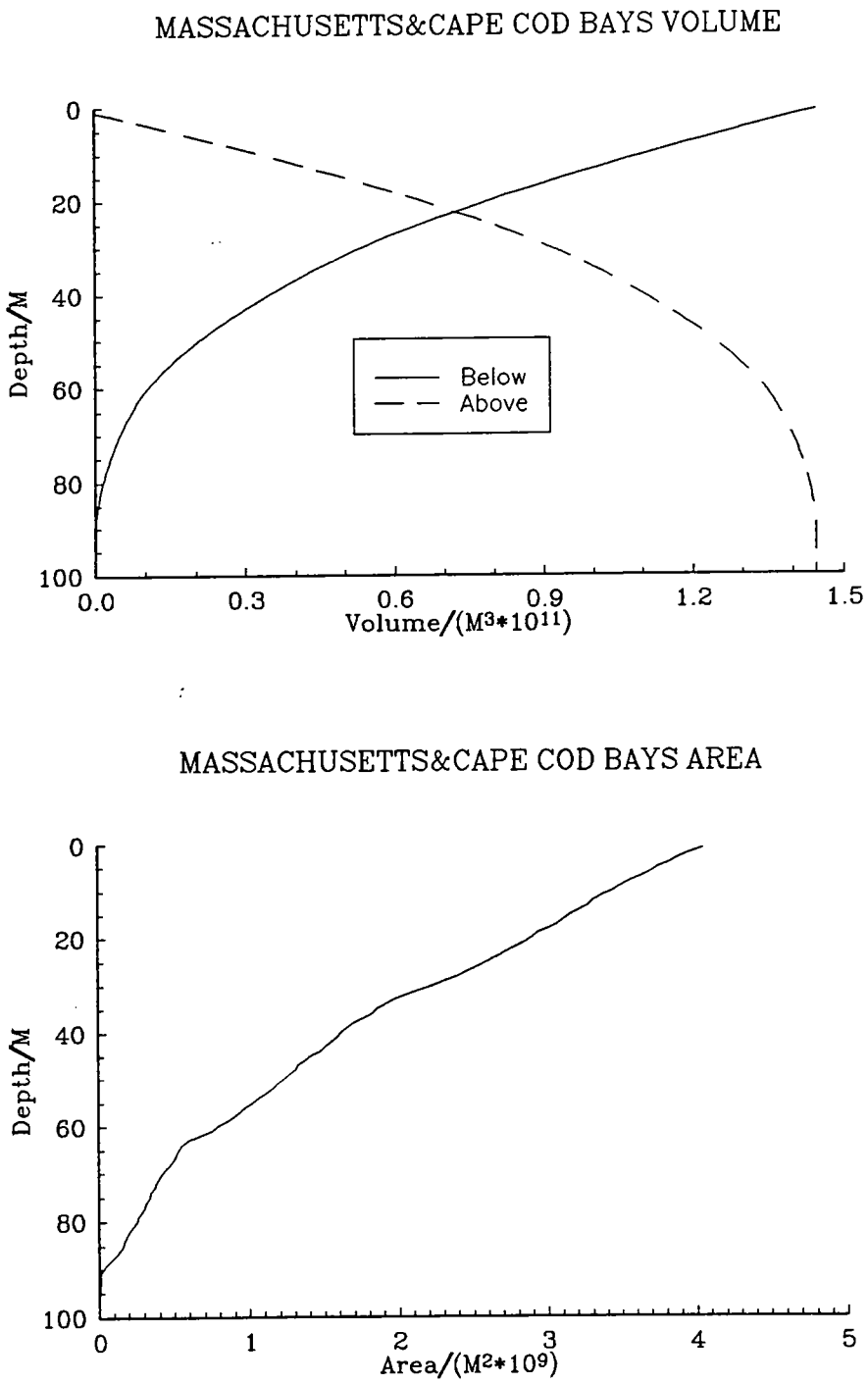

Figure 3.4-2 Volume and area of Massachusetts and Cape Cod Bays, as functions of depth. The volume is plotted both as the volume above a given depth and volume below that depth.

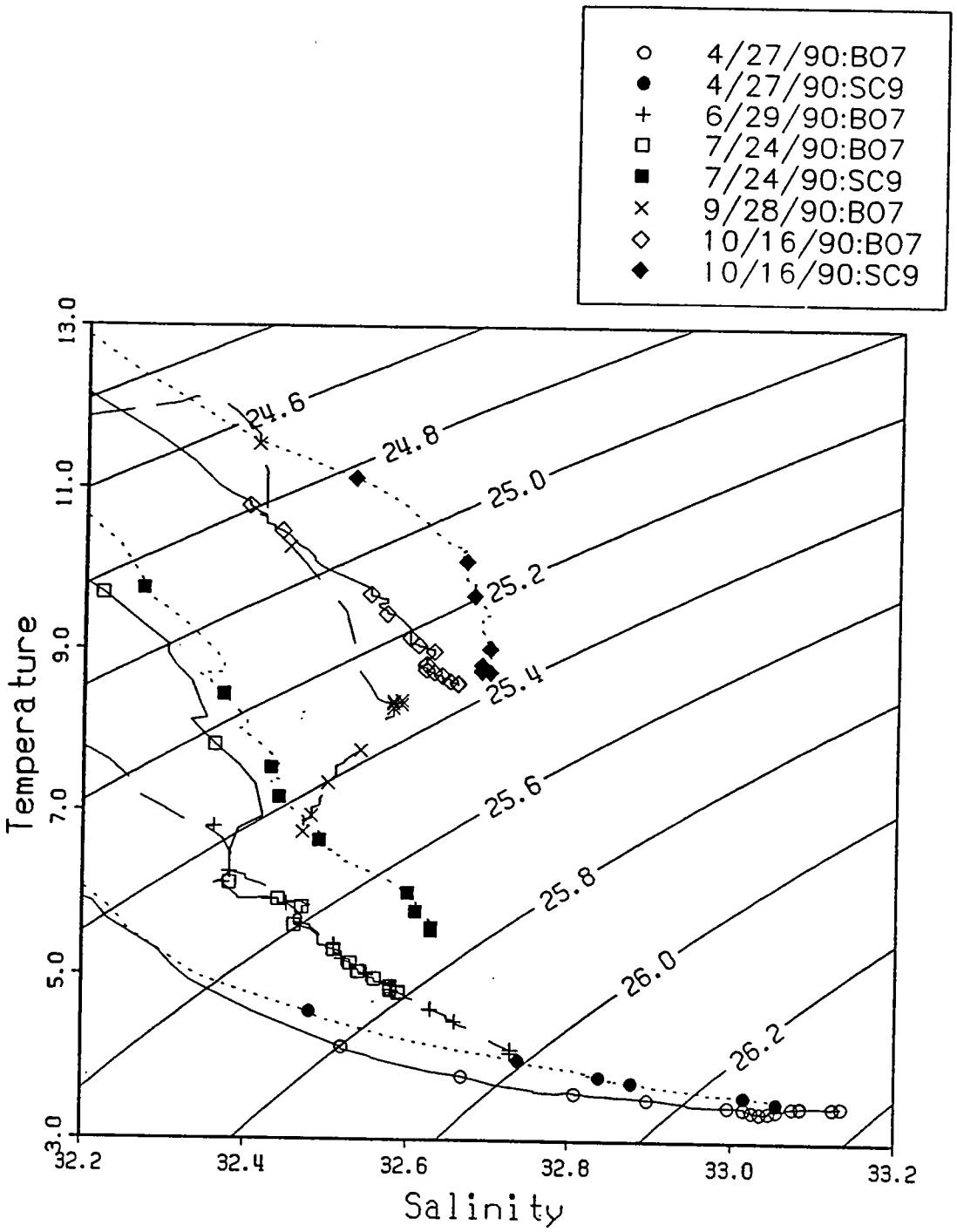

Figure 3.4-3 T-S diagrams for Stellwagen Basin (BO7) and Gulf of Maine (SC9) from April through October, 1990.

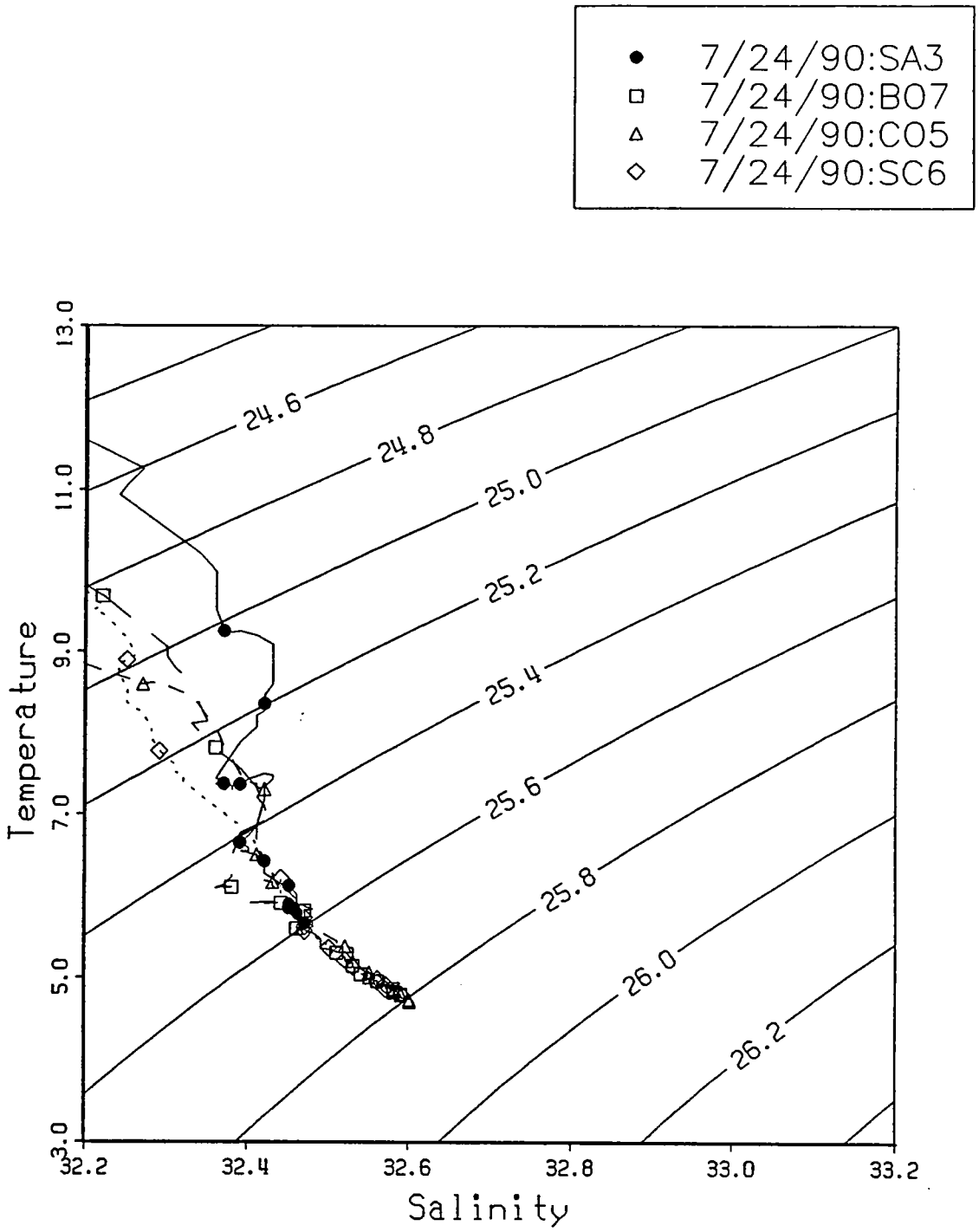

Figure 3.4-4 T-S diagrams for four stations in Stellwagen Basin in July, 1990. All stations had nearly identical T-S characteristics in the deep layer.

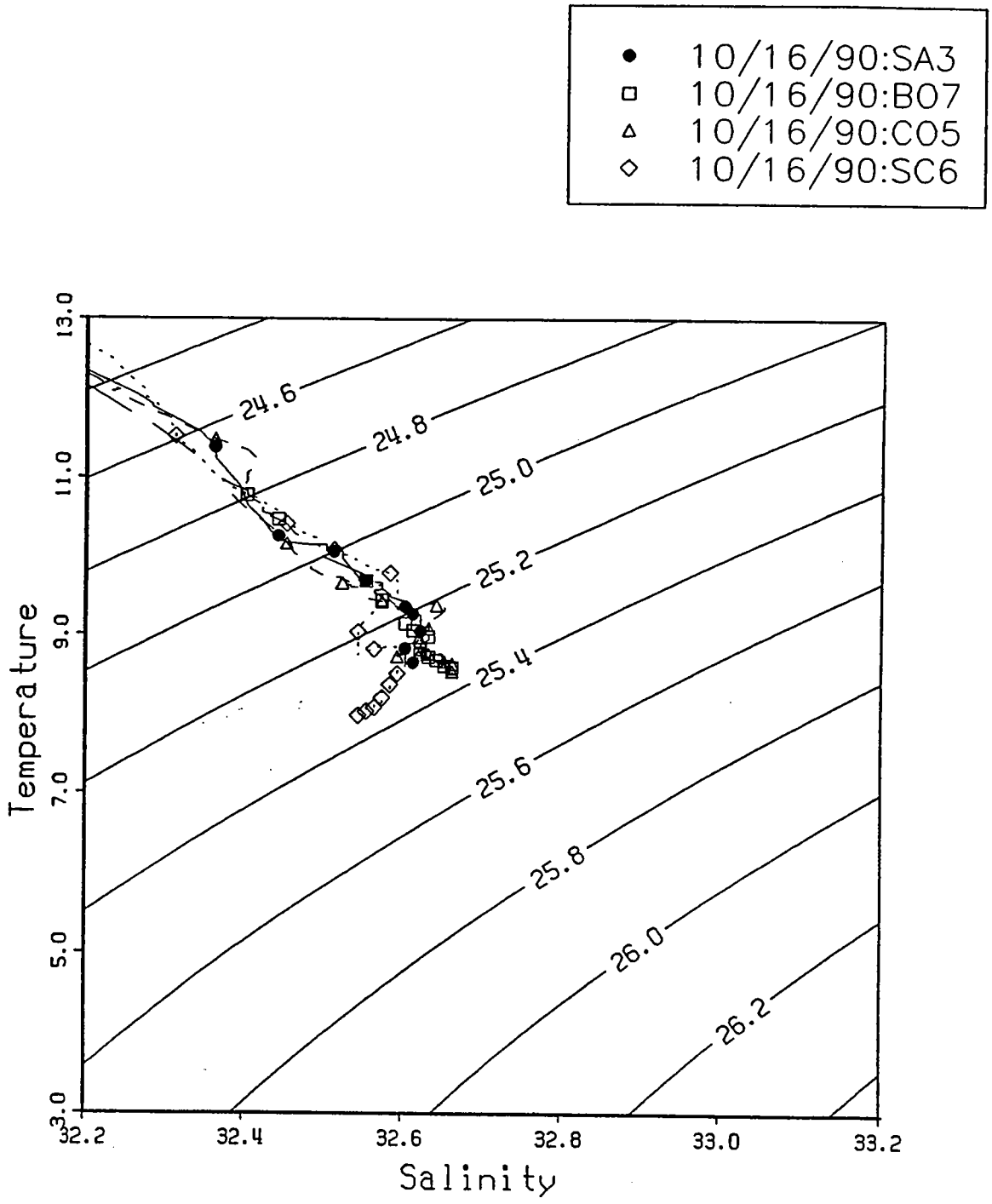

Figure 3.4-5 T-S diagrams for four stations in Stellwagen Basin in October, 1990. Station SC6, the southernmost station of the four, had different deep characteristics than the other three stations, possibly due to advection from the north.

3.5 Suspended Sediment Transport

The Massachusetts Bays Physical Oceanography experiment provided an opportunity to make limited observations to investigate the frequency, extent and principal processes causing sediment resuspension in the Massachusetts Bays. Transport of sediments is important to the overall Bays Program because many contaminants adhere to fine-grained sediments and the transport and long-term fate of particles in the system, both organic and inorganic, affects many aspects of the system. The extent to which particles are resuspended from a site of initial deposition is a key step to their long-term fate.

To monitor resuspended sediments, transmissometers were deployed at stations BB, MN, RP, U6, BS and SC, typically at 10 mab. Observations were converted to beam attenuation that is linearly proportional to suspended sediment concentration for a fixed particle size and composition (Moody et al., 1987). The transmission observations are sometimes difficult to interpret because of the changing concentration and composition of suspended material and are often limited, especially towards the end of the deployment, by biological fouling of the optical windows. However, they provide a useful qualitative measure of resuspension events.

3.5.1 Observations at station BB

The observations at station BB (figure 1-3) show that sediments are episodically resuspended from the seafloor during storms (figure 3.5-1). Resuspension is closely correlated with the strength of oscillatory bottom wave currents that reach 30 cm/s (at 8-10 second periods) during a typical storm. All of the major resuspension events were associated with waves; the increased stress caused by these oscillatory currents, rather than any mean, tidal or wind generated current is the primary stress that resuspends sediments in this region of Massachusetts Bay. Resuspension events in winter last a few days. The concentration of resuspended sediment was largest near the bottom, but increased concentrations were observed at 10 mab and a 5 m from the surface during some events.

Bottom stress (or bottom shear velocity u_{*wave}) caused by waves was calculated using the model of Grant and Madsen (1979) from wave observations obtained at the LNB by NOAA. Theory does not exist for calculating bottom stress from a complete wave spectrum; the wave stress used here was calculated from the significant wave height and period and provides a useful proxy for the actual wave stress on the seafloor. Resuspension events at the station BB were typically observed when this estimate of bottom wave shear velocity exceeded approximately 2.5 cm s^{-1}. During periods of low wave stress (less than 2.5 cm s^{-1}) winds were predominantly from the west and bottom currents at station BB were onshore (figure 3.5-2). During periods

of high bottom wave stress, winds were typically from the north and near bottom currents were alongshore to the southwest and slightly offshore. These observations suggest onshore transport of suspended material during tranquil periods and episodic offshore and southerly alongshore transport of resuspended sediments during storms in the northwestern corner of Massachusetts Bay.

Winds associated with low pressure systems that pass to the east of Massachusetts Bay are typically from the north or northeast and have a large fetch over the Gulf of Maine, generating large waves that propagate into the bay. For storms that pass to the west, winds are from the south or west and the fetch is limited by land. The association of large waves, wind from the north and east, and southerly and offshore flow near the bottom is consistent with this storm climatology.

A time-series sediment trap was deployed at the long-term station (Butman et al., 1992) to provide a measure of the quantity and type of material in suspension. The flux of sediments to the trap is a function of the particle size and concentration in the water column as well as the current flow past the trap. The rates of suspended sediment collection measured since December 1989 suggest a seasonal pattern. In general, the sediment collection rates display a maximum in spring, a minimum in summer, followed by increasing fluxes again in late summer and fall. Large episodic spikes in the fall winter and spring of 1990-91 are associated with individual storms. This seasonal pattern is consistent with the hypothesis that fine-grained, organic-rich sediments accumulate on the bottom in western Massachusetts Bay during the tranquil summer months and then are resuspended and transported in response to storms at the end of the summer season and in the winter.

3.5.2 Observations at U6

Observations at station U6 in the deep part of Stellwagen basin did not show resuspension associated with winter storms. Apparently none of the storms which occurred during the observation period generated waves large enough to cause sufficiently strong currents at 80 m depth to resuspend the sediments. Fluctuations in suspended sediments were observed however that were not associated with any local increase in near bottom current or wave activity. One hypothesis is that these resuspension events were caused by bottom trawling.

It was anticipated that currents associated with the large high-frequency internal waves generated by the tidal flow across Stellwagen Bank in summer (Halpern, 1971; Haury et al., 1983) would be sufficient to resuspend the bottom sediments in Stellwagen Basin. The waves may also break on the western shore of the bay after they propagate across the basin, providing a mechanism in summer for local resuspension. Although there is a significant internal tide at Station U6, it was apparently too close

to the generation region of the internal waves and the high-frequency packets have not had time to form and thus large currents were not observed. The high-frequency internal waves may be extremely important to summer-time resuspension of fine-grained sediment in the Bay and to vertical mixing. Additional field measurements are needed document and assess their role in the Massachusetts Bays.

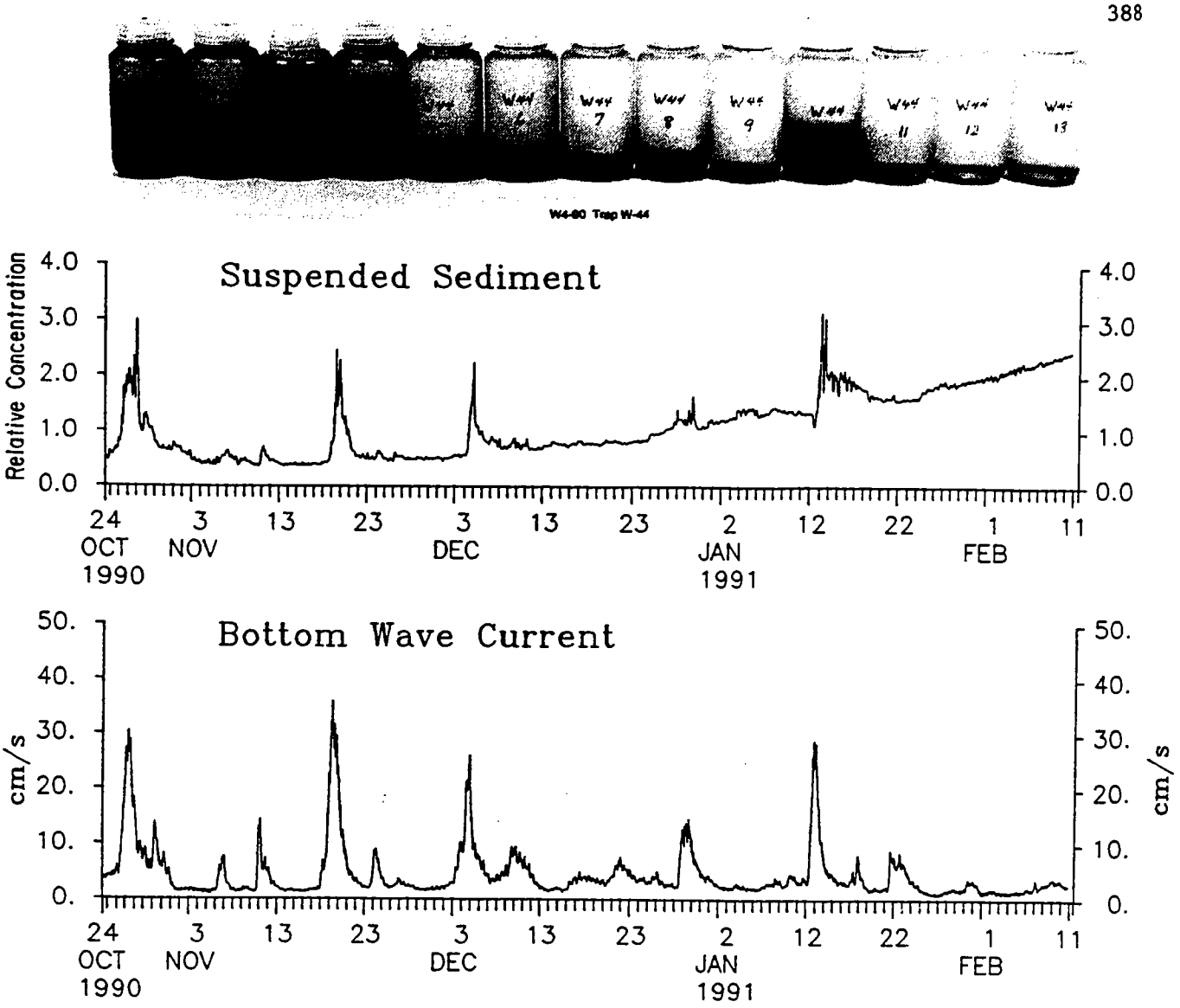

Figure 3.5-1 Photograph of the sample bottles (top) from a time-series sediment trap located 4 meters above the bottom at the long-term monitoring site (station BB) shows the varying amount of material collected during approximately 9-day intervals from October 1990 until February 1991. The turbidity in the bottom water (second panel) is related to the concentration of suspended matter in the water (the upward sloping baseline starting in December is a result of biological fouling of the transmissometer optics used to make the measurements). The close correlation between the four periods of high turbidity in the water column and the four most intense periods of wave activity (bottom panel) indicates that waves are the major cause of resuspension; the rates of sediment collection in the sediment trap bottles also vary with the amount of resuspension. From Butman et al. (1992).

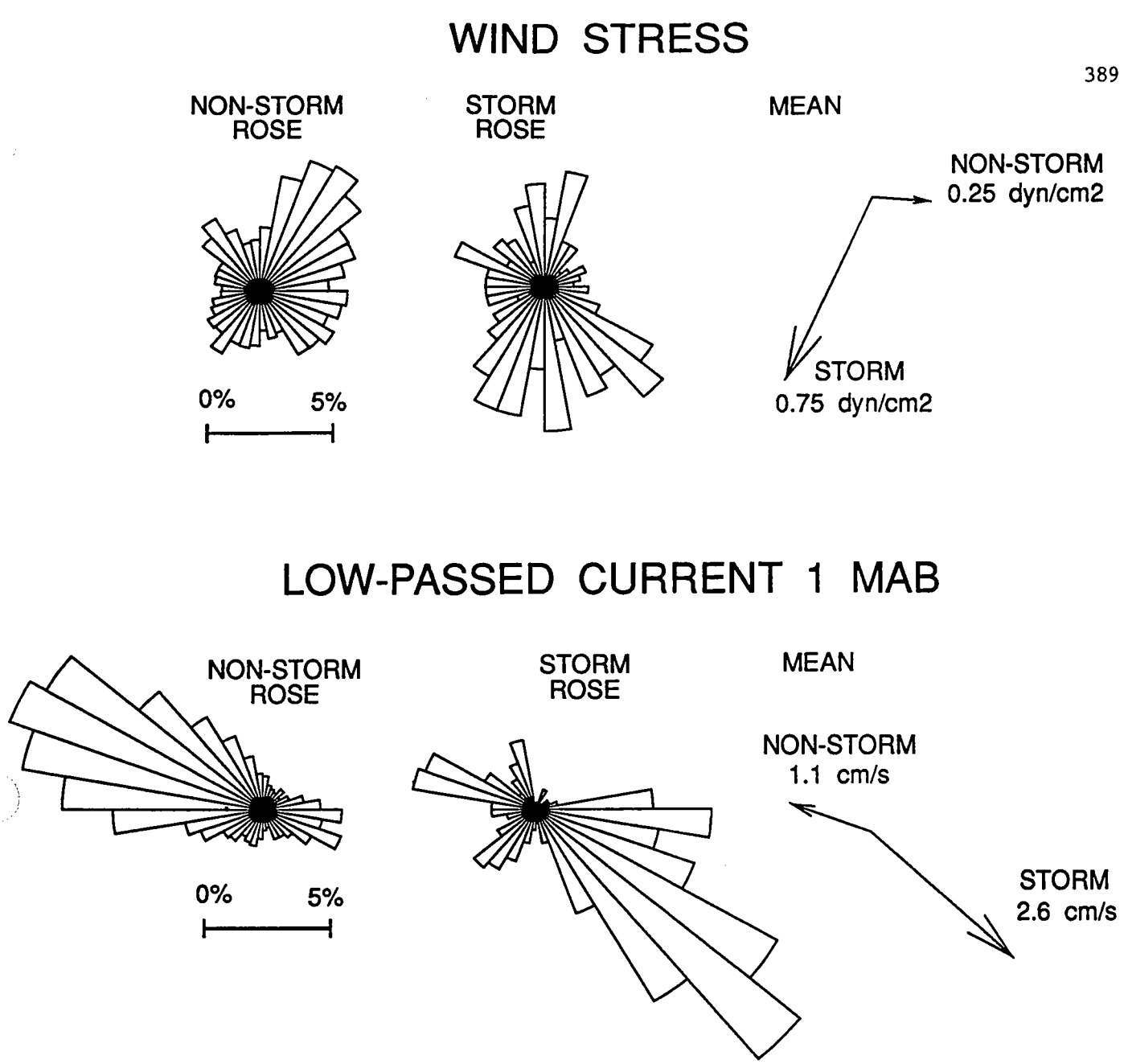

Figure 3.5-2 Histograms of the wind direction at the Large Navigational Buoy and bottom current direction at Station BB during non-storm (u_{*wave} less than 2.5 cm s^{-1}) and storm periods (u_{*wave} greater 2.5 than cm s^{-1}). U_{*wave} is calculated from significant wave height and period measured at the Large Navigational Buoy. Storm periods occurred only 3.6% of the time. The mean wind stress during storm periods is from the northeast. Mean bottom current during non-storm periods is onshore toward Boston Harbor. Mean bottom current during storm periods is southward alongshore toward Cape Cod Bay and slightly offshore toward Stellwagen Basin.

4 Summary, Conclusions and Recommendations

(This section contains the same information that is included in the Executive Summary)

4.1 Summary

This physical oceanographic study of the Massachusetts Bays provided a bay-wide description of the circulation and mixing processes on a seasonal basis. Most of the measurements were conducted between April 1990 and June 1991 and consisted of moored observations to study the current flow patterns, hydrographic surveys to document the changes in water properties, high-resolution surveys of velocity and water properties to provide information on the spatial variability of the flow, drifter deployments to measure the currents, and acquisition of satellite images to provide a bay-wide picture of the surface temperature and its spatial variability.

Key results are:

- There is a marked seasonal variation in stratification in the bays, from well mixed conditions during the winter to strong stratification in the summertime. The stratification acts as a partial barrier to exchange between the surface waters and the deeper waters and causes the motion of the surface waters to be decoupled from the more sluggish flow of the deep waters.
- During much of the year, there is weak but persistent counterclockwise flow around the bays, made up of southwesterly flow past Cape Ann, southward flow along the western shore, and outflow north of Race Point. The data suggest that this residual flow pattern reverses in fall. Fluctuations caused by wind and density variations are typically larger than the long-term mean.
- With the exception of western Massachusetts Bay, flushing of the Bays is largely the result of the mean throughflow. Residence time estimates of the surface waters range from 20–45 days. The deeper water has a longer residence time, but its value is difficult to estimate. There is evidence that the deep waters in Stellwagen Basin are not renewed between the onset of stratification and the fall cooling period.
- Current measurements made near the new outfall site in western Massachusetts Bay suggest that water and material discharged there are not swept away in a consistent direction by a well-defined steady current but are mixed and transported by a variety of processes, including the action of tides, winds, and river

inflow. One-day particle excursions are typically less than 10 km. The outfall is apparently located in a region to the west of the basin-wide residual flow pattern.

- Observations in western Massachusetts Bay, near the location of the future Boston sewage outfall, show that the surficial sediments are episodically resuspended from the seafloor during storms. The observations suggest onshore transport of suspended material during tranquil periods and episodic offshore and southerly alongshore transport of resuspended sediments during storms.

- The spatial complexity of the flow in the Massachusetts Bays is typical of nearshore areas that have irregular coastal shorelines and topography and currents that are forced locally by wind and river runoff as well as by the flow in adjacent regions. Numerical models are providing a mechanism to interpret the complex spatial flow patterns that cannot be completely resolved by field observations and to investigate key physical processes that control the physics of water and particle transport.

4.2 Overall Findings

Water Properties

The water properties in the Bays showed a marked seasonal cycle, varying from cold, well-mixed waters during the winter to strongly stratified conditions during the summer months. Stratification was dominated by salinity variation during the spring, when run-off from the Maine rivers contributed to a reduction of near-surface salinity due to local and regional river discharge. During the summer and fall, temperature variations were the most important contributors to stratification. Variations in water properties were found to be the result of several factors, including internal tides, upwelling and downwelling, and run-off events. Internal tides cause tidal period fluctuations in the height of the thermocline throughout the Bays, most notably in Stellwagen Basin. Upwelling by southwesterly winds causes cold, sub-thermocline water to reach the surface along the western portions of the Bays, with the most intense upwelling occurring in Broad Sound. Downwelling, resulting from northerly or northeasterly winds, causes a weakening of the stratification in the coastal regions.

Circulation

The study indicated that there are several circulation regimes that apparently result from distinct forcing agents. First there is a persistent counterclockwise flow through the Bays that is apparently driven by the large scale circulation of the Gulf of Maine. Second, there are episodic intrusions of relatively fresh, low-density fluid resulting from run-off events in the rivers of the Gulf of Maine, with a lesser contribution from the Charles River and the Massachusetts Water Resources Authority (MWRA) outfalls. Third, there is a wind-driven regime associated with winds from the northwest that reinforced the mean counterclockwise circulation pattern, and finally there is a wind-driven regime associated with southwest–northeast winds that produces significant upwelling or downwelling in the coastal regions and a variable response in the rest of the Bays. Deep currents tend to be weak, particularly during the stratified seasons.

The study confirmed earlier observations that the dominant circulation regime in the Bays is a counterclockwise flow that enters south of Cape Ann, flows south through most of Massachusetts Bay, and exits north of Race Point. This flow regime was found to persist through most of the observation period, the only significant disruption occurring during the fall of 1990, when the circulation pattern appeared to reverse itself. The counterclockwise circulation pattern is most evident in the coastal flow (measured offshore of Scituate and Manomet) and in the outflow north of Race Point. Based on drifter observations, the southward flow appears to extend across Massachusetts Bay as far as Stellwagen Bank, with no obvious intensification in the coastal region. However the mooring in Stellwagen Basin show little evidence of a mean southward flow. This may be the result of tidal rectification of the flow around Stellwagen Bank that resulted in a local current anomaly. Contrary to the overall tendency of the Bays circulation, the region offshore of Boston Harbor does not indicate a significant net southward flow. Cape Cod Bay appears to have a fairly weak net throughflow except during periods of run-off events.

Run-off events were identifiable by decreased near-surface salinity, typically 10–20 days following a peak in run-off in the Maine rivers. The circulation pattern is quite complex during run-off events in the northern portion of Massachusetts Bay, but in the southern portion of the bay and Cape Cod Bay there is a distinct coastal current, which reinforces the mean counterclockwise circulation regime. This pattern of flow through Cape Cod Bay was most clearly evident in drifter trajectories following periods of high run-off. Interestingly, there were no major run-off events in the Bays during the winter months, in spite of some major freshwater flows in the Maine rivers. Apparently the vertical mixing in the western Gulf of Maine is adequate to prevent the development of a coastal current during the winter months.

Wind-driven motions were discerned by statistical analysis of the moored current meter records. The strongest response of the currents is to along-bay winds,

most often being northwesterlies, which drive a southward flow through the middle of the Bays and outflow past Race Point, thus reinforcing the mean circulation. The strongest response to the winds was observed along the coast off Scituate. Southwesterly winds result in upwelling along the coast, causing near-surface temperatures to drop markedly as deep water was carried to the surface. Occasional northeasterly storms cause strong downwelling, which results in weakening of the stratification in the coastal regions.

Deep circulation is weak, and the deep throughflow was not well quantified. Evidence from Stellwagen Basin suggests that there is little horizontal exchange during the spring and summer months, with horizontal transport only becoming important during the fall. This is also suggested by moored data at Race Point.

Exchange Rates

The residence times for the near-surface waters were estimated at 20–40 days, based on the drifters and the moored and drifting velocity data. Lower values were derived from the drifters than the moorings, and the discrepancies may relate on the one hand to the small number of drifters deployed and on the other hand to the sparse spacing of the moored instruments.

The residence time of the deep water was found to vary seasonally. During the unstratified periods, coupling of the deep motion with the surface waters probably results in residence times approaching values of the surface waters. However, the decoupling of the upper and lower portions of the water column during stratified periods causes the deep regions to become much more sluggish during the summertime. There was evidence in Stellwagen Basin that there was essentially no horizontal exchange of deep water between April and October, suggesting that the only deep water exchange was due to vertical mixing. The timescale of vertical mixing was estimated to be approximately 300 days, based on the variations of water properties during the stratified period. Since this timescale exceeds the duration of stratification, the residence time of the deep water during the summer is comparable to the length of time of stratification, or roughly 6 months.

The motion in western Massachusetts Bay, near the future sewage outfall, is qualitatively different than most of the Bays in the sense that it does not exhibit a significant mean circulation. The exchange of water from this portion of the Bays occurs as a result of episodic processes, either by run-off events, winds, or some combination, which causes the fluid to be carried far enough that it is incorporated into the mean counterclockwise circulation.

Perhaps the longest residence times of the surface waters occur in Cape Cod Bay, based on drifter trajectories as well as water properties. There were not adequate data to actually quantify the residence time; in fact it may not be a well-defined

quantity in Cape Cod Bay due to the episodic variation in the circulation regime there. It appears that during periods of freshwater inflow, there is a significant non-tidal flow around the perimeter of Cape Cod Bay. This buoyancy driven flow appears to be impeded by the shallow water in western Cape Cod Bay, resulting in the accumulation of low salinity water in that region. During periods when there is no freshwater inflow, the motions in Cape Cod Bay are weak. One drifter remained in Cape Cod Bay for more than one month during the summer of 1990 before being carried out past Race Point.

4.3 Recommendations

This study provides a solid observational foundation for understanding the physical oceanographic regime of the Massachusetts Bays. Some analysis was undertaken in this study, but by no means does it do justice to the wealth of information contained in these data. All aspects of the physics deserve closer scrutiny than was possible in the timescale of this report. The tidal processes, the density driven flow, and wind-driven processes all should be examined in much greater detail. Only with an understanding of the processes can the results of observations from one particular period be used to draw inferences about the circulation processes occurring at other times.

Numerical modeling is an important means by which to use the knowledge gained about the Bays from this program in a predictive sense. Some early comparisons of the data to model results obtained from the USGS modeling effort suggest that considerable insight into the dynamics and transport processes will come from a combination of three-dimensional modeling and data analysis. Questions will arise in the implementation of the numerical model regarding boundary and initial conditions that may call for additional field measurements.

The need for models is argued in terms of what the present study could never provide. Given the limited resources available, it will not be possible to determine the complex temporal and spatial structure of the exchange between the Bays and the Gulf well enough for quantitative prediction of contamination fluxes. Our observations provide a crude qualitative picture of the flow structures. Models, which represent the physics reasonably well, will be used to provide the essential detailed description. The validity of the model must be tested using observations. The Bays Program observations will be used for that purpose. The model can only work if the conditions along its open boundary are accurately specified. That specification could be provided by very expensive observations and/or results from a "correct" model of the Gulf. In either case, models and observations will have to be integrated — in ways like those used by meteorologists — in order to (1) accurately describe the details of the flow and water property structure at a particular time and (2) make predictions about the

future.

Additional field measurements are also warranted to address important questions that did not receive adequate attention in this study. Vertical mixing and exchange mechanisms are very important to the ecology of the Bays, since they determine the rate at which nutrients can be supplied from the deep waters to the euphotic zone. Additional field work is necessary to provide more quantitative information about rates of vertical exchange by vertical mixing and coastal upwelling.

The impact of the new sewage outfall for Boston obviously provides a major driving force for future studies. Since the outfall plume will be trapped in the lower portion of the thermocline, additional measurements should focus on the circulation of the waters between 15 and 25 m depth. Subsurface drifters would probably be very valuable for describing the general characteristics of the flow at the depths that the plume will be trapped.

We need a better understanding of how and when water enters the Bays. A major forcing agent of the flow in the Bays is freshwater inflow from the Gulf of Maine, yet we still cannot quantify the fraction of that water that enters the Bays. A better understanding of this problem will come from a combination of modeling, additional field measurements and more satellite data analysis.

Finally, we need more interdisciplinary studies, to address the relationship between the physical processes and the ecology of the Bays. Many of the water quality concerns of the Bays are related to impacts on the living resources. We need to be able to quantify the response of the Bays ecosystem to changes in anthropogenic inputs, yet we have little understanding of how the natural forcing agents influence the ecosystem. The physical transport processes play key roles in the ecological response of the Bays; that is why the Massachusetts Bays Program made this large investment in physical oceanographic research. Future ecological research should be cognizant of the physical factors that are influencing distributions of nutrients and organisms, and likewise these ecological studies should provide insights to gain a better understanding of the physical regime.

References

Baines, P.G., 1973. The Generation of Internal Tides by Flat-bump Topography, *Deep-Sea Res.*, **20**, 179–205.

Beardsley, R.C., 1987. A Comparison of the Vector-Averaging Current Meter and New Edgerton, Germeshausen, and Grier, Inc., Vector-Measuring Current Meter on a Surface Mooring in Coastal Ocean Dynamics Experiment I, *J. Geophys. Res.*, **92**, 1845–1859.

Berliand, M.E. and T.G. Berliand, 1952. Determination of Effective Radiation of the Earth as Influenced by Cloud Cover, *Izvestiia Akademii Nauk S.S.S.R., Seriia Geofiziceskaya*, **1**, 64–78.

Bigelow, H.B., 1927. Physical Oceanography of the Gulf of Maine, *Bulletin U.S. Bureau of Fisheries*, **40**(2), 511–1027.

Bottero, J.M., and R.D. Pillsbury, 1987. Evaluation of the S4 Current Meter at Oregon State University, Ref. 88-2, College of Oceanography, Oregon State Univ., Corvallis, 54 pp.

Bowen, I.S., 1926. The Ratio of Heat Losses by Conduction and by Evaporation from Any Water Surface, *Phys. Rev.*, **27**, 779–787.

Brooks, D.A. and D.W. Townsend, 1989. Variability of the Coastal Current and Nutrient Pathways in the Eastern Gulf of Maine, *J. Marine Res.*, **47**, 303–321.

Brown, W.S., 1976. A Seafloor Data Logger, *Polymode News*, **15**, pp. 17.

Brown W.S. and R.C. Beardsley, 1978. Winter Circulation in the Gulf of Maine Part 1. Cooling and Water Mass Formation, *J. Phys. Oceanogr.*, **8**, 265–277.

Brown, W.S., J.D. Irish and A. Bratkovich, 1983a. CODE-1: Moored Temperature and Conductivity Observations, in CODE-1: Moored Array and Large Scale Data Report, ed. L.K. Rosenfeld, WHOI Tech. Rept. No. 83-23, CODE Tech. Rept. No. 21, 117–129.

Brown, W.S., J.D. Irish, and R. Erdman, 1983b. CODE-I: Bottom Pressure Observations, in CODE-I: Moored Array and Large Scale Data Report, ed. L.K. Rosenfield, WHOI Tech. Rept. 82-83, CODE Tech. Rept. 21, 109–116.

Brown, W.S. and J.A. Moody, 1987. Tides, Chapter 9 in Georges Bank, ed. R.H. Backus, MIT Press, Cambridge, MA 100–107.

Brown, W.S., J.D. Irish and C.D. Winant, 1987. A Description of Subtidal Pressure Field Observations on the Northern California Continental Shelf During the Coastal Ocean Dynamics Experiment, *J. Geophys. Res.*, **92**, 1605–1635.

Brown, W.S. and J. Irish, 1992. The Seasonal Evolution of the Geostrophic Circulation in the Gulf of Maine, 1986–87, *J. Phys. Oceanogr.*, **22**(5), 445–473.

Bryden, H., 1976. Horizontal Advection of Temperature and Low-Frequency Motions, *Deep-Sea Res.*, **2**, 1165–1174.

Bumpus, D.F., 1973. A Description of the Circulation on the Continental Shelf of the East Coast of the United States, *Progress in Oceanography*, **6**, 111–157.

Bumpus, D.F., 1974. Review of the Physical Oceanography of Massachusetts Bay. Woods Hole Oceanographic Inst. Tech. Rept. WHOI-74-6, 157 pp.

Bumpus, D.F. and L.M. Lauzier, 1965. Circulation on the Continental Shelf off Eastern North America between Newfoundland and Florida, *American Geographical Society Serial Atlas of the Marine Environment*, Folio 7.

Butman, B., 1975. On the Dynamics of Shallow Water Currents in Massachusetts Bay and on the New England Continental Shelf, Ph.D. Dissertation, Massachusetts Institute of Technology and Woods Hole Oceanographic Institution, Woods Hole Oceanographic Institution Technical Report 77-15.

Butman, B., 1976. Hydrography and Low-frequency Currents Associated with the Spring Runoff in Massachusetts Bay. *Memoiries Societe Royale des Sciences de Liege*, 247–275.

Butman, B., and D.W. Folger, 1979. An Instrument System for Long-term Sediment Transport Studies on the Continental Shelf, *J. Geophys. Res.*, **84**, 1215–1220.

Butman, B., M.H. Bothner , J.C. Hathaway, H.L. Jenter, H.J. Knebel, F.T. Manheim, R.P. and Signell, 1992. Contaminant Transport and Accumulation in Massachusetts Bay and Boston Harbor: A Summary of U.S. Geological Survey Studies. U.S. Geological Survey Open-File Report 92-202, 42 pp.

Cartwright, D., W. Munk and B. Zetler, 1969. Pelagic Tidal Measurements, A Suggested Procedure for Analysis, *EOS*, **50**(7), 472–47.

Chapman, D.C. and R.C. Beardsley, 1989. On the Origin of Shelf Water in the Middle Atlantic Bight, *J. Phys. Oceanogr.*, **19**, 384–391.

Chao, S.Y., 1987. Wind-driven Motion Near Inner Shelf Fronts, *J. Geophys. Res.*, **92**(C4), 3849–3860.

Chao, S.Y., 1988a. River-forced Estuarine Plumes, *J. Phys. Oceanogr.*, **18**, 72–88.

Chao, S.Y., 1988b. Wind-driven Motion of Estuarine Plumes, *J. Phys. Oceanogr.*, **18**, 144–1166.

Chao, S.Y. and W.C. Boicourt, 1986. Onset of Estuarine Plumes, *J. of Phys. Oceanogr.*, **16**, 2137–2149.

Chereskin, T.K., 1983. Generation of Internal Waves in Massachusetts Bay, *J. Geophys. Res.*, **88**, 2649–2661.

Csanady, G.T., 1974. Barotropic Currents Over the Continental Shelf, *J. Phys. Oceanogr.*, **4**, 357–371.

Dahlen, J.M., 1986. The Draper LCD: A Calibrated, Low Cost Lagrangian Drifter. Charles Stark Draper Labs Technical Report CSDL-P-2670, 14 pp.

Davis, R.E., 1985. Drifter Observations of Surface Currents during CODE: the Statistical and Dynamical Views, *J. Geophys. Res.*, **90**, 4756–4772.

Defant, A., 1962. Physical Oceanography, Vol. 2, Pergamon, New York.

Dennis, R.E. and E.E. Long, 1971. A Users Guide to a Computer Program for Harmonic Analysis of Data at Tidal Frequencies, NOAA Tech. Rept. No. 41, U.S. Dept. of Commerce, Washington, D.C.

Dutton, J.A., 1986. The Ceaseless Wind: An Introduction to the Theory of Atmospheric Motion, Dover Publications, Inc., New York, 617 pp.

Fitzgerald, M.G., 1980. Anthropogenic Influence of the Sedimentary Regime of an Urban Estuary–Boston Harbor, Ph.D. Dissertation, MIT-WHOI Joint Program.

Fofonoff, N.P. and R.C. Millard, Jr., 1983. Algorithms for Computation of Fundamental Properites of Seawater, UNESCO Tech. Paper in Mar. Sci., No. 44.

Foreman, M.G.G., 1977. Manual for Tidal Analysis and Prediction, Pacific Marine Science Rept. 77-10, Inst. of Ocean Sciences, Patricia Bay, Victoria, B.C.

Franks, P.J.S., 1990. Dinoflagellate Blooms and Physical Systems in the Gulf of Maine. Ph.D. Dissertation, WHOI-90-23, Woods Hole Oceanographic Institution, Woods Hole, MA, 253 pp.

Gardner, G.B., 1989. Vernal Circulation of Massachusetts Bay, *EOS*, **70**, pp. 356.

Garrett, C.J., 1972. Tidal Resonance in the Bay of Fundy and Gulf of Maine, *Nature*, **238**(5365), 441–443.

Garrett, C.J., 1974. Normal Modes of the Bay of Fundy and the Gulf of Maine, *Canadian Jour. of Earth Science*, **11**, 549–556.

Garvine, R.W., 1987. Estuarine Plumes and Fronts in Shelf Waters: A Layer Model, *J. Phys. Oceanogr.*, **17**, 1877–1896.

Geyer, W.R., 1989. Field Calibration of Mixed-layer Drifters, *J. Atmos. and Ocean. Tech.*, **6**, 333–342.

Glibert, P.M. and T.C. Loder, 1977. Automated Analysis of Nutrients in Sea Water: A Manual of Techniques, WHOI Tech. Rept. 77-47, 46 pp.

Godin, G., 1972. The Analysis of Tides, University of Toronto Press, Toronto.

Grant, W.D. and O.S. Madsen, 1979. Combined Wave and Current Interactions with a Rough Bottom, *J. Geophys. Res.*, **84**, 1797–1808.

Greenberg, D.A., 1983. Modeling the Mean Barotropic Circulation in the Bay of Fundy and the Gulf of Maine, *J. Phys. Oceanogr.*, **13**, 886–904.

Halpern, D., 1971. Observations of Short-period Internal Waves in Massachusetts Bay, *J. Mar. Res.*, **29**, 116–132.

Haugin, E.L., 1992. Personal communication, Bigelow Labs.

Haury, L.R., M.G. Briscoe and M.H. Orr, 1979. Tidally Generated Internal Wave Packets in Massachusetts Bay, *Nature*, **278**, 312–317.

Haury, L.R., P.H. Wiebe, M.H. Orr, and M.G. Briscoe, 1983. Tidally Generated High-frequency Internal Wave Packets and Their Effects on Plankton in Massachusetts Bay, *J. Mar. Res.*, **41**, 43–55.

Hopkins, T.S. and N. Garfield, III, 1979. Gulf of Maine Intermediate Water, *J. Mar. Res.*, **37**, 103–139.

Hopkins, T.S. and S. Raman, 1987. Atmospheric Variables and Patterns, in Georges Banks, ed. R. Backus, MIT Press, Cambridge, MA, 66–73.

Huang, J.C.K. and J.M. Park, 1975. Effective Cloudiness Derived from Ocean Buoy Data, *J. App. Met.*, **14**, 240–245.

Ikeda, M., 1984. Coastal Flows Driven by a Local Density Flux, *J. Geophys. Res.*, **89**(C5), 8008–8016.

Irish, J.D., N.R. Pettigrew, K.Deines and F. Rowe, 1983. A New, Bottom-Mounted, Internally-Recording Doppler Acoustic Profiling Current Meter, IEEE Third Working Symp. on Oceanographic Data Systems, 109–1113.

Irish, J.D., 1985. CODE-2: Moored Temperature and Conductivity Observations, CODE-2: Moored Array and Large-Scale Data Report, ed. R. Limeburner, WHOI Tech. Rept. No. 85-35, CODE Tech. Rept. No. 38, 133–164.

Irish, J.D. and W.S. Brown, 1986. An Archiving and Analysis System for Geophysical Data, Marine Data Systems International Symposium, MDS86, 64–69.

Irish, J.D., J.M. Joy, R.M. Gelinas, and D.D. Ball, September 1987. Quasi-Real Time Measurements of Density in the Gulf of Maine, Proceedings of OCEANS '87, 899–904.

Irish, J.D., 1989. Long Term Measurements of the Variability of the Density Field of the Gulf of Maine, OPAL Tech. Rept. (in revision).

Irish, J.D., 1990. Time Series Measurements of Bottom Pressure, Temperature and Conductivity in the Gulf of Maine: 1986-1987, EOS Tech. Rept. No. EOS-90-TR02, 57 pp.

Irish, J.D., K.E. Morey, G.J. Needell and Jon Wood, 1991. A Current Meter with Intelligent Data System, Environmental Sensors, and Data Telemetry, *IEEE J. Oceanic Eng.*, **16**, 319–328.

Isaji, T. and M. Spaulding, 1984. A Model of the Tidally Induced Residual Circulation in the Gulf of Maine and Georges Bank, *J. Phys. Oceanogr.*, **14**, 1119–1126.

Large, N.G. and S. Pond, 1981. Open Ocean Momentum Flux Measurements in Moderate to Strong Winds, *J. Phys. Oceanogr.*, **11**(3), 324–336.

Loder, T.C. and P.M. Glibert, 1977. Blank and Salinity Corrections for Automated Nutrient Analysis of Estuarine and Seawaters, Technicon International Congress 1976, **2**, 48–56.

Loder, J., 1980. Topographic Rectification of Tidal Currents on the Sides of Georges Bank, *J. Phys. Oceanogr.*, **10**, 1399–1418.

Martini, M. and W. Strahle, in press. A Multi-Sensor Oceanographic Measurement System for Coastal Environments, Oceans '92.

McCullough, J. 1975. Vector-Averaging Current Meter Speed Calibration and Recording Technique, Woods Hole Oceanogr. Inst. Tech. Rept. 75-54, 35 pp.

Menzie and Cura, 1991. Final Report: Sources and Lodging of Pollutants to Massachusetts Bay, Massachusetts Bay Program Final Report.

Metcalf and Eddy, 1984. Application for a Waiver of Secondary Treatment for the Nut Island and Deer Island Treatment Plants, Report prepared for the Metropolitan District Commission.

Moody, J.A., B. Butman, R.C. Beardsley, W.S. Brown, P. Daifuku, J.D. Irish, D.A. Mayer, H.O. Mofjeld, B. Petrie, S. Ramp, P. Smith, W.R. Wright, 1984. Atlas of Tidal Elevation and Current Observations on the Northeast American Continental Shelf and Slope, U.S. Geological Survey Bulletin 1611, U.S. Dept. of Interior, Washington, D.C.

Moody, J.A., B. Butman, M.H. Bothner, 1987. Near-bottom Suspended Matter Concentration on the Continental Shelf Curing Storms; Estimates Based on Insitu Observations of Light Transmission and Particle Size Dependent Transmissometer Calibration, *Continental Shelf Res.*, **7**, 609–628.

Mountain, D.G. and P.F. Jessen, 1987. Bottom Waters of the Gulf of Maine 1978–1983, *J. Mar. Res.*, **45**, 319–345.

Munk, W. and D. Cartwright, 1966. Tidal Spectroscopy and Prediction. *Phil. Trans. Proc. Roy. Soc.*, London, A, 533–581.

Parker, B.B., 1991. The Relative Importance of the Various Nonlinear Mechanisms in a Wide Range of Tidal Interactions (Review), in Tidal Hydrodynamics, ed. B. Parker, John Wiley & Sons, New York, 237–268.

Pederson, A.M., 1969. An Accurate Low-cost Temperature Sensor. Trans. Marine Temperature Measurements Symp., Miami, 135–153.

Pederson, A.M. and M.C. Gregg, 1979. Development of a Small In Situ Conductivity Instrument, *IEEE Jour. Oceanic Eng.*, **OE4**, 69–75.

Pettigrew, N.R. and J.D. Irish, 1983. Evaluation of a Bottom-Mounted Doppler Acoustic Profiling Current Meter, Proc. Oceans'83, 182–186.

Pettigrew, N.R., R.C. Beardsley and J.D. Irish, 1986. Field Evaluations of a Bottom-mounted Acoustic Doppler Profiler and Conventional Current Meter Moorings, IEEE Proc. Third Working Conf. on Current Measurement, 153–162.

Pettigrew, N.R., J.D. Wood, E.H. Pape, G.J. Needell and J.D. Irish, 1987. Acoustic Doppler Current Profiling from Moored Subsurface Floats, Proc. Oceans '87, 110–116.

Ramp, S.R., R.J. Schlitz, and W.R. Wright, 1985. The Deep Flow Through the Northeast Channel, Gulf of Maine, *J. Phys. Oceanogr.*, **15**, 1790–1808.

Rattray Jr., M., J.D. Dworski, and P.E. Kovala, 1969. Generation of Long Waves at the Continental Slope, *Deep-Sea Res.*, **16**, 179–195.

Schureman, P.W., 1941. Manual of Harmonic Analysis and Prediction of Tides, Coast and Geodetic Survey Special Publication No. 98, Revised (1940) Edition, U.S. Dept. of Commerce, Washington, D.C.

Signell, R.P. and W.R. Geyer, 1990. Transient eddy formation around headlands, *J. Geophys. Res.*, **96**, 2561–2576.

Signell, R.P, 1992. Tide- and Wind-Driven Flushing of Boston Harbor, in Proceedings of the 2nd International Conference on Estuarine and Coastal Modeling, edited by M. L. Spaulding, American Society of Civil Engineers, New York, 594–606.

Snodgrass, F.E., 1968. Deep Sea Instrument Capsule, *Science*, **162**, 78–87.

Strickland, J.D.H. and T.R. Parsons, 1972. A Practical Handbook of Sea Water Analysis. (2nd Ed.), *Bull. Fish. Res. Bd. Canada*, **167**, 310.

Sverdrup, H.V., M.W. Johnson and R.H. Fleming, 1946. The Oceans, Their Physics, Chemistry and General Biology, Prentice Hall, Englewood Cliffs, N.J., 1087 pp.

Townsend, D.W., L.M. Cammen, J.P. Christensen, S.G. Ackleson, M.D. Keller, E.M. Haugen, S. Corwin, W.K. Bellows and J.F. Brown, 1990. Winter-Spring Oceanographic Conditions in Massachusetts Bay, Bigelow Laboratory for Ocean Sciences Technical Report 76, 256 pp.

Trask, R.P. and M.G. Briscoe, 1983. Detection of Massachusetts Bay Internal Waves by the Synthetic Aperature Radar (SAR) on SEASAT, *J. Geophys. Res.*, **88**, 1789-1799.

Wearn Jr., R.B. and N.G. Larson, 1982. Measurements of the Sensitivities and Drift of Digiquartz Pressure Sensors, *Deep-Sea Res.*, bf 29, 111–134.

Weller, R.A. and R.E. Davis, 1980. A Vector Measuring Current Meter, *Deep Sea Res.*, **27**, 565–582.

Wood, J.D. and J.D. Irish, September 1987. A Compliant Surface Mooring System for Real Time Data Acquisition, Proceedings of Oceans '87, 652–657.

Woodward, W. and G. Appell, 1973. Report on the Evaluation of a Vector-Averaging Current Meter, NOAA Tech. Memo. NOAA-TM-NOS-NOIC-1, 64 pp.

Wright, D.G., D.A. Greenberg, J.W. Loder and P.C. Smith, 1986. The Steady-state Barotropic Response of the Gulf of Maine and Adjacent Regions to Surface Wind Stress, *J. Phys. Oceanogr.*, **16**, 947–966.